

**OSA Biophotonics Congress:**  
**Biomedical Optics**  
**Clinical and Translational Biophotonics (Translational)**  
**Optics and the Brain (Brain)**  
**Optical Tomography and Spectroscopy (OT&S)**  
**Microscopy, Histopathology and Analytics (Microscopy)**

3–6 April 2018  
The Diplomat Beach Resort  
Hollywood, Florida USA

**Table of Contents**

|                                    |    |
|------------------------------------|----|
| Program Committees .....           | 2  |
| General Information .....          | 3  |
| Special Events .....               | 4  |
| Plenary Speakers .....             | 6  |
| Buyers' Guide .....                | 9  |
| Explanation of Session Codes ..... | 12 |
| Agenda of Sessions .....           | 13 |
| Abstracts .....                    | 18 |
| Key to Authors .....               | 54 |

# Program Committees

## Congress Chair

Elizabeth Hillman, *Columbia University, USA*

## Past Congress Chair

Irene Georgakoudi, *Tufts University, USA*

## Clinical and Translational Biophotonics

Stefan Andersson Engels, *Tyndall National Institute, Ireland, Chair*

Thomas Wang, *University of Michigan, USA, Chair*

Laura Marcu, *University of California Davis, USA, Program Chair*

David Sampson, *University of Western Australia, Australia, Program Chair*

J. Quincy Brown, *Tulane University, USA*

Daniel Elson, *Imperial College London, United Kingdom*

Ewa Goldys, *Macquarie University, Australia*

Michalina Gora, *CNRS, ICube Laboratory, France*

Dimitris Gorpas, *Helmholtz Zentrum München GmbH*

Frederic Leblond, *Polytechnique Montreal, Canada*

Xingde Li, *Johns Hopkins University, USA*

Lothar Lilge, *Princess Margaret Hospital, Canada*

Seemantini Nadkarni, *Harvard Medical School, USA*

Malini Olivo, *Singapore Bioimaging Consortium, Singapore*

Jennifer Phipps, *University of California Davis, USA*

Ronald Sroka, *Ludwig-Maximilians-Universität München, Germany*

Alex Vitkin, *Ontario Cancer Institute, Canada*

Karin Wardell, *Linköping University, Sweden*

Adam Wax, *Duke University, USA*

Victor Yang, *Sunnybrook Health Sciences Centre, Canada*

Elena Zagaynova, *Nizhny Novgorod State Medical Academy, Russia*

## Optics and the Brain

Daniel Cote, *Université Laval, Canada, Chair*

Joseph Culver, *Washington University in St. Louis, USA, Chair*

Erin Buckley, *Emory University, USA*

Michael Crair, *Yale University, USA*

Hod Dana, *HHMI - Janelia Farm Research Campus, USA*

Anna Devor, *University of California San Diego, USA*

Mamadou Diop, *Western University, Canada*

Maria Angela Franceschini, *Massachusetts General Hospital, USA*

Timothy Holy, *Washington University in St. Louis, USA*

Ori Katz, *Hebrew University of Jerusalem, Israel*

Tim Murphy, *University of British Columbia, Canada*

Chris Schaffer, *Cornell University, USA*

Shy Shoham, *Technion Israel Institute of Technology, Israel*

Spencer Smith, *University of North Carolina at Chapel Hill, USA*

Vivek Srinivasan, *University of California Davis, USA*

Francois St-Pierre, *Baylor College of Medicine, USA*

Jack Waters, *Allen Institute for Brain Science, USA*

Meryem Yucel, *Athinoula A. Martinos Center for Biomedical Imaging, USA*

## Optical Tomography and Spectroscopy

Hamid Dehghani, *University of Birmingham, United Kingdom, Chair*

Daniel Razansky, *Technical University of Munich, Germany, Chair*

Turgut Durduran, *ICFO - The Institute of Photonic Sciences, Spain, Program Chair*

Christine Hendon, *Columbia University, USA, Program Chair*

Emmanuel Bossy, *LIPhy, University Grenoble Alpes - CNRS, France*

Erin Buckley, *Emory University, USA*

Regine Choe, *University of Rochester, USA*

Laura Di Sieno, *Politecnico di Milano, Italy*

Andrew Dunn, *University of Texas at Austin, USA*

Andreas Hielscher, *Columbia University, USA*

Jana Kainerstorfer, *Carnegie Mellon University, USA*

Brendan Kennedy, *The University of Western Australia, Australia*

Muyinatu Lediju Bell, *Johns Hopkins University, USA*

Seemantini Nadkarni, *Harvard Medical School, USA*

Brian Pogue, *Dartmouth, USA*

Amir Rosenthal, *Technion Israel Institute of Technology, Israel*

Ulas Sunar, *Wright State University, USA*

Bruce Tromberg, *University of California Irvine, USA*

Ruikang Wang, *University of Washington, USA*

Adam Wax, *Duke University, USA*

Udo Weigel, *Hemophotonics S.L., Castelldefels, Spain*

Martin Wolf, *University of Zurich, Switzerland*

Junjie Yao, *Duke University, USA*

Chao Zhou, *Lehigh University, USA*

## Microscopy, Histopathology and Analytics

Richard Levenson, *University of California Davis, USA, Chair*

Melissa Skala, *University of Wisconsin-Madison, USA, Chair*

Kevin Eliceiri, *University of Wisconsin, USA, Program Chair*

Milind Rajadhyaksha, *Memorial Sloan Kettering Cancer Center, USA, Program Chair*

James Castracane, *SUNY Polytechnic Institute, USA*

Andrew Cohen, *University of Wisconsin-Milwaukee, USA*

Xiaohu Gao, *University of Washington, USA*

Michael Giacomelli, *Massachusetts Institute of Technology, USA*

Jonathan Liu, *University of Washington, USA*

John Tomaszewski, *State University of New York at Buffalo, USA*

Benjamin Vakoc, *Harvard Medical School, USA*

Anna Yaroslavsky, *Harvard Medical School, USA*

# General Information

## Access to the Wireless Internet

OSA is pleased to offer complimentary wireless internet services throughout the meeting space at The Diplomat Beach Resort for all attendees and exhibitors. Activate your computer's wireless radio and select available network and enter password listed below.

Network: The\_Optical\_Society

Passcode: biomed2018

## Registration

Grand Ballroom Foyer

|                    |             |
|--------------------|-------------|
| Monday, 2 April    | 15:00–18:00 |
| Tuesday, 3 April   | 07:00–17:30 |
| Wednesday, 4 April | 07:30–17:30 |
| Thursday, 5 April  | 07:30–17:30 |
| Friday, 6 April    | 07:30–16:00 |

## Early Online Access to Technical Digest

Full Technical Attendees have both early and free continuous online access to the Congress Technical Digest and Post-deadline papers through OSA Publishing's Digital Library. The presented papers can be downloaded individually or by downloading .zip files (.zip files are available for 60 days).

1. Visit the conference website at [www.osa.org/biomed](http://www.osa.org/biomed)
2. Select the "Access digest papers" link on the right hand navigation.
3. Log in using your email address and password used for registration. You will be directed to the conference page where you will see the .zip file link at the top of this page.

[**Note:** if you are logged in successfully, you will see your name in the upper right-hand corner.]

Access is limited to Full Technical Attendees only. If you need assistance with your login information, please use the "forgot password" utility or "Contact Help" link.

## About OSA Publishing's Digital Library

Registrants and current subscribers can access all of the meeting papers, posters and postdeadline papers on OSA Publishing's Digital Library. The OSA Publishing's Digital Library is a cutting-edge repository that contains OSA Publishing's content, including 16 flagship, partnered and co-published peer reviewed journals and 1 magazine. With more than 350,000 articles including papers from over 700 conferences, OSA Publishing's Digital Library is the largest peer-reviewed collection of optics and photonics.

## Poster Presentation PDFs



The PDFs of select poster presentations will be available early June. While accessing the papers in OSA Publishing's Digital Library look for the multimedia symbol.

## Update Sheet and Postdeadline Papers

All technical program changes will be communicated in the onsite Congress Program Update Sheet. All attendees receive this information with registration materials, and we encourage you to review it carefully to stay informed to changes in the program. Postdeadline papers will also be announced on the update sheet. This program contains the latest information up to 9 March 2018.

## Code of Conduct

All conference guests, attendees, and exhibitors are subject to the Code of Conduct policy, the full text of which is available at [https://www.osa.org/en-us/meetings/code\\_of\\_conduct/](https://www.osa.org/en-us/meetings/code_of_conduct/). Conference management reserves the right to take any and all appropriate actions to enforce the Code of Conduct, up to and including ejecting from the Conference individuals who fail to comply with the policy.

# Special Events

## Plenary Sessions

Tuesday, 3 April, 09:00–10:30  
Wednesday, 4 April, 08:00–09:30  
Thursday, 5 April, 08:00–09:30  
Grand Ballroom West

This year's Biomedical Optics Congress will feature six Plenary speakers in three Plenary sessions throughout the week. For more information on the plenary presentations, see the Plenary descriptions on pages 6-8 of this program.

## Joint Poster Sessions

Tuesday, 3 April, 13:30–15:30  
Wednesday, 4 April, 13:30–15:30  
Thursday, 5 April, 13:30–15:30  
Grand Ballroom East

The Congress will feature three joint poster sessions and over 190 poster presentations over the course of three days. Each author is provided with a board on which to display their summary and results of his or her paper. Posters are an integral part of the technical program and offer a unique networking opportunity, where presenters can discuss their results one-to-one with interested parties.

## OSA Biomedical Optics Technical Groups Poster Award

OSA offers several technical groups focused on biomedical optics to provide you with a chance to connect with colleagues working in your area of specialization. As part of this congress, these technical groups are supporting an award for Best Poster Presentation for students and recent graduates. Individuals who applied to be considered for this award have the opportunity to win a monetary prize and an OSA membership. All attendees are also invited to stop by the OSA Technical Group table during this week's poster sessions to learn more about the technical groups within the OSA Biomedical Optics Technical Division.

Hosted by  Technical Groups

## Welcome Reception with Exhibitors

Tuesday, 3 April, 17:30–19:00  
Grand Ballroom East

Join your fellow attendees for the Welcome Reception. Enjoy delectable fare while networking. The reception is open to all full conference attendees. Guest tickets may be purchased for US \$75.

## Student & Early Career Professional Development & Networking Program

Wednesday, 4 April, 12:00–13:30  
Meeting Room 314

Join us for an interactive lunch and learn program focused on professional development within the Biophotonics field. This program will engage students and early career professionals with the key leaders in the field who will share their professional development journey and provide useful tips to those who attend. Lunch will be provided. There is limited space, RSVP required to attend.

Hosted by 

## Dinner Cruise on The Grand Floridian

Wednesday, 4 April, 18:00–20:00  
The Diplomat Beach Resort, Diplomat Landing, Marina Dock

Cruise the Intracoastal waterway and enjoy dinner on a spectacular luxury yacht that offers four decks, a covered sky lounge and a spacious top deck for ocean views. Conference attendees may purchase extra tickets for their guests at the OSA Registration desk. Advance ticket purchase is required.

### Cruise Schedule:

|             |   |
|-------------|---|
| 18:00–18:30 | Boarding at the Diplomat Landing, Marina Dock |
| 18:30       | Cruise Departure                              |
| 18:30–20:00 | Cruise and Dinner Buffet                      |
| 20:00       | Return to Dock                                |
| 21:00       | Final Disembark                               |

## Workshop: Understanding Unconscious Bias

Thursday, 5 April, 12:00–13:30  
Atlantic Ballroom 1

Speaker: Sara Bendoraitis, American University, USA

Research demonstrates that we all have unconscious biases. These biases can result in best and brightest talent made to feel unwelcome, invisible, and not important to the success of the organization. This training will explore concepts and engage participants to better understand implicit bias, increase awareness and understanding the impact on organizational culture and identify ways to promote greater engagement with diversity and inclusion. Program is open to OSA Members and RSVP required to attend.

Hosted by  

## Lost in Translation?: Clinical Trial Challenges Across the Globe

Friday, 6 April, 12:00–13:30  
Grand Ballroom West

The potential for biophotonics technologies to have transformative clinical impact is clear. However, taking a great idea from the bench to the clinic, and then to market is a complex path to navigate. At this lunch event you will hear from a panel of experts who have taken on this challenge in order to deliver their technologies to those who need them. In particular, we will contrast the differences in design features and deployment strategies needed for technologies targeting markets such as the US and Europe, versus technologies for global health – an area well matched to the unique benefits of biophotonics. There will be ample time for questions, discussion and networking. Lunch will be available for purchase outside the meeting room.



### INVEST IN YOUR FUTURE. JOIN OSA TODAY.

Your OSA Membership includes:

- Members-only pricing on OSA meetings and journals
- Subscriptions to OPN & *Physics Today*
- 50 downloads from OSA Publishing
- Technical group memberships

**Get started and save 20% on a one year, individual membership.\***

**Visit [osa.org/join](http://osa.org/join) and enter in discount code 2018OSAM.**

\*Promotion applies to a 1-year individual membership only and excludes those residing in economically developing nations.

ANTIGONE MARINO, Italy



# Plenary Speakers

## Joint Plenary Session I

Tuesday, 3 April, 09:00–10:30  
Grand Ballroom West



### Quanta Image Sensor: Photon counting with high resolution and high frame rate

**Eric R. Fossum**, *Thayer School of Engineering, Dartmouth University, USA*

09:00–09:45

The Quanta Image Sensor will be introduced and recent progress presented from a 1Mpixel, 1000fps, back-illuminated room temperature stacked device. The prototype device features very low dark count rate and high quantum efficiency with further improvements anticipated in the future.

**About the Speaker:** Eric R. Fossum is best known for the invention of the CMOS image sensor “camera-on-a-chip” used in billions of cameras, from smart phones to web cameras to pill cameras and many other applications. He has been a Professor with the Thayer School of Engineering since 2010. He also serves as Dartmouth’s Associate Provost for Entrepreneurship and Technology Transfer. Fossum is a Queen Elizabeth Prize Laureate, the world’s largest engineering prize, a member of the National Academy of Engineering, a National Inventors Hall of Fame inductee, and a Fellow member of the IEEE and OSA.



### Diffuse Optical Monitoring of Biomarkers in Brain and Breast

**Arjun Yodh**, *University of Pennsylvania, USA*

09:45–10:30

Yodh will describe his progress applying diffuse optical monitoring techniques to measure hemodynamics, metabolism, and autoregulation in brain and breast tissues. The brain studies demonstrate potential for usage as a bedside treatment management tool in the neuro-ICU, especially for patients with traumatic brain injury and acute stroke; the breast studies demonstrate potential of optical cancer therapy monitoring, especially for patients undergoing neoadjuvant chemotherapy prior to surgery.

**About the Speaker:** Arjun G. Yodh is the James M. Skinner Professor of Science in the Department of Physics and Astronomy at the University of Pennsylvania. At Penn, he is also Director of The Laboratory for Research on the Structure of Matter (LRSM) and its NSF-supported Materials Science and Engineering Center (MRSEC). Yodh has published over 300 papers (>32,000 citations, h-index 96) about research that spans the fields of Biomedical Optics, Condensed Matter Physics, and Atomic, Molecular & Optical Sciences. His biomedical research is oriented towards diffuse optical imaging and monitoring of brain, breast, and muscle, and towards monitoring of hemodynamic biomarkers during therapy. His group made key contributions to the development of this field starting from its earliest stages, including identification of connections between traditional and

diffuse optics, elucidation of diffuse optical resolution and contrast limits, experimental demonstration of frequency-domain diffuse optical tomography, imaging of exogenous contrast agents in human breast cancer based on both absorption contrast and fluorescence contrast, development of diffuse correlation spectroscopy for measurement of tissue blood flow, first all-optical measurements of tissue oxygen metabolism in human brain, technique validation of the optical methods in pre-clinical and clinical contexts against MRI, Xe-CT, ultrasound and other traditional techniques, and more. Yodh is a Fellow of the OSA, APS, AAAS, and AIMBE.

## Joint Plenary Session II

Wednesday, 4 April, 09:00–10:30  
Grand Ballroom West



### Talking to The Brain in Its Own Language

**Sheila Nirenberg**, *Weill Medical College of Cornell University, USA*

08:00–08:45

Neuroscience research has focused largely on listening to the brain - on taking recordings, analyzing responses, and trying to extract meaning from them. But now we’re entering a new phase where we can go beyond listening and can start talking back to the brain, and we can do it in its own language. This opens the door to new technologies for treating disease. Here we present the development of one such technology: a new kind of neuro-prosthetic for treating blindness. Briefly, it works by converting visual images into meaningful neural signals in real time and then sending the signals on to the brain using an optogenetic interface.

**About the Speaker:** Sheila Nirenberg is a professor at Cornell and the founder of two companies – one that develops new kinds of prosthetic devices, and one that develops new kinds of smart robots. Her lab at Cornell focuses on basic science, and her companies take what’s learned in the lab and use it to develop solutions to real world problems.

The prosthetics company, Bionic Sight, focuses on the development of devices for restoring sight to patients with retinal degenerative diseases. In 2017, the company entered into a collaboration agreement with Applied Genetic Technologies Corporation (NASDAQ:AGTC) and is currently preparing for its first clinical trial. The AI company, NN, focuses on computer vision applications. In 2016, NN licensed its technology to Ford Motor Company (NYSE:F) for use in Ford’s autonomous driving program, and it has recently engaged with other strategic partners on other applications.

Nirenberg has won numerous awards for her innovations, including a MacArthur “genius” Award. Her work on cracking the retina’s neural code and the implications have been featured in TED talks, BBC’s “The Genius Behind...”, Discovery Channel, Scientific American, National Geographic, Bloomberg, as well as peer-reviewed publications.



### Stain-Free Slide-Free Multiphoton Histopathology of Carcinogenesis and Cancer

**Stephen Boppart**, *University of Illinois at Urbana-Champaign, USA*

08:45–09:30

Multiphoton microscopy has emerged as a powerful tool for stain-free slide-free histopathology. We have recently demonstrated a fiber-based nonlinear optical microscope that achieves fast and simultaneous visualization of a variety of intrinsic molecular contrasts within live tissue including auto-fluorescence excited by two/three-photon processes and specially structured molecules by second/third harmonic generation. Results from human subjects with and without breast cancer, and a pre-clinical rat mammary tumor model, show that extracellular vesicles (exosomes and microvesicles) may serve as new biomarkers for breast cancer. Real-time videos also demonstrate the versatility of this imaging platform in tracking cellular events, including tumor cell migration and leukocyte activation in living rats with carcinogen-induced mammary tumors. Histopathology, whether with standard hematoxylin and eosin or special immunohistochemical stains, has been the gold-standard process for the diagnosis of disease. However, due to the intensive time and labor required for the histochemical treatment of the tissue in traditional histopathology, great efforts have been devoted to using label-free optical imaging for the examination of intact biological specimens, even *in vivo*. By shifting to a new excitation wavelength, our fiber-based multimodal nonlinear optical microscope achieves fast and simultaneous visualization of the rich intrinsic molecular information within fresh human breast tissue. In addition to the near-real-time visualization of the authentic tumor microenvironment, quantitative analysis of these multi-dimensional datasets was performed in search for more selective clinical biomarkers. Preliminary analysis conducted on fresh human breast tissue obtained from healthy and cancer subjects showed that a significant portion of extracellular vesicles from the tumor micro- and macro-environment have unique optical signatures in comparison with those from healthy subjects, opening investigations of their physiological role in carcinogenesis and their diagnostic value for cancer. Collectively, the potential exists for real-time stain-free *in vivo* histopathology, promoting imaging-based scientific research, and potentially revealing new image-based biomarkers for diseases such as cancer.

**About the Speaker:** Stephen Boppart heads the Biophotonics Imaging Laboratory at the Beckman Institute and is a full-time faculty member in the Bioimaging Science and Technology group. His home departments are Electrical and Computer Engineering and Bioengineering, with affiliations with the Department of Internal Medicine in the College of Medicine, the Micro and Nanotechnology Laboratory and the Institute for Genomic Biology. Professor Boppart received his PhD in Electrical and Medical Engineering from MIT in 1998 and his MD from Harvard Medical School in 2000. Currently he combines his optical imaging and biophotonics research and teaching with clinical research in novel medical technologies.

### Joint Plenary Session III

Thursday, 5 April, 09:00–10:30  
Grand Ballroom West



### Unraveling the Origins of Endogenous Optical Metabolic Changes

**Irene Georgakoudi**, *School of Engineering, Tufts University, USA*

08:00–08:45

The ability to monitor subcellular functional and structural changes associated with metabolism is essential for understanding tissue development and disease progression. Metabolic perturbations or dysfunctions often play a critical role in numerous diseases, including cancer, obesity, cardiovascular and neurodegenerative disorders. Established methods to assess metabolic processes are either destructive or require the use of exogenous compounds. However, such approaches are limited in their ability to capture the highly dynamic and heterogeneous nature of metabolic responses. In my plenary presentation, I will explain how a combined use of endogenous two-photon intensity and lifetime based fluorescence measurements enable ways to identify changes in specific metabolic pathways. These functional insights can improve understanding of disease development and drug effects.

**About the Speaker:** Irene Georgakoudi has been working on the use of lasers for therapeutic and diagnostic applications since her undergraduate years. She started as a physicist at Dartmouth College and continued her graduate studies in Biophysics at the University of Rochester. Her interests in spectroscopy and spectroscopic imaging using endogenous sources of contrast were founded during her postdoctoral years at the MIT Spectroscopy Lab. After working on the development of fluorescence-based *in vivo* flow cytometry while an Instructor at the Wellman Laboratories for Photomedicine at Massachusetts General Hospital/Harvard Medical School, she moved to Tufts in 2004. She is the author of several patents on the development and use of spectroscopy and imaging to characterize tissues or to detect specific populations of cells and has published numerous peer reviewed manuscripts, review articles and book chapters in these topics. She is the recipient of a Claflin Distinguished Scholar, an NSF Career, and an American Cancer Society Research Scholar award. She has served on the Board of Directors of The Optical Society, and is the Director of the Tufts Advanced Microscopic Imaging Center (TAMIC).



## Using Optical Tweezers to Probe the Role of Tissue Biophysics in Metastasis

**Kandice Tanner**, *Laboratory of Cell Biology, Center for Cancer Research, National Institutes of Health, USA*

08:45–09:30

Tumor latency and dormancy are obstacles in effective treatment of cancer. In the event of metastatic disease, emergence of a lesion can occur at varying intervals from diagnosis and in some cases following successful treatment of the primary tumor. Genetic factors that drive metastatic progression have been identified, such as those involved in cell adhesion, signaling, extravasation and metabolism. Is there a difference in strategy to facilitate outgrowth? Why is there a difference in latency? One missing cue may be the role of tissue biophysics of the brain microenvironment on the infiltrated cells. Here I discuss using optical tweezer based active microrheology to measure the mechanical cues that may influence disseminated tumor cells in different organ microenvironment. I further discuss in vitro and in vivo preclinical models such as 3D culture systems and zebrafish in efforts of providing novel targeted therapeutics.

**About the Speaker:** Kandice Tanner received her doctoral degree in Physics at the University of Illinois, Urbana-Champaign

under Professor Enrico Gratton. She completed post-doctoral training at the University of California, Irvine specializing in dynamic imaging of thick tissues. She then became a Department of Defense Breast Cancer Post-doctoral fellow jointly at University of California, Berkeley and Lawrence Berkeley National Laboratory under Dr. Mina J. Bissell. Dr. Tanner joined the National Cancer Institute as a Stadtman Tenure-Track Investigator in July, 2012, where she integrates concepts from molecular biophysics and cell biology to learn how cells and tissues sense and respond to their physical microenvironment, and to thereby design therapeutics and cellular biotechnology. For her work, she has been awarded the 2013 National Cancer Institute Director's Intramural Innovation Award, the 2015 NCI Leading Diversity award, 2016 Federal Technology Transfer Award, the 2016 Young Fluorescence Investigator award from the Biophysical Society and named as a Young Innovator in Cellular and Molecular Bioengineering, which highlight her scientific accomplishments and service to the greater intramural NIH and extramural scientific community. She also maintains strong connections with the extramural community through service as an editorial board member of Scientific Reports and as a review editor for *Frontiers in Cell and Development Biology*. She currently serves on the Membership Committee of the American Society of Cell Biology, the Minority Affairs Committee of the Biophysical Society and is a Member at large for the Division of Biological Physics of the American Physical Society.

**NEW!**  
**OSA Career Calibrator**

The Optical Society (OSA) and the OSA Foundation (OSAF) have partnered with Cheeky Scientist to launch the Career Calibrator, a new career training platform with world-class resources to support your professional development goals.

This members-only benefit provides exclusive access to:

- **PROFESSIONAL DEVELOPMENT** content for students and professionals who are job searching or looking to transition from academia to industry.
- **GUIDANCE** on building a career transition plan, improving your resume/cv, interview skills and online presence.
- **GENERAL RESOURCES** for building transferrable skills, conducting salary negotiations, navigating immigration laws and more.

For more information visit [osa.org/careercalibrator](http://osa.org/careercalibrator)

# Exhibition / Buyers' Guide

## American Elements

### Sponsor

1093 Broxton Avenue, Suite 2000  
Los Angeles, CA 90024, USA  
P: +1.310.208.0351  
Email: customerservice@americanelements.com  
URL: www.americanelements.com



American Elements is the world's manufacturer of engineered & advanced materials with a catalog of over 16,000 materials including ferro metals, ferro alloys, compounds and nanoparticles; high purity metals, chemicals, semiconductors and minerals; and crystal-grown materials for commercial & research applications including high performance steels, super alloys, automotive, aerospace, military, medical, electronic, and green/clean technologies. American Elements maintains research and laboratory facilities in the U.S. and manufacturing/warehousing in the U.S., Mexico, Europe, & China.

## Axiom Optics

### Sponsor

14 Tyler Street, 3rd Fl.  
Somerville, MA 02143, USA  
P: +1.617.401.2198  
Email: pclenceau@axiomoptics.com



## Energetiq Technology, Inc.

7 Constitution Way  
Woburn, MA 01801, USA  
P: +1.781.939.0763  
F: +1.781.939.0769  
Email: info@energetiq.com



## Hamamatsu Corporation

### Gold Sponsor

360 Foothill Road  
Bridgewater, NJ 08807, USA  
P: +1.908.231.0960  
F: +1.908.231.1539  
Email: marcom@hamamatsu.com  
URL: www.hamamatsu.com



Hamamatsu Corporation is the North American subsidiary of Hamamatsu Photonics K.K. (Japan). We will be introducing our latest instrument for whole slide imaging the S360: an addition to our renowned NanoZoomer line that has proven to be the workhorse for slide scanning in both brightfield and fluorescence applications. Our new product will continue to serve the imaging community with the robust performance and image quality it has come to expect from Hamamatsu.

## ISS, Inc.

1602 Newton Drive  
Champaign, IL 61822-1061, USA  
P: +1.217.359.8681  
F: +1.217.359.7879  
Email: ISS@ISS.com  
URL: www.ISS.com

ISS activities include two product lines: the fluorescence analytical division (spectrofluorometers for time-resolved /steady-state fluorescence measurements) and the medical division (for measurements of oxygen saturation in brain and muscle tissue, fNIRS). A variety of modular components complements the instrumentation: laser diodes, LEDs, high pressure cell and fiber optic sensors; data acquisition cards for FCS and FLIM, laser launchers, galvo-scanning mirrors and detector units. Applications include FRET, FLIM, FCS, FCCS, PCH, STED, and NIRS.

## OSA Publishing

2010 Massachusetts Ave NW  
Washington, DC 20036, USA  
P: +1.202.416.1474  
Email: custerv@osa.org  
URL: www.osapublishing.org

OSA Publishing publishes & distributes the largest collection of peer-reviewed optics and photonics content via the OSA Publishing Digital Library. Covering a variety of disciplines including physics, engineering, biomedical, telecommunications, and energy, this repository of 16 journals, 1 magazine, and hundreds of conference proceedings has the highest number of citations of any other publisher in Optics category.

## Photonics Media

100 West Street, 2nd Floor  
Pittsfield, MA 01201, USA  
P: +1.413.499.0514  
Email: info@photonics.com  
URL: www.Photonics.com

Photonics Media invites you to explore the world of light-based technology at [www.photonics.com](http://www.photonics.com) and on our FREE mobile apps. As the publisher of BioPhotonics, Photonics Spectra, Industrial Photonics, and EuroPhotonics magazines as well as the Photonics Buyers' Guide, Photonics.com, and more, we bring you the news, research and applications articles you need to succeed.



## PicoQuant Photonics North America, Inc.

9 Trinity Drive  
West Springfield, MA 01089, USA  
P: +1.413.562.6161  
F: +1.413.562.6167  
Email: [info@picoquant-usa.com](mailto:info@picoquant-usa.com)  
URL: [www.picoquant-usa.com](http://www.picoquant-usa.com)

Product lines include Pulsed Diode Lasers, Time-Correlated Single Photon Counting (TCSPC) electronics and detectors, fluorescence lifetime spectrometers, time-resolved fluorescence microscopes and upgrade kits for Laser Scanning Microscopes. Applications include Single Molecule Spectroscopy, Fluorescence Lifetime Imaging (FLIM), Fluorescence Resonance Energy Transfer (FRET), Fluorescence Correlation Spectroscopy (FCS), Optical tomography and Quantum Key Distribution.

## Semrock, a unit of IDEX Health and Science



### Silver Sponsor

3625 Buffalo Road, Suite 6  
Rochester, NY 14624 USA  
P: +1.585.594.7000  
Email: [IHSOrders@idexcorp.com](mailto:IHSOrders@idexcorp.com)  
URL: [www.semrock.com](http://www.semrock.com)

Semrock has become the standard in optical filters for the life science industry, applying patented design techniques to create some of the most spectrally sophisticated optical filters on the market. Whether you select from our extensive catalog or we design a custom filter to your exact specifications, you can be confident of our uncompromising quality, reliability, and reproducible results.



The Global Talent Hub for Optics and Photonics

# WORKinOPTICS

**YOUR SOURCE FOR THE BEST JOBS AND  
THE BEST CANDIDATES**

WORKinOPTICS.com provides a state-of-the-art platform to efficiently connect employers and job seekers within the optics and photonics community.

*Your next job opportunity or new hire is just a click away.*

- Post your resume at no charge to reach top employers.
- OSA Industry Development Associates (OIDA) Members get 20 free job postings.

Visit [www.WORKinOPTICS.com](http://www.WORKinOPTICS.com)

# CALL FOR PAPERS:

## OSA Biophotonics Congress Feature Issue in *Biomedical Optics Express*

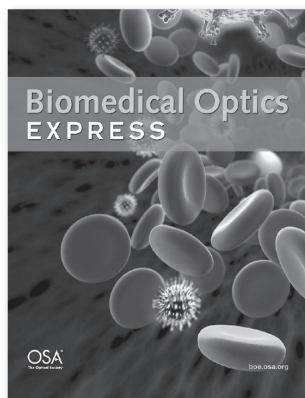
**Submission Deadline:** 15 June 2018

This Feature Issue will highlight topics from the following meetings:

- Clinical and Translational Biophotonics
- Optics and the Brain
- Optical Tomography and Spectroscopy
- Microscopy, Histopathology and Analytics

*Biomedical Optics Express* (BOEx) welcomes expanded submissions from the oral and poster presentations for the conference. While meeting participants are particularly encouraged to submit their work, this feature issue is open to all contributions pertaining to the topics above.

All papers need to present original, previously unpublished work, and will be subject to the standard peer-review process of the Journal. Standard BOEx Article Processing Charges will apply.



### FEATURE ISSUE EDITORS

**Michael Giacomelli**, *Massachusetts Institute of Technology, USA*  
Microscopy, Histopathology and Analytics

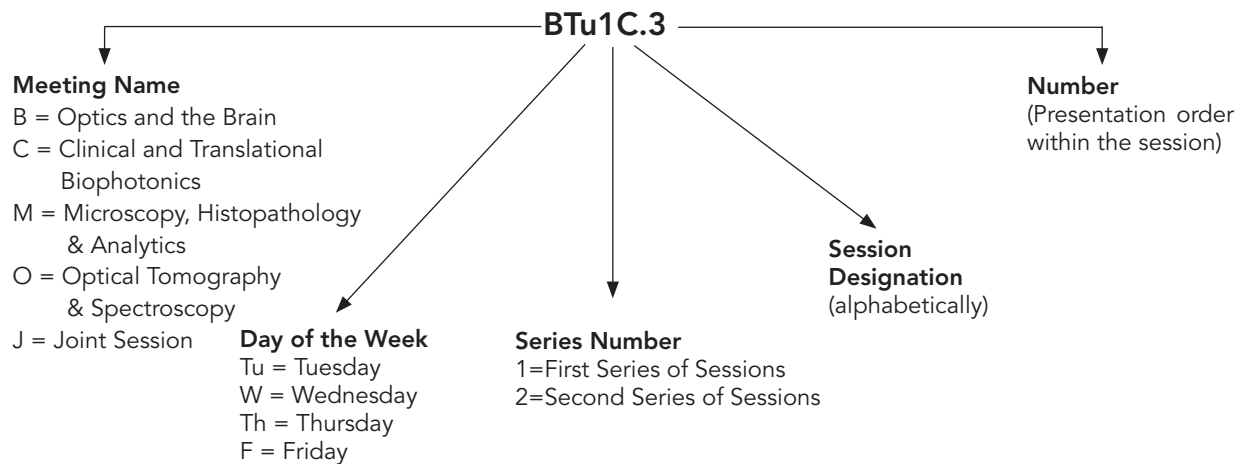
**Christine Hendon**, *Columbia University, USA*  
**Daniel Razansky**, *Helmholtz Center Munich & Technical University of Munich, Germany*  
Optical Tomography and Spectroscopy

**Spencer Smith**, *The University of North Carolina at Chapel Hill, USA*  
Optics and the Brain

**Ronald Sroka**, *Ludwig Maximilian University of Munich, Germany*  
Clinical and Translational Biophotonics

For more information, visit [osapublishing.org/boe/feature.cfm](http://osapublishing.org/boe/feature.cfm)

## Explanation of Session Codes



The first letter of the code designates the meeting (B=Brain, C=Translational, M=Microscopy, O=OT&S, J=Joint). The second element denotes the day of the week (Tu=Tuesday, W=Wednesday, Th=Thursday, F=Friday). The third element indicates the session series in that day (for instance, 1 would denote the first parallel sessions in that day). Each day begins with the letter A in the fourth element and continues alphabetically through a series of parallel sessions. The lettering then restarts with each new series. The number on the end of the code (separated from the session code with a period) signals the position of the talk within the session (first, second, third, etc.). For example, a presentation coded BTu1C.3 indicates that this paper is part of the Brain topical meeting (B) and is being presented on Tuesday (Tu) in the first series of sessions (1), and is the third parallel session (C) in that series and the third paper (3) presented in that session.

Invited papers are noted with **Invited**

Plenaries are noted with **Plenary**

# Agenda of Sessions — Monday, 2 April

|             |  |
|-------------|--|
| 08:00–18:00 | <b>NIRFAST Pre-Conference Training Workshop</b> , Meeting Room 314 (pre-registration required) |
| 08:00–18:00 | <b>MCX'18 Pre-Conference Workshop</b> , Meeting Room 307 (pre-registration required)           |
| 15:00–18:00 | <b>Registration</b> , Grand Ballroom Foyer   |

# Agenda of Sessions — Tuesday, 3 April

|             | Atlantic Ballroom 1   | Atlantic Ballroom 2   | Grand Ballroom West                                      | Atlantic Ballroom 3   |
|-------------|---|---|--|---|
|             | Microscopy  | Translational   | Brain  | OTS   |
| 07:00–17:30 | <b>Registration</b> , Grand Ballroom Foyer  |   |  |   |
| 08:50–09:00 | <b>Opening Remarks</b> , Grand Ballroom West  |   |  |   |
| 09:00–10:30 | <b>JTu1A • Joint Plenary Session I</b> , Grand Ballroom West                                    |   |  |   |
| 10:30–11:00 | <b>Coffee Break and Exhibits</b> , Grand Ballroom East<br><i>Sponsored By: <b>HAMAMATSU</b></i> |   |  |   |
| 11:00–12:30 | <b>MTu2A • Light Sheet Microscopy</b>   | <b>CTu2B • Clinical Therapeutic Guidance</b>                          | <b>BTu2C • Multiscale Connections and Networks</b>       | <b>OTu2D • Diffuse Correlation Spectroscopy, Tomography and Other Laser Speckle Methods</b>           |
| 12:30–13:30 | <b>Lunch Break</b> , On Your Own  |   |  |   |
| 13:30–15:30 | <b>JTu3A • Joint Poster Session I, Coffee Break and Exhibits</b> , Grand Ballroom East          |   |  |   |
| 15:30–17:30 | <b>MTu4A • New Microscopy Techniques</b>  | <b>CTu4B • Optical Techniques for Breast Tumor Margins Assessment</b> | <b>BTu4C • New Technologies for Human Brain Function</b> | <b>OTu4D • Raman, Fluorescence, Mie-Scattering and Other Spectroscopies for Clinical Applications</b> |
| 17:30–19:00 | <b>Welcome Reception with Exhibitors</b> , Grand Ballroom East                                  |   |  |   |

## Key to Conference Abbreviations

|               |  |
|---------------|--|
| Brain         | Optics and the Brain                     |
| Translational | Clinical and Translational Biophotonics  |
| Microscopy    | Microscopy, Histopathology and Analytics |
| OTS           | Optical Tomography and Spectroscopy      |

# Agenda of Sessions — Wednesday, 4 April

|             | Atlantic Ballroom 1   | Atlantic Ballroom 2  | Grand Ballroom West  | Atlantic Ballroom 3   |
|-------------|---|--|--|---|
|             | Microscopy  | Translational  | Brain/OTS  | OTS   |
| 07:30–17:30 | <b>Registration, Grand Ballroom Foyer</b>   |  |  |   |
| 08:00–09:30 | <b>JW1A • Joint Plenary Session II, Grand Ballroom West</b>   |  |  |   |
| 09:30–10:00 | <b>Coffee Break and Exhibits, Grand Ballroom East</b>   |  |  |   |
| 10:00–12:00 | <b>MW2A • Biosensing and Bioimaging</b>   | <b>CW2B • Hemodynamics of the Brain</b>  | <b>BW2C • Rethink the Scan</b>   | <b>OW2D • Diffuse Correlation Spectroscopy: Blood Flow Measurements</b> |
| 12:00–13:30 | <b>Lunch Break, On Your Own</b>   |  |  |   |
| 12:00–13:30 | <b>Student &amp; Early Career Professional Development &amp; Networking Lunch and Learn, Meeting Room 314</b><br><i>(OSA Members Only; RSVP required)</i> |  |  |   |
| 13:30–15:30 | <b>JW3A • Joint Poster Session II, Coffee Break and Exhibits, Grand Ballroom East</b>   |  |  |   |
| 15:30–17:30 | <b>MW4A • Confocal and Multimodal Microscopy</b>  | <b>CW4B • Techniques for Cardiovascular and Peripheral Vascular Disease Assessment</b> | <b>OW4C • Technologies for Non-Invasive Optical in Vivo Brain Imaging and Monitoring</b> | <b>OW4D • Photoacoustic Tomography, Microscopy and Endoscopy</b>        |
| 18:00–21:00 | <b>Dinner Cruise Event, Diplomat Beach Resort, Diplomat Landing, Marina Dock</b><br><i>(Advance Ticket Purchase Required)</i>                             |  |  |   |

## Key to Conference Abbreviations

|               |  |
|---------------|--|
| Brain         | Optics and the Brain                     |
| Translational | Clinical and Translational Biophotonics  |
| Microscopy    | Microscopy, Histopathology and Analytics |
| OTS           | Optical Tomography and Spectroscopy      |

# Agenda of Sessions — Thursday, 5 April

|             | Atlantic Ballroom 1  | Atlantic Ballroom 2  | Grand Ballroom West                          | Atlantic Ballroom 3   |
|-------------|--|--|--|---|
|             | Microscopy   | Translational  | Brain  | OTS   |
| 07:30–17:30 | <b>Registration, Grand Ballroom Foyer</b>  |  |  |   |
| 08:00–09:30 | <b>JTh1A • Joint Plenary Session III, Grand Ballroom West</b>  |  |  |   |
| 09:30–10:00 | <b>Coffee Break and Exhibits, Grand Ballroom East</b>  |  |  |   |
| 10:00–12:00 | <b>MTh2A • Computational Microscopy and Analysis</b>   | <b>CTh2B • Clinical Spectroscopy</b>                       | <b>BTh2C • Brain Disorders: Mouse to Man</b> | <b>OTh2D • Optical Coherence Tomography: Novel Applications</b>                         |
| 12:00–13:30 | <b>Lunch Break, On Your Own</b>  |  |  |   |
| 12:00–13:30 | <b>Workshop: Understanding Unconscious Bias, Atlantic Ballroom 1 (OSA Members Only; RSVP required)</b> |  |  |   |
| 13:30–15:30 | <b>JTh3A • Poster Session III, Coffee Break and Exhibits, Grand Ballroom East</b>                      |  |  |   |
| 15:30–17:30 | <b>MTh4A • Challenges in Clinical Translation</b>  | <b>CTh4B • Optical Techniques for Diseases Diagnostics</b> | <b>BTh4C • Using the Tools</b>               | <b>OTh4D • Tomographic and Spectroscopy Methods for Non-Invasive Imaging of Disease</b> |
| 17:30–18:30 | <b>Postdeadline Papers Session, Atlantic Ballroom 1</b>  |  |  |   |

## Key to Conference Abbreviations

|               |  |
|---------------|--|
| Brain         | Optics and the Brain                     |
| Translational | Clinical and Translational Biophotonics  |
| Microscopy    | Microscopy, Histopathology and Analytics |
| OTS           | Optical Tomography and Spectroscopy      |

# Agenda of Sessions — Friday, 6 April

|             | Atlantic Ballroom 1  | Atlantic Ballroom 2                    | Grand Ballroom West                             | Atlantic Ballroom 3  |
|-------------|--|--|---|--|
|             | Microscopy   | Translational                          | Brain   | OTS  |
| 07:30–16:00 | <b>Registration, Grand Ballroom Foyer</b>  |  |   |  |
| 08:00–09:30 | <b>MF1A • Digital Pathology</b>  | <b>CF1B • Optical Spectroscopy I</b>   | <b>BF1C • Gizmos and Gadgets</b>                | <b>OF1D • Acousto-Optics and Ultrasound-Assisted Optical Tomography</b>    |
| 09:30–10:00 | <b>Coffee Break and Exhibits, Grand Ballroom East</b>  |  |   |  |
| 10:00–12:00 | <b>MF2A • Nonlinear Microscopy</b>   | <b>CF2B • Optical Spectroscopy II</b>  | <b>BF2C • Cerebral Blood Flow in Humans</b>     | <b>OF2D • Devices and Algorithms for Optical Imaging</b>                   |
| 12:00–13:30 | <b>Lunch Break, On Your Own</b>  |  |   |  |
| 12:00–13:30 | <b>Lost in Translation?: Clinical Trial Challenges Across the Globe, Grand Ballroom West</b><br><i>(Lunch will be available for purchase outside the meeting room)</i> |  |   |  |
| 13:30–15:30 | <b>MF3A • Cellular Diagnostics</b>   | <b>CF3B • Optical Spectroscopy III</b> | <b>BF3C • Looking Deeper</b>                    | <b>OF3D • Optical Coherence Tomography: Novel Techniques</b>               |
| 15:30–16:00 | <b>Coffee Break and Exhibits, Grand Ballroom East</b>  |  |   |  |
| 16:00–18:00 | <b>MF4A • Clinical Imaging</b>   | <b>CF4B • OCT and Microscopy</b>       | <b>BF4C • Microscopy, Structure and Anatomy</b> | <b>OF4D • Novel Developments for Clinical and Preclinical Applications</b> |

## Key to Conference Abbreviations

|               |  |
|---------------|--|
| Brain         | Optics and the Brain                     |
| Translational | Clinical and Translational Biophotonics  |
| Microscopy    | Microscopy, Histopathology and Analytics |
| OTS           | Optical Tomography and Spectroscopy      |



REDEFINED

Optimized flexibility, speed and image quality for any scanning need.



Introducing the  
NanoZoomer S360

**HAMAMATSU**  
PHOTON IS OUR BUSINESS

## Grand Ballroom West

08:50–09:00  
Opening Remarks

09:00–10:30  
JTU1A • Joint Plenary Session I

JTu1A.1 • 09:00 **Plenary**

**Quanta Image Sensor: Photon Counting with High Resolution and High Frame Rate**, Eric Fossum<sup>1</sup>; <sup>1</sup>Dartmouth Univ., USA. The Quanta Image Sensor will be introduced and recent progress presented from a 1Mpixel, 1000fps, back-illuminated room temperature stacked device. The prototype device features very low dark count rate and high quantum efficiency with further improvements anticipated in the future.

JTu1A.2 • 09:45 **Plenary**

**Diffuse Optical Monitoring of Biomarkers in Brain and Breast**, Arjun G. Yodh<sup>1</sup>; <sup>1</sup>Univ. of Pennsylvania, USA. I will describe our progress applying diffuse optical monitoring techniques to measure hemodynamics, metabolism, and autoregulation in brain and breast tissues. The brain studies demonstrate potential for usage as a bedside treatment management tool in the neuro-ICU, especially for patients with traumatic brain injury and acute stroke; the breast studies demonstrate potential of optical cancer therapy monitoring, especially for patients undergoing neoadjuvant chemotherapy prior to surgery.

10:30–11:00 Coffee Break and Exhibits, Grand Ballroom East Sponsored By: **HAMAMATSU**

## Atlantic Ballroom 1

Microscopy, Histopathology  
and Analytics

11:00–12:00  
MTu2A • Light Sheet  
Microscopy  
Presider: Richard Levenson, Univ.  
of California Davis, USA

MTu2A.1 • 11:00 **Invited**  
**Quantitative Imaging in 3D Microenvironments Using Advanced Light-Sheet Microscopes**, Reto P. Fiolka<sup>1</sup>; <sup>1</sup>UT Southwestern, USA. To study subcellular dynamics and architecture in 3D requires isotropic resolution, rapid volumetric acquisition and improved optical penetration depth. Here we present microscopes that are optimized for 3D imaging in artificial microenvironments and model organisms.

## Atlantic Ballroom 2

Clinical and Translational  
Biophotonics

11:00–12:30  
CTu2B • Clinical Therapeutic  
Guidance  
Presider: Stefan Andersson  
Engels, Tyndall National Inst.,  
Ireland; Imperial College  
London, UK

CTu2B.1 • 11:00 **Invited**  
**Optics in Radiation Therapy**, Brian W. Pogue<sup>1</sup>; <sup>1</sup>Engineering Science, Dartmouth, USA. Optical tools are widely used in radiotherapy from simple localization to body position mapping. New quantitative optical tools are used for dose mapping including scintillation and Cherenkov measurement.

## Grand Ballroom West

Optics and the Brain

11:00–12:30  
BTu2C • Multiscale Connections  
and Networks  
Presider: Stephane Dieudonné,  
Ecole Normale Supérieure, France

BTu2C.1 • 11:00  
**Fast 3D Imaging and Re-Activation of Neuronal Networks, Dendrites, and Spines in Several Cubic Millimeter Volumes During Visual Learning to Understand Visual Representation**, Balazs Rozsa<sup>1</sup>; <sup>1</sup>Inst Exp Medicine, Hungarian Acad Sci, Hungary. We recorded neuronal networks, dendrites, and spines in several cubic millimeter volumes using novel methods such as multi-cube scanning. We found that, in contrast to previous theories, orientation tuning can change following visual learning.

BTu2C.2 • 11:15  
**Two-Photon Imaging and Manipulation of Neural Networks with High Spatial Resolution and Minimal Crosstalk**, Angelo Forlì<sup>1</sup>, Dania Vecchia<sup>1</sup>, Noemi Binini<sup>1</sup>, Serena Bovetti<sup>1</sup>, Claudio Moretti<sup>1</sup>, Mathias Mahn<sup>2</sup>, Christopher Baker<sup>3</sup>, McLean Bolton<sup>3</sup>, Ofer Yizhar<sup>2</sup>, Tommaso Fellin<sup>1</sup>; <sup>1</sup>Dept. of Neuroscience and Brain Technologies, Istituto Italiano di Tecnologia, Italy; <sup>2</sup>Dept. of Neurobiology, Weizmann Inst. of Science, Israel; <sup>3</sup>Max Planck Florida Inst. for Neuroscience, USA. We combined two-photon holographic stimulation of blue light-sensitive opsins with two-photon imaging of red-shifted fluorescence indicators in the intact mouse neocortex to perform cellular-resolution control of neural excitability with minimal crosstalk between imaging and stimulation.

## Atlantic Ballroom 3

Optical Tomography and  
Spectroscopy

11:00–12:30  
OTu2D • Diffuse Correlation  
Spectroscopy, Tomography and  
Other Laser Speckle Methods  
Presider: Wesley Baker, Univ. of  
Pennsylvania, USA

OTu2D.1 • 11:00  
**Effects of Temporal Gating in Time Domain Diffuse Correlation Spectroscopy for Real Systems**, Lorenzo Colombo<sup>1,2</sup>, Marco Pagliazzi<sup>1</sup>, Sanathana Konugolu Venkata Sekar<sup>2</sup>, Davide Contini<sup>2</sup>, Alberto Dalla Mora<sup>2</sup>, Alessandro Torricelli<sup>2</sup>, Antonio Pifferi<sup>2,3</sup>, Turgut Durdurani<sup>1,4</sup>; <sup>1</sup>ICFO, Spain; <sup>2</sup>Politecnico di Milano, Italy; <sup>3</sup>IFN-CNR, Italy; <sup>4</sup>ICREA, Spain. We propose a model for time domain diffuse correlation spectroscopy which describes the effects of temporal gating for real systems, enabling accurate depth-resolved blood flow measurements. The model is validated with simulations and experiments.

OTu2D.2 • 11:15  
**Correlation Gating Quantifies Optical Properties of Dynamic Media in Transmission Mode**, Dawid M. Borycki<sup>2,1</sup>, Oybek Kholiqov<sup>2</sup>, Vivek J. Srinivasan<sup>2,3</sup>; <sup>1</sup>Polish Academy of Sciences, Poland; <sup>2</sup>Dept. of Biomedical Engineering, Univ. of California Davis, USA; <sup>3</sup>Dept. of Ophthalmology and Vision Science, Univ. of California Davis, USA. We apply correlation gating with interferometric near-infrared spectroscopy (iNIRS) to separate ballistic and scattered light transmitted through thick samples. By analyzing each component, we determine optical properties of a dynamic medium from one measurement set.

Atlantic Ballroom 1

Microscopy, Histopathology and Analytics

MTu2A • Light Sheet Microscopy—Continued

MTu2A.4 • 11:30 **Invited**  
**Pathology-Optimized Open-top Light-sheet Microscopy**, Adam Glaser<sup>1</sup>, Jonathan T. Liu<sup>1</sup>; <sup>1</sup>Univ. of Washington, USA. We present the design of a pathology-optimized open-top light-sheet microscope for imaging fluorescently-labeled tissues. Initial imaging results from a variety of tissue types will be presented.

Atlantic Ballroom 2

Clinical and Translational Biophotonics

CTu2B • Clinical Therapeutic Guidance—Continued

CTu2B.2 • 11:30 **Invited**  
**The Current Role of Optical Technologies in Managing Patients with Barrett's Esophagus**, Norman S. Nishioka<sup>1</sup>; <sup>1</sup>Harvard Medical School, USA. During the past 15 years numerous optical technologies have been used as potential enhancements to the endoscopic management of Barrett's esophagus but despite these efforts, screening and surveillance of Barrett's esophagus remains imperfect. In this presentation, the clinical challenges presented by Barrett's esophagus and potential solutions will be described.

CTu2B.3 • 12:00  
**Head and Neck Cancer Evaluation via Transoral Robotic Surgery with Augmented Fluorescence Lifetime Imaging**, Jennifer Phipps<sup>1</sup>, Jakob Unger<sup>1</sup>, Regina Gandour-Edwards<sup>2</sup>, Michael G. Moore<sup>3</sup>, Arnaud Bewley<sup>3</sup>, D. Gregory Farwell<sup>1</sup>, Laura. Marcu<sup>1</sup>; <sup>1</sup>Dept. of Biomedical Engineering, Univ. of California Davis, USA; <sup>2</sup>Dept. of Pathology, Univ. of California Davis Medical Center, USA; <sup>3</sup>Dept. of Otolaryngology, Univ. of California Davis Medical Center, USA. Fluorescence lifetime imaging (FLIm) was integrated with a da Vinci Surgical System (Intuitive Surgical, Inc.) for exploration of head and neck cancer (N=25 patients). *In vivo* results showed FLIm distinguished between tumor and healthy tissue.

CTu2B.4 • 12:15  
**Noninvasive Autofluorescence Imaging for Tracking and Monitoring the Progression of Oral Premalignant Lesions**, Katelin D. Cherry<sup>1</sup>, Richard Schwarz<sup>1</sup>, Eric Yang<sup>1</sup>, Hawraa Badaoui<sup>2</sup>, Michelle Williams<sup>3</sup>, Nadarajah Vigneswaran<sup>2</sup>, Ann Gillenwater<sup>3</sup>, Rebecca Richards-Kortum<sup>1</sup>; <sup>1</sup>Rice Univ., USA; <sup>2</sup>Diagnostic and Biomedical Sciences, Univ. of Texas School of Dentistry, USA; <sup>3</sup>Univ. of Texas M.D. Anderson Cancer Center, USA. Preliminary results are presented from a longitudinal study in which autofluorescence imaging is used to monitor progression of oral premalignant lesions of patients that were tracked over six years.

Grand Ballroom West

Optics and the Brain

BTu2C • Multiscale Connections and Networks—Continued

BTu2C.3 • 11:30  
**Spatially and Temporally Precise Optical Probing of Neural Activity Readout**, Gilad M. Lerman<sup>1</sup>, Jonathan V. Gill<sup>1</sup>, Dmitry Rinberg<sup>1</sup>, Shy Shoham<sup>1,2</sup>; <sup>1</sup>New York Univ. School of Medicine, USA; <sup>2</sup>Technion - Israel Inst. of Technology, Israel. We developed an all-optical multiphoton system for efficient, high rate (>100 fps) simultaneous stimulation and imaging system and integrated it with a behavioral setup, to dissect activity codes that guide behavior in the olfactory system.

BTu2C.4 • 11:45  
**Using Connectivity to Infer Behavior from Cortical Activity Recorded through Widefield Transcranial Imaging**, shiva salsabilian<sup>1</sup>, Christian R. Lee<sup>1</sup>, David J. Margolis<sup>1</sup>, Laleh Najafizadeh<sup>1</sup>; <sup>1</sup>Rutgers Univ., USA. We present a method utilizing functional connectivity to infer behavior from calcium signals of excitatory neurons that are recorded through widefield imaging in GCaMP6 reporter mice.

BTu2C.5 • 12:00  
**Mesoscale Imaging of Cortical Dynamics During Motor Skill Learning**, Eros Quarta<sup>1</sup>, Anna L. Allegra Mascaro<sup>1,2</sup>, Jessica Lucchesi<sup>1</sup>, Costanza Campaioli<sup>1</sup>, Leonardo Sacconi<sup>1,3</sup>, Francesco Saverio Pavone<sup>1,3</sup>; <sup>1</sup>LENS - Univ. of Florence, Italy; <sup>2</sup>Inst. of Neuroscience, National Research Council, Italy; <sup>3</sup>National Inst. of Optics, National Research Council, Italy. In this work, to shed light on the neural correlates of motor control, we analyze mesoscale cortical activity - via fluorescence imaging - and kinematics of paw movement obtained from mice during motor skill learning.

BTu2C.6 • 12:15  
**Optical Imaging of Functional Connectivity Across Development in the Mouse Cortex**, Rachel M. Rahn<sup>1,2</sup>, Annie R. Bice<sup>1</sup>, Lindsey M. Brier<sup>1</sup>, Joseph D. Dougherty<sup>2,3</sup>, Joseph P. Culver<sup>1,4</sup>; <sup>1</sup>Radiology, Washington Univ., USA; <sup>2</sup>Genetics, Washington Univ., USA; <sup>3</sup>Psychiatry, Washington Univ., USA; <sup>4</sup>Physics, Washington Univ., USA. Imaging functional networks during healthy development is essential to studies of disease in mouse models. Here we report the feasibility of imaging calcium dynamics across five developmental timepoints in a GCaMP6 transgenic mouse during wakefulness.

Atlantic Ballroom 3

Optical Tomography and Spectroscopy

OTu2D • Diffuse Correlation Spectroscopy, Tomography and Other Laser Speckle Methods—Continued

OTu2D.3 • 11:30  
**Time-resolved Diffuse Correlation Spectroscopy based on Commercial Laser Module**, Saeed Samaei<sup>1</sup>, Piotr Sawosz<sup>1</sup>, Anna Gerega<sup>1</sup>, Adam Liebert<sup>1</sup>; <sup>1</sup>Nalecz Inst. of Biocybernetics and Biomedical Engineering, Polish Academy of Sciences, Poland. Time-resolved diffuse correlation spectroscopy makes the potential to measure blood flow at different tissue layers. We developed an instrument based on a commercial laser module, and validated its sensitivity to particle movements at different depths.

OTu2D.4 • 11:45  
**An In-expensive Diffuse Correlation Spectroscopy System using Low Frame Rate Camera**, Murali K<sup>1</sup>, Nandakumaran A K<sup>2</sup>, Turgut Durduran<sup>3</sup>, Hari Varma<sup>1</sup>; <sup>1</sup>Indian Inst. of Technology, Bombay, India; <sup>2</sup>Indian Inst. of Science, India; <sup>3</sup>Inst. of Photonic Sciences, Spain. A novel method based on multi-step Volterra Integral Equation (MVIM) is presented to achieve an in-expensive diffuse correlation spectroscopy system using low frame rate camera. MVIM utilizes multi-exposure-speckle contrast data to recover field autocorrelation function.

OTu2D.5 • 12:00  
**A Recipe for Near Infrared Spectroscopy and Diffuse Correlation Spectroscopy Phantoms with Tunable Optical and Dynamic Properties**, Lorenzo Cortese<sup>1</sup>, Giuseppe Lo Presti<sup>1</sup>, Marco Pagliazzi<sup>1</sup>, Davide Contini<sup>2</sup>, Alberto Dalla Mora<sup>2</sup>, Antonio Pifferi<sup>2</sup>, Sanathana Konugolu Venkata Sekar<sup>2</sup>, Lorenzo Spinelli<sup>3</sup>, Paola Taroni<sup>2,3</sup>, Marta Zanoletti<sup>2</sup>, Udo M. Weigel<sup>4</sup>, Turgut Durduran<sup>1,5</sup>; <sup>1</sup>ICFO-Institut de Ciències Fotòniques, Spain; <sup>2</sup>Dipartimento di Fisica, Politecnico di Milano, Italy; <sup>3</sup>Istituto di Fotonica e Nanotecnologie, Consiglio Nazionale delle Ricerche, Italy; <sup>4</sup>HemoPhotonics S.L., Spain; <sup>5</sup>Institució Catalana de Recerca i Estudis Avançats (ICREA), Spain. We present a recipe of combined liquid phantoms for diffuse correlation spectroscopy and near-infrared spectroscopy with well-defined and easily tunable optical and dynamic properties.

OTu2D.6 • 12:15  
**High-density Speckle Contrast optical Tomography of Brain Activity**, Ernesto Vidal<sup>1</sup>, Tanja Dragojević<sup>1</sup>, Joseph Hollman<sup>1</sup>, Joseph P. Culver<sup>2</sup>, Carles Justicia<sup>3</sup>, Turgut Durduran<sup>1</sup>; <sup>1</sup>ICFO, Spain; <sup>2</sup>Dept. of Radiology, Washington Univ. School of Medicine, USA; <sup>3</sup>Neuroscience, Univ. of Barcelona, Spain. A new method for the tomographic monitoring of cerebral blood flow changes is presented. The method is based on speckle contrast optical tomography (SCOT) to recover 3D brain activation changes due to forepaw stimulation.

12:30–13:30 Lunch Break, On Your Own

13:30–15:30

## JTU3A • Joint Poster Session I, Coffee Break and Exhibits

**JTu3A.1**  
Withdrawn.

**JTu3A.2**  
**Fluorescence Image Contrast Improvement by a Time-domain Method**, Goro Nishimura<sup>1</sup>; <sup>1</sup>Hokkaido Univ., Japan. We have demonstrated a time gate method to enhance the contrast of fluorescence image from an indocyanine green target embedded in a tissue-simulating phantom and discussed the applicability in real time clinical applications.

**JTu3A.3**  
**A Six-channel Multispectral Imager for Simultaneous In Vivo Imaging of Multiple Near-Infrared Fluorescent Markers**, N Misael Garcia<sup>1,2</sup>, Tyler Davis<sup>3</sup>, Kevin Kauffman<sup>3,2</sup>, Radoslav Marinov<sup>1,4</sup>, Viktor Grujev<sup>2,5</sup>; <sup>1</sup>Computer Science and Engineering, Washington Univ. in St. Louis, USA; <sup>2</sup>Electrical and Computer Engineering, Univ. of Illinois Urbana Champaign, USA; <sup>3</sup>Biomedical Engineering, Univ. of Michigan, USA; <sup>4</sup>Inst. of Materials Science and Engineering, Washington Univ. in St. Louis, USA; <sup>5</sup>Beckman Inst. for Advanced Science and Technology, Univ. of Illinois Urbana Champaign, USA. We have created a six-channel multispectral imager for the simultaneous space- and time-detection of color and multiple near-infrared fluorescent molecular markers by integrating the vertically stacked photodetector technology with pixelated spectral interference filters.

**JTu3A.4 • 13:30**  
**Optimization and Validation of BODIPY for Quantification of Steatosis in Donor Transplant Livers**, Carly Askinas<sup>1</sup>, Katherine N. Elfer<sup>1</sup>, David Tulman<sup>1</sup>, Sam J. Luethy<sup>1</sup>, Gretchen Galliano<sup>2</sup>, Ari Cohen<sup>2</sup>, J. Quincy Brown<sup>1</sup>; <sup>1</sup>Tulane Univ., USA; <sup>2</sup>Ochsner Health System, USA. The use of BODIPY, a lipid-specific dye, allows for identification and possible quantification of hepatic steatosis using fluorescence histology. This method could provide rapid quality assessment to safely expand the liver transplantation donor pool.

**JTu3A.5**  
**Multimodal Fast Optical-Electrical Imaging of Interictal Epileptic Spikes**, Mahdi Mahmoudzadeh<sup>1</sup>, Mana Manoochehri<sup>1</sup>, Emilie Bourel<sup>1</sup>, Fabrice Wallois<sup>1</sup>; <sup>1</sup>Medicine, Univ. of Picardie, INSERM U1105, France. Using multimodal-multiscale analysis of Fast Optical, ECoG and HD-EEG data, we demonstrated complex changes in the dynamics of cortical networks at synaptic and non-synaptic level surrounding the interictal epileptic spike (IES).

**JTu3A.6**  
**Calibration of Low Cost, Portable Mueller Matrix Polarimeter**, Mariacarla Gonzalez<sup>1</sup>, Karla Montejo<sup>1</sup>, Karl Krupp<sup>1</sup>, Vijaya Srinivas<sup>2</sup>, Edward DeHoog<sup>3</sup>, Joseph Chue-Sang<sup>1</sup>, Nicole Sevilla<sup>1</sup>, Purnima Madhivanan<sup>1</sup>, Jessica Ramella-Roman<sup>1</sup>; <sup>1</sup>Florida International Univ., USA; <sup>2</sup>Public Health Research Inst. of India, India; <sup>3</sup>Optical Engineering & Analysis LLC, USA. A low-cost, portable Mueller Matrix polarimeter is proposed for diagnosis of cervical cancer in low resource settings. Calibration is conducted with two different methods. Errors associated with this instrument and calibration method are evaluated.

**JTu3A.7**  
**Tissue Oxygenation Changes in Venous Leg Ulcers**, Rebecca J. Kwasinski<sup>1</sup>, Cristianne M. Fernandez<sup>1</sup>, Kevin Leiva<sup>1</sup>, Richard Schutzman<sup>1</sup>, Edwin Robledo<sup>1</sup>, Penelope Kallis<sup>2</sup>, Luis Borda<sup>2</sup>, Francisco Perez-Clavijo<sup>3</sup>, Robert Kirsner<sup>2</sup>, Anuradha Godavarty<sup>1</sup>; <sup>1</sup>Florida International Univ., USA; <sup>2</sup>Univ. of Miami, USA; <sup>3</sup>Podiatry Care Partners, USA. A non-contact near-infrared optical scanner (NIROS) was used to obtain 2D tissue oxygenation maps of venous leg ulcers across weeks of treatment. The oxygenation differences between wound and background were similar as wounds began healing.

**JTu3A.8**  
**Spatial Regularisation based Reconstruction of Quantitative Fluorescence Imaging**, Yijing Xie<sup>1</sup>, Michael Ebner<sup>1</sup>, Victoria Wykes<sup>1</sup>, Anna Miserocchi<sup>1</sup>, Andrew McEvoy<sup>1</sup>, Sebastien Ourselin<sup>1</sup>, Tom Vercauteren<sup>1</sup>; <sup>1</sup>Univ. College London, UK. In 5-ALA-PpIX guided brain tumour resection, PpIX fluoresces in cancerous tissue, thus, allowing for improved tumour delineation compared with white-light guided resection. We propose and evaluate spatial regularisation based reconstruction methods toward accurate quantitative fluorescence imaging.

**JTu3A.9**  
**Threshold Value Based Photodynamic Therapy Treatment Planning Using Full Monte**, Abdul-Amir Yassine<sup>2</sup>, William Kingsford<sup>2</sup>, Jeffrey Cassidy<sup>2</sup>, Vaughn Betz<sup>2</sup>, Lothar Lilge<sup>1</sup>; <sup>1</sup>Univ. Health Network, Canada; <sup>2</sup>Electrical and Computer Engineering, Univ. of Toronto, Canada. Treatment planning for high efficacy therapy must be based on the photodynamic dose delivered and the intrinsic sensitivity of the target and host tissues. A Monte Carlo approach utilizing the Photodynamic Threshold model is presented

**JTu3A.10**  
**Fractal Dimension-based Similarity Evaluation Between Retinal Vessel Segmentation Images**, Marco Antonio Escobar Acevedo<sup>3</sup>, Jose Guzman-Sepulveda<sup>1</sup>, Rafael Guzmán-Cabrera<sup>2</sup>; <sup>1</sup>The College of Optics and Photonics, Univ. of Central Florida, USA; <sup>2</sup>Departamento de Ingeniería Eléctrica, Universidad de Guanajuato, Mexico; <sup>3</sup>Universidad de La Salle Bajío, Mexico. A method that includes the fractal dimension to assess the similarity between retinal vessel segmentation images is presented.

**JTu3A.11**  
**In Vivo Retinal Imaging of Neuroinflammation in a Mouse Model of Traumatic Brain Injury**, Olga V. Minaeva<sup>2,1</sup>, James D. Akula<sup>3,4</sup>, Mark W. Wojnarowicz<sup>2</sup>, R. D. Ferguson<sup>5</sup>, Mircea Mujat<sup>2</sup>, Erich S. Franz<sup>2,1</sup>, Andrew M. Fisher<sup>2,1</sup>, Juliet A. Moncaster<sup>2</sup>, Bertrand R. Huber<sup>2,6</sup>, Lee E. Goldstein<sup>2,1</sup>; <sup>1</sup>College of Engineering, Boston Univ., USA; <sup>2</sup>Boston Univ. School of Medicine, USA; <sup>3</sup>Ophthalmology, Boston Children's Hospital, USA; <sup>4</sup>Ophthalmology, Harvard Medical School, USA; <sup>5</sup>Biomedical Optics, Physical Sciences, Inc, USA; <sup>6</sup>VA Boston Healthcare System, USA. Head trauma is a potent stimulus for brain inflammation. We demonstrate that *in vivo* retinal imaging may be useful for noninvasive diagnosis, prognosis, and monitoring of neuroinflammation following traumatic brain injury.

**JTu3A.12**  
**Ho:YAG-Laser Induced Lithotripsy – in-vitro Investigation on Fragmentation, Dusting and Fluorescence**, Ronald Sroka<sup>2,1</sup>, Thomas Pongratz<sup>2,1</sup>, Stephan Ströbl<sup>2</sup>, Frank Strittmatter<sup>1</sup>, Max Eisel<sup>2,1</sup>; <sup>1</sup>Dept of Urology Ludwig-Maximilians-Universität München, Germany; <sup>2</sup>Laser-Forschungslabor LIFE-Center, Germany. Ho:YAG-laser induced phantom stone destruction results in dusting / fragmentation ratios depending on the laser parameter used. The impact of detection of urinary stone fluorescence during endoscopic laser lithotripsy are investigated and discussed.

**JTu3A.13**  
**A Methodology to Investigate the Relationship Between Cancer Cells cell-cycle Phase and Their Migratory Behaviors**, Kamyar Esmaeili Pourfarhangi<sup>1</sup>, Battuya Bayarmagnai<sup>1</sup>, Andrew Cohen<sup>3</sup>, Bojana Gligorijevic<sup>1,2</sup>; <sup>1</sup>Bioengineering Dept., Temple Univ., USA; <sup>2</sup>Cancer Biology Program, Fox Chase Cancer Center, USA; <sup>3</sup>Electrical and computer engineering, Drexel Univ., USA. We present a methodology integrating live-cell fluorescent microscopy, cell labeling, PDMS fabricated micro-channels (2D) and tumor spheroids (3D), and automated cell tracking in order to investigate cell-cycle phase dependency in invasive behaviors of cancer cells.

**JTu3A.14**  
**Characterization of Collagen Structure by SHG in Tumor Models In-vitro**, Varvara Dudenkova<sup>1,2</sup>, Irina Druzkhova<sup>1</sup>, Maria Lukina<sup>1,2</sup>, Marina Shirmanova<sup>1</sup>, Elena Zagaynova<sup>1</sup>; <sup>1</sup>NIIBMT, Nizhny Novgorod State Medical Academy, Russia; <sup>2</sup>Univ. of Nizhny Novgorod, Russia. The parameters of the mean intensity, coherency and energy were applied for complex quantitative analysis of SHG collagen signal. Dynamics investigation of collagen structure was performed during the interaction of fibroblasts and colon cancer cells.

**JTu3A.15**  
Withdrawn.

**JTu3A.16**  
**Solving the Refractive Index – Thickness Ambiguity in Quantitative Phase Imaging of Primary Neurons in Culture with a Low-Cost Custom-Made 3D-Printed Perfusion Chamber**, Erik Bélanger<sup>1</sup>, Sébastien A. Lévesque<sup>1</sup>, Émile Rioux-Pellerin<sup>1</sup>, Jean-Michel Mugnes<sup>1</sup>, Valérie Watters<sup>1</sup>, Vincent Roy<sup>1</sup>, Alyson Bernatchez<sup>1</sup>, Gabriel Ancill<sup>1</sup>, Pierre Marquet<sup>1</sup>; <sup>1</sup>CRISMQ, Canada. We developed a low-cost custom-made 3D-printed perfusion chamber to solve the refractive index – thickness ambiguity for quantitative phase imaging of primary neurons in culture. We also show successful decoupling experiments during hypo-osmotic and hyper-osmotic challenges.

**JTu3A.17**  
**Programmable Illumination for Multimodal Microscopy Using an Electric Paper (ePaper) display**, Jing Wang<sup>1</sup>, Eric Gerald<sup>2</sup>, Ryan McGorty<sup>1</sup>; <sup>1</sup>Dept. of Physics and Biophysics, Univ. of San Diego, USA; <sup>2</sup>Dept. of Psychological Sciences, Univ. of San Diego, USA. We present a highly-flexible, cost-effective multimodal microscope using a programmable electric paper display. We demonstrate its ability to acquire dark-field and phase contrast images. The display can be used with either incoherent or laser illumination.

**JTu3A.18**  
Withdrawn.

**JTu3A.19**  
Withdrawn.

**JTu3A.20**  
**Compact, Low Power Consumption and Low cost Multi-exposure Speckle Contrast Optical Spectroscopy (SCOS) device for Real-time Measurement of Deep Tissue Blood Flow**, Tanja Dragojević<sup>1</sup>, Joseph L. Hollmann<sup>1</sup>, Davide Portaluppi<sup>2</sup>, Mauro Buttafava<sup>2</sup>, Davide Tamborini<sup>2</sup>, Joseph P. Culver<sup>3,4</sup>, Federica Villa<sup>2</sup>, Turgut Durduan<sup>1,5</sup>; <sup>1</sup>ICFO -The Inst. of Photonic Sciences, Spain; <sup>2</sup>Dipartimento di Elettronica, Informazione e Bioingegneria, Politecnico di Milano, Italy; <sup>3</sup>Dept. of Radiology, Washington Univ. School of Medicine, USA; <sup>4</sup>Dept. of Physics, Washington Univ., USA; <sup>5</sup>Instituto Catalana de Recerca i Estudis Avançats (ICREA), Spain. We present a novel device and a method based on speckle contrast optical spectroscopy (SCOS) for measuring absolute blood flow in deep tissue. The device was validated on healthy adult subjects.

**JTu3A.21**  
**Digital Depth-of-field expansion Using Contrast Pyramid fusion Algorithm for Full-field Optical Angiography**, nanshou wu<sup>1</sup>, Mingyi Wang<sup>1</sup>, Guojian Yang<sup>2</sup>, Zeng Yaguang<sup>1</sup>; <sup>1</sup>Foshan Univ., China; <sup>2</sup>Beijing Normal Univ., China. We propose a method to expand the depth-of-field in full-field optical angiography (FFOA) with absorption intensity fluctuation modulation effect and contrast pyramid fusion algorithm. The experimental results suggest that our methods could be applied to improve the depth of field in FFOA.

**JTu3A.22**  
**Flexible Mid-infrared Photonic Chips for Real-time and Label-Free Biomedical Compounds Detection**, Pao T. Lin<sup>1</sup>; <sup>1</sup>Texas A&M Univ., USA. Chip-scale chemical sensors were demonstrated using mid-infrared flexible aluminum nitride waveguides. Real-time detection of ethanol and water was conducted by measuring waveguide light at  $\lambda=2.7 \mu\text{m}$  corresponding to characteristic -OH absorption.

**JTu3A.23**  
**Validation of a Novel Wearable Technology to Estimate Oxygen Saturation Level and Lactate Threshold Power in the Exercising Muscle**, Parisa Farzam<sup>1</sup>, Zack Starkweather<sup>1</sup>, Maria Angela Franceschini<sup>1</sup>; <sup>1</sup>MGH, Harvard Medical School, USA. We have monitored the oxygen saturation and hemoglobin concentration in thigh muscle of 18 athletes, while cycling on a stationary ergometer to predict the lactate threshold power and thus, a wearable optical sensor can optimize athletes' training regimens.

**JTu3A.24**  
**Automated Data Analysis for Preclinical imaging of bioluminescent Reporter Systems**, ALEXANDER D. Klose<sup>1</sup>, Neal Paragas<sup>1</sup>, Kenneth Li<sup>1</sup>; <sup>1</sup>InVivo Analytics, USA. An automated and operator-independent data analysis tool has been developed that reconstructs the three-dimensional bioluminescent reporter distribution inside small animals, co-registers it to the animal anatomy, and automatically provides a comprehensive study report.

## JTU3A • Joint Poster Session I, Coffee Break and Exhibits—Continued

## JTU3A.25

**A Tool for Quantitative and Systematic Simulation of Diffuse Optical Tomography with a Limited Number of Fixed Sources and Detectors**, Edoardo Ferocino<sup>1</sup>, Antonio Pifferi<sup>1,2</sup>, Simon Aridge<sup>3</sup>, Fabrizio Martelli<sup>4</sup>, Paola Taroni<sup>1,2</sup>, Andrea Farina<sup>5</sup>, <sup>1</sup>Politecnico di Milano, Italy; <sup>2</sup>Istituto di Fotonica e Nanotecnologie, Consiglio Nazionale delle Ricerche, Italy; <sup>3</sup>Centre for Medical Image Computing, Univ. College London, UK; <sup>4</sup>Dipartimento di Fisica e Astronomia, Università degli Studi di Firenze, Italy; <sup>5</sup>Quantitative Time-Domain Diffuse Optical Tomography simulations are systematically performed through a developed tool. Reflectance geometry and fixed sources and detectors provide 4 mm localization error and 80% accuracy on reconstructed absorption in depth (2 cm).

## JTU3A.26

**System Configuration Optimization for Mesoscopic Fluorescence Molecular Tomography**, Fugang Yang<sup>1</sup>; <sup>1</sup>Shandong Inst. of Tech. and Business, China. We report on the optimization of optode configuration for a MFMT system with the detection chain implemented in descanned mode. The optimal illumination as well as detection configuration are identified through an *in silico* study.

## JTU3A.27

**Deep Learning Classification of Cartilage Integrity Using Near Infrared Spectroscopy**, Isaac O. Afara<sup>1</sup>, Jaakko K. Sarin<sup>1</sup>, Simo Ojanen<sup>1</sup>, Mikko Finnilä<sup>1</sup>, Walter Herzog<sup>2</sup>, Simo Saarakkala<sup>2</sup>, Rami Korhonen<sup>1</sup>, Juha Töyräs<sup>1</sup>; <sup>1</sup>Dept. of Applied Physics, Univ. of Eastern Finland, Finland; <sup>2</sup>Research Unit of Medical Imaging, Physics and Technology, Faculty of Medicine, Univ. of Oulu, Finland; <sup>3</sup>Human Performance Lab, Faculty of Kinesiology, Univ. of Calgary, Canada. We apply state-of-the-art machine-learning approach for classification of cartilage integrity based on near infrared spectroscopy. The classifiers achieved maximum sensitivity, specificity and precision of 97.9%, 83% and 91.2%, respectively.

## JTU3A.28

**A Reconstruction Algorithm for Bioluminescence Tomography Based on Sparse and Total Variation Regularizations**, Jinchao Feng<sup>1,2</sup>, Yanan Li<sup>1</sup>, Zhe Li<sup>1,2</sup>, Zhonghua Sun<sup>1,4</sup>, Kebin Jia<sup>1,3</sup>; <sup>1</sup>Beijing Univ. of Technology, China; <sup>2</sup>Beijing Lab of Advanced Information Networks, China; <sup>3</sup>Beijing Key Lab of Computational Intelligence and Intelligent System, Beijing Univ. of Technology, China; <sup>4</sup>Beijing Advanced Innovation Center for Future Internet Technology, Beijing Univ. of Technology, China. A novel reconstruction algorithm for bioluminescence tomography was proposed by combining sparse ( $L_1$  norm) and total variation regularizations. Results of simulation image reconstructions showed that the proposed algorithm could improve the quantification of reconstructed bioluminescence sources.

## JTU3A.29

**Image Resolution Improvements in Optical Imaging: Comparison of Angular vs. Time-domain Restriction of Highly Scattered Photons**, Lagnojita Sinha<sup>2</sup>, Jovan G. Brankov<sup>1</sup>, Kenneth M. Tichauer<sup>2</sup>; <sup>1</sup>Electrical Engineering, Illinois Inst. of Technology, USA; <sup>2</sup>Biomedical Engineering, Illinois Inst. of Technology, USA. Angular and time-domain restriction of highly scattered photons represent two methods of improving optical resolution in scattering media. Here, the advantages/tradeoffs between these approaches for varying medium thicknesses are presented.

## JTU3A.30

**Efficient Jacobian Construction for Hyperspectral Wide-field Diffuse Optical Tomography via "Replay" Monte Carlo**, Ruoyang Yao<sup>2</sup>, Xavier Intes<sup>2</sup>, Qianqian Fang<sup>1</sup>; <sup>1</sup>Dept. of Bioengineering, Northeastern Univ., USA; <sup>2</sup>Dept. of Biomedical Engineering, Rensselaer Polytechnic Inst., USA. "Replay" Monte Carlo provides a fast approach to build spatially and temporally resolved Jacobians for optical tomography. We successfully applied this method to reconstruct optically-thick tissue-like phantom data measured from a hyperspectral wide-field DOT system.

## JTU3A.31

**Frequency Selection with Optical Property Uncertainty Estimates for Spatial Frequency Domain Imaging**, Vivian Pera<sup>1</sup>, Kavon Karroobi<sup>1</sup>, Syeda Tabassum<sup>1</sup>, Fei Teng<sup>1</sup>, Darren M. Roblyer<sup>1</sup>; <sup>1</sup>Boston Univ., USA. We present a method to generate optical property uncertainty estimates from knowledge of diffuse reflectance measurement errors for spatial frequency domain imaging. Our method can help optimize spatial frequency selection for a given application.

## JTU3A.32

**Nonlocal Differential Operators Improve Image Reconstruction in Diffuse Optical Tomography**, Wenqi Lu<sup>1</sup>, Iain Styles<sup>1</sup>; <sup>1</sup>Univ. of Birmingham, UK. We propose a nonlocal Tikhonov regularization to the inverse model in diffuse optical tomography, using a spatial gradient operator defined on irregular meshes. Numerical experiments show that the proposed method can achieve better depth localization and higher image contrast than standard methods.

## JTU3A.33

**Line-field Confocal Optical Coherence Tomography Operating Simultaneously at 760 nm and 1270 nm center Wavelengths**, Arthur Davis<sup>1,2</sup>, Olivier Leveque<sup>2</sup>, Hicham Azimani<sup>2</sup>, David Siret<sup>2</sup>, Arnaud Dubois<sup>1,2</sup>; <sup>1</sup>Institut d'Optique Graduate School, France; <sup>2</sup>DAMAE Medical, France. Dual-band line-field confocal optical coherence tomography is reported for cross-sectional imaging in real-time at 760 nm and 1270 nm center wavelengths simultaneously. Differences in absorption and scattering in skin tissues, *in vivo*, is revealed.

## JTU3A.34

**Cellular Viability Imaging with DLS-OCT**, Julia S. Lee<sup>1</sup>, Collin Polucha<sup>1</sup>, Jonghwan Lee<sup>1</sup>; <sup>1</sup>Brown Univ., USA. DLS-OCT is tested to serve as a means to image the cellular viability with a single-cell resolution in mouse retinal tissue. Multiple metrics have been tested for representation of cellular or tissue viability, including intensity signal, decorrelation, and diffusion coefficient.

## JTU3A.35

**Coupling Polarisation Sensitive Optical Coherence Tomography and Mechanical Indentation to Assess Cartilage Degeneration**, Matthew S. Goodwin<sup>1</sup>, Ashvin Thambayah<sup>1</sup>, Frédérique Vanholsbeeck<sup>1</sup>; <sup>1</sup>Univ. of Auckland, New Zealand. In the past, quantifying difference in degeneration using Polarisation Sensitive Optical Coherence Tomography (PS-OCT) has proven difficult. However, coupling PS-OCT and mechanical indentation has enabled the differentiation of healthy cartilage from early degenerate cartilage.

## JTU3A.36

**Quantitative OCT of Living Rat Kidney**, Yuhong Fang<sup>1</sup>, Weijun Li<sup>1</sup>, Kui Dong<sup>1</sup>, Wei Gong<sup>1</sup>, Shusen Xie<sup>1</sup>, Zheng Huang<sup>1</sup>; <sup>1</sup>Fujian Normal Univ., China. Optical coherence tomography (OCT) is a useful optical biopsy tool. In this study, living rat kidneys were imaged using SD-OCT. Various sizes and shapes of signal free cavities (SFC) in 2D and 3D images were quantitatively analyzed.

## JTU3A.37

**Algebraic Calculation of Back-Projection Operators in Optoacoustic Tomography**, Amir Rosenthal<sup>1</sup>; <sup>1</sup>Technion Israel Inst. of Technology, Israel. A novel method for determining back-projection operators is developed and demonstrated in optoacoustic tomography. The proposed method may be generalized for any imaging surface or detector shape.

## JTU3A.38

**In Vivo Quantifying Molecular Specificity of  $Y_2O_3:Eu:Mg:Ti$  with Dynamic Fluorescence Imaging**, Yungpeng Dai<sup>1</sup>, Xueli Chen<sup>1</sup>, Yuzhu Gong<sup>1</sup>, Xu Cao<sup>1</sup>, Yonghua Zhan<sup>1</sup>, Jimin Liang<sup>1</sup>; <sup>1</sup>Xidian Univ., China. We quantified a type of persistent luminescent nanoparticles ( $Y_2O_3:Eu:Mg:Ti$ ) *in vivo* with dynamic fluorescence imaging to better understand its kinetic properties. The results show that it is expected to be further used in biomedical applications.

## JTU3A.39

**Significance of Covariation Between Arterial Blood Pressure and Total Hemoglobin Concentration in Coherent Hemodynamics Spectroscopy**, Angelo Sassaroli<sup>1</sup>, Kristen Tgavalekos<sup>1</sup>, Sergio Fantini<sup>1</sup>; <sup>1</sup>Tufts Univ., USA. We have performed a detailed study of the significance of covariation between arterial blood pressure and cerebral concentration of total hemoglobin measured with NIRS during a cyclic thigh cuff occlusion and release maneuver.

## JTU3A.40

**Correlation of EEG with Intercranial Pressure and Cerebral Hemodynamics during Burst-Suppression**, Jason Yang<sup>1</sup>, Alexander Ruesch<sup>1</sup>, Samantha Schmitt<sup>2</sup>, Matthew A. Smith<sup>2,3</sup>, Jana M. Kainerstorfer<sup>1,3</sup>; <sup>1</sup>Carnegie Mellon Univ., USA; <sup>2</sup>Eye and Ear Inst., Univ. of Pittsburgh, USA; <sup>3</sup>Center for the Neural Basis of Cognition, USA. The physiological relationship between electroencephalography (EEG), intercranial pressure (ICP), and cerebral hemodynamics is poorly understood. Here we demonstrate work in correlating EEG with hemodynamic responses during burst-suppression states in non-human primates.

## JTU3A.41

**Deep Tissue Multi-Wavelength Spatial Frequency Domain Imaging**, Constance M. Robbins<sup>1</sup>, Guruprasad Raghavan<sup>1</sup>, Jason Yang<sup>1</sup>, James F. Antaki<sup>1</sup>, Jana M. Kainerstorfer<sup>1</sup>; <sup>1</sup>Carnegie Mellon Univ., USA. We demonstrate the potential of spatial frequency domain imaging (SFDI) with tissue compression to image lesions located deep beneath tissue surface, and present a new multi-wavelength SFDI prototype capable of monitoring hemodynamic changes.

## JTU3A.42

**Discrimination of Healthy Skin and Cutaneous Malignant Lesions using FTIR Spectra and their Second Derivatives: A Comparative Study**, Denise M. Zezell<sup>1</sup>, Cassio Lima<sup>1</sup>; <sup>1</sup>Center for Lasers and Applications, IPEN - CNEN/SP, Brazil. PC-LDA statistical method was used to differentiate cutaneous tumor tissue from healthy skin. Discrimination accuracy obtained by raw FTIR spectra was 95% and by second derivatives 92%, besides identifying secondary structure of proteins and collagen.

## JTU3A.43

**Evaluation of Phantoms with Various Water and Lipid Contents by Using a Six-Wavelength Time-Resolved Spectroscopy System**, Etsuko Ohmae<sup>1</sup>, Hiroaki Suzuki<sup>1</sup>, Kenji Yoshimoto<sup>1</sup>, Shu Homma<sup>1</sup>, Norihiro Suzuki<sup>1</sup>, Hiroko Wada<sup>1</sup>, Tetsuya Mimura<sup>1</sup>, Nobuko Yoshizawa<sup>2</sup>, Hiroyuki Ogura<sup>3</sup>, Hatsuko Nasu<sup>2</sup>, Harumi Sakahara<sup>2</sup>, Yutaka Yamashita<sup>1</sup>, Yukio Ueda<sup>1</sup>; <sup>1</sup>Central Research Lab, Hamamatsu Photonics K.K., Japan; <sup>2</sup>Dept. of Radiology, Hamamatsu Univ. School of Medicine, Japan; <sup>3</sup>Dept. of Breast Surgery, Hamamatsu Univ. School of Medicine, Japan. We evaluate a set of solid phantoms, which mainly consist of water and lipid, by using our developed 6-wavelength time-resolved spectroscopy (TRS) system. The results obtained by the system correlate with the expected values.

## JTU3A.44

**Skin Optical Attenuation Coefficient Changes at Heart Rate**, Matheus B. Martinelli<sup>1</sup>, Christian T. Dominguez<sup>1</sup>, Luciano Bachmann<sup>1</sup>, George Cardoso<sup>1</sup>; <sup>1</sup>Universidade de Sao Paulo, Brazil. Video plethysmographic signals arise from subtle color modulations in reflected visible light. We use OCT imaging to show that such signals are due to modulation of the optical properties of superficial skin at rate.

## JTU3A.45

Withdrawn.

## JTU3A.46

**Pseudo-time Ensemble Kalman Filtering for Ultrasound Modulated Optical Tomography**, Saurabh Gupta<sup>1</sup>, Tara Raveendran<sup>2</sup>, Ram Vasu<sup>2</sup>, Debasish Roy<sup>2</sup>; <sup>1</sup>NIT Raipur, India; <sup>2</sup>IISc Bangalore, India; <sup>3</sup>College of Engineering, Trivandrum, India. A pseudo-time, sub-optimal stochastic filtering approach based on derivative free variant of ensemble Kalman filter for solving inverse problem of Ultrasound Modulated Optical Tomography is developed. The proposed scheme enhanced the contrast of reconstructed images.

## JTu3A • Joint Poster Session I, Coffee Break and Exhibits—Continued

## JTu3A.47

**All-Optical Simultaneous Stimulation and Readout of Motor Cortex Activity in Awake Mice**, Francesco Resta<sup>1</sup>, Emilia Conti<sup>1</sup>, Elena Montagnì<sup>1</sup>, Leonardo Sacconi<sup>1,2</sup>, Anna L. Allegra Mascaro<sup>1,3</sup>, Francesco S. Pavone<sup>1,2</sup>, <sup>1</sup>European Lab for Non-Linear Spectroscopy (LENS), Italy; <sup>2</sup>National Inst. of Optics, National Research Council, Italy; <sup>3</sup>Neuroscience Inst., National Research Council, Italy. Excitation spectra overlap between fluorescence indicators and optogenetic tools limits the development of an all-optical system for neural circuits interrogation. Here we describe how we solved the puzzle by combining red-shifted GECI with Channelrhodopsin 2.

## JTu3A.48

**Cell Counting in Targeted Nuclei of Whole Brain Two-Photon Image Data**, Gerald A. Moore<sup>1</sup>, Polona Jager<sup>2</sup>, Alessio Delogu<sup>2</sup>, Simon Schultz<sup>1</sup>, Stephen Brickley<sup>1</sup>, <sup>1</sup>Imperial College London, UK; <sup>2</sup>King's College London, UK. We quantify differences across whole mouse brains by developing a tool for automated cell counting in target nuclei. Validation was performed using the Sox14 mouse model to map the brain-wide distribution of Sox14 positive cells.

## JTu3A.49

**Assessment of Complete Hemodynamic Characteristics of in Vivo Tissues Using a Non-contact Laser Doppler and Total Diffuse Reflectance Spectroscopy System**, Juan Giraldo<sup>1</sup>, Anthony Giordano<sup>1</sup>, Mohamed Almadi<sup>1</sup>, Wei-Chiang Lin<sup>1</sup>, <sup>1</sup>Florida International Univ., USA. A non-contact, combined laser Doppler and total diffuse reflectance spectroscopy system was developed to simultaneously and continuously measure hemoglobin oxygenation, hemoglobin concentration, and regional flow from in vivo tissues.

## JTu3A.50

**Towards Spiroximetry in Adult Humans – How to Increase Amplitude of Respiratory Wave in an Optical Signal**, Piotr Sawosz<sup>1</sup>, Magdalena Morawiec<sup>1</sup>, Wojciech Dabrowski<sup>2</sup>, Przemyslaw Pulawski<sup>1</sup>, Michal Kacprzak<sup>1</sup>, Roman Maniewski<sup>1</sup>, Adam Liebert<sup>1</sup>, <sup>1</sup>Nalecz Inst. of Biocybernetics and Biomedical Engineering, Poland; <sup>2</sup>Dept. of Anaesthesiology and Intensive Therapy, Medical Univ. of Lublin, Poland. We propose a method to increase an amplitude of respiration-related wave in optical signal measured on a head. The method is based on cuff occlusion of abdominal part of the body of the subject.

## JTu3A.51

**Improved Sparse Reconstruction for Fluorescence Molecular Tomography with Poisson Noise Modeling**, Yansong Zhu<sup>2</sup>, Abhinav Kumar Jha<sup>1</sup>, Arman Rahmim<sup>1,2</sup>, Dean Wong<sup>1</sup>, <sup>1</sup>Radiology, Johns Hopkins Univ. School of Medicine, USA; <sup>2</sup>Electrical and Computer Engineering, Johns Hopkins Univ., USA. We present a maximum-likelihood-expectation-maximization (MLEM)-based method that models Poisson noise for improved reconstruction in fluorescence molecular tomography with sparse fluorescence distribution.

## JTu3A.52

**Generating High Quality Tetrahedral Meshes of the Human Head and Applications in fNIRS**, Anh Phong Tran<sup>1</sup>, Qianqian Fang<sup>1</sup>, <sup>1</sup>Northeastern Univ., USA. We report a workflow to efficiently create high-quality tetrahedral meshes of the human brain and head from neuroanatomical scans. We also demonstrate the utility of these accurate brain models for optical brain imaging.

## JTu3A.53

**Review of Time-domain Diffuse Correlation Spectroscopy: From Theory to Human Subject Studies**, Davide Tamborini<sup>1</sup>, Stefan Carp<sup>1</sup>, Xiaojun Cheng<sup>2</sup>, Bernhard Zimmermann<sup>2</sup>, Casey Evans<sup>3</sup>, Oleg Shatrovov<sup>3</sup>, Adrew Siegel<sup>3</sup>, Erik Duerr<sup>3</sup>, Megan Blackwell<sup>3</sup>, David Boas<sup>2</sup>, Maria Franceschini<sup>1</sup>, <sup>1</sup>Massachusetts General Hospital, USA; <sup>2</sup>Boston Univ., USA; <sup>3</sup>MIT Lincoln Lab, USA. We present theoretical models, technological aspects, validation with phantoms and humans subject results of Time-Domain Diffuse Correlation Spectroscopy.

## JTu3A.54

**Noninvasive Continuous Optical Monitoring of Absolute Cerebral Blood Flow in Adult Human Subjects**, Lian He<sup>1</sup>, Wesley Baker<sup>1,2</sup>, Daniel F. Milej<sup>3,5</sup>, Venkaiah C. Kavuri<sup>1</sup>, David R. Busch<sup>1,4</sup>, Mamadou Diop<sup>3,5</sup>, Keith St. Lawrence<sup>3,5</sup>, Ramani Balu<sup>2</sup>, Adrew Kofke<sup>2</sup>, Arjun G. Yodh<sup>1,2</sup>, <sup>1</sup>Dept. of Physics & Astronomy, Univ. of Pennsylvania, USA; <sup>2</sup>Dept. of Anesthesiology and Critical Care, Hospital of the Univ. of Pennsylvania, USA; <sup>3</sup>Dept. of Medical Biophysics, Univ. of Western Ontario, Canada; <sup>4</sup>Division of Neurology, Children's Hospital of Philadelphia, USA; <sup>5</sup>Imaging Division, Lawson Health Research Inst., Canada. We calibrated the DCS blood flow index against contrast-enhanced time-resolved NIRS for absolute cerebral blood flow. Absolute calibration was stable across single days. A "best" calibration coefficient was obtained from the study population.

## JTu3A.55

**Novel X-ray Fluorescent Organic Monomer and Polymer Materials for Optogenetic Applications**, David N. French<sup>1</sup>, Kelli Cannon<sup>2</sup>, Aundrea Bartley<sup>3</sup>, Lori McMahon<sup>3</sup>, Gary Gray<sup>1</sup>, <sup>1</sup>Chemistry, Univ. of Alabama at Birmingham, USA; <sup>2</sup>School of Vision Science, Univ. of Alabama at Birmingham, USA; <sup>3</sup>Neurobiology, Univ. of Alabama at Birmingham, USA. A unique approach to optogenetics has been investigated. Novel organic based materials that down-convert penetrative x-rays to visible light have been synthesized. These materials provide a non-invasive approach to optogenetics.

## JTu3A.56

Withdrawn.

## JTu3A.57

**Wide Field Speckle Imaging and Two Photon Microscopy Close Up for the Investigation of Cerebral Blood Flow in vivo in Murine Model of Obesity**, Haleh Soleimanzad<sup>1,2</sup>, Hirc Gurden<sup>2,3</sup>, Frederic pain<sup>1,2</sup>, <sup>1</sup>Université Paris Sud, France; <sup>2</sup>CNRS, France; <sup>3</sup>Université Paris Denis Diderot, France. A multi exposure speckle imaging system was developed to image superficial blood flow of the mice cortex. The acquisition of speckle contrast for different expositions time allows discriminate moving and static diffusers. In vivo speckle imaging of the mice brain will be presented.

## JTu3A.58

**Monte-Carlo Lookup Table-based Inverse Model for Non-invasive Quantification of Cerebral Optical Properties in Small Animals Using Review of Time-domain Diffuse Correlation Spectroscopy: From Theory to Human Subject Studies**, Seung Yup Lee<sup>1</sup>, Corey Zheng<sup>2</sup>, Erin Buckley<sup>1</sup>, <sup>1</sup>Georgia Inst. of Tech/Emory Univ., USA; <sup>2</sup>Georgia Inst. of Technology, USA. We present a Monte-Carlo simulation-based inverse algorithm to estimate absorption and scattering properties using small separation (<1cm) frequency-domain near-infrared spectroscopy data, and we validate this algorithm in tissue-simulating phantoms and animals.

## JTu3A.59

**Monitoring Acute Stroke in Mouse Model Using Visible-light Optical Coherence Tomography**, Xiao Shu<sup>1</sup>, Qi Liu<sup>1,2</sup>, Siyu Chen<sup>1</sup>, Shanbao Tong<sup>2</sup>, Hao F. Zhang<sup>1</sup>, <sup>1</sup>Northwestern Univ., USA; <sup>2</sup>Shanghai Jiao Tong Univ., China. We applied visible-light optical coherence tomography to monitor the dynamic cerebral blood flow and blood oxygen saturation in an acute stroke mouse model created by distal middle cerebral artery occlusion.

## JTu3A.60

**Chronic Transcranial Fluorescence Imaging of Cortical Neurons with 3-Photon Microscopy**, Kevin Takasaki<sup>1</sup>, Matthew Valley<sup>1</sup>, Emily Turschak<sup>1</sup>, Rui Liu<sup>1</sup>, Jack Waters<sup>1</sup>, <sup>1</sup>Allen Inst. for Brain Science, USA. 3-photon excitation permits fluorescence microscopy through the intact skull. We demonstrate 3-photon fluorescence imaging of neuronal structure and calcium activity in a chronic transcranial window preparation up to 300  $\mu$ m into brain below the intact skull.

## JTu3A.61

**Optical Imaging of Endogenous Lipid Particles Instructs on the Dynamics and Functions of the Cerebrospinal Fluid**, Olivier Thouvenin<sup>1</sup>, Claire Wyart<sup>1</sup>, Pierre-Luc Bardet<sup>1</sup>, Yasmine Cantaut-Belari<sup>2</sup>, Jenna Sternberg<sup>1</sup>, <sup>1</sup>Institut du Cerveau et de la Moelle epiniere (ICM), France. We report the first imaging and quantification of cerebrospinal fluid (CSF) dynamics within the spinal cord of zebrafish larvae. It provides a basis for understanding how CSF selectively transports instructive signals during development and morphogenesis.

## JTu3A.62

**Towards a Full Volumetric Atlas of Cell-specific Neuronal Spatial Organization in the Entire Mouse Brain**, Ludovico Silvestri<sup>1,2</sup>, Antonino Paolo Di Giovanna<sup>2</sup>, Giacomo Mazzamuto<sup>2</sup>, Trygve Leergard<sup>3</sup>, Francesco Orsini<sup>2,4</sup>, Irene Costantini<sup>2</sup>, Jan Bjaalie<sup>3</sup>, Paolo Frasconi<sup>4</sup>, Francesco S. Pavone<sup>2,4</sup>, <sup>1</sup>Istituto Nazionale di Ottica, Italy; <sup>2</sup>European Lab for Non-linear Spectroscopy, Italy; <sup>3</sup>Univ. of Oslo, Norway; <sup>4</sup>Univ. of Florence, Italy. We present a pipeline, based on light-sheet microscopy and high-throughput image analysis, for full-volumetric 3D mapping of the spatial organization of selected neuronal types in the whole mouse brain.

## JTu3A.63

**Self-Calibrated DCS for Monitoring Absolute Cerebral Blood Flow**, Mahro Khalid<sup>2,1</sup>, Daniel F. Milej<sup>2,1</sup>, Ajay Rajaram<sup>2,1</sup>, Androu Abdalmalak<sup>2,1</sup>, Mamadou Diop<sup>2,1</sup>, Keith St. Lawrence<sup>2,1</sup>, <sup>1</sup>Imaging division, Lawson Health Research Inst., Canada; <sup>2</sup>Medical Biophysics, Univ. of Western Ontario, Canada. This Study presents a stand-alone DCS system that incorporates a bolus tracking method to convert the blood flow index measured by DCS into units of absolute blood flow.

## JTu3A.64

**Mobile Phone Camera Based Near-Infrared Spectroscopy Measurements**, Morris D. Vanegas<sup>1</sup>, Stefan Carp<sup>2</sup>, Qianqian Fang<sup>1</sup>, <sup>1</sup>Northeastern Univ., USA; <sup>2</sup>Martinos Center for Biomedical Imaging, Massachusetts General Hospital, USA. We report a wearable camera-based near-infrared spectroscopy technique for low-resource regions. With a mobile phone and LED attachment, we investigate the suitability of low-cost cameras in non-contact tissue oxygenation assessments.

NOTES

## Atlantic Ballroom 1

Microscopy, Histopathology and Analytics

15:30–17:30

## MTu4A • New Microscopy Techniques

Presider: DongKyun Kang, Massachusetts General Hospital, USA

MTu4A.1 • 15:30 **Invited**

**Nondestructive Polarimetric Imaging of Collagen Organization in Articular Cartilage**, Gang Yao<sup>1</sup>; <sup>1</sup>Univ. of Missouri-Columbia, USA. Optical polarization tractography (OPT) was applied to image depth-resolved local fiber orientation and birefringence in articular cartilage samples. The OPT images were further quantified for parametric mapping of subsurface collagen structural changes in cartilage.

MTu4A.2 • 16:00

**Miniature Fourier Ptychographic Microscope Using Mobile Phone Camera Sensors**, Tomas Aidukas<sup>1</sup>, Andrew R. Harvey<sup>1</sup>, Pavan Chandra Konda<sup>1</sup>; <sup>1</sup>School of Physics and Astronomy, Univ. of Glasgow, UK. We report a Fourier ptychographic setup with sub-micron resolution costing around £100 using mobile phone camera sensors. Reconstruction algorithms were developed to overcome the Bayer pattern on these sensors and robust calibration methods have been developed to tackle alignment errors.

MTu4A.3 • 16:15

**Giga-pixel Spinning Time-stretch Quantitative Phase Imaging Cellular Assay**, Dickson M. Siu<sup>1</sup>, Anson H. Tang<sup>1</sup>, Kenneth Wong<sup>1</sup>, Kevin Tsia<sup>1</sup>; <sup>1</sup>Univ. of Hong Kong, Hong Kong. We present a high-throughput adherent-cell assay based on integration of high-resolution time-stretch quantitative phase imaging (QPI) and a modified DVD spinning platform – enabling Giga-pixel QPI and thus large-scale single-cell biophysical phenotyping.

## Atlantic Ballroom 2

Clinical and Translational Biophotonics

15:30–17:30

## CTu4B • Optical Techniques for Breast Tumor Margin Assessment

Presider: Michael Giacomelli, MIT, USA; Laura Marcu, Univ. of California Davis, USA

CTu4B.1 • 15:30 **Invited**

**Preventing Over Treatment Through Smart Health Technologies**, Nirmala Ramanujam<sup>1</sup>; <sup>1</sup>Duke Univ., USA. The cost of cancer care in the U.S. was \$125 billion in 2010 and is projected to increase to \$175 billion by 2020. Total spending on cancer care is driven by the cost to treat an individual patient and the number of patients treated. For example, sipuleucel-T, a novel immunotherapy for metastatic prostate cancer, was found to improve survival by several months in a population of patients with few proven options. However, its cost was more than \$100,000 per patient for a three-dose course of treatment.

CTu4B.2 • 16:00

**Raman-encoded Molecular Imaging (REMI) with SERS Nanoparticles to Guide Lumpectomy**, Yu Wang<sup>1</sup>, Nicholas Reder<sup>3</sup>, Soyoung Kang<sup>1</sup>, Sara Javid<sup>2</sup>, Suzanne M. Dintzis<sup>2</sup>, Jonathan T. Liu<sup>1,3</sup>; <sup>1</sup>Mechanical Engineering, Univ. of Washington, USA; <sup>2</sup>Surgery, Univ. of Washington School of Medicine, USA; <sup>3</sup>Pathology, Univ. of Washington School of Medicine, USA. We demonstrate that spectral imaging of fresh lumpectomy specimens, topically stained with a multiplexed cocktail of biomarker-targeted SERS nanoparticles, allows for rapid (~15 min) detection of residual tumors at the surgical margin surfaces.

CTu4B.3 • 16:15

**Spatial and Spectral Analysis of in-Situ Tumor-Normal Interfaces in Freshly Resected Lumpectomy Slices using Multispectral Structured Light Imaging**, David M. McClatchy<sup>1</sup>, Benjamin W. Maloney<sup>1</sup>, Elizabeth J. Rizzo<sup>2</sup>, Keith D. Paulsen<sup>1,3</sup>, Wendy A. Wells<sup>2,3</sup>, Brian W. Pogue<sup>1,3</sup>; <sup>1</sup>Thayer School of Engineering, Dartmouth College, USA; <sup>2</sup>Pathology, Dartmouth Hitchcock Medical Center, USA; <sup>3</sup>Norris Cotton Cancer Center, Dartmouth Hitchcock Medical Center, USA. A cohort of N=42 breast lesions has been imaged in-situ with a structured light imaging system through an ongoing clinical study. Multispectral, high spatial frequency scatter images provide additional modes contrast across the tumor-normal boundary.

## Grand Ballroom West

Optics and the Brain

15:30–17:30

## BTu4C • New Technologies for Human Brain Function

Presider: Mamadou Diop, Western Univ., Canada

BTu4C.1 • 15:30 **Invited**

**Dual-mode Investigation of Brain Networks Stimulated By Transcranial Photobiomodulation**, Hanli Liu<sup>1</sup>; <sup>1</sup>Univ. of Texas at Arlington, USA. Functional near infrared spectroscopy and electroencephalogram were utilized to investigate metabolic, hemodynamic, and electrophysiological responses to transcranial photobiomodulation, which was delivered to the human forehead with 1064-nm laser. Stimulation-induced alteration in brain networks were discussed.

BTu4C.2 • 16:00 **Invited**

**Interferometric Diffusing-wave Spectroscopy of the Human Brain**, Wenjun Zhou<sup>1</sup>, Oybek Kholiqov<sup>1</sup>, Shau Poh Chong<sup>1</sup>, Vivek J. Srinivasan<sup>1,2</sup>; <sup>1</sup>Department of Biomedical Engineering, University of California Davis, USA; <sup>2</sup>Department of Ophthalmology and Vision Science, University of California Davis School of Medicine, USA. We propose and demonstrate interferometric diffusing-wave spectroscopy (iDWS), which combines a multimode interferometer with a CMOS camera to achieve multispeckle detection, for high-speed measurements of blood flow in the human brain.

## Atlantic Ballroom 3

Optical Tomography and Spectroscopy

15:30–17:00

## OTu4D • Raman, Fluorescence, Mie-Scattering and Other Spectroscopies for Clinical Applications

Presider: Erin Buckley, Emory Univ., USA

OTu4D.1 • 15:30

**Frequency Offset Raman Spectroscopy (FORS) for Subsurface Probing of Highly Scattering Media**, Sanathana Konugolu Venkata Sekar<sup>1</sup>, Sara Mosca<sup>1</sup>, Andrea Farina<sup>2</sup>, Fabrizio Martelli<sup>2</sup>, Paola Taroni<sup>1,2</sup>, Gianluca Valentini<sup>1,2</sup>, Rinaldo Cubeddu<sup>1</sup>, Antonio Pifferi<sup>1,2</sup>; <sup>1</sup>Politecnico di Milano, Italy; <sup>2</sup>Istituto di Fotonica e Nanotecnologie, Consiglio Nazionale delle Ricerche, Italy; <sup>3</sup>Dipartimento di Fisica e Astronomia, Università degli Studi di Firenze, Italy. We present a new technique, Frequency Offset Raman Spectroscopy (FORS) for probing deep layer Raman spectra of diffusive media. It was demonstrated on a tissue mimicking phantom, and shows potential for *in vivo* applications.

OTu4D.2 • 15:45

**Compact Time Domain Diffuse Raman Instrumentation Based on a TCSPC Camera for Depth Probing of Diffusive Media**, Sanathana Konugolu Venkata Sekar<sup>1</sup>, Sara Mosca<sup>1</sup>, Gianluca Valentini<sup>1,2</sup>, Werner Zschratner<sup>3</sup>, Rainer Erdmann<sup>4</sup>, Antonio Pifferi<sup>1,2</sup>; <sup>1</sup>Politecnico di Milano, Italy; <sup>2</sup>Consiglio Nazionale delle Ricerche, Istituto di Fotonica e Nanotecnologie, Italy; <sup>3</sup>Leibniz Inst. for Neurobiology (LIN), Germany; <sup>4</sup>PicoQuant GmbH, Germany. We present a TCSPC camera based compact time domain diffuse Raman instrumentation for depth probing of diffusive media by time gating Raman photons. A compact non-contact probe was developed and demonstrated on tissue mimicking phantoms.

OTu4D.3 • 16:00 **Invited**

**Manifestations Of Pathology in Elastic-Scattering Spectra and Exigencies For Clinical Translation of Diagnostic Spectroscopy**, Irving J. Bigio<sup>1</sup>; <sup>1</sup>Boston Univ., USA. Elastic-scattering spectroscopy is sensitive to micro-architectural changes at the cellular and sub-cellular levels, which are the biomarkers of disease in histopathology. Optical diagnostic accuracy is superior when multiple structural factors are assessed for spectral classification.

**Atlantic Ballroom 1**

Microscopy, Histopathology and Analytics

**MTu4A • New Microscopy Techniques—Continued**

**MTu4A.4 • 16:30** **Invited**  
**Molecularly Targeted Imaging of Oral Cancer**, Thomas Reiner<sup>1</sup>; <sup>1</sup>Gerstner Sloan Kettering School of Biomedical Science, USA. Oral cancers are typically diagnosed late. To address this, we developed a molecularly targeted imaging probe, PARPi-FL, which could be used as a non-invasive tool for early detection. Here, we present preclinical and first-in-human data.

**MTu4A.5 • 17:00** **Invited**  
**Quantitative Differential Interference Contrast Microscopy**, Michael I. Shribak<sup>1</sup>; <sup>1</sup>Marine Biological Lab, USA. We describe modifications in differential interference contrast microscope, which make the microscope quantitative with orientation-independent image contrast. The new microscope produces maps of the optical path difference or dry mass and its gradient.

**Atlantic Ballroom 2**

Clinical and Translational Biophotonics

**CTu4B • Optical Techniques for Breast Tumor Margin Assessment—Continued**

**CTu4B.4 • 16:30**  
**Real-time Visualization of Tumor Margins in Breast Specimen using Fluorescence Lifetime Imaging**, Jakob Unger<sup>1</sup>, Christoph Heibisch<sup>1</sup>, Jennifer Phipps<sup>1</sup>, Morgan Darrow<sup>2</sup>, Richard Bold<sup>3</sup>, Laura Marcu<sup>1</sup>; <sup>1</sup>Biomedical Engineering, Univ. of California, Davis, USA; <sup>2</sup>Dept. of Pathology and Lab Medicine, Univ. of California, Davis, USA; <sup>3</sup>Dept. of Surgery, Univ. of California, Davis, USA. In this work we combine Time-Resolved Fluorescence Spectroscopy with machine learning techniques to provide a real-time assessment of tumor positive resection margins

**CTu4B.5 • 16:45**  
**Intra-operative Assessment of Excision margins During Breast Conserving Surgery by Integrated Raman Microscopy and Autofluorescence Imaging**, Dustin Shipp<sup>1</sup>, Emad Rakha<sup>2</sup>, Alexey Koloydenko<sup>4</sup>, Douglas Macmillan<sup>3</sup>, Ian Ellis<sup>2</sup>, Ioan Notingher<sup>1</sup>; <sup>1</sup>Univ. of Nottingham, UK; <sup>2</sup>School of Medicine, Univ. of Nottingham, UK; <sup>3</sup>The Breast Inst., Nottingham Univ. Hospitals NHS Trust, UK; <sup>4</sup>Mathematics Dept., Royal Holloway, Univ. of London, UK. An automated multimodal spectral imaging system based on auto-fluorescence imaging and Raman micro-spectroscopy was developed to allow label-free molecular diagnosis of surgical resections obtained during breast cancer surgery within 25 minutes.

**CTu4B.6 • 17:00**  
**Neoadjuvant Therapy Monitoring in Breast Cancer Patients with Diffuse Optical Tomography**, Mirella Altoe<sup>1</sup>, Jacqueline Gunther<sup>1</sup>, Emerson Lim<sup>2</sup>, Alessandro Marone<sup>1</sup>, Hyun Keol Kim<sup>3</sup>, Richard S. Ha<sup>3</sup>, Hanina Hibshoosh<sup>4</sup>, Kevin Kalinsky<sup>2</sup>, Dawn Hershman<sup>2</sup>, Andreas H. Hielscher<sup>1,3</sup>; <sup>1</sup>Biomedical Engineering, Columbia Univ., USA; <sup>2</sup>Medicine, Columbia Univ. Medical Center, USA; <sup>3</sup>Radiology, Columbia Univ. Medical Center, USA; <sup>4</sup>Pathology and Cell Biology, Columbia Univ. Medical Center, USA. In a clinical pilot study involving patients undergoing neoadjuvant chemotherapy, we explored evidence that diffuse optical tomography can be used to monitor tumor progression and predict treatment response.

**CTu4B.7 • 17:15**  
**Biodynamic 4D Imaging of Living Cancer Biopsies for Personalized Selection of Chemotherapy**, Zhe Li<sup>1</sup>, Honggu Choi<sup>1</sup>, Shadia Jalal<sup>2</sup>, John Turek<sup>1</sup>, David D. Nolte<sup>1</sup>; <sup>1</sup>Purdue Univ., USA; <sup>2</sup>IU School of Medicine, USA. Clinical trials of biodynamic digital holography in human esophageal and breast cancer identify patients with resistance to chemotherapy. Treatment of ex vivo living cancer biopsies from patients generates intracellular Doppler signatures related to patient chemosensitivity.

**Grand Ballroom West**

Optics and the Brain

**BTu4C • New Technologies for Human Brain Function—Continued**

**BTu4C.3 • 16:30**  
**Decoding Visual Information from High Density Diffuse Optical Tomography Neuroimaging Data**, Kalyan Tripathy<sup>1</sup>, Andrew Fishell<sup>1</sup>, Zachary Markow<sup>1</sup>, Tracy M. Burns-Yocum<sup>1</sup>, Dillan J. Newbold<sup>1</sup>, Pooja Tripathy<sup>1</sup>, Bradley L. Schlaggar<sup>1</sup>, Joseph P. Culver<sup>1</sup>; <sup>1</sup>Radiology, Washington Univ. in St. Louis, USA. Using high density diffuse optical tomography neuroimaging data and a template-matching strategy, we were able to decode detailed information about the position of a checkerboard being viewed by a human subject.

**BTu4C.4 • 16:45**  
**Diffuse Optical Tomography for Noninvasive Functional Brain Imaging in Awake Behaving Humans**, Xianjin Dai<sup>1</sup>, hao yang<sup>2</sup>, huabei jiang<sup>2</sup>; <sup>1</sup>Univ. of Florida, USA; <sup>2</sup>Medical Engineering, Univ. of South Florida, USA. We present a high density diffuse optical tomography (wHD-DOT) system capable of mapping hemodynamics in awake behaving humans. Both phantom and in vivo human subject experiments were conducted to validate the wHD-DOT system.

**BTu4C.5 • 17:00** **Invited**  
**Coherent Hemodynamics Spectroscopy (CHS): A New Way to Look at Cerebral Hemodynamic Oscillations**, Sergio Fantini<sup>1</sup>; <sup>1</sup>Tufts Univ., USA. We present initial clinical measurements of coherent hemodynamics spectroscopy (CHS), a frequency-resolved characterization of the amplitude and phase of coherent cerebral hemodynamics measured with near-infrared spectroscopy (NIRS) and analyzed with a dedicated CHS model.

**Atlantic Ballroom 3**

Optical Tomography and Spectroscopy

**OTu4D • Raman, Fluorescence, Mie-Scattering and Other Spectroscopies for Clinical Applications—Continued**

**OTu4D.4 • 16:30**  
**Comparison of Compressive Basis for Quantitative Single-Pixel Fluorescence Lifetime Imaging**, Marien I. Ochoa<sup>1</sup>, Qi Pian<sup>1</sup>, Xavier Intes<sup>1</sup>; <sup>1</sup>Rensselaer Polytechnic Inst., USA. A hyperspectral single pixel system determined the best patterns for intensity, lifetime and lifetime-FRET quantification. Hadamard Ranked, Sign and Normal, Speckle and Fourier patterns were compared in silico and experimentally, resulting in a better overall performance from Hadamard Ranked basis.

**OTu4D.5 • 16:45**  
**Spectroscopic Evaluation of Post-Traumatic Osteoarthritis in Shetland Ponies**, Jaakko K. Sarin<sup>1,2</sup>, Nikae te Moller<sup>3</sup>, Harold Brommer<sup>3</sup>, René van Weeren<sup>3</sup>, Irina Mancini<sup>2</sup>, Jos Malda<sup>3,4</sup>, Isaac O. Afara<sup>1</sup>, Juha Töyräs<sup>1,2</sup>; <sup>1</sup>Univ. of Eastern Finland, Finland; <sup>2</sup>Diagnostic Imaging Center, Kuopio Univ. Hospital, Finland; <sup>3</sup>Utrecht Univ., Netherlands; <sup>4</sup>Univ. Medical Centre Utrecht, Netherlands. We present preliminary findings on multivariate modeling between cartilage biomechanical properties and spectroscopic measurements, performed in arthroscopic surgery and Lab. Also, generic multivariate regression techniques were compared.

17:30–19:00 Welcome Reception with Exhibitors, Grand Ballroom East

## Grand Ballroom West

08:00–09:30

## JW1A • Joint Plenary Session II

President:

JW1A.1 • 08:00 **Plenary**

**Stain-Free Slide-Free Multiphoton Histopathology of Carcinogenesis and Cancer**, Stephen A. Boppart<sup>1</sup>; <sup>1</sup>Univ of Illinois at Urbana-Champaign, USA. Multiphoton microscopy has emerged as a powerful tool for stain-free slide-free histopathology. We have recently demonstrated a fiber-based nonlinear optical microscope that achieves fast and simultaneous visualization of a variety of intrinsic molecular contrasts within live tissue including auto-fluorescence excited by two/three-photon processes and specially structured molecules by second/third harmonic generation.

JW1A.2 • 08:45 **Plenary**

**Talking to The Brain in Its Own Language**, Shelia Nirenberg<sup>1</sup>; <sup>1</sup>Dept. of Physiology and Biophysics Weill Medical College, Cornell Univ., USA. Neuroscience research has focused largely on listening to the brain - on taking recordings, analyzing responses, and trying to extract meaning from them. But now we're entering a new phase where we can go beyond listening and can start talking back to the brain, and we can do it in its own language. This opens the door to new technologies for treating disease. Here we present the development of one such technology: a new kind of neuro-prosthetic for treating blindness. Briefly, it works by converting visual images into meaningful neural signals in real time and then sending the signals on to the brain using an optogenetic interface.

## 09:30–10:00 Coffee Break and Exhibits, Grand Ballroom East

## Atlantic Ballroom 1

Microscopy, Histopathology and Analytics

10:00–12:00

## MW2A • Biosensing and Bioimaging

President: Alex Walsh, Morgridge Inst. for Research, USA

MW2A.1 • 10:00 **Invited**

**Infrared Spectroscopic Imaging for All-digital Molecular Histopathology**, Rohit Bhargava<sup>1</sup>, Kevin Yeh<sup>1</sup>, Shachi Mittal<sup>1</sup>, Saumya Tiwari<sup>1</sup>; <sup>1</sup>Dept. of Bioengineering and Beckman Inst. for Advanced Science and Technology, Univ. of Illinois at Urbana-Champaign, USA. We present a chemical imaging approach to histopathology wherein image contrast derives from mid-infrared absorption. Fast imaging is developed to scan tissues at high definition and machine learning classifies archival breast tissue with high accuracy.

MW2A.2 • 10:30 **Invited**

**Molecular Imaging in Surgical Pathology and Drug Development**, Nathalie Agar<sup>1</sup>; <sup>1</sup>Harvard Medical School, USA. We apply mass spectrometry and optical imaging applications to provide molecular tissue characterization for surgical decision-making, and to investigate drug distribution in correlation with tissue architecture for the development of brain tumor therapeutics.

## Atlantic Ballroom 2

Clinical and Translational Biophotonics

10:00–12:00

## CW2B • Hemodynamics of the Brain

President: Anita Mahadevan-Jansen, Vanderbilt Univ., USA

CW2B.1 • 10:00 **Invited**

**Time-Domain Diffuse Correlation Spectroscopy: From Theory to Human Subject Studies**, Maria Angela Franceschini<sup>1</sup>; <sup>1</sup>Massachusetts General Hospital, USA. Time-domain diffuse correlation spectroscopy (TD-DCS) is a novel modality which offers dramatic improvements over the capabilities of functional near-infrared spectroscopy (fNIRS) by providing three times higher sensitivity to brain and greatly reduced scalp contamination. We are developing the first wearable, short-separation, gated TD-DCS system.

## CW2B.2 • 10:30

**Non-Invasive Diffuse Optical Quantification of Changes in Cerebral Oxygen Metabolism Following Deep Hypothermia and Circulatory Arrest in a Neonatal Swine Model**, Tiffany Ko<sup>1,2</sup>, Constantine D. Mavroudis<sup>3</sup>, Wesley Baker<sup>2</sup>, Vincent Morano<sup>5</sup>, Kobina Mensah-Brown<sup>2</sup>, Timothy Boorady<sup>2</sup>, Jennifer Lynch<sup>4,5</sup>, David R. Busch<sup>5</sup>, Alexander Schmidt<sup>4</sup>, Javier Gentile<sup>3</sup>, George Bratinov<sup>4</sup>, Yuxi Lin<sup>4</sup>, Sejin Jeong<sup>4</sup>, Richard W. Melchior<sup>7</sup>, Tami M. Rosenthal<sup>7</sup>, Kellie L. Schiavo<sup>7</sup>, Brandon C. Shade<sup>7</sup>, Rui Xiao<sup>8</sup>, Arjun G. Yodh<sup>5</sup>, Todd J. Kilbaugh<sup>4</sup>, Daniel Licht<sup>2</sup>; <sup>1</sup>Bioengineering, Univ. of Pennsylvania, USA; <sup>2</sup>Neurology, Children's Hospital of Philadelphia, USA; <sup>3</sup>Cardiothoracic Surgery, Hospital of the Univ. of Pennsylvania, USA; <sup>4</sup>Critical Care and Anesthesia, Children's Hospital of Philadelphia, USA; <sup>5</sup>Physics and Astronomy, Univ. of Pennsylvania, USA; <sup>6</sup>Biology, James Madison Univ., USA; <sup>7</sup>Perfusion Services, Cardiac Center, Children's Hospital of Philadelphia, USA; <sup>8</sup>Biostatistics, Children's Hospital of Philadelphia, USA. Non-invasive, hybrid frequency-domain diffuse optical spectroscopy (FD-DOS) and diffuse correlation spectroscopy (DCS) were combined to quantify cerebral oxygen metabolism in a neonatal swine model of deep hypothermia and circulatory arrest.

## Grand Ballroom West

Optics and the Brain

10:00–12:00

## BW2C • Rethink the Scan

President: Chris Xu, Cornell Univ., USA

BW2C.1 • 10:00 **Invited**

**SCAPE Microscopy for Multi-scale, High Speed Volumetric Imaging in Neuroscience**, Elizabeth M. Hillman<sup>1</sup>; <sup>1</sup>Columbia Univ., USA. Swept confocally aligned planar excitation (SCAPE) microscopy is a high-speed 3D imaging method that combines light sheet benefits with a simple, single-objective geometry. Latest technological developments and results will be presented.

## BW2C.2 • 10:30

**Partially Coherent Holographic Temporal Focusing for 3D Light Sculpting with Single Neuron Resolution**, Nicolas C. Pegard<sup>1</sup>, Alan Mardinly<sup>1</sup>, Ian A. Oldenburg<sup>1</sup>, Laura Waller<sup>1</sup>, Hillel Adesnik<sup>1</sup>; <sup>1</sup>Univ. of California Berkeley, USA. We propose a two-photon optogenetic photostimulation method that combines partially coherent 3D holography and temporal focusing for precise targeting of individual neurons. Experimental results demonstrate simultaneous illumination of 200 targets with high spatial resolution.

## Atlantic Ballroom 3

Optical Tomography and Spectroscopy

10:30–12:00

## OW2D • Diffuse Correlation Spectroscopy: Blood Flow Measurements

President: Ashwin Parthasarath, Univ. of South Florida, USA

OW2D.1 • 10:00 **Invited**

**Laser Speckle Contrast Imaging of Blood Flow**, Andrew Dunn, University of Texas, USA. Efforts to produce quantitative images with laser speckle imaging are hampered by challenges in relating the measured quantities to the complex underlying microvasculature. This talk will discuss these challenges and introduce new advances and applications.

## OW2D.2 • 10:30

**In vivo Depth Resolved Measurement of Blood Flow with Time Domain Diffuse Correlation Spectroscopy**, Marco Pagliuzzi<sup>1</sup>, Sanathana Konugolu Venkata Sekar<sup>2</sup>, Lorenzo Colombo<sup>1,2</sup>, Edoardo Martinenghi<sup>2</sup>, Jordi Minnema<sup>1</sup>, Rainer Erdmann<sup>3</sup>, Davide Contini<sup>2</sup>, Alberto Dalla Mora<sup>2</sup>, Alessandro Torricelli<sup>2</sup>, Antonio Pifferi<sup>2,4</sup>, Turgut Durduran<sup>1,5</sup>; <sup>1</sup>ICFO, Spain; <sup>2</sup>Politecnico di Milano, Italy; <sup>3</sup>Picoquant GmbH, Germany; <sup>4</sup>IFN-CNR, Italy; <sup>5</sup>ICREA, Spain. We have achieved continuous path length resolved diffuse correlation spectroscopy *in vivo* by means of an actively mode-locked Ti:Sapphire laser that allows high coherence pulses, thus enabling adequate signal-to-noise ratio in relatively fast (~1s) temporal resolution.

## Atlantic Ballroom 1

Microscopy, Histopathology and Analytics

### MW2A • Biosensing and Bioimaging—Continued

**MW2A.3 • 11:00** **Invited**  
**Photonic Crystal Resonant Coupling to Nanoantennas and Applications for Digital Resolution Biosensing**, Brian T. Cunningham<sup>1</sup>; <sup>1</sup>Univ of Illinois at Urbana-Champaign, USA. Using nanoparticles as nanoantennas to efficiently couple with the resonant modes of a photonic crystal, amplification of surface enhanced Raman spectroscopy and resonant enhanced absorption provides high signal-to-noise mechanisms for single-event sensing of biomolecular interactions.

## Atlantic Ballroom 2

Clinical and Translational Biophotonics

### CW2B • Hemodynamics of the Brain—Continued

**CW2B.3 • 10:45**  
**Coherent Hemodynamic Oscillations Induced in the Human Brain by Paced Breathing and Cyclic Thigh-cuffs Inflation**, Nishanth Krishnamurthy<sup>1</sup>, Angelo Sassaroli<sup>1</sup>, Kristen Tgavalekos<sup>1</sup>, Thao T. Pham<sup>1</sup>, Sergio Fantini<sup>1</sup>; <sup>1</sup>Tufts Univ., USA. We compare cerebral hemodynamic oscillations in the brain induced by two protocols. Pneumatic thigh-cuffs can produce similar results to paced breathing, and are more practical for coherent hemodynamics spectroscopy in a clinical population.

**CW2B.4 • 11:00**  
**The Impact of Hyperventilation Therapy on Cerebral Blood Flow and Oxygenation in Traumatic Brain Injured Patients Measured by Diffuse Optics**, Susanna Tagliabue<sup>1</sup>, Michal Kacprzak<sup>2</sup>, Federica Maruccia<sup>1,3</sup>, Julia Scheel<sup>1</sup>, Lidia Castro<sup>3</sup>, Marilyn Riveiro Vilaboa<sup>3,6</sup>, Anna Rey-Perez<sup>3,6</sup>, María Antonia Poca<sup>3</sup>, Juan Sa-huquillo<sup>3,4</sup>, Turgut Durduran<sup>1,5</sup>; <sup>1</sup>ICFO-Institut de Ciències Fotòniques, Spain; <sup>2</sup>Inst. of Biocy-bernetics and Biomedical Engineering, Poland; <sup>3</sup>Neurotraumatology and Neurosurgery Research Unit (UNINN), Vall d'Hebron Univ. Research Inst. (VHIR), Spain; <sup>4</sup>Dept. of Neurosurgery, Vall d'Hebron Univ. Hospital, Universidad Autònoma de Barcelona, Spain; <sup>5</sup>Institució Catalana de Recerca i Estudis Avançats (ICREA), Spain; <sup>6</sup>Neurotraumatology Intensive Care Unit, Vall d'Hebron Univ. Hospital, Universidad Autònoma de Barcelona, Spain. Cerebral blood flow and hemoglobin concentration measured by diffuse correlation spectroscopy and time-resolved spectroscopy in patients with traumatic brain injury show different behaviour during hyper-ventilation therapy according to the functioning of the treatment.

**CW2B.5 • 11:15**  
**Prediction of Return of Spontaneous Circulation During Cardiopulmonary Resuscitation using Frequency-Domain Diffuse Optical Spectroscopy in a Pediatric Swine Model of Asphyxial Cardiac Arrest**, Tiffany Ko<sup>1,2</sup>, Constantine D. Mavroudis<sup>3</sup>, Timothy Boorady<sup>2</sup>, Kobina Mensah-Brown<sup>2</sup>, Ryan Morgan<sup>4</sup>, Andrew Lautz<sup>4</sup>, George Bratinov<sup>4</sup>, Yuxi Lin<sup>4</sup>, Sejin Jeong<sup>4</sup>, Vinay M. Nadkarni<sup>4</sup>, Robert A. Berg<sup>4</sup>, Robert M. Sutton<sup>4</sup>, Arjun G. Yodh<sup>5</sup>, Todd J. Kilbaugh<sup>4</sup>, Daniel Licht<sup>2</sup>; <sup>1</sup>Bioengineering, Univ. of Pennsylvania, USA; <sup>2</sup>Neurology, Children's Hospital of Philadelphia, USA; <sup>3</sup>Cardiothoracic Surgery, Hospital of the Univ. of Pennsylvania, USA; <sup>4</sup>Critical Care and Anesthesia, Children's Hospital of Philadelphia, USA; <sup>5</sup>Physics and Astronomy, Univ. of Pennsylvania, USA. Continuous non-invasive quantification of cerebral hemodynamics using frequency-domain diffuse optical spectroscopy (FD-DOS) during cardiopulmonary resuscitation (CPR) provides an early prognostic indicator of CPR success during pediatric cardiac arrest.

## Grand Ballroom West

Optics and the Brain

### BW2C • Rethink the Scan—Continued

**BW2C.3 • 10:45**  
**Wide Area Profiling of Neuronal Function Using Hadamard Microscopy**, Vicente J. Parot<sup>1,2</sup>, Samouil L. Farhi<sup>3</sup>, Abhinav Grama<sup>4,5</sup>, Masahito Yamagata<sup>4,5</sup>, Ahmed Abdelfattah<sup>4</sup>, Yoav Adam<sup>7</sup>, Shan Lou<sup>7</sup>, Jeong J. Kim<sup>7</sup>, Robert E. Campbell<sup>8</sup>, David D. Cox<sup>4,5</sup>, Adam E. Cohen<sup>7,8</sup>; <sup>1</sup>Biophysics Program, Harvard Univ., USA; <sup>2</sup>Division of Health Science and Technology, Massachusetts Inst. of Technology, USA; <sup>3</sup>Chemical Biology Program, Harvard Univ., USA; <sup>4</sup>Dept. of Molecular and Cellular Biology, Harvard Univ., USA; <sup>5</sup>Center for Brain Science, Harvard Univ., USA; <sup>6</sup>Dept. of Chemistry, Univ. of Alberta, Canada; <sup>7</sup>Dept. of Chemistry and Chemical Biology, Harvard Univ., USA; <sup>8</sup>Howard Hughes Medical Inst., USA. Fluorescence background and light scattering impede all-optical mapping of neural function in intact tissue. Hadamard microscopy enabled simultaneous optogenetic stimulation and fluorescence recording of Ca<sup>2+</sup> responses in six thousand neurons in acute brain slices.

**BW2C.4 • 11:00**  
**Volumetric Imaging of Neural Activity employing an Overdrive Spatial Light Modulator**, Rui Liu<sup>1</sup>; <sup>1</sup>Allen Inst. for Brain Science, USA. We report an overdrive liquid crystal spatial light modulator based two-photon fluorescence microscope, capable of recording neural activity from a volume of 500  $\mu\text{m}$ s  $\times$  500  $\mu\text{m}$ s  $\times$  200  $\mu\text{m}$ s at  $\sim$ 5 Hz.

**BW2C.5 • 11:15**  
**High Accuracy Two-Photon Population Imaging of GCaMP6 Signals with Fast Smart Line Scan**, Marco Brondi<sup>1</sup>, Manuel Molano-Mazón<sup>2</sup>, Stefano Panzeri<sup>2</sup>, Tommaso Fellin<sup>1</sup>; <sup>1</sup>Dept. of Neuroscience and Brain Technologies, Istituto Italiano di Tecnologia, Italy; <sup>2</sup>Center for Neuroscience and Cognitive Systems, Istituto Italiano di Tecnologia, Italy. We present a method to perform imaging of GCaMP6 signals with high accuracy for single action potential detection over populations of neurons in the mouse brain using galvanometric mirrors and fast smart line scan trajectories.

## Atlantic Ballroom 3

Optical Tomography and Spectroscopy

### OW2D • Diffuse Correlation Spectroscopy: Blood Flow Measurements—Continued

**OW2D.3 • 10:45**  
**Spatial and Temporal Blood Flow Changes Provided by Diffuse Correlation Tomography during Bone Healing in a Murine Fracture Model**, Jingxuan Ren<sup>1</sup>, Songfeng Han<sup>1</sup>, Danielle E. Desa<sup>1</sup>, Ashley R. Proctor<sup>1</sup>, Gabriel A. Ramirez<sup>1</sup>, Nathaniel E. Barber<sup>1</sup>, Amanda M. Forti<sup>1</sup>, Danielle S. Benoit<sup>1</sup>, Regine Choe<sup>1</sup>; <sup>1</sup>Univ. of Rochester, USA. A non-contact diffuse correlation tomography technique was applied for measuring blood flow changes during bone healing in a murine fracture model. The spatial and temporal blood flow changes were observed.

**OW2D.4 • 11:00**  
**EMCCD-based Speckle Contrast Diffuse Correlation Tomography of Tissue Blood Flow Distribution**, Mingjun Zhao<sup>1</sup>, Chong Huang<sup>1</sup>, Daniel Irwin<sup>1</sup>, Siavash Mazdeyasna<sup>1</sup>, Ahmed Bahrani<sup>1</sup>, Nneamaka Agochukwu<sup>1</sup>, Lesley Wong<sup>1</sup>, Guoqiang Yu<sup>1</sup>; <sup>1</sup>Univ. of Kentucky, USA. We developed a novel EMCCD-based speckle contrast diffuse correlation tomography (scDCCT) system for 3-dimensional imaging of deep tissue blood flow distribution. The system has been validated in tissue-simulating phantoms and applied in human tissues.

**OW2D.5 • 11:15**  
**Pilot Study of Blood Flow Markers during Neoadjuvant Chemotherapy**, Jeffrey M. Cochran<sup>1</sup>, So H. Chung<sup>1</sup>, Anais Leproux<sup>2</sup>, Wesley Baker<sup>3,1</sup>, David R. Busch<sup>1</sup>, Bruce J. Tromberg<sup>2</sup>, Arjun G. Yodh<sup>1</sup>; <sup>1</sup>Univ. of Pennsylvania, USA; <sup>2</sup>Univ. of California Irvine, USA; <sup>3</sup>Children's Hospital of Philadelphia, USA. We performed a pilot longitudinal study of blood flow measurements during neoadjuvant chemotherapy for breast cancer and investigated potential correlations between pathologic complete responders and early blood-flow markers.

## Atlantic Ballroom 1

Microscopy, Histopathology and Analytics

### MW2A • Biosensing and Bioimaging—Continued

MW2A.4 • 11:30

**Nanoscale Imaging of Chromatin with Labeled and Label-Free Super-Resolution Microscopy and Partial-Wave Spectroscopy**, Adam Eshel<sup>1</sup>, Yue Li<sup>2</sup>, Xiang Zhou<sup>1</sup>, Graham Spicer<sup>1</sup>, The-Quyen Nguyen<sup>1</sup>, Luay M. Almassalha<sup>1</sup>, John E. Chandler<sup>1</sup>, Scott Gladstein<sup>1</sup>, Biqin Dong<sup>1,3</sup>, Cheng Sun<sup>3</sup>, Hao F. Zhang<sup>1</sup>, Vadim . Backman<sup>1</sup>; <sup>1</sup>Biomedical Engineering, Northwestern Univ., USA; <sup>2</sup>Applied Physics, Northwestern Univ., USA; <sup>3</sup>Mechanical Engineering, Northwestern Univ., USA. We demonstrate a multimodal imaging system that combines partial-wave spectroscopic microscopy and spectroscopic super-resolution microscopy to study chromatin topology. This instrument allows nanoscale visualization of labeled and unlabeled chromatin with molecular and structural contrast.

MW2A.5 • 11:45

**Spectroscopic Stimulated Raman Scattering Imaging of Highly Dynamic Specimens through Matrix Completion**, Haonan Lin<sup>1</sup>, Chien-Sheng Liao<sup>1</sup>, Pu Wang<sup>2</sup>, Nan Kong<sup>3</sup>, Ji-Xin Cheng<sup>1</sup>; <sup>1</sup>Boston Univ., USA; <sup>2</sup>Vibronix Inc., USA; <sup>3</sup>Purdue Univ., USA. We report a sparse spectroscopic stimulated Raman scattering imaging which improves acquisition speed by an order of magnitude through randomly sub-sampling the spectroscopic image followed by a low-rank matrix completion algorithm, enabling label-free real-time metabolic imaging of fungal cells.

## Atlantic Ballroom 2

Clinical and Translational Biophotonics

### CW2B • Hemodynamics of the Brain—Continued

CW2B.6 • 11:30

**Microvascular Cerebral Blood Flow Fluctuations Due to Periodic Apneas in Acute Ischemic Stroke**, Clara Gregori Pla<sup>1</sup>, Stella Avtzi<sup>1</sup>, Gianluca Cotta<sup>1</sup>, Giacomo Giacalone<sup>2</sup>, Federica Maruccia<sup>1</sup>, Pol Camps-Renom<sup>3</sup>, Joan Martí-Fàbregas<sup>3</sup>, Raquel Delgado-Mederos<sup>3</sup>, Mercedes Mayos<sup>3,4</sup>, Turgut Durduran<sup>1,5</sup>; <sup>1</sup>ICFO -The Inst. of Photonic Sciences, Spain; <sup>2</sup>San Raffaele Scientific Inst., Italy; <sup>3</sup>Hospital de la Santa Creu i Sant Pau, Spain; <sup>4</sup>CIBER Enfermedades Respiratorias (CibeRes) (CB06/06), Spain; <sup>5</sup>Institució Catalana de Recerca i Estudis Avançats (ICREA), Spain. Diffuse correlation spectroscopy monitoring revealed periodic fluctuations in the microvascular cerebral blood flow of acute ischemic stroke patients. A follow-up study revealed that the origin of such fluctuations was due to undiagnosed apneas.

CW2B.7 • 11:45

**Fetal Cerebral Blood Flow and Hemodynamics in a Model of Acute Ischemia in the Rabbit Fetus**, Giuseppe Lo Presti<sup>1</sup>, Lorenzo Cortese<sup>1</sup>, Sergio Berdún<sup>2</sup>, Elisenda Eixarch<sup>2,3</sup>, Eduard Gratacós<sup>2,3</sup>, Turgut Durduran<sup>1,4</sup>; <sup>1</sup>ICFO, Spain; <sup>2</sup>Fetal i+D, Fetal Medicine Research Center, BCNatal, Spain; <sup>3</sup>Barcelona Center for Maternal-Fetal and Neonatal Medicine (Hospital Clinic and Hospital Sant Joan de Deu), IDIBAPS, BCNatal, Spain; <sup>4</sup>ICREA, Spain. Variations of cerebral blood flow during acute ischemia and total hemoglobin concentration were monitored in rabbit fetuses using a hybrid device based on diffuse correlation spectroscopy and near infrared diffuse optical spectroscopy

## Grand Ballroom West

Optics and the Brain

### BW2C • Rethink the Scan—Continued

BW2C.6 • 11:30

**Video-rate Volumetric Neuronal Imaging Using 3D Targeted Illumination**, Sheng Xiao<sup>1</sup>, Hua-an Tseng<sup>2</sup>, Howard Gritton<sup>2</sup>, Xue Han<sup>2</sup>, Jerome Mertz<sup>2</sup>; <sup>1</sup>Dept. of Electrical & Computer Engineering, Boston Univ., USA; <sup>2</sup>Dept. of Biomedical Engineering, Boston Univ., USA. We describe a simple widefield based fast volumetric microscopy technique. Our technique enables neuronal imaging up to 500 X 500 X 240 μm 3D field of view at 100 Hz with high contrast and signal-to-noise ratio.

BW2C.7 • 11:45

**In Vivo Long-term Cortical Photoacoustic Microscopy Using Ultrasound-sensitive Chronic Cranial Window**, Biqin Dong<sup>1</sup>, Hao Li<sup>1</sup>, Xiao Shu<sup>1</sup>, Xian Zhang<sup>1</sup>, Hao F. Zhang<sup>1</sup>, Cheng Sun<sup>1</sup>; <sup>1</sup>Northwestern Univ., USA. We report an ultrasound-sensitive cranial window integrated with a highly sensitive micro-ring resonator ultrasound detector. We demonstrated implantation of the functional cranial window in mice and performed long-term intravital photoacoustic microscopy of cortex vasculature.

## Atlantic Ballroom 3

Optical Tomography and Spectroscopy

### OW2D • Diffuse Correlation Spectroscopy: Blood Flow Measurements—Continued

OW2D.6 • 11:30

**Implementation of Diffuse Correlation Spectroscopy to Measurements of Cerebral Blood Flow in Mice**, Bharat B. Sanders<sup>1</sup>, Eashani Sathialingam<sup>1</sup>, Seung Yup Lee<sup>1</sup>, Leah Bryan<sup>2</sup>, Courtney McCracken<sup>2</sup>, Erin Buckley<sup>1,2</sup>; <sup>1</sup>Wallace H. Coulter Dept. of Biomedical Engineering, Georgia Inst. of Technology and Emory Univ., USA; <sup>2</sup>Dept. of Pediatrics, Emory Univ. School of Medicine, USA. We translate diffuse correlation spectroscopy, which has commonly been used in humans and large animals, to a preclinical mouse model, wherein we characterize intra-user and inter-user repeatability along with verifying the accuracy of the measurements.

OW2D.7 • 11:45

**Employing Diffuse Correlation Spectroscopy and the Fluorescent Microsphere Technique for Murine Skeletal Muscle Blood Flow Measurement**, Ashley R. Proctor<sup>1</sup>, Gabriel A. Ramirez<sup>1</sup>, Songfeng Han<sup>2</sup>, Ziping Liu<sup>1</sup>, Tracy M. Bubel<sup>3</sup>, Regine Choe<sup>1,4</sup>; <sup>1</sup>Dept. of Biomedical Engineering, Univ. of Rochester, USA; <sup>2</sup>Inst. of Optics, Univ. of Rochester, USA; <sup>3</sup>Center for Visual Science, Univ. of Rochester, USA; <sup>4</sup>Dept. of Electrical and Computer Engineering, Univ. of Rochester, USA. The sensitivity of diffuse correlation spectroscopy (DCS) to blood flow changes in the quadriceps femora of mice treated with nicotinamide was tested. The correlation between DCS and the gold-standard fluorescent microsphere technique is presented.

12:00–13:30 Lunch Break, On Your Own

12:00–13:30 Student & Early Career Professional Development & Networking Lunch and Learn, (OSA Members Only; RSVP required)

13:30–15:30

## JW3A • Joint Poster Session II, Coffee Break and Exhibits

## JW3A.1

**A Vascular Optical Spectroscopic Measurement (VOSM) System for Monitoring Peripheral Artery Disease Patients**, Christopher Fong<sup>1</sup>, Jennifer W. Hoi<sup>1</sup>, Youngwan Kim<sup>1</sup>, Hyun Keol Kim<sup>1</sup>, andrea Hielscher<sup>1</sup>; <sup>1</sup>Columbia Univ., USA. A diffuse optical spectroscopic system suitable for intraoperative use for vascular surgery is characterized. A case example of its use for a patient before and after angioplasty is presented.

## JW3A.2

**PV[O]H Signals Intravascular Blood Loss in the Rat**, Bin Deng<sup>1</sup>, Seth Fillioe<sup>1</sup>, Paul Dent<sup>1</sup>, Charles Peterson<sup>1</sup>, James Mostrom<sup>1</sup>, Richard Steinmann<sup>1</sup>, Joshua Satalin<sup>1</sup>, Jerry Goodisman<sup>1</sup>, Gary Nieman<sup>1</sup>, Sriram Narsipur<sup>1</sup>, Joseph Chaiken<sup>1</sup>; <sup>1</sup>Syracuse Univ., USA. PV[O]H is a new noninvasive optical technique that measures hematocrit and vascular volume with unprecedented sensitivity, precision and bandwidth. We show that PV[O]H can reflect intravascular blood loss in seconds in a rat model.

## JW3A.3

**Automated Handling Device for Circumferential Gigapixel Microscopy of Whole Prostate Resections**, Sam J. Luehly<sup>1</sup>; <sup>1</sup>Biomedical Engineering, Tulane Univ., USA. The intraoperative correction of radical prostatectomy positive surgical margins relies on rapid and automated sample processing and imaging. This work demonstrates the feasibility of fully-automated circumferential prostate surface imaging in 10 minutes at subcellular resolution.

## JW3A.4

**LED-based Photoacoustic Imaging of Medical Devices with Carbon Nanotube-polydimethylsiloxane Composite Coatings**, Wenfeng Xia<sup>1,2</sup>, Sacha Noimark<sup>1,3</sup>, Eftymios Maneas<sup>1,2</sup>, Mithun K. Singh<sup>4</sup>, Sebastien Ourselin<sup>1,5</sup>, Simeon J. West<sup>6</sup>, Adrien E. Desjardins<sup>1,2</sup>; <sup>1</sup>Wellcome / EPSRC Centre for Interventional and Surgical Sciences, Univ. College London, UK; <sup>2</sup>Dept. of Medical Physics and Biomedical Engineering, Univ. College London, UK; <sup>3</sup>Dept. of Chemistry, Univ. College London, UK; <sup>4</sup>Research and Business Development Division, PreXion Corporation, Netherlands; <sup>5</sup>Centre for Medical Imaging Computing, Univ. College London, UK; <sup>6</sup>Dept. of Anaesthesia, Univ. College Hospital, UK. Invasive medical devices such as needles and catheters can have low visibility with ultrasound imaging. Here, we demonstrate that visibility can be greatly improved using LED-based photoacoustic imaging in combination with optically absorbing nanocomposite coatings.

## JW3A.5

Withdrawn.

## JW3A.6

**3D Computational Cytology Using Dual-view Inverted Selective Plane Illumination Microscopy (diSPIM)**, Bihe Hu<sup>1</sup>, Daniel Bolus<sup>1</sup>, Katherine N. Elfer<sup>1</sup>, Carly Swan<sup>1</sup>, Jay Tellis<sup>1</sup>, J. Quincy Brown<sup>1</sup>; <sup>1</sup>Tulane Univ., USA. To overcome the current limitations of cytopathology, 3D cytological imaging has been tested using dual-view inverted selective plane illumination microscopy (diSPIM) on human buccal cells, which shows the potential of diSPIM for high-throughput 3D cytology.

## JW3A.7

**Time Resolved Imaging for Tumor Diagnosis and Detection of Chemotherapy Response**, Elena Zagaynova<sup>1</sup>, Marina Shirmanova<sup>1</sup>, Maria Lukina<sup>1</sup>, Varvara Dudenkova<sup>1,2</sup>, Vladislav Scheslavskiy<sup>3</sup>, Vadim Elagin<sup>1</sup>, Ekaterina Gubarkova<sup>1</sup>, Irena Shlivko<sup>1</sup>; <sup>1</sup>Nizhny Novgorod State Medical Academy, Russia; <sup>2</sup>bLobachevsky State Univ. of Nizhny Novgorod, Russia; <sup>3</sup>Becker and Hickl GmbH, Germany. Early response of cancer cells to chemotherapeutic drugs were studied using FLIM/PLIM imaging. The dynamics of energy metabolism, intracellular pH, oxygen under chemotherapy were evaluated. In patients we have showed possibilities to distinguish benign and malignant pigmented lesions.

## JW3A.8

**Monitoring Joint Blood Flow with DCE TR-NIRS to Assess Treatment Response in Rheumatoid Arthritis**, Seva Ioussoufovitch<sup>1</sup>, Laura Morrison<sup>1</sup>, Lise Desjardins<sup>1</sup>, Jennifer Hadway<sup>1</sup>, Keith St. Lawrence<sup>1,3</sup>, Ting-Yim Lee<sup>3,1</sup>, Frank Beier<sup>4</sup>, Mamadou Diop<sup>3,1</sup>; <sup>1</sup>Lawson Health Research Inst., Canada; <sup>2</sup>Biomedical Engineering, Western Univ., Canada; <sup>3</sup>Medical Biophysics, Western Univ., Canada; <sup>4</sup>Physiology and Pharmacology, Western Univ., Canada; <sup>5</sup>Robarts Research Inst., Canada. Dynamic contrast-enhanced (DCE) TR-NIRS was used to monitor joint blood flow in a rat model of rheumatoid arthritis (RA) during disease induction and treatment. Preliminary results suggest DCE TR-NIRS can monitor treatment response in RA.

## JW3A.9

**Estimation of Chlorine-based Photosensitizer Penetration Depth Prior to PDT Procedure from Two-wavelength Excitation Fluorescence Measurements**, Aleksander Khilov<sup>1</sup>, Mikhail Kirillin<sup>1</sup>, Daria Loginova<sup>1</sup>, Ilya Turchin<sup>1</sup>; <sup>1</sup>IAP RAS, Russia. The ratio of fluorescence signals upon excitation of chlorine-based photosensitizers at peaks of 402 and 662 nm provides evaluation of photosensitizer penetration depth in biotissues. Monte Carlo simulations are in good agreement with phantom experiment.

## JW3A.10

**Continuous and Minimally Invasive Measurement of Blood Flow in the Spinal Cord**, David R. Busch<sup>2</sup>, Wei Lin<sup>3</sup>, Alissa Cutrone<sup>4</sup>, Brandon J. Kovarovic<sup>3</sup>, jakub tatka<sup>4</sup>, Chia C. Goh<sup>3</sup>, Arjun G. Yodh<sup>1</sup>, James Barsi<sup>5</sup>, Thomas F. Floyd<sup>2</sup>; <sup>1</sup>Physics, Univ. of Pennsylvania, USA; <sup>2</sup>Anesthesiology and Pain Management, Univ. of Texas Southwestern, USA; <sup>3</sup>Biomedical Engineering, Stony Brook Univ., USA; <sup>4</sup>Anesthesiology, Stony Brook Univ., USA; <sup>5</sup>Orthopedics, Stony Brook Univ., USA. Surgery and trauma commonly cause spinal cord ischemia. We have developed a catheter-based optical tool to continuously monitor spinal cord blood flow intraoperatively in a ovine model of spinal surgery.

## JW3A.11

**Mid-Infrared Photonic Chip for Label-free Glucose Sensing**, Pao T. Lin<sup>1</sup>; <sup>1</sup>Texas A&M Univ., USA. A chip-scale glucose sensor was developed using nitride optical waveguides at  $\lambda = 2.70\text{--}3.70\ \mu\text{m}$  because these spectral regions, which overlap with the characteristic O-H and C-H stretch absorptions. A detection limit better than 0.5 ng is experimentally demonstrated.

## JW3A.12

**Quantitative Analyses on Second Harmonic Generation Microscopy Images of Collagen in Ex Vivo Basal Cell Carcinoma Samples in Comparison to Normal Skin**, Norbert Kiss<sup>2,3</sup>, Dora Haluszka<sup>2,3</sup>, Kende Lorincz<sup>2</sup>, Szabolcs Bozsanyi<sup>3</sup>, Norbert Wikonkál<sup>3</sup>, Robert Szipocsi<sup>2,1</sup>; <sup>1</sup>R&D Ultrafast Lasers Kft., Hungary; <sup>2</sup>Wigner RCP, Hungary; <sup>3</sup>Semmelweis Univ., Hungary. We carried out quantitative analyses including fast Fourier transform and CT-FIRE algorithms on images captured by second harmonic generation microscopy for the identification of basal cell carcinoma in ex vivo human skin samples.

## JW3A.13

**Biomaterials as Second Harmonic Probes for Bioimaging and Diagnostic Applications**, Ming Ni<sup>1</sup>, Shuangmu Zhuo<sup>2</sup>; <sup>1</sup>YachayTech Univ., Ecuador; <sup>2</sup>Fujian Normal Univ., China. Some biomaterials also hold potentials to be second harmonic probes for bioimaging. I will give three examples to illustrate in this regard: collagen, DNA, and polysulfone. Their diagnostic applications will be also discussed.

## JW3A.14

**Temporal Deep Learning Classification of Digital Hologram Reconstructions of Multicellular Samples**, Tomi Pitkäaho<sup>1</sup>, Aki Manninen<sup>2</sup>, Thomas J. Naughton<sup>1</sup>; <sup>1</sup>Dept. of Computer Science, Maynooth Univ., Ireland; <sup>2</sup>Oulu Center for Cell-Matrix Research, Faculty of Biochemistry and Molecular Medicine, Univ. of Oulu, Finland. Digital holographic microscopy allows label-free capture of the full wavefront of light from an object using a low intensity laser. Using numerical reconstructions as an input to deep convolutional neural networks, detection of tumorigenic samples is feasible.

## JW3A.15

Withdrawn.

## JW3A.16

**Novel Fluorescence Imaging Approach in Deep Tissue Based on Sonoluminescence**, hao yang<sup>1</sup>, chaolong song<sup>2</sup>, huabei jiang<sup>1</sup>; <sup>1</sup>Univ. of South Florida, USA; <sup>2</sup>School of Mechanical Engineering and Electronic Information, China. We present a novel approach to effectively excite fluorescence molecules in deep tissue (> 2cm) using focused ultrasound. The sonoluminescence generated by a well-focused ultrasound beam is used to excite the fluorescence molecules.

## JW3A.17

**Role of Refractive Index Mismatch in Backward Nonlinear Optical Imaging**, Jarmo N. van der Kolk<sup>1</sup>, Charalambos Kioulos<sup>1</sup>, Antonino Calà Lessina<sup>1</sup>, Stéphane Bancelin<sup>2</sup>, François Légaré<sup>2</sup>, Lora Ramunno<sup>1</sup>; <sup>1</sup>Univ. of Ottawa, Canada; <sup>2</sup>Centre Énergie Matériaux et Télécommunication, Institut National de la Recherche Scientifique, Canada. Epi nonlinear optical imaging is used to image subresolution features. We find a refractive index mismatch between background medium and object affects imaging significantly. We study second harmonic generation microscopy of collagen fibrils as example.

## JW3A.18

**Fast, High-Quality Histology of Cleared Tissue Samples by Polygon-Based Multiphoton Microscopy**, Eben Olson<sup>1</sup>, Michael J. Levene<sup>2</sup>, Richard Torres<sup>1</sup>; <sup>1</sup>Yale Univ., USA; <sup>2</sup>Applique Technologies, LLC, USA. A polygon mirror-based, stage-scanning multiphoton microscopy approach is presented for rapidly obtaining, high-resolution images at depth from optically-cleared tissue samples, capable of substituting for physically-sectioned slides and enabling high-quality, large, 3D histologic reconstructions.

## JW3A.19

**Focusing Through Mouse Skull Using Wavefront Shaping**, Nektarios Koukourakis<sup>1</sup>, Moritz Kreysing<sup>2</sup>, Jürgen Czarske<sup>1</sup>; <sup>1</sup>Lab for Measurement and Sensor System Technique, TU Dresden, Germany; <sup>2</sup>Max-Planck Inst. of Molecular Cell Biology and Genetics, Germany. We focus through 400  $\mu\text{m}$  thick mouse skull using digital optical phase conjugation based on guide stars and discuss approaches to use backscattered light to determine the descrambling phase mask.

## JW3A.20

**Fast Diffuse Correlation Spectroscopy with Low-Cost Microcontroller**, Arindam Biswas<sup>1</sup>, Dillon A. Buffone<sup>1</sup>, Ashwin B. Parthasarathy<sup>1</sup>; <sup>1</sup>Univ. of South Florida, USA. We describe and demonstrate acquisition of Diffuse Correlation Spectroscopy data at up to 70 Hz measurement rates, using a low-cost embedded Arduino Due Board.

## JW3A.21

**Simulating DCT and SCOT in the transport regime**, Ugo Tricoli<sup>1</sup>, Callum Macdonald<sup>1</sup>, Turgut Durdurand<sup>2</sup>, Anabela Da Silva<sup>1</sup>, Vadim Markel<sup>1</sup>; <sup>1</sup>Inst. Fresnel, AMU, France; <sup>2</sup>ICFO, Spain. We apply first order perturbation theory to the scalar radiative transport equation for the temporal field auto-correlation function to study DCT and SCOT sensitivity to changes in the Brownian motion of the constituent scattering particles.

## JW3A.22

**Diffuse Correlation Tomography Geometry Optimization with Genetic Algorithm Using Singular Value Analysis**, Vincent Ralph D. Ching-Roa<sup>1</sup>, Songfeng Han<sup>2</sup>, Jingxuan Ren<sup>1</sup>, Gabriel A. Ramirez<sup>1</sup>, Seung Hyun Kim<sup>1</sup>, Regine Choe<sup>1</sup>; <sup>1</sup>Dept. of Biomedical Engineering, Univ. of Rochester, USA; <sup>2</sup>Inst. of Optics, Univ. of Rochester, USA. Singular value analysis is used to evaluate image resolution in raster scanning remission geometry for diffuse correlation tomography. Effect of scanning density was investigated, and probe geometry was optimized using genetic algorithm.

## JW3A • Joint Poster Session II, Coffee Break and Exhibits—Continued

## JW3A.23

**All Optical Real Time Method for Laser Speckle Pattern Tracking of Non-Contact Biomedical Parameters**, Ariel Schwarz<sup>1</sup>, Ran Califa<sup>2</sup>, Zeev Zalesky<sup>1</sup>, Nisan Ozana<sup>1</sup>, Amir Shemer<sup>1</sup>, Javier Garcia<sup>3</sup>, mark golberg<sup>1</sup>, Zeev Markman<sup>2</sup>, <sup>1</sup>Engineering, Bar Ilan Univ., Israel; <sup>2</sup>ContinUse Biometrics, Israel; <sup>3</sup>Universitat de València, Spain. A novel all optical method for laser speckle tracking of non-contact biomedical parameters is presented. The new technique enables a replacement of the expensive DSP solutions with all-optical low cost design. Method was experimentally demonstrated.

## JW3A.24

**A Novel 32 x 32, 224 Events/s Time Resolved SPAD Image Sensor for Near-Infrared Optical Tomography**, Scott Lindner<sup>1,2</sup>, Chao Zhang<sup>3</sup>, Ivan Antolovic<sup>3</sup>, Alexander Kalyanov<sup>1</sup>, Jingjing Jiang<sup>1</sup>, Linda Ahnen<sup>1</sup>, Aldo di Costanzo<sup>1</sup>, Juan Mata Pavia<sup>1</sup>, Salvador Sanchez Majos<sup>1</sup>, Edoardo Charbon<sup>2,3</sup>, Martin Wolf<sup>1</sup>, <sup>1</sup>Univ. of Zurich, Switzerland; <sup>2</sup>Advanced Quantum Architecture Lab, EPFL, Switzerland; <sup>3</sup>Circuits and Systems, TU Delft, Netherlands. To increase the spatial resolution of near-infrared optical tomography, we successfully designed and tested a 32x32 time-resolved SPAD image sensor with unprecedented sensitivity in the near-infrared and fast image acquisition speed.

## JW3A.25

**Novel Approach to Spatial Frequency Domain Fluorescence Diffuse Optical Tomography for Tumor Imaging**, Sanghoon Chong<sup>1</sup>, Vadim A. Markel<sup>1</sup>, Ashwin B. Parthasarathy<sup>2</sup>, Yihong Ong<sup>1,3</sup>, Frank A. Moscatelli<sup>4</sup>, Arjun G. Yodanis<sup>1</sup>, <sup>1</sup>Univ. of Pennsylvania, USA; <sup>2</sup>Dept. of Electrical Engineering, Univ. of South Florida, USA; <sup>3</sup>Dept. of Radiation Oncology, Hospital of the Univ. of Pennsylvania, USA; <sup>4</sup>Dept. of Physics, New York Univ., USA. We discovered a limitation of SVD-based analytic inversion algorithm for spatial frequency domain fluorescence diffuse optical tomography. We illustrate the issue and introduce an algorithm to overcome this challenge.

## JW3A.26

**An Approach to Improve Temporal Response of Single Photon Avalanche Photodiode for Time-resolved Diffuse Optical Tomography (DOT)**, Ahmed C. Kadhim<sup>1</sup>, Ahmad Azzahrani<sup>1</sup>, Susan Earles<sup>1</sup>, <sup>1</sup>Electrical and Computer Engineering, Florida Inst. of Technology, USA. A proposed approach of single photon avalanche photodiode based time-resolved DOT is introduced. It is supported by mathematical model of dark count rate as a function of gating voltage to further improve the DOT features.

## JW3A.27

**Non-Invasive Assessment of Deep Buried Flap Viability with Time-Resolved Optical Monitoring: Results on Pigs**, Anne PLANAT-CHRETIEN<sup>1</sup>, Audrey DOT<sup>2</sup>, Mathieu Perriolat<sup>1</sup>, Michel Berger<sup>1</sup>, Rodolphe Lartizien<sup>3</sup>, Jean-Luc Coll<sup>2,4</sup>, Georges Bettega<sup>3,4</sup>, <sup>1</sup>CEA-LETI, France; <sup>2</sup>Inst. for Advanced Biosciences, France; <sup>3</sup>Centre Hospitalier Annecy Genevois, France; <sup>4</sup>INSERM-UGA U1209, CNRS UMR 5309, France. With an optimized Time-Resolved acquisition system and probe, we detected and identified both arterial and venous occlusions and recoveries of deep buried flaps. Our results were cross-validated with a PtO2 clinical LICOX invasive reference.

## JW3A.28

**Laparoscopic Diffuse Optical Spectroscopy of Underlying Vessel Structures: A Model of the Detectability of a Long Cylindrical Inclusion Bisecting the Source-detector Pair**, Daqing (Daching) Piao<sup>1</sup>, Sanjay Patel<sup>2</sup>, <sup>1</sup>Oklahoma State Univ., USA; <sup>2</sup>Univ. of Oklahoma Health Sciences Center, USA. We present a model regarding laparoscopic detectability of a long absorbing tubular inclusion parallel to the medium surface and bisecting the source-detector-pair. The model agrees with measurements in an aqueous medium using a 10mm probe.

## JW3A.29

**Estimating Mechanical Properties of Bovine Knee Ligaments and Tendons with Near Infrared Spectroscopy**, Jari E. Tornainen<sup>1,2</sup>, Aapo Ristaniemi<sup>1</sup>, Lauri Stenroth<sup>1</sup>, Juha Töyräs<sup>1,2</sup>, <sup>1</sup>Dept. of Applied Physics, Univ. of Eastern Finland, Finland; <sup>2</sup>Diagnostic Imaging Center, Kuopio Univ. Hospital, Finland. In this study, mechanical properties of bovine knee ligament and tendon samples were estimated using near infrared spectroscopy (NIRS). Properties related to sample stress-relaxation characteristics were found to be suitable for NIRS-based estimation.

## JW3A.30

**How Should the New Generation of Detectors for Diffuse Optics Be? A Systematic Simulation Study**, Laura Di Sieno<sup>1</sup>, Anurag Behera<sup>1</sup>, Antonio Pifferi<sup>1,2</sup>, Fabrizio Martelli<sup>2</sup>, Alberto Dalla Mora<sup>1</sup>, <sup>1</sup>Politecnico di Milano, Italy; <sup>2</sup>Consiglio Nazionale delle Ricerche, Istituto di Fotonica e Nanotecnologie, Italy; <sup>3</sup>Dipartimento di Fisica e Astronomia, Università degli Studi di Firenze, Italy. In this work we report a comprehensive simulation study in which we quantify the effects of all parameters affecting the Instrument Response Function of a time-domain system in terms of sensitivity to an optical perturbation.

## JW3A.31

**Spatially-enhanced Data Analysis Method for Time-resolved NIRS to Determine Tissue Optical Properties**, Lin Yang<sup>1</sup>, Heidrun Wabnitz<sup>1</sup>, Dirk Grosenick<sup>1</sup>, Thomas Gladysz<sup>1</sup>, Rainer Macdonald<sup>1</sup>, <sup>1</sup>Physikalisch-Technische Bundesanstalt (PTB), Germany. The estimation of optical properties is investigated by combining temporally and spatially-resolved diffuse reflectance measurements. Through restricting the degrees of freedom by analytical relations, optical properties can be obtained more rapidly and accurately.

## JW3A.32

**Adaptability and Performance of Low-Cost OCT System for use in Benchtop Optical Coherence Microscopy**, Evan T. Jelly<sup>1</sup>, Yang Zhao<sup>1</sup>, Michael Crose<sup>1</sup>, Sanghoon Kim<sup>1</sup>, Brian Cox<sup>1</sup>, Ge Song<sup>1</sup>, Adam Wax<sup>1</sup>, <sup>1</sup>Duke Univ., USA. We present a feasible application for performing en face optical coherence microscopy using a low-cost OCT engine and a commercially available inverted microscope.

## JW3A.33

**Optogenetic Cardiac Control in Drosophila Using Red-light**, Jing Men<sup>1</sup>, Angelika Wyzlic<sup>1</sup>, Luisa Göpfert<sup>2</sup>, Airong Li<sup>2</sup>, Rudolph Tanzi<sup>3</sup>, Chao Zhou<sup>1</sup>, <sup>1</sup>Lehigh Univ., USA; <sup>2</sup>Hamburg Univ. of Applied Sciences, Germany; <sup>3</sup>Massachusetts General Hospital and Harvard Medical School, USA. Red-shifted opsins (ReaChR and halorhodopsin) were expressed in *Drosophila melanogaster* heart in order to achieve optogenetic pacing using red-light excitation. Controlled heart function was demonstrated *in vivo* throughout the *Drosophila* life cycle.

## JW3A.34

Withdrawn.

## JW3A.35

**Data Compression of Time-lapse Optical Coherence Tomography Images Based On Low-rank Plus Sparse Reconstruction**, Yuye Ling<sup>1</sup>, James P. McLean<sup>1</sup>, Christine P. Hendon<sup>1</sup>, <sup>1</sup>Columbia Univ., USA. Optical coherence tomography (OCT) is a promising candidate for observing dynamic processes via time-lapse imaging. We suggested that a faithful recovery of the dynamic signals could be achieved based on a low-rank plus sparse (L+S) reconstruction of under-sampled data.

## JW3A.36

**Multiscale Optoacoustic Measurements of Blood Oxygen Saturation in VIS-NIR Wavelength Range with the Ultrawideband Ultrasonic Detector: An In Vitro Study**, Valeriya Perekatova<sup>1</sup>, Ilya Turchin<sup>1</sup>, Mikhail Kirillin<sup>1</sup>, Daria Loginova<sup>1</sup>, Pavel Subochev<sup>1</sup>, <sup>1</sup>IAP RAS, Russia. The results of optoacoustic calibration-free measurements of effective optical attenuation of whole blood *in vitro* at 532-1069 nm wavelengths are presented. The potential of multiscale optoacoustic *in vivo* measurements of blood oxygen saturation is discussed.

## JW3A.37

**Discrimination of Ionizing Radiation Effects on Bone Using Fourier Transform Infrared Spectroscopy Using K-means**, Pedro Castro<sup>1</sup>, Denise M. Zezell<sup>1</sup>, <sup>1</sup>Center for Lasers and Applications, IPEN - CNEN/SP, Brazil. We demonstrated the feasibility of using ATR-FTIR spectroscopy associated with k-means clustering to evaluate the recognition of different doses. Our results open up new possibilities for protein monitoring relating to dose responses.

## JW3A.38

**Near-infrared Spectroscopy: A Potential Tool for Mapping Meniscus Properties**, Juho P. Ala-Myllymäki<sup>1</sup>, Juha Töyräs<sup>1</sup>, Isaac O. Afara<sup>1</sup>, <sup>1</sup>Univ. of Eastern Finland, Finland. Near-infrared spectroscopy is a promising tool for estimating the composition and biomechanical properties of meniscus. Here, we developed a predictive model was created for mapping meniscus biomechanical properties based on near-infrared spectroscopy.

## JW3A.39

**Submicron Position-resolved Raman Spectra for Characterizing Laser-trapped Single Airborne Particles**, Aiambé Kalume<sup>1</sup>, chuiji wang<sup>2</sup>, Joshua Snatarpia<sup>3</sup>, Yongle Pan<sup>1</sup>, <sup>1</sup>US Army Research Lab, USA; <sup>2</sup>Mississippi State u, USA; <sup>3</sup>Snadia National Labs, USA. We developed a technique that can measure submicron-position-resolved Raman spectra from laser-trapped airborne aerosol particles. Different spectra and evaporation processes were observed from different positions within a droplet of diethyl phthalate, glycerol, or their mixture.

## JW3A.40

**Depth-Resolved Measurements of Oscillatory Hemodynamics in Cerebral Near-Infrared Spectroscopy**, Kosar Khaksari<sup>1</sup>, Angelo Sassaroli<sup>1</sup>, Kristen Tgavalekos<sup>1</sup>, Sergio Fantini<sup>1</sup>, <sup>1</sup>Tufts Univ., USA. We propose a NIRS method based on 1-long and 2-short source-detector distances to identify superficial (extracerebral) and cerebral hemodynamic oscillations. We emphasize the relative amplitude and phase of oxy- and deoxy-hemoglobin oscillations in the brain.

## JW3A.41

**Light Transport Modeling for Accurate Pressure Modulation Calibration of Extra-cerebral Contribution to DCS Cerebral Blood Flow Monitoring in Adult Subjects**, Stefan Carp<sup>1</sup>, Parisa Farzam<sup>1</sup>, Parya Farzam<sup>1</sup>, Juliette Selb<sup>2</sup>, Jason Z. Qu<sup>1</sup>, Maria Franceschini<sup>1</sup>, <sup>1</sup>Massachusetts General Hospital, USA; <sup>2</sup>Boston Univ., USA. DCS monitoring of cerebral blood flow in adult subjects requires accounting for extracerebral contributions to the signal. We explore the impact of the choice of model on using the recently proposed pressure modulation method for calibrating the extracerebral contribution.

## JW3A.42

**Rapid and In Situ Optical Detection of Trace Lithium in Tissue**, Condon Lau<sup>1</sup>, Irfan Ahmed<sup>1</sup>, <sup>1</sup>City Univ. of Hong Kong, Hong Kong. Lithium-based medications are used against many mental disorders. However, lithium's distribution in organs is poorly characterized due to limitations in detection. To address this need, laser induced breakdown spectroscopy is developed for rapid and in situ detection of lithium in tissues.

## JW3A.43

**Advances in Single-Photon Detection and Timing for Time Domain Multi-Wavelength Optical Mammography**, Edoardo Ferocino<sup>1</sup>, Edoardo Martinenghi<sup>1</sup>, Alberto Dalla Mora<sup>1</sup>, Antonio Pifferi<sup>1,2</sup>, Rinaldo Cubeddu<sup>1,2</sup>, Paola Taroni<sup>1,2</sup>, <sup>1</sup>Politecnico di Milano, Italy; <sup>2</sup>Istituto di Fotonica e Nanotecnologie, Consiglio Nazionale delle Ricerche, Italy. To enhance photon harvesting and improve data quality, an 8-channel compact SiPM probe and TDC acquisition replace PMTs and TCSPC boards in a time-resolved optical mammograph still providing similar performances for optical properties estimation.

## JW3A • Joint Poster Session II, Coffee Break and Exhibits—Continued

## JW3A.44

**Coregistered and Segmented Tissue Oxygenation Maps onto White Light Images of Diabetic Foot Ulcers**, Edwin A. Robledo<sup>1</sup>, Richard Schutzman<sup>1</sup>, Cristianne M. Fernandez<sup>1</sup>, Fang Ruogu<sup>3</sup>, Kevin Leiva<sup>1</sup>, Rebecca J. Kwasinski<sup>1</sup>, Penelope Kallis<sup>2</sup>, Luis Borda<sup>2</sup>, Robert Kirsner<sup>2</sup>, Francisco Perez-Clavijo<sup>4</sup>, Anuradha Godavarty<sup>1</sup>; <sup>1</sup>Florida International Univ., USA; <sup>2</sup>Univ. of Miami, USA; <sup>3</sup>Univ. of Florida, USA; <sup>4</sup>Podiatry Care Partners Inc., USA. Regions of reduced tissue oxygenation in diabetic foot ulcers were segmented using graph cuts algorithms. These segmented oxygenation maps were coregistered onto their respective white light images, during weekly assessment of wound healing.

## JW3A.45

**Multi-wavelengths Photo Magnetic Imaging**, Farouk Nouzi<sup>1</sup>, Hakan Erkol<sup>1</sup>, alex luk<sup>1</sup>, Maha Algarawia<sup>1</sup>, Mehrnaz Mehrabi<sup>1</sup>, gultekin gulsen<sup>1</sup>; <sup>1</sup>Univ. of California Irvine, USA. We present the preliminary results obtained using the first multi-wavelengths Photo-Magnetic Imaging system. Results show that our multi-wavelengths PMI image reconstruction algorithm is able to provide bio-tissue chromophores concentration with high spatial and quantitative accuracy.

## JW3A.46

**Quantitative Optical Discrimination of Benign and Malignant Human Colon Pathologies Using Spatial Frequency Domain Modulated Imaging**, Sreyankar Nandy<sup>1</sup>; <sup>1</sup>Washington Univ. in St. Louis, USA. A spatial frequency domain imaging (SFDI) was used to image ex vivo human colon tissues. Significant differences were observed between absorption, scattering, scatter slope, total hemoglobin and spatial heterogeneities of benign and malignant tissue groups.

## JW3A.47

**Separating Systemic and Functional Components of the Hemodynamic Signal: A Comparison Using Two Techniques**, Amber Williams<sup>1</sup>, Karthik Vishwanath<sup>1</sup>, Rebeca de Jesus<sup>1</sup>, Vrinda Kalia<sup>1</sup>; <sup>1</sup>Miami Univ., USA. Hemodynamic changes were measured using functional near-infrared spectroscopy from subjects undergoing cold-pressor (sham) tasks. Systemic and functional components of these signals were calculated by minimizing the average mutual information or by using NIRFAST-based 3D reconstruction.

## JW3A.48

**Learning Biomarkers of Disease from Non-Invasive Measurements of Blood Flow**, Jakob Krzyston<sup>1</sup>, Seung Yup Lee<sup>1,2</sup>, Erin Buckley<sup>1,2</sup>, Eva Dyer<sup>1,2</sup>; <sup>1</sup>Georgia Inst. of Technology, USA; <sup>2</sup>Emory Univ., USA. Imaging techniques providing high resolution measurements of cortical blood flow can be used to characterize the state of the brain. Here we describe computational methods for processing measurements of blood flow to identify biomarkers of disease.

## JW3A.49

**High Sensitivity Photoacoustic Imaging System for Cerebral Cortex using Tightly Focused Beams and Contrast Agents**, Yu-Hang Liu<sup>1</sup>, Kim Chuan Chan<sup>1</sup>, Yu Xu<sup>1</sup>, Aishwarya Bandla<sup>1</sup>, Nitish Thakor<sup>1,2</sup>; <sup>1</sup>Singapore Inst. for Neurotechnology (SINAPSE), National Univ. of Singapore, Singapore; <sup>2</sup>Dept. of Biomedical Engineering, Johns Hopkins Univ., USA. Detection sensitivity (signal-to-noise ratio) of the real-time photoacoustic imaging was enhanced by using multiple measures, including the tightly focused dot/line beams and the exogenous contrast agents, supported by results of the *in vivo* cerebrovascular imaging.

## JW3A.50

**Hybrid Broadband NIRS/Diffuse Correlation Spectroscopy System for Simultaneous Monitoring of Cerebral Perfusion and Cytochrome C Oxidase**, Ajay Rajaram<sup>1,3</sup>, Gemma Bale<sup>2</sup>, Matthew D. Kewin<sup>1,3</sup>, Ilias Tachtsidis<sup>2</sup>, Keith St. Lawrence<sup>1,3</sup>, Mamadou Diop<sup>1,3</sup>; <sup>1</sup>Medical Biophysics, Western Univ., Canada; <sup>2</sup>Medical Physics and Biomedical Engineering, Univ. College London, UK; <sup>3</sup>Lawson Health Research Inst., Canada. This article reports on the development and demonstration of a novel optical system combining broadband near-infrared spectroscopy and diffuse correlation spectroscopy to provide simultaneous acquisition of cerebral perfusion and cytochrome c oxidase.

## JW3A.51

**Improvements in Functional Diffuse Optical Tomography Maps by Global Motion Censoring Techniques**, Arefeh Sherafati<sup>1</sup>, Adam T. Eggebrecht<sup>1</sup>, Karla M. Bergonzzi<sup>1</sup>, Tracy M. Burns-Yocum<sup>1</sup>, Joseph P. Culver<sup>1</sup>; <sup>1</sup>Washington Univ. in St. Louis, USA. Head motion produces artifact that disrupts optical neuroimaging data. Global variance in the temporal derivative (GVTD) across all measurements or voxels time-traces, provides a motion censoring technique that improves the functional connectivity maps.

## JW3A.52

**Importance of Left Dorsolateral Prefrontal Cortex in Moral Judgment Using Functional Near-Infrared Spectroscopy**, Hadis Dashtestani<sup>1,2</sup>, Rachel Zaragoza<sup>1</sup>, Riley Keranian<sup>1</sup>, Kristine Knutson<sup>1</sup>, Milton Hale<sup>2</sup>, Afroz Anderson<sup>1</sup>, Amir Gandjbakhche<sup>1</sup>; <sup>1</sup>NIH, USA; <sup>2</sup>Computer Science, UMBC, USA. We used fNIRS to investigate the neural processes of moral judgment (MJ). Left dorsolateral PFC was significantly more activated during impersonal MJ (less emotional) in non-utilitarian decisions.

## JW3A.53

**Ca2+ Decomposition into Signal and Noise Components for Multisite Ca2+ Imaging**, Mariana Potcoava<sup>1</sup>, Shelagh Rodriguez<sup>1</sup>, Simon Alford<sup>1</sup>; <sup>1</sup>Univ. of Illinois at Chicago, USA. We developed a de-noising methodology to automatically remove the fluorescence background and the non-stationary baseline in Ca2+ imaging, and enhance the signal/noise ratio for Ca2+ fluorescence transients evoked by single synaptic events under physiological conditions.

## JW3A.54

**Optical Monitoring of Cerebral Hemodynamics in Acute Stroke Patients During Mechanical Thrombectomy**, Parisa Farzam<sup>1</sup>, Henrikas Vaitkevicius<sup>2</sup>, Mohammad A. Aziz-Sultan<sup>2</sup>, Parya Farzam<sup>1</sup>, Alfred P. See<sup>2</sup>, Maria Franceschini<sup>1</sup>, Nirav J. Patel<sup>2</sup>; <sup>1</sup>Harvar Medical School, Massachusetts General Hospital, USA; <sup>2</sup>Department of Neurosurgery, Brigham and Women's Hospital, USA. This study uses diffuse correlation spectroscopy (DCS) to monitor blood flow during mechanical thrombectomy, a novel catheter-based treatment in acute ischemic stroke patients, to assist the surgeons observing the flow changes in realtime, towards a personalized therapy.

## JW3A.55

**Mechanistic Understanding of Transcranial Photobiomodulation Stimulated by Infrared Laser on the Human Forehead**, Xinlong Wang<sup>1</sup>, Divya D. Reddy<sup>1</sup>, Sahil Nalawade<sup>1</sup>, Douglas Barrett<sup>1</sup>, Francisco Gonzalez-Lima<sup>2</sup>, Hanli Liu<sup>1</sup>; <sup>1</sup>UT-Arlington, USA; <sup>2</sup>UT-Austin, USA. We measured laser- and heat-induced cerebral responses of the human forehead during placebo-controlled photobiomodulation by 1064-nm laser. Significant enhancement in cerebral cytochrome-c-oxidase and hemodynamics was observed, revealing physiological mechanisms of transcranial photobiomodulation.

## JW3A.56

**Does Light Propagate Better Along Pyramidal Apical Dendrites in Cerebral Cortex?**, Martin Thunemann<sup>1</sup>, Torbjørn V. Ness<sup>1,3</sup>, Kivilmir Kilic<sup>2</sup>, Christopher G. Ferri<sup>2</sup>, Sava Sakadzic<sup>2</sup>, Anders M. Dale<sup>4</sup>, Yeshiahu Fainman<sup>5</sup>, David A. Boas<sup>6</sup>, Gaute T. Einevoll<sup>3,7</sup>, Anna Devor<sup>6,5</sup>; <sup>1</sup>Radiology, Univ. of California, San Diego, USA; <sup>2</sup>Neurosciences, Univ. of California, San Diego, USA; <sup>3</sup>Norwegian Univ. of Life Sciences, Norway; <sup>4</sup>Biomedical Engineering, Boston Univ., USA; <sup>5</sup>Martinos Center for Biomedical Imaging, Harvard Medical School, USA; <sup>6</sup>Neurosciences and Radiology, Univ. of California, San Diego, USA; <sup>7</sup>Dept. of Physics, Univ. of Oslo, Norway; <sup>8</sup>Electrical and Computer Engineering, Univ. of California, San Diego, USA. Simulation studies of light propagation in cerebral cortex often assume homogeneous and direction-independent scattering; however, direct measurements revealed significant directional dependence with implications for optogenetics and diffuse optical tomography.

## JW3A.57

**Refined Utah Optrode Array and  $\mu$ LED Array for Deep Cortical Optogenetic Stimulation in Primates**, Robert Scharf<sup>1</sup>, Christopher Reiche<sup>1</sup>, Niall McAlinden<sup>2</sup>, Yunzhou Cheng<sup>2</sup>, Rohit Sharma<sup>1</sup>, Enyuan Xie<sup>2</sup>, Prashant Tathireddy<sup>1</sup>, Alessandra Angelucci<sup>1</sup>, Christine Kallmayer<sup>3</sup>, Keith Mathieson<sup>2</sup>, Loren Rieth<sup>1</sup>, Steve Blair<sup>1</sup>; <sup>1</sup>Univ. of Utah, USA; <sup>2</sup>Univ. of Strathclyde, UK; <sup>3</sup>Fraunhofer IZM, Germany. We fabricated a deep optogenetic cortical stimulation device (10x10 glass waveguide array) using wafer dicing, etching and annealing. A  $\mu$ LED array delivers light through individual shanks. A silicon interposer layer with optical vias prevents crosstalk.

## JW3A.58

**Serial Optical Coherence Scanner for Imaging Neurodegenerative Diseases**, Chao Liu<sup>1</sup>, Orion Rainwater<sup>1</sup>, Harry Orr<sup>1</sup>, Taner Akkin<sup>1</sup>; <sup>1</sup>Univ. of Minnesota, USA. Serial optical coherence scanner combines optical coherence tomography with a tissue slicer, which enables the visualization of the microstructures in the brain and provides quantitative contrasts for pathological changes in neurodegeneration diseases.

## JW3A.59

**Detecting Ultra-low Light Level Signals with Optical Fiber Probe for Intrinsic Neural Signals *in vivo***, Wen-Ju Pan<sup>1</sup>, Waqas Majeed<sup>1</sup>, Jacob Billings<sup>1</sup>, Shella Keilholz<sup>1</sup>; <sup>1</sup>Emory Univ., USA. A photodiode in photovoltaic mode was introduced for ultra-low-light-level detection to study brain activity in rats using a miniaturized probe. Studies conducted with simultaneous measurement of 3 wavelengths demonstrated clear optical responses to neuronal activity.

## JW3A.60

**MesoScope Upgrade: Dual Plane Remote Focusing Imaging System for Recording of Ca<sup>2+</sup> Signals in Neural Ensembles**, Dmitri Tsyboulski<sup>1</sup>, Natalia Orlova<sup>1</sup>, Jerome Lecoq<sup>1</sup>, Peter Saggau<sup>1</sup>; <sup>1</sup>Allen Inst., USA. We present a modification of a commercial system known as MesoScope that utilizes principles of temporal multiplexing and remote focusing, and allows simultaneous imaging from two regions of interest arbitrarily positioned in axial direction.

## JW3A.61

**Design of a Wavefront-Engineered Multiphoton Microscope (WEMM) for Imaging Awake and Behaving Mouse**, Rui Liu<sup>1</sup>; <sup>1</sup>Allen Inst. for Brain Science, USA. We report a multiphoton microscope design allowing excitation from 900 nm to 1320 nm and all the scanners and wavefront shaping device conjugated to the back pupil for imaging mouse brain during visual behavior.

## JW3A.62

**Dual-color Three-photon Microscopy for Deep Imaging of Neural Tissue**, Lamiae Abdeladim<sup>1</sup>, Khmaies Guesmi<sup>2</sup>, Pierre Mahou<sup>1</sup>, Samuel Tozer<sup>3</sup>, Takuma Kumamoto<sup>3</sup>, Julia Ferrer-Ortas<sup>1</sup>, Nicolas Dray<sup>4</sup>, Karine Loulier<sup>2</sup>, Marc Hanna<sup>2</sup>, Patrick Georges<sup>2</sup>, Jean Livet<sup>3</sup>, Willy Supatto<sup>1</sup>, Frédéric Druon<sup>2</sup>, Emmanuel Beaupaire<sup>1</sup>; <sup>1</sup>Ecole Polytechnique, Lab for Optics and Biosciences, CNRS, INSERM, France; <sup>2</sup>Lab Charles Fabry, Institut d'Optique Graduate School, CNRS, Paris-Saclay Univ., France; <sup>3</sup>Institut de la Vision, INSERM, UPMC, CNRS, France; <sup>4</sup>Zebrafish Neurogenetics Unit, Developmental and Stem Cell Biology Dept., Institut Pasteur, CNRS, France. We demonstrate dual-color three-photon imaging of red and green fluorescent proteins in neural tissue using a novel ultrafast laser design providing simultaneous excitation at 1300 and 1700 nm.

JTh3A • Poster Session III, Coffee Break and Exhibits—Continued

JW3A.63

**Simultaneous Monitoring of Intravascular and Extravascular Oxygen Tension and Cerebral Blood Flow in Rat Brain During Forepaw Stimulation**, Sanghoon Chong<sup>1</sup>, Yihong Ong<sup>1,2</sup>, Mirna E. Khatib<sup>1</sup>, Tatiana V. Esipova<sup>1</sup>, Ashwin B. Parthasarathy<sup>3</sup>, Joel H. Greenberg<sup>1</sup>, Arjun G. Yodh<sup>1</sup>, Sergei A. Vinogradov<sup>1</sup>; <sup>1</sup>Univ. of Pennsylvania, USA; <sup>2</sup>Dept. of Radiation Oncology, Hospital of the Univ. of Pennsylvania, USA; <sup>3</sup>Dept. of Electrical Engineering, Univ. of South Florida, USA. We studied rat somatosensory cortex *in vivo* responses to functional activation based on real-time measurements of intravascular and extravascular oxygen tension using two-color phosphorescence lifetime spectroscopy and cerebral blood flow using laser speckle contrast imaging.

JW3A.64

**Comparison of Cerebral Blood Flow Measurements with Diffuse Correlation Spectroscopy and Coherent Hemodynamics Spectroscopy**, Thao T. Pham<sup>1</sup>, Kristen Tgavalekos<sup>1</sup>, Angelo Sassaroli<sup>1</sup>, Nishanth Krishnamurthy<sup>1</sup>, Sergio Fantini<sup>1</sup>; <sup>1</sup>Biomedical Engineering, Tufts Univ., USA. We found a good agreement between the temporal dynamics of cerebral blood flow measured with diffuse correlation spectroscopy (DCS) and with near-infrared spectroscopy (NIRS) in conjunction with coherent hemodynamics spectroscopy (CHS).

JW3A.65

**Mechanisms of Vascular Function in Cerebrospinal Fluid Waste Metabolites Clearance Perivascular System**, Xinglei Liu<sup>1</sup>, Yiming Cheng<sup>1</sup>, James Haorah<sup>1</sup>, Kevin D. Belfield<sup>1</sup>; <sup>1</sup>New Jersey Inst. of Technology, USA. Through *in vivo* two-photon fluorescence microscopy experiments, the clearance of water-insoluble large size cerebrospinal fluid metabolites regulated by brain arterial endothelium and smooth muscle cells through perivascular dynamic exchange was studied.

JW3A.66

**Blood Flow Biomarkers Measured with Diffuse Correlation Spectroscopy Elucidate Mechanisms of Cognitive Dysfunction After Repetitive Concussion**, Levi Wood<sup>1</sup>, Alyssa Pybus<sup>2</sup>, Bharat Sanders<sup>2</sup>, Amanda Liew<sup>1</sup>, Erin Buckley<sup>2,3</sup>; <sup>1</sup>Biology, Georgia Inst. of Technology, USA; <sup>2</sup>Biomedical Engineering, Georgia Inst. of Technology and Emory Univ., USA; <sup>3</sup>Pediatrics, Emory Univ., USA. Using non-invasive diffuse correlation spectroscopy measurements of cerebral blood flow, we identify an early functional biomarker of cognitive outcome after repetitive concussion, and we explore potential pathological mechanisms of cognitive deficits.

JW3A.67

**High-throughput Optical Investigation into Intact Murine Brains**, Jian Ren<sup>1,2</sup>, Heejin Choi<sup>3</sup>, Kwanghun Chung<sup>3,4</sup>, Brett Bouma<sup>1,2</sup>; <sup>1</sup>Wellman Center for Photomedicine, Massachusetts General Hospital, Harvard, USA; <sup>2</sup>Harvard Medical School, USA; <sup>3</sup>Inst. for Medical Engineering and Science, MIT, USA; <sup>4</sup>Picower Inst. for Learning and Memory, MIT, Cambridge, USA. Coherent detection of scattered photon from complex biological systems has unique advantages. By controlling light scattering via tissue clearing, we developed a coherent imaging approach enabling label-free volumetric investigation of intact murine brains at high-throughput.

Wednesday, 4 April

NOTES

Large empty rectangular box for taking notes, containing horizontal lines.

## Atlantic Ballroom 1

Microscopy, Histopathology and Analytics

15:30–17:30

### MW4A • Confocal and Multimodal Microscopy

Presider: Milind Rajadhyaksha, Memorial Sloan Kettering Cancer Center, USA

MW4A.1 • 15:30 **Invited**

**Toward Smaller, More Useable Clinical Confocal Microscopes with Advanced Scanning and Integrated Wide-Field Guidance**, David L. Dickensheets<sup>1</sup>, Tianbo Liu<sup>1</sup>, Seth Kreitinger<sup>1</sup>, Gary Peterson<sup>2</sup>, Milind Rajadhyaksha<sup>2</sup>, <sup>1</sup>Montana State Univ., USA; <sup>2</sup>Memorial Sloan Kettering Cancer Center, USA. MEMS 3D scanning dramatically shrinks an instrument while preserving image quality, enabling pencil probes or endoscopic tools with the performance of benchtop instruments. An integrated wide-field camera provides real-time dermoscopic guidance during confocal sampling.

MW4A.2 • 16:00 **Invited**

**Spectrally Encoded Confocal Microscopy for Comprehensive and Low-cost In Vivo Cellular Imaging**, DongKyun Kang<sup>1</sup>, <sup>1</sup>College of Optical Sciences, Univ. of Arizona, USA. In spectrally encoded confocal microscopy (SECM), spectral spread of the imaging light is used to conduct line confocal imaging. Here we present various SECM devices and their uses in clinical applications.

## Atlantic Ballroom 2

Clinical and Translational Biophotonics

15:30–17:30

### CW4B • Techniques for Cardiovascular and Peripheral Vascular Disease Assessment

Presider: Hongki Yoo, Hanyang Univ., South Korea

CW4B.1 • 15:30 **Invited**

**Label-free Multimodal Intravascular Optical Imaging for Cardiovascular Disease**, Hongki Yoo<sup>1</sup>, <sup>1</sup>Hanyang Univ., Korea (the Republic of). We present multimodal intravascular optical imaging combining optical coherence tomography and fluorescence lifetime imaging. It can provide new opportunities to investigate vascular pathobiology and diagnose cardiovascular disease, by simultaneously visualizing plaque morphology and biochemical composition.

CW4B.2 • 16:00

**In Vivo Intravascular Photoacoustic Tomography for Depth-Resolved Lipid-Rich Plaque Assessment**, Yingchun Cao<sup>1,2</sup>, Ayeeshik Kole<sup>2,1</sup>, Jie Hui<sup>1</sup>, Michael Sturek<sup>2,1</sup>, Ji-Xin Cheng<sup>3,1</sup>, <sup>1</sup>Purdue Univ., USA; <sup>2</sup>Indiana Univ. School of Medicine, USA; <sup>3</sup>Boston Univ., USA. With a quasi-collinear imaging catheter and functional sheath material, we successfully implemented intravascular photoacoustic tomography for *in vivo* imaging of rabbit aorta, with localization and quantification analysis of lipid distribution in arterial walls.

CW4B.3 • 16:15

**Correlation Between Ulcer Healing and Vascular Hemodynamic Observed with Diffuse Optical Spectroscopy**, Alessandro Marone<sup>1</sup>, Jennifer W. Hoi<sup>1</sup>, Christopher Fong<sup>1</sup>, Youngwan Kim<sup>1</sup>, Hyun Keol Kim<sup>1</sup>, Danielle R. Bajakian<sup>1</sup>, Andreas H. Hielscher<sup>1</sup>, <sup>1</sup>Columbia Univ., USA. Patients affected by peripheral arterial disease are prone to have ulcers in their feet. The healing or worsening of these wounds are correlated with vascular hemodynamic changes observed with diffuse optical spectroscopy.

## Atlantic Ballroom 3

Optical Tomography and Spectroscopy

15:30–17:30

### OW4C • Technologies for Non-Invasive Optical in-Vivo Brain Imaging and Monitoring

Presider: Jana Kainerstorfer, Carnegie Mellon Univ., USA

OW4C.1 • 15:30 **Invited**

**Individualizing critical care delivery - New opportunities**, Daniel Licht<sup>1</sup>, <sup>1</sup>The Children's Hospital of Philadelphia, USA. The delivery of care for infants born with critical congenital malformations has moved beyond improving survival and is focused on improving long-term neurodevelopmental outcomes. Advanced optics now opens a rare opportunity to guide therapies for individual patients.

OW4C.2 • 16:00

**The BabyLux Device: Baseline Hemodynamic and Optical Properties of the Newborn Brain and the Reproducibility of the Measurements**, Martina Giovannella<sup>1</sup>, Bjørn Andresen<sup>2</sup>, Agnese De Carli<sup>3</sup>, Marco Pagliuzzi<sup>1</sup>, Monica Fumagalli<sup>3</sup>, Gorm Greisen<sup>2</sup>, Davide Contini<sup>4</sup>, Antonio Pifferi<sup>4,5</sup>, Lorenzo Spinelli<sup>5</sup>, Turgut Durduran<sup>1,6</sup>, Udo M. Weigel<sup>7</sup>, Alessandro Torricelli<sup>4,5</sup>, <sup>1</sup>ICFO, Spain; <sup>2</sup>Dept. of Neonatology, Rigshospitalet, Denmark; <sup>3</sup>Fondazione IRCCS Ca' Granda Ospedale Maggiore Policlinico, Italy; <sup>4</sup>Dip di Fisica, Politecnico di Milano, Italy; <sup>5</sup>Istituto di Fotonica e Nanotecnologie, Consiglio nazionale delle ricerche, Italy; <sup>6</sup>Institució Catalana de Recerca i Estudis Avançats (ICREA), Spain; <sup>7</sup>HemoPhotonics S.L., Spain. We present reproducibility of baseline hemodynamic and optical properties of the newborn brain measured with the BabyLux device that integrates diffuse correlation spectroscopy and time resolved near infrared spectroscopy. We compare experimental results with simulations.

OW4C.3 • 16:15

**Intracranial Pressure Changes Derived from Near Infrared Spectroscopy Measurements in Non-Human Primates**, Alexander Ruesch<sup>1</sup>, Samantha Schmitt<sup>2</sup>, Jason Yang<sup>1</sup>, Matthew A. Smith<sup>2,3</sup>, Jana M. Kainerstorfer<sup>1,3</sup>, <sup>1</sup>Dept. of Biomedical Engineering, Carnegie Mellon Univ., USA; <sup>2</sup>Dept. of Ophthalmology, Eye and Ear Inst., Univ. of Pittsburgh, USA; <sup>3</sup>Center for the Neural Basis of Cognition, USA. Measuring intracranial pressure (ICP) is a highly invasive procedure. We show ICP changes calculated from non-invasive near-infrared spectroscopy-measured hemodynamics, using non-parametric transfer function analysis in a hydrocephalus model on non-human primates.

## Grand Ballroom West

Optical Tomography and Spectroscopy

15:30–17:30

### OW4D • Photoacoustic Tomography, Microscopy and Endoscopy

Presider: Muyinatu Lediju Bell, Johns Hopkins Univ., USA

OW4D.1 • 15:30 **Invited**

**Photoacoustic Spectroscopy to Guide Cardiovascular Interventions**, Gijs van Soest<sup>1</sup>, Sophies Iskander-Rizk<sup>1</sup>, Min Wu<sup>2</sup>, Antonius van der Steen<sup>1,3</sup>, Pieter Kruijnga<sup>1,3</sup>, <sup>1</sup>Thoraxcenter Erasmus MC, Netherlands; <sup>2</sup>Eindhoven Univ. of Technology, Netherlands; <sup>3</sup>ImPhys, Delft Univ. of Technology, Netherlands. Photoacoustic imaging combines deep-viewing ultrasonic imaging with chemically specific optical contrast. I will discuss how endogenous tissue contrast can be used for guiding cardiovascular interventions, capitalizing on specific absorption contrasts associated with pathology and therapeutic effect.

OW4D.2 • 16:00

**Innovative Approach For Including Dual Mode Ultrasound And Volumetric Imaging Capability Within A Medical Photoacoustic Imaging Camera System**, Navalgund Rao<sup>2</sup>, Francis Kalloor<sup>3</sup>, Bhargava Chinni<sup>1</sup>, Zichao Han<sup>2</sup>, Vikram Dogra<sup>1</sup>, <sup>1</sup>Univ. of Rochester, USA; <sup>2</sup>Imaging Sciences, Rochester Inst. of Technology, USA; <sup>3</sup>Dept. of Electrical Engineering, Indian Inst. of Technology, India. Acoustic lens based focusing enables affordable fabrication of a photoacoustic imaging camera. We describe further innovations that add volumetric imaging and co-registered dual mode ultrasound to the existing photoacoustic system.

OW4D.3 • 16:15

**Accelerated Time Domain Quantitative Photoacoustic Tomography (TD-qPAT) based on Graphic Processing Units (GPU) for Clinical Application of Breast Cancer Imaging**, Tianqi Shan<sup>1</sup>, <sup>1</sup>Univ. of Florida, USA. We present a GPU-based method to accelerate the image reconstruction using TD-qPAT, reducing the reconstruction time from days to minutes and making it feasible as a powerful tool in clinical applications of breast cancer imaging.

## Atlantic Ballroom 1

Microscopy, Histopathology and Analytics

## MW4A • Confocal and Multimodal Microscopy—Continued

MW4A.3 • 16:30

**Multimodal Confocal Imaging of Renal Fine Needle Aspiration Samples**, Xin Feng<sup>1</sup>, Peter R. Jermain<sup>1</sup>, Anna N. Yaroslavsky<sup>1</sup>; <sup>1</sup>Univ. of Massachusetts Lowell, USA. Methylene Blue (MB) stained cancer and normal human renal cells were imaged using multimodal confocal microscopy. The results indicate that fluorescence polarization of MB is significantly higher in cancer cells as compared to normal.

MW4A.4 • 16:45

**Multi-Spectral Imaging of Rare-Earth-Doped Nanoparticles Using Line-Scanning Confocal Microscopy**, Carolina Bobadilla Mendez<sup>1</sup>, Harini Kantamneni<sup>1</sup>, Vidya Ganapathy<sup>1</sup>, Mei Chee Tan<sup>2</sup>, Prabhas V. Moghe<sup>1</sup>, Mark C. Pierce<sup>1</sup>; <sup>1</sup>Rutgers Univ., USA; <sup>2</sup>Engineering Product Development, Singapore Univ. of Technology and Design, Singapore. We demonstrate the ability of multi-spectral confocal microscopy to distinguish the visible upconversion emissions from erbium- and thulium-doped nanoparticles under 980 nm illumination in breast cancer cell lines.

MW4A.5 • 17:00 **Invited**

**Integrated Multimodality Microscopy and Confocal Raman Spectroscopy for In Vivo Skin Evaluation and Diagnosis**, Haishan Zeng<sup>2,1</sup>; <sup>1</sup>Imaging Unit - Integrative Oncology Dept., BC Cancer Agency Research Centre, Canada; <sup>2</sup>Dermatology and Skin Science, Univ. of British Columbia, Canada. We developed an integrated system for label-free *in-vivo* skin morphology and biochemical analysis. It provides simultaneous, co-registered reflectance confocal microscopy and multiphoton microscopy imaging and performs targeted Raman spectroscopy of interested microstructures under imaging guidance.

## Atlantic Ballroom 2

Clinical and Translational Biophotonics

## CW4B • Techniques for Cardiovascular and Peripheral Vascular Disease Assessment—Continued

CW4B.4 • 16:30

**Label-free Fluorescence Lifetime Imaging for Assessment of Carotid Artery Grafts**, Alba Alfonso Garcia<sup>1</sup>, Anne K. Haudenschild<sup>1</sup>, Laura Marcu<sup>1</sup>; <sup>1</sup>Univ. of California Davis, USA. Fluorescence lifetime imaging via a fiber-optic interface quantitatively differentiates biochemical composition of porcine carotid arteries originating from anatomical location and freeze-thaw processing. This work provides a framework for future non-destructive evaluation of vascular grafts *in-vivo*.

CW4B.5 • 16:45

**Intraoperative Assessment of Blood Coagulability using Coherence-gated Light Scattering**, Jose Guzman-Sepulveda<sup>1</sup>, William M. DeCamp<sup>1,2,3</sup>, Aristide Dogariu<sup>1</sup>; <sup>1</sup>CREOL, The College of Optics and Photonics, Univ. of Central Florida, USA; <sup>2</sup>College of Medicine, Univ. of Central Florida, USA; <sup>3</sup>Pediatric Cardiothoracic Surgery, The Heart Center, Arnold Palmer Hospital for Children, USA. We developed an optical technique capable of measuring *in-vivo* the coagulation status of blood. This technique is fiber optic-based, non-invasive, and permits continuous, in-line assessment of blood condition during clinical procedures such as cardiovascular surgery.

CW4B.6 • 17:00

**Monitoring Surgical Intervention in PAD Patients with Diffuse Optical Spectroscopy – Initial Case Studies**, Jennifer W. Hoi<sup>1</sup>, Christopher J. Fong<sup>1</sup>, Youngwan Kim<sup>1</sup>, Alessandro Marone<sup>1</sup>, Hyun K. Kim<sup>1</sup>, Danielle R. Bajakian<sup>1</sup>, Andreas H. Hielscher<sup>1</sup>; <sup>1</sup>Columbia Univ., USA. We present initial results from monitoring surgical interventions in peripheral-artery-disease (PAD) patients with diffuse optical spectroscopy (DOS). DOS measures show promise as an early predictor of treatment success.

## Atlantic Ballroom 3

Optical Tomography and Spectroscopy

## OW4C • Technologies for Non-Invasive Optical in-Vivo Brain Imaging and Monitoring—Continued

OW4C.4 • 16:30

**Validation of a Hyperspectral NIRS Method for Measuring Oxygen Saturation by Comparison to Time-Resolved NIRS**, Matthew D. Kewin<sup>1,2</sup>, Daniel F. Milej<sup>1,2</sup>, Androu Abdalmalak<sup>1,2</sup>, Ajay Rajaram<sup>1,2</sup>, Mamadou Diop<sup>1,2</sup>, Sandrine de Ribaupierre<sup>3,2</sup>, Keith St. Lawrence<sup>1,2</sup>; <sup>1</sup>Medical Biophysics, Univ. of Western Ontario, Canada; <sup>2</sup>Lawson Health Research Inst., Canada; <sup>3</sup>Clinical Neurological Sciences, Univ. of Western Ontario, Canada. A validation study was conducted to show that broadband NIRS could measure similar changes in cerebral oxygen saturation as time-resolved NIRS. Experiments were conducted in piglets in which inhaled oxygen was progressively decreased.

OW4C.5 • 16:45

**A Diffuse Optical Tomography System for Whole-Brain Functional Imaging in Mice Using Multiple Camera Views**, Zachary Markow<sup>1</sup>, Matthew D. Reisman<sup>2</sup>, Adam Q. Bauer<sup>3</sup>, Adam T. Eggebrecht<sup>3</sup>, Mark A. Anastasio<sup>2</sup>, Joseph P. Culver<sup>4</sup>; <sup>1</sup>Biomedical Engineering, Washington Univ. in St. Louis, USA; <sup>2</sup>Physics, Washington Univ. in St. Louis, USA; <sup>3</sup>Radiology, Washington Univ. in St. Louis, USA; <sup>4</sup>Radiology, Biomedical Engineering, Physics, Washington Univ. in St. Louis, USA; <sup>5</sup>Biomedical Engineering, Electrical and Systems Engineering, Radiology, Radiation Oncology, Washington Univ. in St. Louis, USA. A diffuse optical tomography system was constructed for noninvasively imaging blood and calcium contrasts related to neural activity throughout the whole mouse brain. System design, measurement registration, imaging methods, and simulated imaging performance are discussed.

OW4C.6 • 17:00

**Diffusive Reflectance Spectroscopy to Enhance Safety during Brain Biopsy Procedure**, Fabien Picot<sup>1</sup>, Andréanne Goyette<sup>1</sup>, Julien Pichette<sup>1</sup>, Marie-André Tremblay<sup>1</sup>, Joannie Desroches<sup>1</sup>, Sami Obaid<sup>2</sup>, Simon Lessard<sup>2</sup>, Gilles Soulez<sup>2</sup>, Frederic Leblond<sup>1</sup>; <sup>1</sup>Ecole Polytechnique de Montreal, Canada; <sup>2</sup>Centre de Recherche du Centre Hospitalier de l'Université de Montréal, Canada. To address the risk of bleeding during brain biopsy procedure, we propose an integrated imaging system based on diffusive reflectance spectroscopy. An *in vivo* experiment was conducted on swine's brain to validate it, using computational tomography (CT) as our Gold Standard.

## Grand Ballroom West

Optical Tomography and Spectroscopy

## OW4D • Photoacoustic Tomography, Microscopy and Endoscopy—Continued

OW4D.4 • 16:30

**Quantification of Chromophore Concentrations from Multispectral 3D Photoacoustic Images Using an Adjoint Monte-Carlo-based Inversion**, Jens Buchmann<sup>1</sup>, Bernhard Kaplan<sup>2</sup>, Samuel Powell<sup>3</sup>, Steffen Prohaska<sup>2</sup>, Jan Lauffer<sup>4</sup>; <sup>1</sup>Institut für Optik und Atomare Physik, Technische Universität Berlin, Germany; <sup>2</sup>Zuse Institut Halle-Wittenberg, Germany. An adjoint Monte-Carlo model was used to recover absolute chromophore concentrations and their ratios from 3D photoacoustic (PA) images. The method is an important step towards functional quantitative PA tomography (qPAT) in deep tissue.

OW4D.5 • 16:45

**Image Enhancement in Acoustic Resolution Photoacoustic Angiography**, Pavel Subochev<sup>1</sup>, Irina Mikhaylova<sup>1</sup>, Ekaterina Smolina<sup>1</sup>, Valeriya Perekatova<sup>1</sup>, Mikhail Kirillin<sup>1</sup>, Anna Orlova<sup>1</sup>, Ilya Turchin<sup>1</sup>; <sup>1</sup>Institute of Applied Physics, Russia. Acoustic resolution photoacoustic microscopy (AR-PAM) at 532 nm optical wavelength is an efficient raster-scan imaging technique allowing high contrast visualization of blood vessels. The talk will review our recent experience in AR-PAM angiography image enhancement.

OW4D.6 • 17:00

**Analysis of Reconstruction Errors in Photoacoustic Tomography with Negatively Focused Ultrasound Detectors**, Gilad Drozdov<sup>1</sup>, Amir Rosenthal<sup>1</sup>; <sup>1</sup>Technion Israel Inst. of Technology, Israel. We analyze the response of negatively focused acoustic detectors in both time and frequency domains and show how the approximations made in the virtual detector approach lead to image distortion and artifacts.

### Atlantic Ballroom 1

Microscopy, Histopathology and Analytics

**MW4A • Confocal and Multimodal Microscopy—Continued**

### Atlantic Ballroom 2

Clinical and Translational Biophotonics

**CW4B • Techniques for Cardiovascular and Peripheral Vascular Disease Assessment—Continued**

**CW4B.7 • 17:15**  
Non-invasive Cardiovascular Disease Assessment with Miniaturized Multi-beam Laser Doppler Vibrometry, Yanlu Li<sup>1,2</sup>, Stephen Greenwald<sup>3</sup>, Daniela Tommasin<sup>4</sup>, Jinghao Zhu<sup>1,2</sup>, Patrick Segers<sup>4</sup>, Soren Aasmul<sup>5</sup>, Mirko de Melis<sup>5</sup>, Matthieu Duperron<sup>6</sup>, Peter O'Brien<sup>6</sup>, Ralf Schüler<sup>7</sup>, Roel Baets<sup>1,2</sup>; <sup>1</sup>Photonics Research Group, Ghent Univ.-imec, Belgium; <sup>2</sup>Center for Nano- and Biophotonics, Ghent Univ., Belgium; <sup>3</sup>Blizard Inst., Queen Mary Univ. of London, UK; <sup>4</sup>IBiTech-bioMMeda, Ghent Univ., Belgium; <sup>5</sup>Medtronic Bakken Research Center, Netherlands; <sup>6</sup>Photonic Packaging Group, Tyndall National Inst., Ireland; <sup>7</sup>SIOS Messtechnik GmbH, Germany. A miniaturized 2x6-beam laser Doppler vibrometry sensor for non-invasive detection of cardiovascular disease is demonstrated. The pulse wave velocity is retrieved from preliminary experiments both on phantoms and on human subjects.

### Atlantic Ballroom 3

Optical Tomography and Spectroscopy

**OW4C • Technologies for Non-Invasive Optical in-Vivo Brain Imaging and Monitoring—Continued**

**OW4C.7 • 17:15**  
NeuroDOT: A New Neuroimaging Toolbox for DOT, David Muccigrosso<sup>1</sup>, Joseph P. Culver<sup>1</sup>, Adam T. Eggebrecht<sup>1</sup>; <sup>1</sup>Washington Univ. School of Medicine, USA. NeuroDOT provides a MATLAB-based self-contained toolbox that addresses common challenges in processing of functional near infrared spectroscopy (fNIRS) and diffuse optical tomography (DOT) data and supports multiple common pre-processing and analytical pipelines.  
Plenary Room

### Grand Ballroom West

Optical Tomography and Spectroscopy

**OW4D • Photoacoustic Tomography, Microscopy and Endoscopy—Continued**

**OW4D.7 • 17:15**  
Single-Cell Optical-Resolution Photoacoustic Microscopy, Yizhi Liang<sup>1</sup>, Chao Liu<sup>1</sup>, Long jin<sup>2</sup>, Li-dai Wang<sup>1</sup>; <sup>1</sup>City Univ. of Hong Kong, Hong Kong; <sup>2</sup>Jinan Univ., China. We present the development of single-cell photoacoustic microscopy. A multi-wavelength laser source is developed with 2-MHz pulse repetition rate, 220-ns wavelength switch time, and hundreds of nano-Joules pulse energy. We demonstrate in vivo photoacoustic imaging of single red blood cells.

**18:00–21:00 Dinner Cruise Event, Diplomat Beach Resort, Diplomat Landing, Marina Dock**  
(Advance Ticket Purchase Required)

Wednesday, 4 April

## Save the Date!

# Biophotonics Congress: Optics in the Life Sciences

15-17 April 2019

Loews Ventana Canyon Resort  
Tucson, Arizona, USA

Bio-Optics: Design and Application

Novel Techniques in Microscopy

Optical Molecular Probes, Imaging and Drug Delivery

Optical Trapping Applications

Optics and the Brain

[www.osa.org/lifesciencesOPC](http://www.osa.org/lifesciencesOPC)

## Grand Ballroom West

08:00–09:30

## JTh1A • Joint Plenary Session III

JTh1A.1 • 08:00 **Plenary**

**Unraveling the Origins of Endogenous Optical Metabolic Changes using a Multi-Parametric Approach**, Irene Georgakoudi<sup>1</sup>, Zhiyi Liu<sup>1</sup>, Dimitra Pouli<sup>1</sup>, Carlo Alonzo<sup>1</sup>, Antonio Varone<sup>1</sup>, Sevasti Karaliota<sup>2</sup>, Kyle P. Quinn<sup>1,3</sup>, Karl Munger<sup>2</sup>, Katia P. Karalis<sup>2</sup>; <sup>1</sup>Dept. of Biomedical Engineering, Tufts Univ., USA; <sup>2</sup>Biomedical Research Foundation, Academy of Athens, Greece; <sup>3</sup>Developmental, Molecular and Chemical Biology, Sackler School of Graduate Biomedical Sciences, Tufts Univ., USA; <sup>4</sup>Dept. of Biomedical Engineering, Univ. of Arkansas, USA. We report on the combined use of endogenous two-photon intensity and lifetime based fluorescence measurements to identify changes in specific metabolic pathways. Such functional insights can improve understanding of disease development and drug effects.

JTh1A.2 • 8:45 **Plenary**

**Using Optical Tweezers to Probe the Role of Tissue Biophysics in Metastasis**, Kandice Tanner, Laboratory of Cell Biology, Center for Cancer Research, National Institutes of Health, USA. Tumor latency and dormancy are obstacles in effective treatment of cancer. In the event of metastatic disease, emergence of a lesion can occur at varying intervals from diagnosis and in some cases following successful treatment of the primary tumor. Genetic factors that drive metastatic progression have been identified, such as those involved in cell adhesion, signaling, extravasation and metabolism. Is there a difference in strategy to facilitate outgrowth? Why is there a difference in latency? One missing cue may be the role of tissue biophysics of the brain microenvironment on the infiltrated cells. Here I discuss using optical tweezer based active microrheology to measure the mechanical cues that may influence disseminated tumor cells in different organ microenvironment. I further discuss in vitro and in vivo preclinical models such as 3D culture systems and zebrafish in efforts of providing novel targeted therapeutics.

09:30–10:00 Coffee Break and Exhibits, Grand Ballroom East

## Atlantic Ballroom 1

Microscopy, Histopathology  
and Analytics

10:00–12:00

MTh2A • Computational  
Microscopy and Analysis

Presider: Anna Yaroslavsky,  
Harvard Medical School, USA

MTh2A.1 • 10:00 **Invited**

**A Multiresolution Deep Learning Framework for Automated Annotation of Reflectance Confocal Microscopy Images**, Kivanc Kose<sup>1</sup>, Alican Bozkurt<sup>3</sup>, Christi Alessi-Fox<sup>2</sup>, Melissa Gill<sup>4</sup>, Dana H. Brooks<sup>3</sup>, Jennifer G. Dy<sup>3</sup>, Milind M. Rajadhyaksha<sup>1</sup>; <sup>1</sup>Dermatology, Memorial Sloan Kettering Cancer Center, USA; <sup>2</sup>Caliber Imaging and Diagnostics, USA; <sup>3</sup>Electrical and Computer Engineering, Northeastern Univ., USA; <sup>4</sup>Skin Medical Research and Diagnostics, P.L.L.C., USA. Morphological tissue patterns in RCM images are critical in diagnosis of melanocytic lesions. We present a multiresolution deep learning framework that can automatically annotate RCM images for these diagnostic patterns with high sensitivity and specificity.

## Atlantic Ballroom 2

Clinical and Translational  
Biophotonics

10:00–12:00

## CTh2B • Clinical Spectroscopy

Presider: To be Determined

CTh2B.1 • 10:00 **Invited**

**Convergence of Nanoimaging and Biology: Can Engineering Lead to a Cancer Cure?**, Vadim . Backman<sup>1,2</sup>; <sup>1</sup>Biomedical Engineering, and Medicine, Northwestern Univ., USA; <sup>2</sup>Cancer and Physical Sciences, Robert H. Lurie Comprehensive Cancer Center, USA. Super-resolution optical nanoscopy and the physics-based modeling of gene expression can help decipher the gene expression code, elucidate early events in carcinogenesis, and lead to new cancer screening and physico-chemical approaches to anti-cancer therapy.

## Grand Ballroom West

Optics and the Brain

10:00–12:00

BTh2C • Brain Disorders:  
Mouse to Man

Presider: To be Determined

BTh2C.1 • 10:00

**Functional Recovery After Stroke is Negatively Influenced by Contralateral Homotopic Activity**, Adam Q. Bauer<sup>1</sup>, Andrew Kraft<sup>1</sup>, Grant A. Baxter<sup>1</sup>, Annie R. Bice<sup>1</sup>, Michael Bruchas<sup>1</sup>, Jin-Moo Lee<sup>1</sup>, Joseph P. Culver<sup>1</sup>; <sup>1</sup>Washington Univ. in St Louis, USA. We combined optogenetic targeting with optical intrinsic signal imaging to examine how contralateral activity in excitatory neurons affected functional recovery after stroke. Recovery was assessed through measures of cortical remapping, functional connectivity, and limb-use asymmetry.

BTh2C.2 • 10:15

**All-Optical Rehabilitation Promotes Motor Recovery in a Mouse Model of Stroke**, Emilia Conti<sup>1</sup>, Anna L. Allegra Mascaro<sup>1,2</sup>, Francesco Resta<sup>1</sup>, Leonardo Sacconi<sup>1,3</sup>, Maria Pasquini<sup>4</sup>, silvestro micera<sup>4,5</sup>, Francesco S. Pavone<sup>1,3</sup>; <sup>1</sup>LENS European Lab for non linear, Italy; <sup>2</sup>Neuroscience Inst., CNR, Italy; <sup>3</sup>National Inst. of Optics, Italy; <sup>4</sup>Istituto Superiore S'ant'Anna di Pisa, Italy; <sup>5</sup>Ecole Polytechnique Federale de Lausanne, Switzerland. Performing in vivo imaging on Thy1-GCaMP6f mice we want to investigate how the optical stimulation of the peri-infarct area impacts on motor recovery after stroke in the primary motor cortex.

## Atlantic Ballroom 3

Optical Tomography and  
Spectroscopy

10:00–12:00

OTh2D • Optical Coherence  
Tomography: Novel  
Applications

Presider: To be Determined

OTh2D.1 • 10:00 **Invited**

**Intra-operative Color Mapping of Brain Cancer Infiltration with Real-time Quantitative OCT**, Xingde Li<sup>1</sup>; <sup>1</sup>Johns Hopkins Univ., USA. We present recent updates on quantitative OCT for guiding brain cancer surgery in real time. Results from pilot intra-operative imaging of more than 20 human subject will be discussed.

## Atlantic Ballroom 1

Microscopy, Histopathology and Analytics

### MTh2A • Computational Microscopy and Analysis—Continued

**MTh2A.2 • 10:30** **Invited**  
**Machine Learning Enabled Computational Imaging and Sensing**, Aydogan .Ozcan<sup>1</sup>; <sup>1</sup>Univ. of California Los Angeles, USA. We provide an overview of some of our recent work on the use of machine learning techniques, including e.g., deep neural networks, in advancing computational imaging and sensing systems, also covering their biomedical applications.

**MTh2A.3 • 11:00**  
**The ImageJ Ecosystem: An Open and Extensible Platform for Biomedical Image Analysis**, Curtis T. Rueden<sup>1</sup>, Kevin Eliceiri<sup>1,2</sup>; <sup>1</sup>LOCI, Univ. of Wisconsin, USA; <sup>2</sup>Morgridge Institute for Research, USA. ImageJ is an image analysis program that features a recordable macro language, and extensible plug-in architecture. We describe new developments including a new plugin framework that enables more image formats, scripting languages, and enhanced visualization.

## Atlantic Ballroom 2

Clinical and Translational Biophotonics

### CTh2B • Clinical Spectroscopy—Continued

**CTh2B.2 • 10:30**  
**Characterization of Autism Spectrum Disorder by Functional Near Infrared Spectroscopy (fNIRS)**, Ulas Sunar<sup>1</sup>; <sup>1</sup>Wright State Univ., USA. We characterized autism spectrum disorder by hemodynamic parameters measured with functional near infrared spectroscopy (fNIRS).

**CTh2B.3 • 10:45**  
**Optical Guidance System for Deep Brain Stimulation Surgery – from Experimental Studies to Clinical Use**, Karin Wårdell<sup>1</sup>, Peter Zsigmond<sup>2</sup>, Johan Richter<sup>1,2</sup>, Simone Hemm<sup>3,1</sup>; <sup>1</sup>Dept. of Biomedical Engineering, Linköping Univ., Sweden; <sup>2</sup>Dept. of Neurosurgery and Clinical and Experimental Medicine, Linköping Univ., Sweden; <sup>3</sup>Inst. for Medical and Analytical Technologies, Univ. of Applied Sciences and Arts Northwestern Switzerland, Switzerland. Laser Doppler flowmetry has been adapted for optical guidance during stereotactic deep brain stimulation (DBS) surgery. It has been used in more than 130 DBS implantations. The necessary steps to go from experimental studies to clinical use in the neurosurgical setting are reviewed.

**CTh2B.4 • 11:00**  
**Withdrawn.**

**CTh2B.5 • 11:15**  
**Interstitial PDT in Brain Tumors - Investigations and Developments**, Ronald Sroka<sup>2,1</sup>, Niklas Markwardt<sup>2,1</sup>, Nikolas Dominik<sup>2,1</sup>, Herbert Stepp<sup>2,1</sup>, Adrian Rühm<sup>2,1</sup>; <sup>1</sup>Dept of Urology Ludwig-Maximilians-Universität München, Germany; <sup>2</sup>Laser-Forschungslabor LIFE Center, Germany. Malignant gliomas are a devastating brain tumor disease with very poor prognosis. Stereotactic approaches for light based techniques useful for taking biopsy, interstitial PDT and spectral monitoring during iPDT are presented.

## Grand Ballroom West

Optics and the Brain

### BTh2C • Brain Disorders: Mouse to Man—Continued

**BTh2C.3 • 10:30**  
**Multi-spectral Photoacoustic Tracking of Non-invasive Photothrombotic Ischemic Stroke**, Dene Ringuette<sup>1,2</sup>, Joshua Lockwood<sup>1</sup>, Adam C. Waspe<sup>3</sup>, Peter L. Carlen<sup>1,2</sup>, philippe monnier<sup>2,4</sup>, Ofer Levi<sup>1,5</sup>; <sup>1</sup>Inst. of Biomaterial and Biomedical Engineering, Univ. of Toronto, Canada; <sup>2</sup>Fundamental Neurobiology, Krembil Research Inst., Canada; <sup>3</sup>Dept. of Medical Imaging, Univ. of Toronto, Canada; <sup>4</sup>Dept. of Physiology, Univ. of Toronto, Canada; <sup>5</sup>The Edward S. Rogers Sr. Dept. of Electrical & Computer Engineering, Univ. of Toronto, Canada. Whole brain cross-sectional changes in blood oxygenation were tracked during focal murine ischemia. Arteriole-scale fast dynamics suggest local flow redistribution during stroke onset. Our results support the suitability of photoacoustic imaging for pre-clinical stroke research.

**BTh2C.4 • 10:45**  
**Optical Imaging in a Mouse Model of Glioma Identifies Different Causes for Proximal and Distal Disruptions to Functional Connectivity**, Inema Orukari<sup>1</sup>, Joshua S. Siegel<sup>2</sup>, Adam Q. Bauer<sup>3</sup>, Grant A. Baxter<sup>3</sup>, Joshua S. Shimony<sup>3</sup>, Joshua B. Rubin<sup>4</sup>, Joseph P. Culver<sup>1,3</sup>; <sup>1</sup>Biomedical Engineering, Washington Univ. in St Louis, USA; <sup>2</sup>Neurology, Washington Univ. in St Louis, USA; <sup>3</sup>Radiology, Washington Univ. in St Louis, USA; <sup>4</sup>Pediatrics, Washington Univ. in St Louis, USA. The relationship between glioma growth and functional connectivity disruptions is poorly understood. Functional connectivity optical intrinsic imaging enables assessment functional connectivity in a mouse model of glioma growth.

**BTh2C.5 • 11:00**  
**Near Infra-Red Spectroscopy (NIRS) in Urea Cycle Disorders and Typically Developing Children**, Fatima Chowdhry<sup>1</sup>, Andrea Gropman<sup>2</sup>, Afrouz Anderson<sup>1</sup>, Hadis Dashtestani<sup>1</sup>, Amir Ganjibakche<sup>1</sup>; <sup>1</sup>National Insts of Health, USA; <sup>2</sup>Childrens National Medical Center, USA. To test whether NIRS can be used to monitor cognitive brain function and detect markers for differentiation of neurocognitive variance in children with urea cycle disorders as compared to typically developing children who serve as controls.

**BTh2C.6 • 11:15**  
**Near Infrared Spectroscopy (NIRS) Reveals the Effect Epinephrine on Cerebral Oxygen Delivery and Metabolism During Cardiac Arrest**, Reyhaneh Nosrati<sup>1,2</sup>, Steve Lin<sup>3,4</sup>, Paul Dorian<sup>3,4</sup>, Vladislav Toronov<sup>1</sup>; <sup>1</sup>Physics, Ryerson Univ., Canada; <sup>2</sup>Sunnybrook Health Sciences Centre, Canada; <sup>3</sup>Keenan Research Centre of the Li Ka Shing Knowledge Inst., St. Michael's Hospital, Canada; <sup>4</sup>Univ. of Toronto, Canada. We studied the effect of epinephrine administration (bolus and continuous infusion) during cardiac arrest and resuscitation on 9 pigs using near infrared spectroscopy. Results showed only epinephrine boluses transiently improved cerebral oxygen delivery and metabolism.

## Atlantic Ballroom 3

Optical Tomography and Spectroscopy

### OTh2D • Optical Coherence Tomography: Novel Applications—Continued

**OTh2D.2 • 10:30**  
**Toward Interstitial Magnetic Hyperthermia Dosimetry via Magnetomotive Optical Coherence Elastography**, Pin-Chieh Huang<sup>1,2</sup>, Darold R. Spillman<sup>1</sup>, Boris Odintsov<sup>1</sup>, Nahil A. Sobh<sup>1,3</sup>, Stephen A. Bopp<sup>1,2</sup>; <sup>1</sup>Beckman Inst. for Advanced Science and Technology, Univ. of Illinois at Urbana-Champaign, USA; <sup>2</sup>Dept. of Bioengineering, Univ. of Illinois at Urbana-Champaign, USA; <sup>3</sup>Center for Nanoscale Science and Technology, Univ. of Illinois at Urbana-Champaign, USA. Magnetic hyperthermia (MH) dosage can be inferred by changes in heat-induced stiffness. A novel magnetomotive optical coherence elastography (MM-OCE) configuration is proposed, where the MH heating seed is also utilized to enable shear wave elastography.

**OTh2D.3 • 10:45**  
**Simultaneous Bright and Dark Field Optical Coherence Tomography Using Few-Mode Fiber Detection for Neuropathology Imaging**, Pablo Eugui<sup>1</sup>, Antonia Lichtenegger<sup>1</sup>, Marco Augustin<sup>1</sup>, Danielle Harper<sup>1</sup>, Martina Muck<sup>2</sup>, Thomas Roetzer<sup>2</sup>, andreas wartak<sup>1</sup>, Christoph K. Hitznerberger<sup>1</sup>, Adelheid Woehrer<sup>2</sup>, Bernhard Baumann<sup>1</sup>; <sup>1</sup>Medical Univ. of Vienna, Austria; <sup>2</sup>Inst. of Neurology, Medical Univ. of Vienna, Austria. Few-mode fibers enable single-shot bright and dark field (BRAD) detection for OCT by collecting the backscattered light into different fiber modes. We demonstrate BRAD imaging with enhanced contrast for characterizing ex vivo tumorous tissue.

**OTh2D.4 • 11:00**  
**Dual-modality Optical Spectroscopy and Optical Coherence Tomography Ablation Catheter for Intra-procedural Assessment of Cardiac Lesion Development**, Rajinder P. Singh-Moon<sup>1</sup>, Xinwen Yao<sup>2</sup>, Mohammad Zaryab<sup>1</sup>, Vivek Iyer<sup>1</sup>, Christine Hendon<sup>1</sup>; <sup>1</sup>Columbia Univ., USA; <sup>2</sup>John Hopkins Univ., USA. We report the development of a dual-modal ablation catheter incorporating optical coherence tomography (OCT) and optical spectroscopy (OS) for improved assessment of acute endocardial ablation lesions. Validation is performed in ex vivo and in vivo porcine experimental models.

**OTh2D.5 • 11:15**  
**High-throughput Optical Coherence Tomography Imaging for Drug Screening with 3D Tumor Spheroids**, Yongyang Huang<sup>1</sup>, Qiongyu Guo<sup>1</sup>, Jinyun Zou<sup>1</sup>, Xiaofang Wang<sup>1</sup>, Steven Titus<sup>2</sup>, Marc Ferrer<sup>2</sup>, Chao Zhou<sup>1</sup>; <sup>1</sup>Electrical & Computer Engineering, Lehigh Univ., USA; <sup>2</sup>National Center for Advancing Translational Sciences, National Insts of Health, USA. We developed an ultrahigh-speed optical coherence tomography system that was capable of performing live, longitudinal characterization of three-dimensional (3D) tumor spheroids for high-throughput screening (HTS) of anti-cancer drugs.

## Atlantic Ballroom 1

Microscopy, Histopathology and Analytics

### MTh2A • Computational Microscopy and Analysis—Continued

**MTh2A.4 • 11:30** **Invited**  
**Integration of Histocytometry and Bioinformatics: Leveraging Large Scale Bioimage Processing to Predict Patient Survival**, Andries Zijlstra<sup>1</sup>, Adel Eskaros<sup>1</sup>, Tatiana novitskaya<sup>1</sup>; <sup>1</sup>Pathology, Microbiology and Immunology, Vanderbilt Univ. Medical Center, USA. Digitization of histological stains in conjunction with computer-guided image analysis has enabled single-cell histocytometry of patient tissues. By implementing data-driven bioinformatics we leveraged this expanded dimension of cell profiling for clinical predictions.

## Atlantic Ballroom 2

Clinical and Translational Biophotonics

### CTh2B • Clinical Spectroscopy—Continued

**CTh2B.6 • 11:30** **Invited**  
**Biomedical Optics: From Bench to Bedside in Cancer Treatment**, Theo J. Ruers<sup>1</sup>; <sup>1</sup>Netherlands Cancer Inst., Netherlands. During cancer surgery tumor resection margins are often difficult to define. Here we present the concept of image guided surgery by means of optical imaging tools using diffuse reflectance spectroscopy, showing accuracies of over 90%

## Grand Ballroom West

Optics and the Brain

### BTh2C • Brain Disorders: Mouse to Man—Continued

**BTh2C.7 • 11:30**  
**Monitoring Cerebral Blood Flow And Oxygenation During Cardiac Surgery**, Parisa Farzam<sup>1</sup>, Stefan Carp<sup>1</sup>, Juliette Selb<sup>1,3</sup>, Parya Farzam<sup>1</sup>, Melissa Wu<sup>1</sup>, Maria Franceschini<sup>1</sup>, Jason Z. Qu<sup>2</sup>; <sup>1</sup>Harvard Medical School, Massachusetts General Hospital, USA; <sup>2</sup>Dept. of Anesthesia, Critical Care and Pain Medicine, Massachusetts General Hospital, USA; <sup>3</sup>Neurophotonics Center, Biomedical Engineering Dept., Boston Univ., USA. Brain injury is a devastating adverse event of cardiac surgery due to compromised blood supply to the brain. This study uses optical techniques to monitor cerebral hemodynamics during cardiac surgery to continuously evaluate brain perfusion

**BTh2C.8 • 11:45**  
**Fluorescence Guidance for Brain Tumor Biopsies**, Neda Haj-Hosseini<sup>1</sup>, Johan Richter<sup>1,2</sup>, Lisa Kobayashi Frisk<sup>1</sup>, Peter Milos<sup>2</sup>, Martin Hallbeck<sup>3</sup>, Karin Wårdell<sup>1</sup>; <sup>1</sup>Dept. of Biomedical Engineering, Linköping Univ., Sweden; <sup>2</sup>Dept. of Neurosurgery and Dept. of Clinical and Experimental Medicine, Linköping Univ. Hospital, Sweden; <sup>3</sup>Dept. of Pathology and Dept. of Clinical and Experimental Medicine, Linköping Univ., Sweden. To provide guidance during stereotactic biopsy in brain tumors, fluorescence spectroscopy was used in ten patients. It was shown that the fiber optical probe could provide real-time guidance with clear fluorescence in all patients.

## Atlantic Ballroom 3

Optical Tomography and Spectroscopy

### OTH2D • Optical Coherence Tomography: Novel Applications—Continued

**OTH2D.6 • 11:30**  
**Characterization of Human Endomyocardium Using a Human Cardiac Optical Coherence Tomography Atlas**, Yu Gan<sup>1</sup>, Theresa Lye<sup>1</sup>, Xinwen Yao<sup>1</sup>, Charles Marboe<sup>2</sup>, Christine Hendon<sup>1</sup>; <sup>1</sup>Electrical Engineering, Columbia Univ., USA; <sup>2</sup>Departement of Pathology and cell biology, Columbia Univ. Medical Center, USA. We present a human cardiac optical coherence tomography atlas. The atlas enables characterization of key features of the human endomyocardial anatomy, which could be used to identify substrates for guidance of intracardiac procedures.

**OTH2D.7 • 11:45**  
**Human Retinal Imaging by Visible-light Optical Coherence Tomography**, Hao F. Zhang<sup>1</sup>, Xiao Shu<sup>1</sup>, Siyu Chen<sup>1</sup>, Wenzhong Liu<sup>2</sup>, Amani Fawzi<sup>1</sup>; <sup>1</sup>Northwestern Univ., USA; <sup>2</sup>Opticent Health, USA. We developed visible-light optical coherence tomography ophthalmoscope for *in vivo* human retinal imaging, which reveals both high resolution anatomical structure and functional hemodynamic information of retinal tissue.

---

12:00–13:30 Lunch Break, *On Your Own*

---

---

12:00–13:30 Workshop: Understanding Unconscious Bias, *(OSA Members Only; RSVP required)*

---

13:30–15:30

## JTh3A • Poster Session III, Coffee Break and Exhibits

## JTh3A.1

**An Indexing Method Based on Diffuse Optical Spectroscopy for Surface Identification of Livers with Parenchymal Fibrosis Stages Unacceptable for Transplantation**, Daqing (Daching) Piao<sup>1</sup>, Halen Borron<sup>2</sup>, Alan Hawxby<sup>3</sup>, Harlan Wright<sup>4</sup>, Erin Rubin<sup>5</sup>, <sup>1</sup>Oklahoma State Univ., USA; <sup>2</sup>College of Medicine, Univ. of Oklahoma Health Sciences Center, USA; <sup>3</sup>Oklahoma Transplant Center, USA; <sup>4</sup>Dept. of Pathology, Univ. of Oklahoma Health Sciences Center, USA. Surface diffuse optical spectroscopy was used to assess 12 livers rejected from transplantation. A quantitation method correctly distinguished all 3 livers with the Ishak fibrosis stages  $\geq 2$  in the presence of various other pathologies.

## JTh3A.2

Withdrawn.

## JTh3A.3

**A Mobile Phone Based Reflectance Pulse Oximeter**, Morris D. Vanegas<sup>1</sup>, Bernhard B. Zimmermann<sup>2</sup>, Sule Sahin<sup>1</sup>, Stefan Carp<sup>2</sup>, Qianqian Fang<sup>3</sup>, <sup>1</sup>Northeastern Univ., USA; <sup>2</sup>Martinos Center for Biomedical Imaging, Massachusetts General Hospital, USA. We report a mobile-phone based reflectance pulse oximeter for use in resource-poor regions. The developed prototype was validated against a reference device in a breath-holding study.

## JTh3A.4

**Intact Primate Brain Tissue Identification Using a Completely Fibered Coherent Raman Spectroscopy System**, Damon DePaoli<sup>1,2</sup>, Nicolas Lapointe<sup>1,2</sup>, Younes Messaddeq<sup>2</sup>, Martin Parent<sup>1</sup>, Daniel Côté<sup>1,2</sup>, <sup>1</sup>CERVO Brain Research Center, Université Laval, Canada; <sup>2</sup>Centre d'optique, photonique et laser, Université Laval, Canada. Using a portable fiber-laser, we present CARS spectroscopy at the tip of a commercial silica optical fiber. Validating the system's utility, we show the delineation of brain tissue types, at high speeds, along mock deep brain stimulation electrode trajectories in primates.

## JTh3A.5

**Effect of Optical Coherence Tomography Resolution on the Assessment of Dental Enamel Indications**, Christine C. Sahyoun<sup>1</sup>, Hresh M. Subhash<sup>2</sup>, Deborah Peru<sup>2</sup>, Roger Ellwood<sup>2</sup>, Lynette Zaidel<sup>2</sup>, LaTonya Kilpatrick<sup>2</sup>, Mark C. Pierce<sup>1</sup>, <sup>1</sup>Biomedical Engineering, Rutgers, The State Univ. of New Jersey, USA; <sup>2</sup>Colgate-Palmolive Company, USA. We have implemented optical coherence tomography with different light sources and imaging optics to provide varying spatial resolution and field-of-view. We examined the impact of these parameters on visualization and quantification of dental enamel indications.

## JTh3A.6

**Tissue Oxygenation Maps of Diabetic Foot Ulcers: Longitudinal Studies**, Cristianne M. Fernandez<sup>1</sup>, Rebecca J. Kwasinski<sup>1</sup>, Kevin Leiva<sup>1</sup>, Richard Schutzman<sup>1</sup>, Edwin Robledo<sup>1</sup>, Penelope Kallis<sup>2</sup>, Luis Borda<sup>2</sup>, Francisco Perez-Clavijo<sup>3</sup>, Robert Kirsner<sup>4</sup>, Anuradha Godavarty<sup>5</sup>, <sup>1</sup>Florida International Univ., USA; <sup>2</sup>Univ. of Miami, USA; <sup>3</sup>Podiatry Care Partners, USA. Near Infrared (NIR) imaging was performed on diabetic foot ulcers to obtain 2D tissue oxygenation maps during longitudinal studies of wound healing. The difference in wound to periwound's oxygenation became insignificant as the wound healed.

## JTh3A.7

**Evaluating the Aging of the Scars After Cancer Removal by Using Multispectral Diagnostic Device**, Marta Lange<sup>1</sup>, Emilija Vija Plorina<sup>1</sup>, Aleksandrs Derjabo<sup>1</sup>, Ilze Lihacova<sup>1</sup>, Ilze Osina<sup>1</sup>, Dmitrijs Bliznuks<sup>2</sup>, Janis Spigulis<sup>1</sup>, <sup>1</sup>Univ. of Latvia, Latvia; <sup>2</sup>Riga Technical Univ., Latvia; <sup>3</sup>Oncology Centre of Latvia, Riga Eastern Univ. Hospital, Latvia. An evaluation of scars after removal of skin lesions was performed using custom-made diagnostic device with auto-fluorescence principle at 405nm LED excitation. Trend of increasing intensity ratio of AF in scars with age was observed.

## JTh3A.8

**The Complex Evaluation of Breast Cancer Metabolism and Blood Supply in Neoadjuvant Polychemotherapy**, Mikhail V. Pavlov<sup>1</sup>, Tatyana Kalganova<sup>2</sup>, German Golubiatnikov<sup>3</sup>, Vladimir Plekhanov<sup>3</sup>, Anna Orlova<sup>3</sup>, Pavel Rykhtik<sup>1</sup>, Lubov Shkalova<sup>1</sup>, Ilya Turchin<sup>3</sup>, Natalia Shakhova<sup>3</sup>, Anna Maslennikova<sup>2,4</sup>, <sup>1</sup>Volga Region Medical Center, Russia; <sup>2</sup>State Medical Academy, Russia; <sup>3</sup>Inst. of Applied Physics RAS, Russia; <sup>4</sup>Lobachevsky State Univ., Russia. Dynamics of breast tumor's oxygenation and tumor blood flow during neoadjuvant chemotherapy was determined by diffuse optical spectroscopy and ultrasound investigation. Oxygenation and blood flow dynamics demonstrated variable changes depending on tumor response.

## JTh3A.9

Withdrawn.

## JTh3A.10

**Novel Multifunctional Porphyrine Pigments for Bimodal Tumor Diagnostics, Photodynamic Therapy and Real Time Monitoring of Its Progress by Intracellular Viscosity Sensing**, Larisa Klaphina<sup>1,2</sup>, <sup>1</sup>Inst. of Organometallic Chemistry, Russia; <sup>2</sup>Biology, N.I. Lobachevsky State Univ., Nizny Novgorod, Russia, Russia. We report a series of novel red-emitting cyananyl porphyrine pigments which are found to be an excellent platform for bimodal tumor diagnostic agents and intracellular viscosity sensors. They also work as efficient PDT sensitizers upon irradiation with red light.

## JTh3A.11

**Breath Hold Paradigm Assesses Regions of Reduced Oxygenation in Diabetic Foot Ulcers**, Kevin Leiva<sup>1</sup>, Jagadeesh Mahadevan<sup>1</sup>, Kacie Kaile<sup>1</sup>, Richard Schutzman<sup>1</sup>, Edwin A. Robledo<sup>1</sup>, Dinesh Khandavilli<sup>1</sup>, Sivakumar Narayanan<sup>2</sup>, Varalakshmi Muthukrishnan<sup>2</sup>, Mohan Viswanathan<sup>2</sup>, Anuradha Godavarty<sup>3</sup>, <sup>1</sup>Florida International Univ., USA; <sup>2</sup>Dr. Mohan Diabetes Specialties Centre, India. Tissue oxygenation varied in diabetic foot ulcers compared to controls as assessed from temporal changes with respect to a breath hold paradigm. Clinical application of this approach can assess extent of healing of DFUs.

## JTh3A.12

**A Rotatable Trans-rectal Probe for Simultaneous Ultrasound and Optical Imaging of Prostate**, Hyun Keol Kim<sup>1</sup>, Jong hwan Lee<sup>1</sup>, Emerson Lim<sup>1</sup>, andrea Hielscher<sup>1</sup>, <sup>1</sup>COLUMBIA UNIV., USA. We present a novel rotatable trans-rectal probe coupled with commercial trans-rectal ultrasound (TRUS) probe, which allows for simultaneous bimodal imaging of prostate with near-infrared light and ultrasound.

## JTh3A.13

**A 12-wavelength NIR Spectral Tomography (NIRST) System for Monitoring Breast Tumor Response to Neoadjuvant Chemotherapy**, Shudong Jiang<sup>1</sup>, Yan Zhao<sup>1</sup>, Xu Cao<sup>1,2</sup>, Erica B. Bernhardt<sup>1</sup>, Peter A. Kaufman<sup>1</sup>, Brian W. Pogue<sup>1</sup>, Keith D. Paulsen<sup>1</sup>, <sup>1</sup>Dartmouth College, USA; <sup>2</sup>School of Life Sciences and Technology, Xidian Univ., China. The total data acquisition time of simultaneous acquisition involving six FD and six CW wavelengths are less than 100 seconds. 10 patients who undergoing Neoadjuvant Chemotherapy have been imaged by this system.

## JTh3A.14

**Molecular Imaging of Breast Cancer and Retina by Means of Raman Spectroscopy and Chemometrics**, Mónica Marro Sánchez<sup>1</sup>, Pablo Loza-Álvarez<sup>2</sup>, <sup>1</sup>ICFO - The Inst. of Photonic Sciences, Spain. The interpretation of Raman spectra is complex for biomedical applications. We developed novel multivariate approaches based in Multivariate Curve Resolution and PLS-DA allowing us to study complex Raman images of retina neuroinflammation and breast cancer.

## JTh3A.15

**A Comparative Study Between Acid-etching and Er,Cr:YSGG Laser Irradiation on Enamel Surface Evaluated by OCT and SEM**, Daniela Lopes<sup>2</sup>, Claudia Mota<sup>2</sup>, Daisa Pereira<sup>1</sup>, Denise M. Zzell<sup>1</sup>, Anderson S. Gomes<sup>2</sup>, <sup>1</sup>Center for Lasers and Applications, IPEN - CNEN/SP, Brazil; <sup>2</sup>Physics Dept., UFPE, Brazil. This study aimed to evaluate the effects of Er,Cr:YSGG laser irradiation and acid-etching on enamel surface, aiming to improve the bond strength between enamel and composite materials, through optical coherence tomography and scanning electron microscopy.

## JTh3A.16

**A Comprehensive Analytical Based Computational Technique for Laser Induced Heat in a Gold Nano-particle Embedded Turbid Medium**, Hakan Erkol<sup>1</sup>, Farouk Nouzi<sup>1</sup>, alex luk<sup>1</sup>, Mehrnaz Mehrabi<sup>1</sup>, Burcin Unlu<sup>2</sup>, gultekin gulsen<sup>1</sup>, <sup>1</sup>Univ. of California, Irvine, USA; <sup>2</sup>Physics, Bogazici Univ., Turkey. We present a computational method to provide laser parameters determining the increase in temperature for thermal therapy applications.

## JTh3A.17

**A Dual-Mesh Monte Carlo Algorithm Using a Coarse Tetrahedral Mesh and Voxel Output**, Shijie Yan<sup>1</sup>, Anh Phong Tran<sup>2</sup>, Qianqian Fang<sup>3,1</sup>, <sup>1</sup>Electrical and Computer Engineering, Northeastern Univ., USA; <sup>2</sup>Chemical Engineering, Northeastern Univ., USA; <sup>3</sup>Bioengineering, Northeastern Univ., USA. We report a new technique to accelerate mesh-based Monte Carlo (MMC) photon transport simulations by using a coarsely tessellated tetrahedral mesh to represent tissue boundaries and a voxelated space to store output fluence.

## JTh3A.18

**Assessing Matrix Reorganization in a Hormone-sensitive 3D Breast Tissue Model**, Zhiyi Liu<sup>1</sup>, <sup>1</sup>Tufts Univ., USA. We report a quantitative metric, 3D directional variance, which characterizes the organization of collagen fibers in a 3D context, and apply it to the assessment of collagen remodeling in a hormone-sensitive 3D breast tissue model.

## JTh3A.19

**Noninvasive Characterization of PEGylated Transferrin Probe Delivery Using Lifetime-based FRET**, Sez-Jade Chen<sup>1</sup>, Nattawut Sinsuebphon<sup>1</sup>, Alena Rudkouskaya<sup>2</sup>, Margarida Barroso<sup>2</sup>, Xavier Intes<sup>1</sup>, <sup>1</sup>Rensselaer Polytechnic Inst., USA; <sup>2</sup>Dept. of Molecular and Cellular Physiology, Albany Medical College, USA. Lifetime-based FRET was used to compare the intracellular delivery of PEGylated and non-PEGylated probes *in vitro* and *in vivo* for applications in transferrin-based drug delivery.

## JTh3A.20

**Optical Analysis Discriminates Meningioma from Normal Surrounding Tissue**, Hussein Mehdine<sup>1,5</sup>, Fanny Poulon<sup>1</sup>, Marjorie Juchaux<sup>1</sup>, Pascale varlet<sup>2,3</sup>, Bertrand Devaux<sup>4</sup>, Johan Pallud<sup>4,3</sup>, Darine Abi Haïdar<sup>1,5</sup>, <sup>1</sup>IMNC Lab, UMR 8165-CNRS/IN2P3, Paris-Saclay Univ., 91405, France; <sup>2</sup>Neuropathology Dept., Sainte-Anne Hospital, 75014, France; <sup>3</sup>IMA BRAIN, INSERMU894, Centre de Psychiatrie et de Neurosciences, France; <sup>4</sup>Neurosurgery Dept., Sainte-Anne Hospital, 75014, France; <sup>5</sup>Université Paris Diderot, Sorbonne Paris Cité, F-75013, France. Our goal is to find the scattering and the absorption coefficient of different meningioma and healthy tissues.

## JTh3A.21

**Superresolved Magnetic Imaging of Cells with Nanodiamonds**, Martina Barbiero<sup>1</sup>, Stefania Castelletto<sup>2</sup>, Qiming Zhang<sup>1</sup>, Mirren Charney<sup>3</sup>, Ye Chen<sup>3</sup>, Sarah Russell<sup>3</sup>, Min Gu<sup>1</sup>, <sup>1</sup>Lab of Artificial-Intelligence Nanophotonics, RMIT Univ., Australia; <sup>2</sup>School of Engineering, RMIT Univ., Australia; <sup>3</sup>Centre for Micro-Photonics, Swinburne Univ., Australia. We report on the optically detected magnetic resonance of nitrogen-vacancy centres in blinking nanodiamonds to measure magnetic fields from magnetically-labeled MCF10A cells. Magnetic fields imaging is reconstructed with a localization microscope down to 25 nm.

## JTh3A.22

Withdrawn.

## JTh3A.23

**Mid-infrared Photonic Chips for Real-time Breath Biomarkers Analysis**, Pao T. Lin<sup>1</sup>, <sup>1</sup>Texas A&M Univ., USA. Real-time gas biomarker analysis on-a-chip was demonstrated using a mid-infrared microcavity. CH<sub>4</sub>, CO<sub>2</sub>, and N<sub>2</sub>O were selected as analytes due to their strong absorption bands at  $\lambda = 3.25 - 3.50 \mu\text{m}$ ,  $4.20 - 4.35 \mu\text{m}$ .

## JTh3A.24

**Fluctuation-based Super-resolution Photoacoustic Imaging**, Sergey Vilov<sup>1</sup>, Bastien Arnal<sup>1</sup>, Thomas Chaigne<sup>2</sup>, Ori Katz<sup>3</sup>, Emmanuel Bossy<sup>1</sup>, <sup>1</sup>Univ. Grenoble Alpes, CNRS, Lab. Interdisciplinaire de Physique (LIPhy), France; <sup>2</sup>Bioimaging and Neurophotonics Lab, NeuroCure Cluster of Excellence, Germany; <sup>3</sup>Dept. of Applied Physics, Hebrew Univ. of Jerusalem, Israel. We propose a SOFI-based high-order statistical analysis of photoacoustic signal fluctuations resulting from motion of optical absorbers for super-resolution photoacoustic imaging. This technique can be potentially used for *in vivo* imaging without contrast agents.

## JTh3A • Poster Session III, Coffee Break and Exhibits—Continued

## JTh3A.25

**Spectroscopic Analysis with a Monolithic Micro-structured Microsphere-Fiber Probe,** Stephen Holler<sup>1</sup>, Bernadette Haig<sup>1</sup>, Ryan Riviere<sup>1</sup>, <sup>1</sup>Fordham Univ., USA. Micro-structured fiber-optic probes are convenient means for delivering laser light in *in vivo* applications but are not used for light collection. We demonstrate bidirectional utilization through spectroscopic analysis of cancerous tissue and captured particulate matter.

## JTh3A.26

**Label-free and Nondestructive Method for Cell Viability Assessment with Two-photon Fluorescence Microscopy,** yang li<sup>1</sup>, Neal Saini<sup>3</sup>, XUN CHEN<sup>1</sup>, Tong Ye<sup>1,2</sup>, <sup>1</sup>Dept. of Bioengineering, Clemson Univ., USA; <sup>2</sup>Dept. of Regenerative Medicine and Cell Biology, Medical Univ. of South Carolina, USA; <sup>3</sup>College of Medicine, Medical Univ. of South Carolina, USA. We imaged cartilage tissues excised from rat tibia condyles with fluorescence from either intrinsic fluorophores or live/dead labeling dye upon two-photon excitation. The results suggested that the fluorescence ratio of NAD(P)H/FAD reflects chondrocyte viability.

## JTh3A.27

**Stepwise Optical Saturation Microscopy: Obtaining Super-Resolution Images with Conventional Fluorescence Microscopes,** Yide Zhang<sup>1</sup>, David Benirschke<sup>1</sup>, Scott S. Howard<sup>1</sup>, <sup>1</sup>Electrical Engineering, Univ. of Notre Dame, USA. We propose stepwise optical saturation (SOS) microscopy, in which two conventional fluorescence images are linearly combined to extend the resolution by 41%. We experimentally perform the SOS microscopy with one-photon (confocal) and multiphoton excitation fluorescence.

## JTh3A.28

**Multispectral Total-variation Reconstruction Applied to Lens-free Microscopy,** Lionel HERVE<sup>1</sup>, Cédric Allier<sup>1</sup>, Pierre Blandin<sup>1</sup>, Fabrice Navarro<sup>1</sup>, Mathilde Menneveau<sup>1</sup>, Thomas Bordy<sup>1</sup>, Olivier Cioni<sup>1</sup>, Sophie Morales<sup>1</sup>, <sup>1</sup>CEA-LETI, France. Lens-free microscopy RGB-acquisitions are processed with an inverse problem approach: a multispectral total variation criterion is defined and minimized with the conjugate gradients method. Reconstruction results show the method is efficient to recover observed samples.

## JTh3A.29

**Interferometric Spectral Modulation of sub-100-fs Pump Pulses for High Chemical Contrast, Background Free, Real Time CARS Imaging,** Gabor Molnar<sup>3</sup>, Adam Krolopp<sup>1</sup>, Norbert Kiss<sup>4</sup>, Gabor Tamas<sup>5</sup>, Robert Szpocs<sup>1,2</sup>, <sup>1</sup>R&D Ultrafast Lasers Kft., Hungary; <sup>2</sup>Wigner RCP, Hungary; <sup>3</sup>Univ. of Szeged, Hungary; <sup>4</sup>Semmelweis Univ., Hungary. A simple, fast interferometric spectral modulation technique is proposed for nonresonant background suppression during CARS imaging. We demonstrate that the proposed setup is also suitable for real time stain-free histopathology of the brain.

## JTh3A.30

**Localization-based Super-resolution Photoacoustic Imaging,** Sergey Vilov<sup>1</sup>, Bastien Arnal<sup>1</sup>, Emmanuel Bossy<sup>1</sup>, <sup>1</sup>Univ. Grenoble Alpes, CNRS, Lab. Interdisciplinaire de Physique (LIPhy), France. We demonstrate that localization-based super-resolution techniques initially introduced in optics can be adapted to achieve super-resolution in photoacoustic imaging. We envision the possibility of super-localization photoacoustic *in vivo* imaging based on medical contrast agents.

## JTh3A.31

**Two-photon Laser Scanning Stereomicroscopy for Fast Volumetric Imaging,** XUN CHEN<sup>1</sup>, Yanlong Yang<sup>2</sup>, Baoli Yao<sup>2</sup>, Yang Li<sup>1</sup>, Tong Ye<sup>1,2</sup>, <sup>1</sup>CLEMSON, USA; <sup>2</sup>Xi'an Inst. of Optics and Precision Mechanics, China; <sup>3</sup>Medical Univ. of South Carolina, USA. We describe the design and implementation of two-photon lasers scanning stereomicroscopy, which allows viewing dynamic processes in three-dimensional (3D) space stereoscopically in real-time at the speed of 1.4 volumes per second.

## JTh3A.32

**The Effects of Blood Flow Velocity and Blood Volume on Acousto-Optic Signals,** Michal Balberg<sup>2</sup>, Pinhas Girschovitz<sup>1</sup>, Noam Racheli<sup>1</sup>, Revital Shechter<sup>1</sup>, Sergio Fantini<sup>3</sup>, <sup>1</sup>Ornim Medical Ltd., Israel; <sup>2</sup>Holon Inst. of Technology, Israel; <sup>3</sup>Tufts University, USA. Acousto optics signals depend linearly on the velocity of flow and the volume density of scattering particles. Such linear dependence has different slopes for different densities, allowing for the separate assessment of flow and density.

## JTh3A.33

**Novel Diffuse Correlation Spectroscopy for Simulations Estimation of Hemoglobin Concentration, Oxygen Saturation, and Blood Flow,** Parisa Farzam<sup>1</sup>, Davide Tamborini<sup>1</sup>, Bernhard B. Zimmermann<sup>1</sup>, Kuan C. Wu<sup>1</sup>, David Boas<sup>2</sup>, Maria Franceschini<sup>1</sup>, <sup>1</sup>Harvard Medical School, Massachusetts General Hospital, USA; <sup>2</sup>Neurophotonics Center, Biomedical Engineering Dept., Boston Univ., USA. We developed a stand-alone multi-distance multi-wavelength diffuse correlation spectroscopy, able to simultaneously measure tissue optical properties and blood flow, by taking advantage of both the light intensity decay over source-detector separations and the autocorrelation at three wavelengths.

## JTh3A.34

**Conformable, Wearable and Scalable Imaging Bands for Assessing Joints Diseases,** Youngwan Kim<sup>1</sup>, Alessandro Marone<sup>1</sup>, Sarah M. Thompson<sup>1</sup>, Johanan N. Sowah<sup>1</sup>, Henry J. Shulevitz<sup>1</sup>, Hyun K. Kim<sup>1</sup>, Ioannis Kymissis<sup>1</sup>, Andreas H. Hielscher<sup>1</sup>, <sup>1</sup>Columbia Univ., USA. Flexible imaging band shows its conformability and scalability for assessing joint diseases such as rheumatoid arthritis. This imaging band supports high-fidelity data acquisition, allowing dynamic optical measurement and tomographic image reconstruction in the field of diffuse optical tomography.

## JTh3A.35

**Solitary vs Gaussian Waves Gating of InGaAs/InP Avalanche Photodiode to Stabilize Dark Count Rate as Excess Voltage Increases,** Ahmad Azzahrani<sup>1</sup>, Ahmed C. Kadhim<sup>1</sup>, Susan Earles<sup>1</sup>, Muhammad Riaz<sup>1</sup>, <sup>1</sup>Electrical and Computer Engineering, Florida Inst. of Technology, USA. A mathematical model for dark count rate of soliton gated InGaAs/InP SPAD is developed. Results are compared with published experimental counts of Gaussian gating. Simulation results show DCR is not affected by increasing  $V_{EX}$ .

## JTh3A.36

**Quantitative Measurement of Fluorescein Sodium for Multi-plexed Fluorescence Spectroscopy in Brain,** Jaime J. Bravo<sup>1</sup>, Keith D. Paulsen<sup>1</sup>, David Roberts<sup>1</sup>, Jonathan Olson<sup>1</sup>, <sup>1</sup>Dartmouth College, USA. A fluorescence correction algorithm was developed for fluorescein sodium (FS), which when paired with an accurate white light analysis algorithm allows for accurate quantification of FS. The model will be further explored using *in vivo* measurements containing both FS and protoporphyrin IX.

## JTh3A.37

**Spectrally Constrained Approach of Spatially Resolved Spectroscopy: Towards a Better Estimate of Tissue Oxygenation,** JOSHUA DEEPAK VEESA<sup>1</sup>, Hamid Dehghani<sup>1</sup>, <sup>1</sup>Univ. of Birmingham, UK. A method based on spatially resolved spectroscopy is developed, which directly recovers the scaled chromophore concentrations and scattering parameter of the tissue. This method provides a more accurate estimate of tissue oxygenation, regardless of the unknown tissue scatter.

## JTh3A.38

**Fast Monte Carlo Photon Transport Simulations for Heterogeneous Computing Systems,** Leiming Yu<sup>1</sup>, Fanny Nina-Paravecino<sup>1</sup>, David Kaeli<sup>1</sup>, Qianqian Fang<sup>1</sup>, <sup>1</sup>Northeastern Univ., USA. We develop a high performance Monte Carlo (MC) photon transport simulation package using the OpenCL framework for heterogeneous computing systems. The scalable and portable performance over a wide range of modern computing devices are characterized.

## JTh3A.39

**Near Infrared Spectroscopy Setup for Concurrent Spectroscopic, Invasive and MRI Investigations in Rats,** Thomas Gladysz<sup>1</sup>, Alexander Hoppe<sup>1</sup>, Kathleen Cantow<sup>2</sup>, Sarah Brix<sup>2</sup>, Bert Flemming<sup>2</sup>, Andreas Pohlmann<sup>2</sup>, Erdmann Seeliger<sup>2</sup>, Thoralf Niendorf<sup>2</sup>, Dirk Grosenick<sup>1</sup>, <sup>1</sup>Physikalisch-Technische Bundesanstalt, Germany; <sup>2</sup>Institut für Vegetative Physiologie, Charité - Universitätsmedizin Berlin, Germany; <sup>3</sup>Berlin Ultrahigh Field Facility (B.U.F.F.), Max-Delbrueck Center for Molecular Medicine, Germany. We describe a multispectral NIRS setup designed to measure the hemodynamics and oxygenation in rat kidney in a preclinical MRI scanner. The challenges tackled include small tissue size, instrumental geometry and the necessary depth resolution.

## JTh3A.40

**Preliminary Results of a Handheld, Low-cost, and Multi-wavelength Spatial Frequency Domain Imaging System for Ex Vivo Cancer Characterization,** Mohsen Erfanzadeh<sup>1</sup>, Sreyankar Nandy<sup>2</sup>, Patrick D. Kumavor<sup>1</sup>, Quing Zhu<sup>2</sup>, <sup>1</sup>Biomedical Engineering, Univ. of Connecticut, USA; <sup>2</sup>Biomedical Engineering, Washington Univ. in St. Louis, USA. We present a handheld and low-cost spatial frequency domain imaging system that utilizes up to 9 LEDs. Its feasibility is evaluated by imaging human wrist *in vivo* and it is used for characterization of ex vivo ovarian and colon cancer samples.

## JTh3A.41

**Noising in Monte Carlo Photon Transport Simulation Using GPU-accelerated Adaptive Non-Local Mean Filter,** Yaoshen Yuan<sup>1</sup>, Leiming Yu<sup>1</sup>, Qianqian Fang<sup>2</sup>, <sup>1</sup>Electrical and Computer Engineering Dept., Northeastern Univ., USA; <sup>2</sup>Bioengineering Dept., Northeastern Univ., USA. We propose a GPU-accelerated adaptive non-local-mean filter to reduce the stochastic noise presented in Monte Carlo photon transport simulations. After filtering, the noise in the output is comparable to that obtained using roughly 10-fold photons.

## JTh3A.42

**Extraction of Group Velocity Dispersion (GVD) Value from Standard Fourier Domain OCT Data,** Sylwia Kolenderska<sup>1</sup>, Bastian Braeuer<sup>1</sup>, Ehsan Vaghefi<sup>1</sup>, Frederique Vanholsbeeck<sup>1</sup>, <sup>1</sup>Univ. of Auckland, New Zealand. We propose a simple, numerical procedure for dispersion mapping of an object, which can be easily used for every OCT dataset acquired from a Fourier domain system employing light source of sufficiently broad spectral bandwidth.

## JTh3A.43

**Use of Photoacoustic Spectroscopy to Evaluate Photosensitizer Penetration into Dentin,** Mauro L. Baesso<sup>2</sup>, Ingrid G. Occhi-Alexandre<sup>3</sup>, Mitsue Fujimaki<sup>1</sup>, Francielle Sato<sup>2</sup>, Lidiane V. Castro-Hoshino<sup>2</sup>, Pedro L. Rosalen<sup>3</sup>, Raquel S. Terada<sup>1</sup>, Antonio Medina Neto<sup>2</sup>, Antonio C. Bento<sup>2</sup>, <sup>1</sup>Dentistry Dept., State Univ. of Maringá, Brazil; <sup>2</sup>Physics, State Univ. of Maringá, Brazil; <sup>3</sup>School of Dentistry of Piracicaba, Univ. of Campinas, Brazil. Photodynamic Therapy has been used in dental carious lesions treatment. Erythrosine penetration into sound and decayed dentin was measured by photoacoustic spectroscopy. Besides, Raman spectroscopy was effective for evaluating the spectral response of dentin.

## JTh3A.44

**Quantitative Image Correction Using Semi-automated Image Correction Using Semi-automated Fully-automatic Segmentation of Hybrid Photoacoustic and Ultrasound Images,** Elena Merčep<sup>2,1</sup>, Berkan Lafci<sup>3,1</sup>, José Luis Deán-Ben<sup>4</sup>, Daniel Razansky<sup>2,4</sup>, <sup>1</sup>iThera Medical, Germany; <sup>2</sup>Faculty of Medicine, Technical Univ. of Munich, Germany; <sup>3</sup>Faculty of Informatics, Technical Univ. of Munich, Germany; <sup>4</sup>Inst. for Biological and Medical Imaging, Helmholtz Center Munich, Germany. To reduce errors in spectral recovery, fluence correction is commonly performed on reconstructed photoacoustic images and requires input on illumination geometry and object boundaries. For latter, we proposed automatic segmentation method and characterized its performance against the ground truth.

## JTh3A • Poster Session III, Coffee Break and Exhibits—Continued

## JTh3A.45

**Computational Performance of Time-Resolved Diffuse Optical Tomography in a Two-Layer Brain Model**, David Orive Miguel<sup>1,2</sup>, Lionel HERVE<sup>1</sup>, Jérôme MARS<sup>2</sup>, Laurent CONDAT<sup>2</sup>, Jean-Marc DINTEN<sup>1</sup>, Sophie Morales<sup>1</sup>; <sup>1</sup>CEA, France; <sup>2</sup>GIPSA-lab, Univ. Grenoble Alpes, CNRS, France. We evaluate Mellin-Laplace algorithm in a two-layer brain model with Monte-Carlo generated data. Results show accurate absorption estimation and the flexibility of the algorithm to detect each layer thickness.

## JTh3A.46

**The Use of Optical Coherence Tomography for the Evaluation of the Effects of an Infrared Laser on Dentin Demineralization**, Patricia A. Ana<sup>2</sup>, Elizabete d. Silva<sup>2</sup>, Carolina Benetti<sup>2</sup>, Marcello M. Amaral<sup>1</sup>, Denise M. Zezell<sup>1</sup>, Anderson S. Gomes<sup>3</sup>; <sup>1</sup>Center for Lasers and Applications, Nuclear and Energy Research Inst., Brazil; <sup>2</sup>Center for Engineering, Modeling and Applied Social Sciences, UFABC, Brazil; <sup>3</sup>Physics Dept., UFPE, Brazil. The effect of Er,Cr:YSGG laser on dentin demineralization was evaluated by optical coherence tomography, which was able to quantify and to evidence that this laser is a promissory alternative for preventing dentin caries.

## JTh3A.47

**Improving Optical Coherence Tomography Contrast for Assessing Biologic Constructs via TiO<sub>2</sub>**, Denzel E. Faulkner<sup>1</sup>, Cassandra E. Roberge<sup>1</sup>, David Kingsley<sup>1</sup>, Charles J. Sloat<sup>1</sup>, David T. Corr<sup>1</sup>, Xavier Intes<sup>1</sup>; <sup>1</sup>Rensselaer Polytechnic Inst., USA. Optical Coherence Tomography is an established imaging modality that plays an increased role in assessing biomanufactured constructs. Herein, a scattering agent, TiO<sub>2</sub>, was used to improve OCT image quality of tumor aggregates with minimal cytotoxicity.

## JTh3A.48

**Detection of Vascular Plaque from Optical Coherence Tomography Images Using Hidden Markov Random Field Based Segmentation**, Ammu Prakash<sup>1</sup>, Mark Hewko<sup>2</sup>, Michael Sowa<sup>2</sup>, Sherif S. Sherif<sup>1</sup>; <sup>1</sup>Univ. of Manitoba, Canada; <sup>2</sup>National Research Council Canada, Canada. We implemented a method to detect vascular plaque from optical coherence tomography images using hidden Markov random field based segmentation. We validated our segmentation results using both histology and photographic images of vascular plaque samples.

## JTh3A.49

**Tolerance of Reconstructed Diffuse Optical Tomographic Breast Images to Experimental Errors**, Bin Deng<sup>1</sup>, Mats Lundqvist<sup>2</sup>, Qianqian Fang<sup>3</sup>, Stefan A. Carp<sup>1</sup>; <sup>1</sup>Martinos Center for Biomedical Imaging, USA; <sup>2</sup>Philips Healthcare, Sweden; <sup>3</sup>Dept. of Bioengineering, Northeastern Univ., USA. Accurate and reproducible quantification of HbT in longitudinal imaging is essential for the successful translation of NIR-DOT. We performed a simulation study on 5 breast phantoms to estimate the impact of various experimental errors on reconstructing optical properties and tumor characteristics.

## JTh3A.50

**Elemental Analysis of Mammary Glands with Laser Induced Laser Spectroscopy**, Irfan Ahmed<sup>1</sup>, Condon Lau<sup>1</sup>; <sup>1</sup>City Univ. of Hong Kong, Hong Kong. Physiological functions of biological cell in breast tissues crucially depend on the trace elements present. Here, laser induced breakdown spectroscopy has been developed to perform the trace elemental analysis. Lithium ( $p < 0.05$ ) trace in breast tissue may affect its overall elemental concentration.

## JTh3A.51

**Noise Characteristics of a Single-pixel Macroscopic Fluorescence Lifetime Imaging System**, Qi Pian<sup>1</sup>, Ruoyang Yao<sup>1</sup>, Xavier Intes<sup>1</sup>; <sup>1</sup>Dept. of Biomedical Engineering, Rensselaer Polytechnic Inst., USA. We report the noise characteristics of a hyperspectral single-pixel macroscopic fluorescence lifetime imaging (MFLI) platform. The joint effect of detector noise and photon noise on system performance is analyzed and characterized by *in vitro* study.

## JTh3A.52

**Mapping Cortical Effects of Childhood Malnutrition Using High-Density Diffuse Optical Tomography**, Andrew Fishell<sup>1,2</sup>, Ed Richter<sup>3</sup>, Claudia Valdes<sup>4</sup>, Marcela Riverá<sup>4</sup>, Adam T. Eggebrecht<sup>1</sup>, Christopher Smyser<sup>5,1</sup>, Ana Maria Arbelaez<sup>6</sup>, Joseph P. Culver<sup>1,2</sup>; <sup>1</sup>Radiology, Washington Univ. in St. Louis, USA; <sup>2</sup>Biology and Biomedical Sciences, Washington Univ. in St. Louis, USA; <sup>3</sup>Electrical Engineering, Washington Univ. in St. Louis, USA; <sup>4</sup>Centro Medico Imbanaco, Colombia; <sup>5</sup>Neurology, Washington Univ. in St. Louis, USA; <sup>6</sup>Pediatric Endocrinology, Washington Univ. in St. Louis, USA; <sup>7</sup>Biomedical Engineering, Washington Univ. in St. Louis, USA. Early life stressors, including malnutrition, result in irreversible deviations from the trajectory of typical brain development. Here, we demonstrate the feasibility of mapping and tracking these deviations using a field-ready High-Density Diffuse Optical Tomography system.

## JTh3A.53

**Functional Brain Connectivity Distinguishes Surgical Skill Learning with Surgical Simulators**, Arun Nemani<sup>1</sup>, Suvranu De<sup>1</sup>, Xavier Intes<sup>1</sup>; <sup>1</sup>Biomedical Engineering, Rensselaer Polytechnic Inst., USA. Surgical skill assessment metrics measure performance but do not address the underlying neurophysiology associated with skill acquisition. Here, we investigate fNIRS-based measures of high functional connectivity in cortical regions associated with increased surgical skill proficiency.

## JTh3A.54

**Spatiotemporal Characterization of Brain Function Via Multiplex Visibility Graph**, Li Zhu<sup>1</sup>, Sasan Haghani<sup>1</sup>, Laleh Najafizadeh<sup>1</sup>; <sup>1</sup>Rutgers Univ., USA. fNIRS signals recorded at resting-state and during task are analyzed using multilayer visibility graph (MVG). Results show that MVG can provide new insights for studying spatiotemporal characteristics of brain function.

## JTh3A.55

**Quantitative Assessment of Image Quality of Sparse Functional Near Infrared Spectroscopy vs High-Density Diffuse Optical Tomography**, Tracy M. Burns-Yocum<sup>1</sup>; <sup>1</sup>Washington Univ. School of Medicine, USA. We evaluated image quality of three sparse fNIRS arrays extracted from and compared to a previously published data set containing subject-matched HD-DOT and fMRI and show that overlapping measurements are required for fMRI-comparable images.

## JTh3A.56

**Transcranial Laser Stimulation Increases Power of Brain Oscillations and Information Flow Measured by EEG**, Xinlong Wang<sup>1</sup>, Jacek Dmochowski<sup>2</sup>, Francisco Gonzalez-Lima<sup>3</sup>, Hanli Liu<sup>1</sup>; <sup>1</sup>UT-Arlington, USA; <sup>2</sup>The City College of New York, USA; <sup>3</sup>UT-Austin, USA. We conducted placebo-controlled 1064 nm Transcranial Laser Stimulation (TLS) on 20 human foreheads. Significant alterations of EEG power and information flow were observed, indicating important neurophysiological benefits of photoneuromodulation by 1064 nm laser.

## JTh3A.57

**Withdrawn.**

## JTh3A.58

**The Relationship Between the Slow Oscillation and Underlying Resting State Cortical Activity During Anesthesia and NREM Sleep**, Lindsey M. Brier<sup>1</sup>, Eric C. Landsness<sup>1</sup>, Armand Mensen<sup>2</sup>, Patrick Wright<sup>1</sup>, Grant A. Baxter<sup>1</sup>, Abraham Z. Snyder<sup>1</sup>, Adam Q. Bauer<sup>1</sup>, Jin-Moo Lee<sup>1</sup>, Joseph P. Culver<sup>1</sup>; <sup>1</sup>Washington Univ. in St. Louis, USA; <sup>2</sup>Neurology, Univ. Hospital, Switzerland. The slow oscillation (SO) is a cortical quasi-periodic excitatory neural wave during NREM sleep. We use wide field GCaMP6 imaging with behavioral state staging to define the SO as a superposition onto ongoing intrinsic activity.

## JTh3A.59

**Transmission Measurement of Brain Activity in vivo**, Wen-Ju Pan<sup>1</sup>, Jacob Billings<sup>1</sup>, Maysam Nezafati<sup>1</sup>, Waqas Majeed<sup>1</sup>, Shella Keilholz<sup>1</sup>; <sup>1</sup>Emory Univ., USA. Localized transmission measurement of intrinsic optical signal of neuronal activity was examined *in-vivo* in the rat brain for the first time. Enhanced light output during neuronal activity was observed, linked to neural swelling signals.

## JTh3A.60

**Designing Large Field-of-view Two Photon Microscopy Using Optical Invariant Analysis**, Jonathan Bumstead<sup>1</sup>, Jasmine Park<sup>1</sup>, Ike Rosen<sup>1</sup>, Andrew Kraft<sup>1</sup>, Patrick Wright<sup>1</sup>, Matthew D. Reisman<sup>1</sup>, Daniel C. Cote<sup>2</sup>, Joseph P. Culver<sup>1</sup>; <sup>1</sup>Washington Univ. in Saint Louis, USA; <sup>2</sup>Universite Laval, Canada. Conventional two photon microscopy (TPM) is capable of imaging neural dynamics with subcellular resolution, but is limited to a field of view (FOV)  $< \varnothing 1$ mm. We present a strategy for extending the FOV to  $\varnothing 7$ mm while maintaining cellular resolution.

## JTh3A.61

**Optical Monitoring of Oxygen Saturation and Tissue Blood Flow in Skeletal Muscle**, Zhe Li<sup>1</sup>, Jinchao Feng<sup>1</sup>, Zhonghua Sun<sup>1</sup>, Pengyu Liu<sup>1</sup>, Kebin Jia<sup>1</sup>, Wesley Baker<sup>2</sup>, Arjun G. Yodanis<sup>2</sup>; <sup>1</sup>Beijing Univ. of Technology, China; <sup>2</sup>Univ. of Pennsylvania, USA. Near-infrared spectroscopy and diffuse correlation spectroscopy were applied to measure oxygen saturation and blood flow changes in skeletal muscle. Comparison results between healthy subjects and peripheral artery disease patients were given in this study.

## JTh3A.62

**Multi-wavelength Time-resolved NIRS Measurements in Pigs During Inflow and Washout of ICG: Assessment of Extracerebral Signal Contamination**, Anna Geregá<sup>1</sup>, Martyna Lachowska<sup>1</sup>, Laura Morrison<sup>2</sup>, Keith St. Lawrence<sup>2,3</sup>, Adam Liebert<sup>1</sup>; <sup>1</sup>Inst. of Biocybernetics and Biomedical Engineering, Poland; <sup>2</sup>Imaging Division, Lawson Health Research Inst., Canada; <sup>3</sup>Dept. of Medical Biophysics, Western Univ., Canada. Multi-wavelength, time-resolved diffuse reflectance signals were measured on pigs during dynamic inflow of ICG. Data were collected on the scalp, incised scalp and directly on the brain to assess extracerebral signal contamination.

## JTh3A.63

**Resting-State Functional Connectivity Measured By Diffuse Correlation Spectroscopy**, Chien Poon<sup>1</sup>, Jun Li<sup>1</sup>, Jeremy G. Kress<sup>1</sup>, Daniel J. Rohrbach<sup>1</sup>, Ulas Sunar<sup>1</sup>; <sup>1</sup>Biomedical Engineering, Wright State, USA. We used Diffuse Correlation Spectroscopy to show that Resting State Functional Connectivity in dorsolateral-dorsolateral region is significantly stronger than inferior-dorsolateral regions in nine adult subjects, in line with previous observations with functional near-infrared spectroscopy.

## JTh3A.64

**Software Tools for Efficient Processing of High-Resolution 3D Images of Macroscopic Brain Samples**, Giacomo Mazzamuto<sup>1</sup>, Ludovico Silvestri<sup>1,2</sup>, Irene Costantini<sup>1</sup>, Francesco Orsini<sup>3</sup>, Matteo Roffilli<sup>4</sup>, Paolo Frascioni<sup>3</sup>, Leonardo Sacconi<sup>1,2</sup>, Francesco S. Pavone<sup>1,2</sup>; <sup>1</sup>European Lab for Non Linear Spectroscopy (LENL), Italy; <sup>2</sup>National Inst. of Optics (INO-CNR), Italy; <sup>3</sup>Dept. of Information Engineering (DINFO), Univ. of Florence, Italy; <sup>4</sup>Bioretics srl, Italy. We present a software pipeline for high throughput stitching and processing of high-resolution tomographies of whole mouse brains. We then employ machine learning techniques for automatic segmentation and classification of neurons in the acquired datasets.

NOTES

Thursday, 5 April

## Atlantic Ballroom 1

Microscopy, Histopathology  
and Analytics

15:30–17:30

### MTh4A • Challenges in Clinical Translation

Presider: Michael Giacomelli,  
MIT, USA

MTh4A.1 • 15:30 **Invited**

**Challenges, Opportunities and New Models to Enhance Translation of Fundamental Research to Patient Care**, Gabriela Apiou-Sbirlea<sup>1</sup>; <sup>1</sup>Massachusetts General Hospital, USA. This lecture will review challenges that academic scientists in biomedical optics have to overcome in order to translate new discoveries to clinical practice and discuss novel research and training models to accelerate the process.

MTh4A.2 • 16:00 **Invited**

**Bringing Biophotonics to Dermatology Patients: Experiences of a New Cutaneous Imaging Clinic**, Fuyao Chen<sup>1,2</sup>, Jianing Wang<sup>3</sup>, Inga Saknite<sup>1</sup>, Melanie D. Patterson<sup>1</sup>, Dan Fabbric<sup>4,5</sup>, Benoit Dawant<sup>3,2</sup>, Madan H. Jagasia<sup>5</sup>, Eric Tkaczyk<sup>1,6</sup>; <sup>1</sup>Dermatology, Vanderbilt Univ. Medical Center, USA; <sup>2</sup>Biomedical Engineering, Vanderbilt Univ., USA; <sup>3</sup>Electrical Engineering and Computer Science, Vanderbilt Univ., USA; <sup>4</sup>Bioinformatics, Vanderbilt Univ. Medical Center, USA; <sup>5</sup>Medicine / Hematology and Oncology, Vanderbilt Univ. Medical Center, USA; <sup>6</sup>Veterans Administration Medical Center, USA. We explore challenges and opportunities for clinical implementation of optical technologies in dermatology. Examples include a confocal diagnostic service and cross-polarized 3D photography to train neural networks for assessments following stem cell transplantation.

MTh4A.3 • 16:30 **Invited**

**The Challenges and Prospects of Microscopy and Biophotonics in Low Resource Settings**, Benjamin Wilson<sup>1</sup>, Matthew Horning<sup>1</sup>, Courosh Mehanian<sup>1</sup>, Charles Delahunt<sup>1</sup>, Liming Hu<sup>1</sup>, Mayoore Jaiswal<sup>1</sup>, Shawn McGuire<sup>1</sup>, David Bell<sup>2</sup>; <sup>1</sup>Intellectual Ventures Lab, USA; <sup>2</sup>Global Good Fund, USA. Developing technologies that target low resource setting applications requires unique considerations in hardware and process design. This presentation will discuss some of these considerations while giving examples of outcomes and lessons learned from a variety of microscopy and optics-related projects.

## Atlantic Ballroom 2

Clinical and Translational  
Biophotonics

15:30–17:30

### CTh4B • Optical Techniques for Diseases Diagnostics

Presider: Juergen Popp,  
Friedrich-Schiller-Universität  
Jena, Germany

CTh4B.1 • 15:30 **Invited**

**Optical Biopsies Using Multimodal Imaging - Chances and Limitations**, Juergen Popp<sup>1,2</sup>; <sup>1</sup>Friedrich-Schiller-Universität Jena, Germany; <sup>2</sup>Leibniz Inst. of Photonic Technology, Germany. Optical multimodal imaging are very promising methods with large potential for use in the solution of current diagnostic medical problems with respect to noninvasively differentiate between pathological and normal tissue under intraoperative conditions.

CTh4B.2 • 16:00 **Invited**

**Optical dental Care for Children, from Caries Prediction to Therapy Monitoring**, Eric J. Seibel<sup>1</sup>, Yaxuan Zhou<sup>1</sup>, Jasmine Y. Graham<sup>1</sup>, Leonard Y. Nelson<sup>1</sup>; <sup>1</sup>Univ. of Washington, USA. Dentists rely on visual examination for diagnosing tooth decay which lacks quantification. To predict enamel demineralization, pH is spectrally mapped using fluorescence. To monitor enamel healing, lesion extent is measured using infrared endoscopic imaging.

CTh4B.3 • 16:30

**Longitudinal Monitoring of Skin Wounds In Vivo Using Label-free Multiphoton Microscopy**, Jake D. Jones<sup>1</sup>, Hallie E. Ramser<sup>1</sup>, Alan Woessner<sup>1</sup>, Kyle P. Quinn<sup>1</sup>; <sup>1</sup>Univ. of Arkansas, USA. *In vivo* label-free multiphoton microscopy reveals differences in both an optical redox ratio of NADH and FAD, as well as fluorescence lifetime, between diabetic and non-diabetic wounds monitored longitudinally over 10 days.

## Grand Ballroom West

Optics and the Brain

15:30–17:30

### BTh4C • Using the Tools

Presider: Anna Devor, Univ. of  
California San Diego, USA

BTh4C.1 • 15:30 **Invited**

**Investigating the Properties of the Cerebrospinal Fluid in the Vertebrate Spinal Cord**, Claire Wyart<sup>1</sup>, Olivier Thouvenin<sup>1</sup>; <sup>1</sup>ICM Paris, France. We will present the dynamics of cerebrospinal fluid flow revealed by dynamic full field OCT on endogenous particles in combination with imaging of exogenous beads to capture the dynamics of particles in the central canal.

BTh4C.2 • 16:00 **Invited**

**Multiphoton Ultrafast Local Volume Excitation (ULOVE) Through Acousto-optic Wavefront Shaping to Record and Control Neuronal Activity**, Stephane Dieudonné<sup>1</sup>; <sup>1</sup>Ecole Normale Supérieure, France. Technologies for recording and manipulating transmembrane potential *in vivo* in defined neuronal populations with high fidelity will be essential to understand how information is represented, processed, and propagated in the brain. Genetically encoded voltage indicators (GEVIs) and optogenetic actuators are especially promising as they can be expressed in defined cell types and are compatible with long-term chronic imaging *in vivo*.

BTh4C.3 • 16:30

**High-resolution Hippocampal Imaging in Mice Navigating in a Flat Real-world Environment**, Mary Ann Go<sup>1</sup>, Simon Schultz<sup>1</sup>; <sup>1</sup>Imperial College London, UK. We present the first demonstration of two-photon calcium imaging in the hippocampus of head-fixed mice performing a spatial memory task in an air-lifted platform. This approach enables behavioral testing with functional imaging in a real-world environment.

## Atlantic Ballroom 3

Optical Tomography and  
Spectroscopy

15:30–17:30

### OTh4D • Tomographic and Spectroscopy Methods for Non-Invasive Imaging of Disease

Presider: Regine Choe, Univ. of  
Rochester, USA

OTh4D.1 • 15:30 **Invited**

**Optical Quantification of Collagen and Breast Cancer: Lesion Classification and Risk Estimate**, Paola Taroni<sup>1</sup>, Antonio Pifferi<sup>1</sup>, Rinaldo Cubeddu<sup>1</sup>, Francesca Ieva<sup>1</sup>, Anna Maria Paganoni<sup>1</sup>, Francesca Abbate<sup>2</sup>, Enrico Cassano<sup>2</sup>; <sup>1</sup>Politecnico di Milano, Italy; <sup>2</sup>European Inst. of Oncology, Italy. Collagen content quantified through 7-wavelength (635-1060 nm) time domain diffuse optical mammography in 200 women proved key to discriminate malignant from benign breast lesions, to measure breast density, and to estimate breast cancer risk.

OTh4D.2 • 16:00

**Identifying an Optimal Time Window for Predicting Response to Neoadjuvant Chemotherapy Using Breast Cancer Subtypes and Hemoglobin Parameters Assessed by US-guided Optical Tomography**, Qing Zhu<sup>1,3</sup>, Susan Tannenbaum<sup>2</sup>, Scott Kurtzman<sup>4</sup>, Patricia DeFusco<sup>5</sup>, Andrew Ricci<sup>4</sup>, Hamed Vavadi<sup>7</sup>, Feifei Zhou<sup>1</sup>, Chen Xu<sup>8</sup>; <sup>1</sup>Washington Univ. in St. Louis, USA; <sup>2</sup>Cancer Center, Univ. of Connecticut Health Center, USA; <sup>3</sup>ECE, Univ. of Connecticut, USA; <sup>4</sup>Waterbury Hospital, USA; <sup>5</sup>Hartford Hospital, USA; <sup>6</sup>BME, Univ. of Connecticut, USA; <sup>7</sup>New York City College of Technology City Univ. of New York (CUNY), USA. The study has identified an optimal time window for predicting breast cancer pathological response to neoadjuvant chemotherapy (NAC) based on tumor subtypes, pretreatment total-hemoglobin level and early changes of total-hemoglobin following NAC.

OTh4D.3 • 16:15

**Tissue Oxygen Saturation Predicts Response to Breast Cancer Neoadjuvant Chemotherapy within 10 Days**, Jeffrey M. Cochran<sup>1</sup>, David R. Busch<sup>1</sup>, Anais Leproux<sup>2</sup>, Bruce J. Tromberg<sup>2</sup>, Arjun G. Yodh<sup>1</sup>; <sup>1</sup>Univ. of Pennsylvania, USA; <sup>2</sup>Univ. of California Irvine, USA. Non-hypoxic levels of tumor oxygen saturation within 10 days of the first dose of therapy predict pathologic complete response to breast cancer neoadjuvant chemotherapy in a 33 subject clinical trial.

OTh4D.4 • 16:30

**Impact of Transmitted and Reflected Lights on Medical Imaging in a Parallel-plane Diffuse Optical Tomography System for Breast Cancer Detection**, hao yang<sup>1</sup>, hanlin sun<sup>2</sup>, Xianlin wei<sup>3</sup>, Taixiang shi<sup>4</sup>, huabei jiang<sup>1</sup>; <sup>1</sup>Univ. of South Florida, USA; <sup>2</sup>Saratoga High School, USA; <sup>3</sup>Hualoha Medical Inc, China; <sup>4</sup>Hualoha Medical Inc, China. We present phantom experimental results based on a parallel-plane DOT system for breast cancer imaging. Three source/detector patterns are compared. For the first time, we demonstrate that the transmission model provides the best image quality.

## Atlantic Ballroom 1

Microscopy, Histopathology and Analytics

### MTh4A • Challenges in Clinical Translation—Continued

**MTh4A.4 • 17:00** **Invited**  
**Making Breast Cancer Diagnoses in Low-Resource Settings**, Jane Brock<sup>1</sup>, <sup>1</sup>Brigham & Womens Hospital, USA. Point-of-Care Technology methods of tissue biopsy handling, imaging and prognostic marker evaluation can obviate current expensive processes requiring highly skilled technicians, that currently limit breast cancer diagnosis and therapeutic decision making in low-resource settings.

## Atlantic Ballroom 2

Clinical and Translational Biophotonics

### CTh4B • Optical Techniques for Diseases Diagnostics—Continued

**CTh4B.4 • 16:45**  
**Dynamical NIR FRET for Non-Invasive Monitoring in vivo Target-Receptor Engagement**, Nattawut Sinsuebphon<sup>1</sup>, Alena Rudkouskaya<sup>2</sup>, Margarida Barroso<sup>2</sup>, Xavier Intes<sup>1</sup>; <sup>1</sup>Rensselaer Polytechnic Inst., USA; <sup>2</sup>Albany Medical College, USA. The dynamics of target-receptor engagement in small animals was assessed by FRET measurement using two imaging instruments. Intensity- and lifetime-based measurements could detect the interaction in the targeted organ but not in non-targeted organ.

**CTh4B.5 • 17:00**  
**Macroscopic Raman Imaging on Tooth for Caries Detection**, Shan Yang<sup>1</sup>; <sup>1</sup>Jackson State Univ., USA. This work reports a Raman imaging setup for full scale (~7 mm in diameter) tooth mapping for mineral concentration distribution of enamel layer. The results indicate that Raman imaging is suitable for dental caries detection.

**CTh4B.6 • 17:15**  
**Optical Fiber Long-Period Grating with Nanoscale Coatings for Rapid Identification of Bacterial Infections**, James . Heflin<sup>1</sup>, Kelly McCutcheon<sup>1</sup>, Aloka Bandara<sup>1</sup>, Ziwei Zuo<sup>1</sup>, Ben Fox<sup>1</sup>, Siddharth Ramachandran<sup>2</sup>, Alfred Ritter<sup>3</sup>, Thomas Inzana<sup>1</sup>; <sup>1</sup>Virginia Tech, USA; <sup>2</sup>Boston Univ., USA; <sup>3</sup>Virginia nanoTech, USA. Rapid identification (<1 hour) of the bacteria methicillin-resistant *Staphylococcus* and *Histophilus somni* are demonstrated using an ionic self-assembled multilayer (ISAM) film deposited on the surface of a long-period grating (LPG) optical fiber.

## Grand Ballroom West

Optics and the Brain

### BTh4C • Using the Tools—Continued

**BTh4C.4 • 16:45**  
**Minimally Invasive Microscopy Using GRIN Lens Microendoscopes**, Pavan Chandra Konda<sup>2</sup>, Julia Edgar<sup>1</sup>, Susan Barnett<sup>1</sup>, Andrew R. Harvey<sup>2</sup>; <sup>1</sup>Inst. of Infection, Immunity & Inflammation, Univ. of Glasgow, UK; <sup>2</sup>School of Physics and Astronomy, Univ. of Glasgow, UK. We report a custom epi-fluorescent microscope setup using GRIN lens microendoscopes for minimally invasive microscopic imaging in rodents. A simple scanning system and deconvolution provides high quality wide field-of-view images through these highly aberrated endoscopes.

**BTh4C.5 • 17:00** **Invited**  
**Fast Confocal Fluorescence Imaging in Freely-Behaving Mice**, Clara Dussaux<sup>1</sup>, Jozsua Fodor<sup>1</sup>, Vivien Szabo<sup>2</sup>, Yan Chastagnier<sup>2</sup>, Jean-François Léger<sup>1</sup>, Laurent Bourdieu<sup>1</sup>, Julie Perroy<sup>2</sup>, Cathie Ventalon<sup>1</sup>; <sup>1</sup>Ecole Normale Supérieure, France; <sup>2</sup>Institut de Génomique Fonctionnelle, France. We developed a novel fiberscope that allows fast (up to 300Hz) line-scanning and multipoint-scanning confocal imaging in freely-behaving mice, using a DMD. Fluorescence imaging of microvasculature and neuronal activity will be presented.

## Atlantic Ballroom 3

Optical Tomography and Spectroscopy

### OTh4D • Tomographic and Spectroscopy Methods for Non-Invasive Imaging of Disease—Continued

**OTh4D.5 • 16:45**  
**The LUCA Project - Laser and Ultrasound Co-Analyzer for Thyroid Nodules: Overview and Current Status**, Lorenzo Cortese<sup>1</sup>, Gloria Aranda<sup>2</sup>, Mauro Buttava<sup>3</sup>, Davide Contini<sup>4</sup>, Alberto Dalla Mora<sup>4</sup>, Sixte de Fraguier<sup>5</sup>, Hamid Dehghan<sup>6</sup>, Eduardo Garcia<sup>7</sup>, Ramon Gomis<sup>2</sup>, Felicia Hanzu<sup>2</sup>, Katharina Krischak<sup>8</sup>, Giuseppe Lo Presti<sup>1</sup>, Mireia Mora<sup>2</sup>, Antonio Pifferi<sup>4</sup>, Marco Renza<sup>9</sup>, Bogdan Rosinski<sup>7</sup>, Sanathana Konugolu Venkata Sekar<sup>4</sup>, Mattia Squarcia<sup>2</sup>, Paola Taroni<sup>4</sup>, Alberto Tosi<sup>3</sup>, Udo M. Weigel<sup>7</sup>, Stanislaw Wojtkiewicz<sup>8</sup>, Pamela Zolda<sup>8</sup>, Turgut Durduran<sup>10</sup>; <sup>1</sup>ICFO, Spain; <sup>2</sup>DIBAPS, Spain; <sup>3</sup>Politecnico di Milano, Italy; <sup>4</sup>Politecnico di Milano, Italy; <sup>5</sup>ECM - ECHO CONTROL MEDICAL, S.A.S., France; <sup>6</sup>Univ. of Birmingham, UK; <sup>7</sup>HemoPhotonics S.L., Spain; <sup>8</sup>The European Inst. for Biomedical Imaging Research, Austria; <sup>9</sup>VERMON S.A., France; <sup>10</sup>CREA, Spain. We present the current status of the LUCA-project whose aim is to develop an innovative device combining ultrasound and diffuse optics for an improved screening of the thyroid cancer.

**OTh4D.6 • 17:00**  
**3D Pathophysiological Changes in Healthy Finger Joints During Cuff Occlusion**, Daniel Lighter<sup>1</sup>, Iain Styles<sup>2</sup>, Andrew Filer<sup>2</sup>, Hamid Dehghani<sup>2</sup>; <sup>1</sup>Sci-Phy-4-Health Centre for Doctoral Training, Univ. of Birmingham, UK; <sup>2</sup>School of Computer Science, Univ. of Birmingham, UK; <sup>3</sup>Rheumatology, Inst. of Inflammation and Ageing, College of Medical and Dental Sciences, Univ. of Birmingham, UK. Changes in 3D pathophysiological images for healthy finger joints during cuff occlusion are presented, recovered using multispectral diffuse optical tomography, to evaluate its potential use for early detection of rheumatoid arthritis.

**OTh4D.7 • 17:15**  
**Demonstration of Dual Channel Fluorescent Optical Projection Tomography to Guide Lymph Node Pathology**, Veronica C. Torres<sup>1</sup>, Cynthia Li<sup>1</sup>, Lagnojita Sinha<sup>1</sup>, Jovan G. Brankov<sup>2</sup>, Kenneth M. Tichauer<sup>1</sup>; <sup>1</sup>Biomedical Engineering, Illinois Inst. of Technology, USA; <sup>2</sup>Electrical Engineering, Illinois Inst. of Technology, USA. Mesoscopic imaging with early photon dual wavelength fluorescent optical projection tomography provides 3D maps of metastases in lymph nodes to guide pathology and reduce the high rate of false negatives in cancer staging.

**17:30–18:30 Postdeadline Papers Session, Atlantic Ballroom 1**  
 See the Congress Update sheet for the PDP schedule of talks.

**Atlantic Ballroom 1**

Microscopy, Histopathology and Analytics

**Atlantic Ballroom 2**

Clinical and Translational Biophotonics

**Grand Ballroom West**

Optics and the Brain

**Atlantic Ballroom 3**

Optical Tomography and Spectroscopy

07:30–17:00 Registration, Grand Ballroom Foyer

**08:00–09:30****MF1A • Digital Pathology***Presider: Kivanc Kose, Memorial Sloan Kettering Cancer Center, USA***MF1A.1 • 08:00** **Invited**

**Applications of Structured Light Microscopy in Clinical Pathology**, J. Quincy Brown<sup>1</sup>, Andrew Sholl<sup>1</sup>; <sup>1</sup>Tulane Univ., USA. Structured light microscopy, including structured illumination microscopy (SIM) and selective plane illumination microscopy (SPIM), has a number of compelling applications in clinical pathology, including large-area rapid 2D imaging for core biopsy and tumor margin assessment, rapid nondestructive 3D cytology, and comprehensive 3D analysis of tumor architecture with isotropic resolution. This talk will briefly introduce our work in these areas, focusing on the use of SIM in tumor margin imaging.

**MF1A.2 • 08:30** **Invited**

**SLIM Tissue Scanner for Cancer Diagnosis and Prognosis in Both Stained and Unstained Tissues**, Gabriel Popescu<sup>1</sup>; <sup>1</sup>Univ of Illinois at Urbana-Champaign, USA. We developed spatial light interference microscopy with a color camera (cSLIM), which reports on tumor microenvironment in both stained and unstained tissue slices, with nanoscale sensitivity and industry-standard throughput.

**08:00–09:30****CF1B • Optical Spectroscopy I***Presider: Theo Ruers, Netherlands Cancer Inst., Netherlands***CF1B.1 • 08:00** **Invited**

**Translation of a Label-Free Intraoperative Approach for the Identification of Parathyroid Glands During Neck Surgeries**, Anita Mahadevan-Jansen<sup>1</sup>; <sup>1</sup>Vanderbilt Univ., USA. Current status in label-free intraoperative approaches to aid surgeons in real-time, parathyroid identification during neck surgeries, will be presented. The focus will be translation from bench to prototype and its evaluation in a clinical setting.

**CF1B.2 • 08:30**

**Multimodal Spectral Histopathology for Detection of Residual Tumour during Basal Cell Carcinoma Surgery**, Radu Boitor<sup>1</sup>, Kenny Kong<sup>1</sup>, Dustin Shipp<sup>1</sup>, Sandeep Varma<sup>2</sup>, Alexey Koloydenko<sup>3</sup>, Kusum Kulkarni<sup>4</sup>, Somaia Elsheikh<sup>4</sup>, Tom Bakker Schut<sup>5</sup>, Peter Caspers<sup>5</sup>, Gerwin Puppels<sup>5</sup>, Ioan Notingher<sup>1</sup>; <sup>1</sup>School of Physics and Astronomy, Univ. of Nottingham, UK; <sup>2</sup>Circle Nottingham Ltd NHS Treatment Centre, UK; <sup>3</sup>Mathematics Dept., Royal Holloway Univ. of London, UK; <sup>4</sup>Dept. of Pathology, Nottingham Univ. Hospitals NHS Trust, UK; <sup>5</sup>RiverD International, Netherlands. We present a fully-automated device combining auto-fluorescence imaging and Raman spectroscopy capable of investigating skin resection margins in 30 minutes. The table top-device can easily fit in a surgery theatre.

**CF1B.3 • 08:45**  
Withdrawn.**08:00–09:00****BF1C • Gizmos and Gadgets***Presider: Daniel Cote, Universite Laval, Canada***BF1C.1 • 08:00** **Invited**

**Network Analysis of Optical Imaging Data**, Patrick Desrosiers<sup>1,2</sup>; <sup>1</sup>Universite Laval, Canada; <sup>2</sup>CERVO Brain Research Centre, Canada. Recent developments in light microscopy and optogenetics permit to record the calcium or electrical activity of large populations of neurons with high spatial resolution. Such neural activity imaging, however, generates big and complex datasets that make the analyst's task harder, especially when it comes to characterizing the neural network at different scales. This will give a practical overview of methods and tools that are used at different stages of the data analysis process, including cell bodies segmentation, extraction of time series, assessment of connectivity between neurons, and detection of mesoscopic structures (neuron communities) in networks.

**BF1C.2 • 08:30** **Invited**

**Portable and Modular Light Sheet Microscopy Platform**, Jan Huisken<sup>1</sup>; <sup>1</sup>Morgridge Inst. for Research, USA. The most advanced microscopes are developed in physics labs and disseminating the technology is a challenge. Here we propose a portable, modular light sheet microscope system that makes this imaging technology easily accessible to biologists.

**08:00–09:30****OF1D • Acousto-Optics and Ultrasound-Assisted Optical Tomography***Presider: Stefan Andersson Engels, Tyndall National Inst., Ireland; Sylvain Gigan, Laboratoire Kastler-Brossel, France***OF1D.1 • 08:00** **Invited**

**Transmission Matrix Approach to Focusing and Imaging in Scattering Media**, Sylvain Gigan<sup>1,2</sup>; <sup>1</sup>Laboratoire Kastler-Brossel, France; <sup>2</sup>Sorbonne Université, France. I will review various approaches to controlling light in and through scattering media, exploiting the knowledge of the transmission matrix, not only for focusing through and in a medium, but also to control the point-spread function or control an ultrashort pulse.

**OF1D.2 • 08:30**

**Modeling Acousto-Optical Tomography With Optical Phase Conjugation Using Transmission Matrix Formalism**, Michael Raju<sup>1,2</sup>, Jacqueline Gunther<sup>1</sup>, Stefan Andersson Engels<sup>1,2</sup>; <sup>1</sup>Tyndall National Inst., Ireland; <sup>2</sup>Physics, Univ. College Cork, Ireland. A 2D electromagnetic wave transport modeling with optical phase information for simulating acousto-optical tomography is formulated using T-Matrix (translation matrix) and transmission matrix formalisms by cascading slabs of periodic collections of infinite cylinders.

**OF1D.3 • 08:45**

**Theoretical Study of Combined Acousto-optical Tomography and Slow Light Filters**, Jacqueline Gunther<sup>1</sup>, Andreas Walther<sup>2</sup>, Lars Rippe<sup>2</sup>, Stefan Kröll<sup>2</sup>, Stefan Andersson Engels<sup>1,3</sup>; <sup>1</sup>Tyndall National Inst., Ireland; <sup>2</sup>Physics, Lund Univ., Sweden; <sup>3</sup>Physics, Univ. College Cork, Ireland. Monte Carlo simulations were used to determine the contrast-to-noise ratio of acousto-optical imaging with slow light filters versus imaging depth. Both reflection and transmission setups were considered. The theoretical model showed that imaging through 12 cm of breast tissue could be plausible.

## Atlantic Ballroom 1

Microscopy, Histopathology  
and Analytics

### MF1A • Digital Pathology— Continued

MF1A.3 • 09:00

**MUSE: A Novel Approach for Slide-free Microscopy**, Farzad Fereidouni<sup>1</sup>, Richard M. Levenson<sup>1</sup>; <sup>1</sup>*Univ. of California, Davis, USA*. Microscopy with UV-surface excitation (MUSE) is a novel technique for rapid, slidefree tissue imaging. This non-destructive, full-color approach replaces standard histology, generates diagnostic-quality images within minutes, and is suitable for remote settings.

MF1A.4 • 09:15

**Virtual H&E Whole-mount Fluorescence Histology of the Entire Prostate Surface for Real-time Surgical Guidance**, Katherine N. Elfer<sup>1</sup>, David Tulman<sup>1</sup>, Sam J. Luethy<sup>1</sup>, Andrew Sholl<sup>1</sup>, Jonathan Silberstein<sup>1</sup>, J. Quincy Brown<sup>1</sup>; <sup>1</sup>*Tulane Univ., USA*. We demonstrate the first fluorescent virtual-H&E of the entire surface of an intact radical prostatectomy margin via DRAQ5 and Eosin imaging with VR-SIM. We also confirm that D&E does not affect clinical downstream fluorescent assays.

## Atlantic Ballroom 2

Clinical and Translational  
Biophotonics

### CF1B • Optical Spectroscopy I—Continued

CF1B.4 • 09:00

**Quantitative Analyses of SHG Endomicroscopy Images of Cervical Collagen Network for Detecting Preterm Birth in Mouse Models**, Wenxuan Liang<sup>1</sup>, Vorada Sakulsaengprapha<sup>1</sup>, Katherine Luby-Phelps<sup>2</sup>, Mala Mahendroo<sup>2</sup>, Xingde Li<sup>1</sup>; <sup>1</sup>*Johns Hopkins Univ., USA*; <sup>2</sup>*Univ. of Texas Southwestern Medical Center, USA*. SHG endomicroscopy imaging performed on cervical collagen is described. Subsequent image analyses quantify the morphological differences between normal and preterm pregnancy mice cervical tissue images.

CF1B.5 • 09:15

**Robotic Wide-Field Optical Biopsy Endoscopy**, Fernando B. Avila Rencoret<sup>1</sup>, George P. Mylonas<sup>2</sup>, Daniel S. Elson<sup>1</sup>; <sup>1</sup>*Dept. of Surgery and Cancer, The Hamlyn Centre for Robotic Surgery, Imperial College London, UK*; <sup>2</sup>*Dept. of Surgery and Cancer, Imperial College London, UK*. This paper describes a novel robotic framework for wide-field optical biopsy endoscopy, characterizes *in vitro* its spatial and spectral resolution, real time hyperspectral tissue classification, and demonstrates its feasibility on fresh porcine cadaveric colon.

## Grand Ballroom West

Optics and the Brain

### BF1C • Gizmos and Gadgets— Continued

## Atlantic Ballroom 3

Optical Tomography and  
Spectroscopy

### OF1D • Acousto-Optics and Ultrasound-Assisted Optical Tomography—Continued

OF1D.4 • 09:00

**A Calibration Method for Diffuse Optical Tomography Based on Extracted Target Depth and Size from Ultrasound Images**, Hamed Vavadi<sup>1</sup>, Quing Zhu<sup>1</sup>; <sup>1</sup>*Univ. of Connecticut, USA*. In this abstract a calibration method based on depth and size information provided from ultrasound images is introduced. The method utilizes the forward data simulated by finite element method to calibrate the reconstructed absorption map.

OF1D.5 • 09:15

**Improved Two Step Reconstruction Method in Ultrasound Guided Diffuse Optical Tomography**, K M Shihab Uddin<sup>1</sup>, Atahar Mostafa<sup>1</sup>, Mark A. Anastasio<sup>1</sup>, Quing Zhu<sup>1</sup>; <sup>1</sup>*Washington Univ. in St Louis, USA*. For ill-posed and ill-conditioned DOT inverse problem, a two-step reconstruction method is proposed. This method obtains an initial solution from the Truncated Pseudoinverse method and uses it for conjugate-gradient based inverse mapping of optical properties.

---

09:30–10:00 Coffee Break and Exhibits, Grand Ballroom East

---

## Atlantic Ballroom 1

Microscopy, Histopathology and Analytics

10:00–11:45

**MF2A • Nonlinear Microscopy**  
Presider: Marica Ericson, Univ. of Gothenburg, Sweden

**MF2A.1 • 10:00**

**Multiphoton Imaging of Surgical Pathology**, Michael G. Giacomelli<sup>1</sup>, Tadayuki Yoshitake<sup>2</sup>, Lucas C. Cahill<sup>1</sup>, Beverly Faulkner-Jones<sup>2</sup>, James Connolly<sup>2</sup>, Daihung Do<sup>3</sup>, James Fujimoto<sup>1</sup>; <sup>1</sup>EECS, MIT, USA; <sup>2</sup>Pathology, Beth Israel Deaconess Medical Center, USA; <sup>3</sup>Dermatology, Beth Israel Deaconess Medical Center, USA. Fluorescent imaging combined with H&E-rendering algorithms can provide histological imaging of surgical specimens more rapidly than conventional histology. We present results imaging breast and skin cancer specimens using highspeed multiphoton microscopy.

**MF2A.2 • 10:15**

**Multicolor Two-photon Imaging of Endogenous Fluorophores in Living Tissues by Wavelength Mixing**, Chiara Stringari<sup>1</sup>, Lamiae Abdeladim<sup>1</sup>, Pierre Mahou<sup>1</sup>, Guy Malkinson<sup>1</sup>, Sébastien BRIZION<sup>2</sup>, Jean-Baptiste Galey<sup>2</sup>, Willy Supatto<sup>1</sup>, Renaud Legouis<sup>3</sup>, Ana-Maria Pena<sup>2</sup>, Emmanuel Beaufreire<sup>1</sup>; <sup>1</sup>LAB FOR OPTICS AND BIOSCIENCES, Ecole Polytechnique, CNRS, INSERM, France; <sup>2</sup>L'Oréal Research and Innovation, France; <sup>3</sup>Inst. for Integrative Biology of the Cell, CEA, CNRS, Univ Paris Sud, Université Paris Saclay, France. Here, we report on efficient and simultaneous multicolor two-photon excitation of endogenous fluorophores with absorption spectra spanning the 750-1040nm range, using wavelength mixing.

**MF2A.3 • 10:30**

**Patterned Illumination Wide-Field Two-Photon Microscopy for Enhanced Axial Resolution and Deep Imaging**, Jong K. Park<sup>1</sup>, Dushan Waddu-wage<sup>1</sup>, Peter T. So<sup>1</sup>; <sup>1</sup>MIT, USA. We demonstrate a simple and programmable implementation of pattern scanning temporal focusing technique, by employing a digital micromirror device, for enhancing axial resolution.

## Atlantic Ballroom 2

Clinical and Translational Biophotonics

10:00–12:00

**CF2B • Optical Spectroscopy II**  
Presider: Melissa Suter, Harvard Medical School, USA

**CF2B.1 • 10:00** **Invited**

**Developing Quantitative Optical Imaging Endpoints for Clinical Medicine**, Bruce J. Tromberg<sup>1</sup>; <sup>1</sup>Univ. of California Irvine, USA. We present the development and validation of quantitative, label-free imaging endpoints based on Multiphoton Microscopy and Diffuse Optical Imaging for differential diagnosis and outcome prediction in patients with melanoma, breast cancer, and metabolic disease.

**CF2B.2 • 10:30**

**Non-invasive, Simultaneous Quantification of Vascular Oxygenation, Glucose Uptake and Mitochondria Membrane Potential in a Flank Tumor Model**, Caigang Zhu<sup>1</sup>, Hannah Martin<sup>1</sup>, Martin Li<sup>1</sup>, Brian Crouch<sup>1</sup>, Amy Martinez<sup>1</sup>, Gregory Palmer<sup>1</sup>, Mark Dewhurst<sup>1</sup>, Nimmi Ramanujam<sup>1</sup>; <sup>1</sup>Duke Univ., USA. For the first time, we performed simultaneous *in vivo* spectroscopy of tissue hemoglobin, 2-NBDG, and TMRE in a preclinical model, to successfully capture vascular and metabolic parameters *in vivo* in solid tumors.

## Grand Ballroom West

Optics and the Brain

10:00–12:00

**BF2C • Cerebral Blood Flow in Humans**  
Presider: Maria Angela Franceschini, Harvard Medical School

**BF2C.1 • 10:00** **Invited**

**Latest on Our Gizmos & Gadgets Based on Speckle Statistics to Measure the Cerebral Bloodflow of the Human Brain**, Turgut Durduran<sup>1</sup>; <sup>1</sup>ICFO -The Inst. of Photonic Sciences, Spain. I will present the latest advances in developing scalable, portable, low-cost monitors for measuring cerebral blood flow. These methods based on diffuse correlation spectroscopy and speckle contrast optical spectroscopy will be put in the context of their on-going clinical translation and pilot validations.

**BF2C.2 • 10:30**

**Quantification of Cerebral Blood Flow in Adults by Dynamic Contrast-Enhanced NIRS: Validation against MRI**, Daniel F. Milej<sup>1,3</sup>, Lian He<sup>2</sup>, Androu Abdalmalak<sup>1,3</sup>, Wesley Baker<sup>4</sup>, Udunna C. Anazodo<sup>1,3</sup>, Sudipto Dolui<sup>5</sup>, Venkaiah C. Kavuri<sup>4</sup>, Mamadou Diop<sup>1,3</sup>, William Pavlosky<sup>3</sup>, Ramani Balu<sup>5</sup>, John A. Detre<sup>5</sup>, Adrew Kofke<sup>4</sup>, Arjun G. Yodh<sup>2</sup>, Keith St. Lawrence<sup>1,3</sup>; <sup>1</sup>Dept. of Medical Biophysics, Univ. of Western Ontario, Canada; <sup>2</sup>Dept. of Physics and Astronomy, Univ. of Pennsylvania, USA; <sup>3</sup>Imaging Division, Lawson Health Research Inst., Canada; <sup>4</sup>Dept. of Anesthesiology and Critical Care, Univ. of Pennsylvania, USA; <sup>5</sup>Dept. of Neurology, Univ. of Pennsylvania, USA. An optics-MRI perfusion validation study investigated whether time-resolved contrast-enhanced NIRS can measure cerebral blood flow changes induced by altering arterial PCO<sub>2</sub>. Strong correlation between flow estimates from MRI and contrast-enhanced NIRS was found.

## Atlantic Ballroom 3

Optical Tomography and Spectroscopy

10:00–12:00

**OF2D • Devices and Algorithms for Optical Imaging**  
Presider: Adam Eggebrecht, Washington Univ. in St Louis, USA

**OF2D.1 • 10:00** **Invited**

**Hyperspectral Imaging for Improved Early Cancer Detection in Endoscopy**, Sarah Bohndiek<sup>1</sup>; <sup>1</sup>Univ. of Cambridge, UK. Exploiting spectral properties of light can assist in defining tissue disease state during endoscopy. Here, I will discuss recent efforts in our Lab to develop hyperspectral endoscopy hardware for early cancer detection in the oesophagus.

**OF2D.2 • 10:30**

**Improving Functional Diffuse Optical Tomography Reconstruction Quality Utilizing Frequency Domain Measurements**, Matthaïos Doulgerakis-Kontoudis<sup>1</sup>, Adam T. Eggebrecht<sup>2</sup>, Joseph P. Culver<sup>2,3</sup>, Hamid Dehghani<sup>1</sup>; <sup>1</sup>Univ. of Birmingham, UK; <sup>2</sup>Dept. of Radiology, Washington Univ. School of Medicine, USA; <sup>3</sup>Dept. of Biomedical Engineering, Washington Univ. in St. Louis, USA. Simulations on 24 subject specific models suggest that the combination of phase shift and amplitude attenuation information in fDOT neuroimaging improves the localization and resolution of the reconstructions, by 42% and 24% respectively, compared to attenuation only data.

## Atlantic Ballroom 1

Microscopy, Histopathology  
and Analytics

### MF2A • Nonlinear Microscopy—Continued

**MF2A.4 • 10:45** **Invited**  
Imaging T Cell Metabolism for Activity and Heterogeneity Analysis, Alex Walsh<sup>1</sup>; <sup>1</sup>US Air Force Research Lab, USA. Fluorescence imaging of NAD(P)H and FAD reveals metabolic differences between T cell subtypes. Heterogeneity analysis of optical imaging endpoints reveals intra- and inter-donor heterogeneity in T cell populations and activation.

**MF2A.5 • 11:15** **Invited**  
Exploring the Combination of Large Area Widefield Fluorescence Imaging with Multiphoton Microscopy in the Detection of Oral Epithelial Neoplasia, Gracie Vargas<sup>1</sup>, Rahul Pal<sup>1</sup>, Paula Villarreal<sup>1</sup>, Tyra Brown<sup>1</sup>, Suimin Qiu<sup>1</sup>, Susan D. McCammon<sup>1,2</sup>; <sup>1</sup>Univ. of Texas Medical Branch, USA; <sup>2</sup>Univ. of Alabama in Birmingham, USA. This study examines the potential pairing large area widefield fluorescence imaging with microscopic MPM imaging in a hamster model for oral neoplasia and pilot human oral cancer samples.

## Atlantic Ballroom 2

Clinical and Translational  
Biophotonics

### CF2B • Optical Spectroscopy II—Continued

**CF2B.3 • 10:45**  
Broadband (600-1100 nm) Diffuse Optical Characterization of Thyroid Tissue Constituents and Application to *in vivo* Thyroid Studies, Sanathana Konugolu Venkata Sekar<sup>1</sup>, Andrea Farina<sup>2</sup>, Alberto Dalla Mora<sup>1</sup>, Paola Taroni<sup>1,2</sup>, Claus Lindner<sup>3</sup>, Mireia Mora<sup>4,5</sup>, Marco Pagliazzi<sup>2</sup>, Mattia Squarcia<sup>6</sup>, Irene Halperin<sup>4,5</sup>, Felicia Hanzu<sup>4,5</sup>, Hamid Dehghani<sup>7</sup>, Turgut Durduran<sup>3,8</sup>, Antonio Pifferi<sup>1,2</sup>; <sup>1</sup>Politecnico di Milano, Italy; <sup>2</sup>Istituto di Fotonica e Nanotecnologie, Consiglio Nazionale delle Ricerche, Italy; <sup>3</sup>The Barcelona Inst. of Science and Technology, ICFO-Institut de Ciències Fotòniques, Spain; <sup>4</sup>IDIBAPS, Fundació Clinic per la Recerca Biomèdica, Spain; <sup>5</sup>Hospital Clinic of Barcelona, Endocrinology and Nutrition Dept., Spain; <sup>6</sup>Hospital Clinic of Barcelona, Neuroradiology Dept., Spain; <sup>7</sup>School of Computer Science, Univ. of Birmingham, UK; <sup>8</sup>Institució Catalana de Recerca i Estudis Avançats (ICREA), Spain. We present the first broadband (600-1350 nm) diffuse optical characterization of thyroglobulin and tyrosine, which are thyroid-specific tissue constituents. *In vivo* measurements on the thyroid of 6 subjects enabled their quantification for functional and diagnostic applications.

**CF2B.4 • 11:00**  
Light Scattering Spectroscopy Diagnoses Pancreatic Cystic Lesions *In Vivo*, Le Qiu<sup>1</sup>, Lei Zhang<sup>1</sup>, Vladimir Turzhitsky<sup>1</sup>, Douglas K. Pleskow<sup>1</sup>, Ram Chuttani<sup>1</sup>, Tyler M. Berzin<sup>1</sup>, Manddeep Sawhney<sup>1</sup>, Edward Vitkin<sup>1</sup>, Umar Khan<sup>1</sup>, Yuri Zakharov<sup>1</sup>, Irving Itzkan<sup>1</sup>, Lev T. Perelman<sup>1</sup>; <sup>1</sup>Harvard Univ., USA. Millions of Americans have pancreatic cystic lesions, the only readily identifiable precursors of deadly pancreatic cancer. We report a light scattering spectroscopic technique that predicts the malignant potential of pancreatic cystic lesions *in vivo*.

**CF2B.5 • 11:15**  
In Vivo Photoacoustic Tracking Migration of Mesenchymal Stem Cells in Multiple Myeloma Model, Yajing Liu<sup>2,1</sup>, liming nie<sup>2</sup>; <sup>1</sup>caltech, USA; <sup>2</sup>Xiamen Univ., China. Continuous tracking of the migration of mesenchymal stem cells (MSCs) is essential to understand their role in cancer. Herein, we use ultra-sensitive photoacoustic microscopy (PAM) for tracking MSCs at cell level and guiding photothermal therapy.

## Grand Ballroom West

Optics and the Brain

### BF2C • Cerebral Blood Flow in Humans—Continued

**BF2C.3 • 10:45**  
A Novel Fiberless Diffuse Speckle Contrast Flowmeter for Tissue Blood Flow Measurement, Mingjun Zhao<sup>1</sup>, Chong Huang<sup>1</sup>, Siavash Mazdeyasna<sup>1</sup>, Elie G. Abu Jawdeh<sup>1</sup>, Henrietta S. Bada<sup>1</sup>, Guoqiang Yu<sup>1</sup>; <sup>1</sup>Univ. of Kentucky, USA. We reported a novel, low-cost, compact, fiberless, diffuse speckle contrast flowmeter consisting of a laser diode and a bare CCD/CMOS chip for tissue blood flow measurement. We validated the system in tissue phantoms and explored its applications in human tissues.

**BF2C.4 • 11:00** **Invited**  
Quantitative Tissue Spectroscopy Techniques for Measuring Cerebral Perfusion and Metabolism, Mamadou Diop<sup>1</sup>; <sup>1</sup>Western Univ., Canada. The brain constitutes 2% of the total body weight but accounts for 20% and 25% of total body basal oxygen and glucose consumption, respectively. As well, the brain has very limited energy storage; thus, it relies on adequate blood flow for oxygen and glucose delivery, and disruption in supply can have devastating effects on the brain.

## Atlantic Ballroom 3

Optical Tomography and  
Spectroscopy

### OF2D • Devices and Algorithms for Optical Imaging—Continued

**OF2D.3 • 10:45**  
Label-free, Non-invasive Mapping of Water and Lipid Content in Tissue with Structured Shortwave-infrared Imaging (SSI), Yanyu Zhao<sup>1</sup>, Matthew B. Applegate<sup>1</sup>, John P. Dumas<sup>2</sup>, Mark C. Pierce<sup>2</sup>, Darren Roblyer<sup>1</sup>; <sup>1</sup>Boston Univ., USA; <sup>2</sup>Rutgers, The State Univ. of New Jersey, USA. We present a label-free imaging method for non-invasive mapping of tissue water and lipid content using quantitative short-wave infra-red imaging. Intralipid phantom results are shown along with an *in vivo* demonstration of brown fat classification.

**OF2D.4 • 11:00**  
Fluorescence Lifetime Imaging with Compressive Sensing through Deep Convolutional Neural Network, Ruoyang Yao<sup>1</sup>, Marien I. Ochoa<sup>1</sup>, Xavier Intes<sup>1</sup>, Pingkun Yan<sup>1</sup>; <sup>1</sup>Dept. of Biomedical Engineering, Rensselaer Polytechnic Inst., USA. We designed a Convolutional Neural Network to directly reconstruct both intensity and lifetime images from raw compressive time-resolved measurements. It provides better simulated and experimental results with significantly reduced time compared to the traditional workflow.

**OF2D.5 • 11:15**  
Brillouin Elastography for Non-contact Mechanical Mapping of Spinal Cord Repair, Juergen W. Czarske<sup>1</sup>, Raimund Schluöbler<sup>1</sup>, Stephanie Möllmert<sup>1</sup>, Jochen Guck<sup>1</sup>; <sup>1</sup>Technische Universität Dresden, Germany. Non-contact, three-dimensional, subcellular measurements of elasticity of cells and tissue are presented. We demonstrate a systematic application of Brillouin elastography to quantify the mechanical properties of native larval zebrafish tissues *in vivo*.

## Atlantic Ballroom 1

Microscopy, Histopathology  
and Analytics

MF2A • Nonlinear  
Microscopy—Continued

## Atlantic Ballroom 2

Clinical and Translational  
Biophotonics

CF2B • Optical Spectroscopy  
II—Continued

CF2B.6 • 11:30

**Blood-flow-informed Photodynamic Therapy(PDT) Improves Therapeutic Efficacy**, Yihong Ong<sup>1</sup>, Joann Miller<sup>1</sup>, Timothy C. Zhu<sup>1</sup>, Arjun G. Yodh<sup>1</sup>, Theresa M. Busch<sup>1</sup>; <sup>1</sup>Univ. of Pennsylvania, USA. We demonstrate a noninvasive system for real-time monitoring of tumor blood flow and automatic adjustment of treatment light fluence-rate to conserve tumor perfusion during PDT. Improved efficacy was observed using blood-flow informed light delivery.

CF2B.7 • 11:45

**Early Pressure Injury Prediction using Non-invasive Optical Methods**, Alec Lafontant<sup>4</sup>, Michael Neidrauer<sup>4</sup>, Michael Weingarten<sup>1</sup>, Rose Ann DiMaria-Ghalili<sup>2</sup>, Guy Fried<sup>3</sup>, Peter Lewin<sup>4</sup>, Leonid Zubkov<sup>4</sup>; <sup>1</sup>College of Medicine, Drexel Univ., USA; <sup>2</sup>College of Nursing and Health Professions, Drexel Univ., USA; <sup>3</sup>Magee Rehabilitation Hospital, USA; <sup>4</sup>School of Biomedical Engineering, Drexel Univ., USA. Diffuse correlation spectroscopy was used to measure blood flow index in rehabilitation patients with spinal cord injuries. Significant differences in BFI were found between those who developed pressure injuries compared with those whose redness disappeared.

## Grand Ballroom West

Optics and the Brain

BF2C • Cerebral Blood Flow in  
Humans—Continued

BF2C.5 • 11:30 **Invited**

**Diffuse Correlation Spectroscopy to Elucidate Mechanisms of Brain Injury**, Erin Buckley<sup>1</sup>; <sup>1</sup>Emory Univ., USA. Using non-invasive diffuse correlation spectroscopy measurements, we discovered that low cerebral blood flow is a functional biomarker of cognitive and pathological outcome after repetitive head injury. We exploit this predictive capability to explore acute mechanisms that drive contemporaneous hemodynamic changes as well as chronic outcome post-injury.

## Atlantic Ballroom 3

Optical Tomography and  
Spectroscopy

OF2D • Devices and  
Algorithms for Optical  
Imaging—Continued

OF2D.6 • 11:30 **Invited**

**Novel Technologies for Time-Domain Diffuse Optics: Miniaturized Wearable Devices and Bioresorbable Optical Fibers**, Alberto Dalla Mora<sup>1</sup>, Laura Di Sieno<sup>1</sup>, Sanathana Konugolu Venkata Sekar<sup>1</sup>, Andrea Farina<sup>2</sup>, Davide Contini<sup>1</sup>, Nadia G. Boetti<sup>3</sup>, Daniel Milanese<sup>4,5</sup>, Jan Nissinen<sup>6</sup>, Antonio Pifferi<sup>1</sup>; <sup>1</sup>Politecnico di Milano, Italy; <sup>2</sup>Consiglio Nazionale delle Ricerche, Italy; <sup>3</sup>Istituto Superiore Mario Boella, Italy; <sup>4</sup>Politecnico di Torino, Italy; <sup>5</sup>Consiglio Nazionale delle Ricerche, Italy; <sup>6</sup>Univ. of Oulu, Finland. Time-Domain Diffuse Optics is undergoing fascinating technology advancements. After a brief review of recent innovations, here we present a miniaturized pulsed source enabling wearable systems and the ex-vivo validation of implantable bioresorbable optical fiber.

---

12:00–13:30 Lunch Break, On Your Own

---

---

12:00–13:30 **Lost in Translation?: Clinical Trial Challenges Across the Globe**, Grand Ballroom West  
(Lunch will be available for purchase outside the meeting room)

---

## Atlantic Ballroom 1

Microscopy, Histopathology and Analytics

13:30–15:30

### MF3A • Cellular Diagnostics

Prsident: Adam Glaser, Univ. of Washington, USA

MF3A.1 • 13:30 **Invited**

**Providing CLARITY: 3D Imaging of Biomarkers in Tumor Samples**, Yi Chen<sup>1</sup>, Qi Shen<sup>1</sup>, Yesim Gokmen-Polar<sup>2</sup>, Sunil Badve<sup>2</sup>, Laurie Goodman<sup>1</sup>; <sup>1</sup>*Clearlight Diagnostics, USA*; <sup>2</sup>*Pathology and Lab Medicine, Indiana Univ. School of Medicine, USA*. The CLARITY method was used to transform core needle biopsies from patients with breast cancer, into optically transparent tissues, followed by multiplexed immunostaining and 3D imaging of key biomarkers. This data was compared to conventional FFPE thin-section methods. Manual pathology scoring of the 3D images from CLARITY processed samples demonstrated concordant results when compared to a set of 2D images scored throughout a similar sized FFPE block from the same patient.

MF3A.2 • 14:00 **Invited**

**Nucleus and Cytoplasm Segmentation Using Full-Field Optical Coherence Tomography**, Chia-Kai Chang<sup>1</sup>, Sheng-Lung .Huang<sup>1</sup>; <sup>1</sup>*Graduate Inst. of Photonics and Optoelectronics, National Taiwan Univ., Taiwan*. Using cellular-resolution optical coherence tomography, a random rayburst sampling framework was developed to extract 3D morphological features of skin cells and tissues. The nuclei and cytoplasm volumes and spatial distribution of keratinocytes were quantitatively obtained.

## Atlantic Ballroom 2

Clinical and Translational Biophotonics

13:30–15:30

### CF3B • Optical Spectroscopy III

Prsident: Bruce Tromberg, Univ. of California Irvine, USA

CF3B.1 • 13:30

**Predicting Chemotherapeutic Response with Hemodynamic Parameters from Diffuse Correlation Spectroscopy and Diffuse Optical Spectroscopy**, gabriel Ramirez<sup>1</sup>, Ashley R. Proctor<sup>1</sup>, Songfeng Han<sup>1</sup>, Regine Choe<sup>1</sup>; <sup>1</sup>*Biomedical Engineering, Univ. of Rochester, USA*. Longitudinal hemodynamic parameters were quantified in 4T1 murine breast cancer under chemotherapy using diffuse correlation and optical spectroscopies. A hemodynamic model to predict chemotherapeutic response within two weeks of intervention is being developed.

CF3B.2 • 13:45

**Optical Quantification of Placenta Oxygenation with Ultrasound Integrated Frequency-Domain NIRS**, Lin Wang<sup>1</sup>, Tiffany Ko<sup>1</sup>, Lian He<sup>1</sup>, Venkaiah C. Kavuri<sup>1</sup>, Ashwin B. Parthasarathy<sup>2</sup>, Wesley Baker<sup>1</sup>, Nadav Schwartz<sup>1</sup>, Arjun G. Yodh<sup>1</sup>; <sup>1</sup>*Univ. of Pennsylvania, USA*; <sup>2</sup>*Electrical Engineering, Univ. of South Florida, USA*. We built a heterodyne frequency-domain near-infrared spectroscopy (NIRS) instrument integrated with ultrasound for investigation of placenta physiology. The instrument was characterized and first measurements quantified placenta vascular oxygenation in healthy human subjects.

CF3B.3 • 14:00

**A Real-time Photoacoustic-ultrasound Dual Modality Functional Imaging System for Clinical Study**, Lingyi Zhao<sup>1</sup>, Fang Yang<sup>2</sup>, Meng Yang<sup>3</sup>, Tao Han<sup>1</sup>, Lei Zhu<sup>2</sup>, Yuxin Jiang<sup>3</sup>, Changhui Li<sup>1</sup>; <sup>1</sup>*Peking Univ., China*; <sup>2</sup>*Shenzhen Mindray Bio -Medical Electronics Co., China*; <sup>3</sup>*Dept. of Ultrasonography, Chinese Academy of Medical Sciences & Peking Union Medical College, China*. We reported a dual-modality Photoacoustic-ultrasound imaging system, which can provide both ultrasound and functional photoacoustic imaging simultaneously. We demonstrated its performance via multiple clinical human studies, including thyroid cancer and breast tumor.

CF3B.4 • 14:15

**Near Infrared Light Propagation Modeling of Infant Lung with Light Source Placed Inside Intubated Airway**, Andrea L. Pacheco Tobo<sup>1,2</sup>, Emilie Krite Svanberg<sup>3</sup>, Eugene Dempsey<sup>4</sup>, Stefan Andersson Engels<sup>1,2</sup>; <sup>1</sup>*Tyndall, Ireland*; <sup>2</sup>*Dept. of Physics, Univ. College Cork, Ireland*; <sup>3</sup>*Dept. of Clinical Sciences, Anesthesiology and Intensive Care Medicine, Skåne Univ. Hospital, SE-221 85, Sweden*; <sup>4</sup>*INFANT Center, Cork Univ. Maternity Hospital, Ireland*. We simulate light propagation in 3D numerical model of infant thorax at 761 nm with light source placed inside the trachea and detectors over the skin between axilla and sternum.

## Grand Ballroom West

Optics and the Brain

13:30–15:30

### BF3C • Looking Deeper

Prsident: Spencer Smith, Univ of North Carolina at Chapel Hill, USA

BF3C.1 • 13:30 **Invited**

**In Vivo Deep Imaging of the Brain**, Chris Xu<sup>1</sup>; <sup>1</sup>*Cornell Univ., USA*. The long wavelength windows of 1300 and 1700 nm are well suited for deep imaging within scattering biological tissues. In vivo nonlinear imaging of neuronal structure and function deep within intact animal brains is presented.

BF3C.2 • 14:00

**In Vivo Brain Imaging with Non-Degenerate 2-Photon Microscopy**, Sanaz Sadegh<sup>1</sup>, Mu-Han Yang<sup>2</sup>, Christopher G. Ferri<sup>1</sup>, Martin Thunemann<sup>3</sup>, Payam A. Saisan<sup>1</sup>, Erik A. Rodriguez<sup>2</sup>, Stephen R. Adams<sup>4</sup>, Sergei A. Vinogradov<sup>5</sup>, Yeshaiahu Fainman<sup>6</sup>, Anna Devor<sup>7,8</sup>; <sup>1</sup>*Neurosciences, Univ. of California, San Diego, USA*; <sup>2</sup>*Electrical and Computer Engineering Graduate Program, Univ. of California, San Diego, USA*; <sup>3</sup>*Radiology, Univ. of California, San Diego, USA*; <sup>4</sup>*Dept. of Pharmacology, Univ. of California, San Diego, USA*; <sup>5</sup>*Dept.s of Biochemistry and Biophysics and of Chemistry, Univ. of Pennsylvania, USA*; <sup>6</sup>*Dept. of Electrical and Computer Engineering, Univ. of California, San Diego, USA*; <sup>7</sup>*Neurosciences and Radiology, Univ. of California San Diego, USA*; <sup>8</sup>*Martinos Center for Biomedical Imaging, MGH, Harvard Medical School, USA*. We demonstrate that non-degenerate 2-photon excitation offers a ~3-fold increase in excitation efficiency compared to degenerate 2-photon excitation and realize this advantage for in vivo brain imaging, trading the excitation efficiency for laser power.

BF3C.3 • 14:15

**Combining Near-infrared Excitation with Swept Confocally-aligned Planar Excitation (SCAPE) Microscopy for Fast, Volumetric Imaging in Mouse Brain**, Hang Yu<sup>1</sup>, P. T. Galwaduge<sup>1</sup>, Venkatakaushik Voleti<sup>1</sup>, Kripa B. Patel<sup>1</sup>, Mohammed A. Shaik<sup>1</sup>, Wenzhe Li<sup>1</sup>, Elizabeth M. Hillman<sup>1</sup>; <sup>1</sup>*Columbia Univ., USA*. We report our recent progress in combining near-infrared excitation with SCAPE microscopy for fast, volumetric imaging in mouse brain in vivo.

## Atlantic Ballroom 3

Optical Tomography and Spectroscopy

13:30–15:30

### OF3D • Optical Coherence Tomography: Novel Techniques

Prsident: Chao Zhou, Lehigh Univ., USA

OF3D.1 • 13:30 **Invited**

**Molecular Imaging with Optical Coherence Tomography and its Biomedical Applications**, Adam de la Zerdá<sup>1</sup>; <sup>1</sup>*Stanford Univ., USA*. We developed a way to turn OCT into a molecular imaging modality through the development of novel nanoparticles. We explored its application in neurosurgery and in visualizing the role of the immune system in tumors.

OF3D.2 • 14:00

**Automatic Measurement of Crimped Collagen Fiber Insertion Angle in Optical Coherence Tomography Images of the Anterior Cruciate Ligament**, James P. McLean<sup>1</sup>, Dovina Qu<sup>1</sup>, Helen Lu<sup>1</sup>, Christine Hendon<sup>1</sup>; <sup>1</sup>*Columbia Univ., USA*. We demonstrate an automatic method for quantifying collagen fiber orientation at the Anterior Cruciate Ligament ligament-to-bone insertion regions in Optical Coherence Tomography images. The integrated spatial filter automatically rejects orientations corresponding to crimped fiber features.

OF3D.3 • 14:15

**Speckle Reduction in Optical Coherence Tomography at Video Rate**, Yang Zhao<sup>1</sup>, Kengyeh K. Chu<sup>1</sup>, Will J. Eldridge<sup>1</sup>, Evan T. Jelly<sup>1</sup>, Michael Crose<sup>1</sup>, Adam Wax<sup>1</sup>; <sup>1</sup>*Duke Univ., USA*. We present a single-shot video-rate speckle reduction technique for OCT using an adaptation of the dual window method. This technique requires no hardware modification and offers ~25% reduction in speckle contrast without reducing spatial resolution.

## Atlantic Ballroom 1

Microscopy, Histopathology  
and Analytics

### MF3A • Cellular Diagnostics— Continued

**MF3A.3 • 14:30** **Invited**  
**Real-Time Imaging of Invadopodia in Tumor Microenvironment Context**, Aviv Bergman<sup>2</sup>, Bojana Gligorijevic<sup>1</sup>; <sup>1</sup>Temple Univ., USA; <sup>2</sup>Systems & Computational Biology, Albert Einstein College of Medicine, USA. We use intravital multiphoton microscopy in mouse models of breast carcinoma to understand cancer cell metastasis. We demonstrate that invadopodia *in vivo* are necessary for metastasis and that they can be eliminated by microenvironment modulation.

**MF3A.4 • 15:00**  
**Ultra-large-scale single-cell quantitative phase imaging**, Kelvin C. Lee<sup>1</sup>, Maolin Wang<sup>1</sup>, Hayden So<sup>1</sup>, Kevin Tsia<sup>1</sup>; <sup>1</sup>Electrical and Electronic Engineering, The Univ. of Hong Kong, Hong Kong. We demonstrate an interferometry-free, high-resolution and high-throughput quantitative-phase imaging platform, *multi-ATOM*, enabling ultra-large-scale single-cell image analysis (>1,000,000 cells) in the context of label-free cancer cell screening in blood.

**MF3A.5 • 15:15**  
**High-resolution 3D Phase Microscopy from Intensity**, Shwetadwip Chowdhury<sup>1</sup>, Regina Eckert<sup>1</sup>, Michael Chen<sup>1</sup>, Laura Waller<sup>1</sup>; <sup>1</sup>UC Berkeley, USA. We present a microscope system for high-resolution complex-field tomography from intensity-only measurements with illumination angle scanning. Preliminary results using a multi-slice framework show promise in visualizing the 3D structure of a cluster of 3  $\mu\text{m}$  transparent microspheres.

## Atlantic Ballroom 2

Clinical and Translational  
Biophotonics

### CF3B • Optical Spectroscopy III—Continued

**CF3B.5 • 14:30**  
**Mesoscopic Imaging of Actinic Skin Damage Using Spatial Frequency Domain Imaging**, Ulas Sunar<sup>1</sup>; <sup>1</sup>Wright State Univ., USA. We characterized skin tissue from mild photodamage to actinic keratosis (AK) by differences in total hemoglobin concentrations assessed by spatial frequency domain imaging.

**CF3B.6 • 14:45**  
**Intraoperative Assessment of Blood Flow Variations in Tissue Flaps Using Noncontact Diffuse Correlation Spectroscopy**, Mingjun Zhao<sup>1</sup>, Chong Huang<sup>1</sup>, Li Chen<sup>1</sup>, Jeffrey Rada-baugh<sup>1</sup>, Rony Aouad<sup>1</sup>, Nneamaka Agochukwu<sup>1</sup>, Lesley Wong<sup>1</sup>, Guoqiang Yu<sup>1</sup>; <sup>1</sup>Univ. of Kentucky, USA. We developed and used a novel noncontact diffuse correlation spectroscopy (ncDCS) device to quantify blood flow variations in mastectomy skin flaps and head/neck free transfer flaps during surgery, with the goal of predicting postoperative flap necrosis.

**CF3B.7 • 15:00**  
**Non-invasive Photoacoustic 3D Imaging of Non-Melanoma Skin Cancers in Asian Population**, Amalina E. Attia<sup>1</sup>, Sai Yee Chuah<sup>2</sup>, Daniel Razansky<sup>3,4</sup>, Chris Jun Hui Ho<sup>1</sup>, Xiuting Li<sup>1</sup>, Steven Tien Guan Thng<sup>2</sup>, Malini C. Olivo<sup>1</sup>; <sup>1</sup>Lab of Bio-optical Imaging, Singapore Bioimaging Consortium, Singapore; <sup>2</sup>National Skin Centre, Singapore; <sup>3</sup>Inst. for Biological and Medical Imaging, Germany; <sup>4</sup>Helmholtz Center Munich, Germany. Herein, Multispectral Photoacoustic Tomography (MSOT) was utilized to map non-melanoma skin cancers on Asian patients to obtain their lesion dimensions. The dimensions were then correlated from the measurements acquired from histology, showing good correlation via intraclass correlation coefficient.

**CF3B.8 • 15:15**  
**Retina and Choroid Imaging with Transcranial Back-illumination**, Timothy D. Weber<sup>1</sup>, Jerome Mertz<sup>1,2</sup>; <sup>1</sup>Dept. of Biomedical Engineering, Boston Univ., USA; <sup>2</sup>Photonics Center, Boston Univ., USA. We present an alternative illumination scheme for retinal imaging. It is based on near-infrared light delivered transcranially at the temple and light diffusion towards the retina. This unique transmission geometry simplifies absorption measurements and enables clear imaging as deep as the choroid.

## Grand Ballroom West

Optics and the Brain

### BF3C • Looking Deeper— Continued

**BF3C.4 • 14:30**  
**Fluorescence Endoscope for Deep Brain Imaging With Minimal Tissue Damage Using a Singlemode Fiber**, Francois Cote<sup>1,2</sup>, Joel Crepeau<sup>1,2</sup>, Nicolas Lapointe<sup>1,2</sup>, Damon DePaoli<sup>1,2</sup>, Cleophae Akitegetse<sup>1</sup>, Martin Levesque<sup>1</sup>, Daniel C. Cote<sup>1,2</sup>; <sup>1</sup>Cervo Brain Research Centre, Canada; <sup>2</sup>Centre d'Optique, Photonique et Laser, Canada. We designed a new endoscopic system with a 125  $\mu\text{m}$ -diameter singlemode fiber that use micro-optics at its tip to provide a large field of view of 400x400  $\mu\text{m}^2$  that is unrelated to the GRIN diameter.

**BF3C.5 • 14:45**  
**Ultra-Thin Flexible Two-Photon Lensless Endoscopy Using Multicore Optical Fibers**, Viktor Tsvirkun<sup>1</sup>, Siddharth Sivankutty<sup>1</sup>, Olivier Vanvincq<sup>2</sup>, Gérald Bouwmans<sup>2</sup>, Rosa Cossart<sup>3</sup>, Esben R. Andresen<sup>2,1</sup>, Hervé Rigneault<sup>1</sup>; <sup>1</sup>Institut Fresnel, France; <sup>2</sup>IRCIJA, PhLAM CNRS, France; <sup>3</sup>INMED Institut de Neurobiologie de la Méditerranée, INSERM, France. We present our recent progress in developing a two-photon lensless endoscope based on ultrathin multicore fiber and wavefront shaping. We discuss the field-of-view extension, intrinsic group delay and bending compensation in such devices with the aim of imaging the deep brain with minimal invasion.

**BF3C.6 • 15:00** **Invited**  
**Deep Tissue Optical Focusing and Optogenetic Modulation with Time-reversed Ultrasonically Encoded Light**, Haowen Ruan<sup>1</sup>, Changhui Yang<sup>1</sup>; <sup>1</sup>California Inst. of Technology, USA. Time-reversed ultrasonically encoded (TRUE) focusing enables noninvasive optical focusing beyond the optical diffusion limit. We demonstrated its application for optogenetic modulation of neural activity in 800- $\mu\text{m}$ -thick acute mouse brain slices at 532-nm wavelength.

## Atlantic Ballroom 3

Optical Tomography and  
Spectroscopy

### OF3D • Optical Coherence Tomography: Novel Techniques—Continued

**OF3D.4 • 14:30**  
Withdrawn.

**OF3D.5 • 14:45**  
**Full-Field OCT Technique for High Speed Event-Based Optical Flow and Particle Tracking**, Xavier Berthelon<sup>1</sup>, Guillaume Chenegros<sup>1</sup>, Nicolas Libert<sup>2</sup>, Jose-Alain Sahel<sup>1</sup>, Kate Grieve<sup>1,3</sup>, Ryad Benosman<sup>1</sup>; <sup>1</sup>Institut de la Vision, France; <sup>2</sup>Departement of Anaesthesia and Intensive Care, Hopital d'Instruction des Armees Percy, France; <sup>3</sup>Clinical Investigation Center, Quinze Vingts National Ophthalmology Hospital, France. We present a method to extract speed and density of microparticles at several kHz using a neuromorphic camera with a FF-OCT setup. This method performs faster and more efficiently than existing techniques in real time.

**OF3D.6 • 15:00**  
Withdrawn.

**OF3D.7 • 15:15**  
**Design and Implementation of a Low-Cost, Portable OCT System**, Ge Song<sup>1</sup>, Sanghoon Kim<sup>1</sup>, Michael Crose<sup>1</sup>, Brian Cox<sup>1</sup>, William Brown<sup>1</sup>, Adam Wax<sup>1</sup>; <sup>1</sup>Duke Univ., USA. We present a low-cost (under \$7,200), portable OCT system to improve ease of access outside of large eye centers. We demonstrate comparable imaging performance to current commercial OCT systems in *ex vivo* tissue samples.

15:30–16:00 Coffee Break and Exhibits, Grand Ballroom East

## Atlantic Ballroom 1

Microscopy, Histopathology and Analytics

16:00–18:00

### MF4A • Clinical Imaging

President: Eric Tkaczyk, Vanderbilt Univ., USA

MF4A.1 • 16:00 **Invited**

**Noninvasive Histopathological Imaging by Using Harmonic Generation Microscopy for Onsite Differential Diagnosis and Treatment Assessment**, Chi-Kuang Sun<sup>1</sup>; <sup>1</sup>National Taiwan Univ., Taiwan. With excitation light in the 1300nm penetration window, third-harmonic-generation microscopy can provide the highest penetration, viability, and 3D resolution for noninvasive histopathological imaging of skin lesions for onsite differential diagnosis and treatment assessment.

MF4A.2 • 16:30 **Invited**

**Application of Non-invasive Diagnostic Techniques for Management of Skin Lesions in 21st Century**, Attiya Haroon<sup>1</sup>, Babar Rao<sup>1</sup>; <sup>1</sup>Dept. of Dermatology, Rutgers-Robert Wood Johnson Medical School, USA. Non-invasive imaging techniques are painless and quick approach to manage skin lesions in 21st century. We are presenting a literature review of in vivo diagnostic techniques from last decades using pub med literature.

## Atlantic Ballroom 2

Clinical and Translational Biophotonics

16:00–18:00

### CF4B • OCT and Microscopy

President: To be Determined

CF4B.1 • 16:00 **Invited**

**Assessing Airway Remodeling, Structure and Function in Allergic Asthma using Optical Coherence Tomography**, Melissa Suter<sup>1</sup>; <sup>1</sup>Massachusetts General Hospital, Harvard Medical School, USA. Excessive contraction of airway smooth muscle leading to bronchoconstriction is responsible for airflow obstruction in individuals with asthma. We used PS-OCT to assess airway smooth muscle microstructure and function in asthmatic and healthy subjects in vivo.

CF4B.2 • 16:30

**Oblique Scanning Laser Ophthalmoscopy (oSLO) Allows Simultaneous Retinal Fluorescence Tomography with Optical Coherence Tomography**, Ji Yi<sup>1</sup>, Lei Zhang<sup>1</sup>, Weiye Song<sup>1</sup>, Di Shao<sup>1</sup>, Sui Zhang<sup>2</sup>, Steven Ness<sup>1</sup>, Sayon Roy<sup>1</sup>, Manishi Desai<sup>1</sup>; <sup>1</sup>Boston Univ., USA; <sup>2</sup>Dana Faber Cancer Institute, USA. We have developed a novel volumetric retinal fluorescence imaging method termed oblique scanning laser ophthalmoscopy (oSLO). By using a method of oblique illumination and angled detection, oSLO achieved simultaneous fluorescence tomography with optical coherence tomography.

CF4B.3 • 16:45

**Structural OCT Middle Ear Imaging Correlated with Functional Wideband Acoustic Immittance Measurements**, Jungeun Won<sup>1</sup>, Guillermo L. Monroy<sup>1</sup>, Pin-Chieh Huang<sup>1</sup>, Malcolm C. Hill<sup>2,3</sup>, Michael A. Novak<sup>2,3</sup>, Ryan G. Porter<sup>2,3</sup>, Eric Chaney<sup>1</sup>, Ronit Barkalifa<sup>1</sup>, Stephen A. Boppart<sup>1,3</sup>; <sup>1</sup>Univ of Illinois at Urbana-Champaign, USA; <sup>2</sup>Carle Foundation Hospital, USA; <sup>3</sup>Carle-Illinois College of Medicine, USA. Wideband acoustic immittance (WAI) measurements characterize middle ear function, but effects of pathologies are not thoroughly understood. Co-acquired OCT and WAI measurements from pediatric subjects were correlated to investigate varied acoustic responses in otitis media.

## Grand Ballroom West

Optics and the Brain

16:00–18:00

### BF4C • Microscopy, Structure and Anatomy

President: Jan Huisken, Morgridge Inst. for Research, USA

BF4C.1 • 16:00 **Invited**

**3d Human Brain Digital Histopathology**, Francesco S. Pavone<sup>1</sup>; <sup>1</sup>European Lab for Non-Linear Spectroscopy, Italy. In this project we perform a quantitative analysis of brain cytoarchitecture to study the three-dimensional reconstruction of the human neural networks at cellular resolution expanding the histopathological studies to the third dimension

BF4C.2 • 16:30

**An Automated Pipeline for the Collection, Transfer, and Processing of Large-scale Tomography Data**, Ming Du<sup>1</sup>, Rafael Vescovi<sup>2</sup>, Ryan Chard<sup>3</sup>, Narayanan Kasthuri<sup>2</sup>, Chris Jacobsen<sup>4,5</sup>, Eva Dyer<sup>6</sup>, Doga Gursoy<sup>5</sup>; <sup>1</sup>Dept. of Materials Science and Engineering, Northwestern Univ., USA; <sup>2</sup>Dept. of Neurobiology, Univ. of Chicago, USA; <sup>3</sup>Computing, Environment, and Life Sciences, Argonne National Lab, USA; <sup>4</sup>Dept. of Physics and Astronomy, Northwestern Univ., USA; <sup>5</sup>Advanced Photon Source, Argonne National Lab, USA; <sup>6</sup>Dept. of Biomedical Engineering, Georgia Inst. of Technology and Emory Univ., USA. We introduce an automated and scalable data collection, transfer, and processing pipeline for tomographic measurement of centimeter-sized mouse brains with sub-micrometer resolution. Parallelized computation is implemented in data processing to allow fast handling of tera-voxel sized datasets.

BF4C.3 • 16:45

**Investigating Pathological Features of Alzheimer's Disease in Human and Mouse Brain Tissue with Visible Light Optical Coherence Microscopy**, Antonia Lichtenegger<sup>1,2</sup>, Martina Muck<sup>1,2</sup>, Pablo Eugui<sup>1,2</sup>, Danielle Harper<sup>1,2</sup>, Marco Augustin<sup>1,2</sup>, Christoph K. Hitzberger<sup>1,2</sup>, Adelheid Woehrer<sup>1,3</sup>, Bernhard Baumann<sup>1,2</sup>; <sup>1</sup>Medical Univ. of Vienna, Austria; <sup>2</sup>Center for Medical Physics and Biomedical Engineering, Austria; <sup>3</sup>Inst. of Neurology, General Hospital, Austria. Human and mouse brains exhibiting Alzheimer's disease hallmarks were investigated using a visible light optical coherence microscope. This high-resolution imaging technique in combination with optical clearing is a powerful tool to investigate microscopic pathological features.

## Atlantic Ballroom 3

Optical Tomography and Spectroscopy

16:00–18:00

### OF4D • Novel Developments for Clinical and Preclinical Applications

President: Lorenzo Cortese, ICFO, Spain

OF4D.1 • 16:00 **Invited**

**Noninvasive Optical Monitoring of Cerebral Blood Flow, Critical Closing Pressure, and Arteriole Compliance in Adult Human Subjects**, Wesley Baker<sup>1,2</sup>, Ashwin B. Parthasarathy<sup>3,4</sup>, Lian He<sup>4</sup>, Venkaiah C. Kavuri<sup>4</sup>, Mamadou Diop<sup>5,6</sup>, Daniel F. Mile<sup>5,6</sup>, David R. Busch<sup>4,7</sup>, Kimberly P. Gannon<sup>8</sup>, Michael T. Mullen<sup>8</sup>, John A. Detre<sup>9</sup>, Daniel Licht<sup>2</sup>, Keith St. Lawrence<sup>5,6</sup>, Ramani Balu<sup>8</sup>, W. Andrew Kofke<sup>1</sup>, Arjun G. Yodh<sup>4</sup>; <sup>1</sup>Anesthesiology and Critical Care, Univ. of Pennsylvania, USA; <sup>2</sup>Neurology, Children's Hospital of Philadelphia, USA; <sup>3</sup>Univ. of South Florida, USA; <sup>4</sup>Univ. of Pennsylvania, USA; <sup>5</sup>Medical Biophysics, Univ. of Western Ontario, Canada; <sup>6</sup>Imaging, Lawson Health Research Inst., Canada; <sup>7</sup>Anesthesiology & Pain Management and Neurology, Univ. of Texas Southwest, USA; <sup>8</sup>Neurology, Univ. of Pennsylvania, USA. We validated a novel approach for measurement of critical closing pressure with near-infrared light via comparison to Doppler ultrasound measurements in healthy adults. We further measured arteriole compliance and cerebral blood flow with the approach.

OF4D.2 • 16:30

**In vivo Study of the Layered Structure on the Abdomen by Broadband Time-Domain Diffuse Optical Spectroscopy**, Antonio Pifferi<sup>1,2</sup>, Sanathana Konugolu Venkata Sekar<sup>1</sup>, Andrea Farina<sup>2</sup>, Claudia Guadagno<sup>1</sup>, Lorenzo Spinelli<sup>2</sup>, Pranav Lanka<sup>1</sup>, Rinaldo Cubeddu<sup>1</sup>, Enzo Nisoli<sup>3</sup>, Paola Taroni<sup>1,2</sup>; <sup>1</sup>Dipartimento di Fisica, Politecnico di Milano, Italy; <sup>2</sup>Istituto di Fotonica e Nanotecnologie, Consiglio Nazionale delle Ricerche, Italy; <sup>3</sup>Dept. of Medical Biotechnology and Translational Medicine, Univ. of Milan, Italy. We investigate the effect of depth heterogeneity in the abdomen by multidistance time-domain diffuse optical spectroscopy on 4 volunteers finding a higher water content in shallower regions, possibly due to fat heterogeneity and/or dermis contributions.

OF4D.3 • 16:45

**Near-infrared Spectroscopy Based Arthroscopic Evaluation of Human Knee Joint Cartilage, Through Automated Selection of an Anatomically Specific Regression Model**, Mithilesh Prakash<sup>1</sup>, Antti Joukainen<sup>2,1</sup>, Jaakko K. Sarin<sup>1</sup>, Lassi Rieppo<sup>1</sup>, Isaac O. Afara<sup>1</sup>, Juha Töyräs<sup>1,3</sup>; <sup>1</sup>Univ. of Eastern Finland, Finland; <sup>2</sup>Dept. of Orthopedics, Traumatology and Hand Surgery, Kuopio Univ. Hospital, Finland; <sup>3</sup>Diagnostic Imaging Center, Kuopio Univ. Hospital, Finland. We compared the performance of generalized versus anatomical-specific models for prediction of cartilage properties using visible and near infrared spectroscopy. The results indicate that anatomical-specific models have the potential for enhanced predictive performance.

## Atlantic Ballroom 1

Microscopy, Histopathology and Analytics

### MF4A • Clinical Imaging—Continued

#### MF4A.3 • 17:00 **Invited**

**Laser Scanning Microscopy Targeting Dermatology - Insights from Research and Translational Inertia**, Marica Ericson<sup>1</sup>; <sup>1</sup>Sahlgrenska Univ. Hospital, Sweden. The technology allowing for non-invasive histopathological analysis patients' first visits is already available; however, the implementation is hampered by translational inertia. Despite extensive technological advances, several hurdles remain to be overcome in order to enable instant diagnostics. This paper will review some of the important challenges encountered from research primary focusing on multiphoton laser scanning microscopy for experimental dermatology. The conclusions will concern implications of laser scanning microscopy as non-invasive techniques in more general, and propose some ideas to facilitate clinical translation.

#### MF4A.4 • 17:30 **Invited**

**Multimodal Optical and Terahertz Biopsy of Nonmelanoma Skin Cancers**, Cecil S. Joseph<sup>1</sup>, Rakesh Patel<sup>1</sup>, Victor Neel<sup>2</sup>, Robert Giles<sup>1</sup>, Anna N. Yaroslavsky<sup>1</sup>; <sup>1</sup>Univ. of Massachusetts Lowell, USA; <sup>2</sup>Massachusetts General Hospital, USA. We investigated the utility of multimodal cross-polarized terahertz and optical biopsy for the accurate detection of nonmelanoma skin cancers. Our quantitative and multimodal imaging approach yields a sensitivity and specificity of 96% and 99%, respectively.

## Atlantic Ballroom 2

Clinical and Translational Biophotonics

### CF4B • OCT and Microscopy—Continued

#### CF4B.4 • 17:00

**A Dual-modal, Dual-channel, Mesoscopic-scale Theranostic Endoscope for Quantitative Imaging, Monitoring, and Light-triggering of Chemodrug Release from Liposomes in Vivo**, Ulas Sunar<sup>1</sup>; <sup>1</sup>Wright State Univ., USA. We present a dual-modal, dual-channel, mesoscopic flexible endoscope that allows quantitative reflectance and fluorescence imaging for quantitative imaging, light delivery and monitoring of local drug concentrations in an ovarian cancer model in mice.

#### CF4B.5 • 17:15

**In Vivo Monitoring of Radiation-induced Changes of Oral Mucosa of Using Optical Coherence Tomography**, Anna V. Maslennikova<sup>1,2</sup>, Marina Sirotkina<sup>1</sup>, Elena S. Sedova<sup>1</sup>, Grigory V. Gelikonov<sup>2</sup>, Lev A. Matveev<sup>3</sup>, Alexander Moiseev<sup>3</sup>, Elena B. Kiseleva<sup>1</sup>, Sergey Ksenofontov<sup>3</sup>, Vladimir Y. Zaitsev<sup>3</sup>, Elena Zagaynova<sup>1</sup>, Natalia D. Gladkova<sup>1</sup>, Felix Feldchtein<sup>1</sup>, Alex Vitkin<sup>4</sup>; <sup>1</sup>Nizhny Novgorod State Medical Academy, Russia; <sup>2</sup>Biophysics, Lobachevsky Univ., Russia; <sup>3</sup>Inst. of Applied Physics RAS, Russia; <sup>4</sup>Univ. of Toronto, Canada. We report on in vivo monitoring of oral mucosa in 25 patients during the course of radiotherapy using multifunctional optical coherence tomography. Image quantification demonstrated an increase of vascular metrics before visual signs of mucositis occur.

#### CF4B.6 • 17:30

**Scanning Angle-Resolved Low Coherence Interferometry System for Clinical Detection of Cervical Dysplasia**, Derek S. Ho<sup>1</sup>, Kengyeh K. Chu<sup>1</sup>, Zachary Steelman<sup>1</sup>, Adam Wax<sup>1</sup>; <sup>1</sup>Duke Univ., USA. We present the design of a scanning a/LCI instrument which uses the depth-resolved reflectivity profile to identify the cervical transformation zone and guide a/LCI measurements of nuclear morphology for detection of cervical dysplasia in vivo.

#### CF4B.7 • 17:45

**Ultrahigh Resolution Optical Coherence Microscopy for Cervical Cancer Diagnosis**, Xianxu Zeng<sup>1</sup>, Xiaohan Zhang<sup>4</sup>, Canyu Li<sup>4</sup>, Xiaofang Wang<sup>1,4</sup>, Jason R. Jerwick<sup>1</sup>, Tao Xu<sup>1,2</sup>, Yuan Ning<sup>1,3</sup>, Yihong Wang<sup>5</sup>, Linlin Zhang<sup>4</sup>, Zhan Zhang<sup>4</sup>, Yutao Ma<sup>2</sup>, Chao Zhou<sup>1</sup>; <sup>1</sup>Lehigh Univ., USA; <sup>2</sup>Wuhan Univ., China; <sup>3</sup>Tianjin Univ., China; <sup>4</sup>Zhengzhou Univ., China; <sup>5</sup>Brown Univ., USA. Cervical cancer is the fourth most common cancer worldwide. Current screening tools cannot provide real-time results or localize suspicious regions. Optical coherence microscopy can provide optical biopsies of human cervical tissue with cellular resolution

## Grand Ballroom West

Optics and the Brain

### BF4C • Microscopy, Structure and Anatomy—Continued

#### BF4C.4 • 17:00 **Invited**

**High-throughput 3D Histology on Intact Tissues Based on Optical Elastic Scattering**, Jian Ren<sup>1</sup>; <sup>1</sup>Massachusetts General Hospital, Harvard, USA. Elastic scattering can be exploited for high-throughput 3D histopathological investigation in complex biological systems, such as whole brains. From various aspects, this talk will introduce current opportunities and challenges in this rapid-growing and promising field.

#### BF4C.5 • 17:30

**Extended Depth of Field in Confocal Microscopy**, Amaury Badon<sup>1</sup>, Jerome Mertz<sup>1</sup>; <sup>1</sup>Biomedical Engineering, Boston Univ., USA. We present a new type of confocal microscope that simultaneously image at four different depths, thus providing volumetric imaging at video rate. Our technique is an attractive tool for in vivo high-speed volumetric calcium imaging.

#### BF4C.6 • 17:45

**Improve Axial Resolution in Line-Scanning Temporal Focusing Microscopy with Global Optimum Adaptive Optics**, Lingjie Kong<sup>1</sup>, Yuanlong Zhang<sup>1</sup>, Hao Xie<sup>1</sup>, Qionghai Dai<sup>1</sup>; <sup>1</sup>Tsinghua Univ., China. Axial resolution in line-scanning temporal focusing microscopy is deteriorated by the inhomogeneity of biological tissues. We propose the global optimum adaptive optics to compensate tissue-induced dispersions, and demonstrate the improvement in neuronal imaging in vivo.

## Atlantic Ballroom 3

Optical Tomography and Spectroscopy

### OF4D • Novel Developments for Clinical and Preclinical Applications—Continued

#### OF4D.4 • 17:00

**Multimodal Breast Cancer Imaging Using Coregistered Dynamic DOT and Digital Breast Tomosynthesis**, Bin Deng<sup>2</sup>, Bernhard B. Zimmermann<sup>1</sup>, Bhawana Singh<sup>2</sup>, Qianqian Fang<sup>3</sup>, Jayne Cormier<sup>1</sup>, Richard Moore<sup>1</sup>, Daniel B. Kopans<sup>1</sup>, Mansi Saksena<sup>1</sup>, David A. Boas<sup>2,4</sup>, Stefan A. Carp<sup>2</sup>; <sup>1</sup>Radiology, MGH, USA; <sup>2</sup>Martinos Center for Biomedical Imaging, USA; <sup>3</sup>Dept. of Bioengineering, Northeastern Univ., USA; <sup>4</sup>Dept. of Biomedical Engineering, Boston Univ., USA. We describe a dynamic diffuse optical tomographic (DOT) apparatus designed for tight integration with commercial digital breast tomosynthesis (DBT) scanners and providing a fast (up to 1 Hz) image acquisition rate to enable tracking hemodynamic changes induced by the mammographic breast compression.

#### OF4D.5 • 17:15

**Time Domain Near-Infrared Optical Tomography with Time-of-Flight SPAD Camera: The New Generation**, Alexander Kalyanov<sup>1</sup>, Jingjing Jiang<sup>1</sup>, Scott Lindner<sup>1,2</sup>, Linda Ahnen<sup>1</sup>, Aldo di Costanzo<sup>1</sup>, Juan Mata Pavia<sup>1</sup>, Salvador Sanchez Majos<sup>1</sup>, Chao Zhang<sup>1</sup>, Edoardo Charbon<sup>2,3</sup>, Martin Wolf<sup>1</sup>; <sup>1</sup>Biomedical Optics Research Lab, Univ. of Zurich, Switzerland; <sup>2</sup>Advanced Quantum Architecture Lab, EPFL, Switzerland; <sup>3</sup>Applied Quantum Architectures, Delft Univ. of Technology, Netherlands. We present the first Lab results of the new generation of time domain near-infrared optical tomography setup, which is based on a time-of-flight 32x32 SPAD camera with high photon detection probability in the NIR range.

#### OF4D.6 • 17:30

**Perfusion Model to Quantify Blood Flow in Peripheral Artery Disease Patients**, Weihao Xu<sup>1</sup>, Alessandro Marone<sup>1</sup>, Christopher Fong<sup>1</sup>, Jennifer W. Hoi<sup>1</sup>, Hyun Keol Kim<sup>2</sup>, Danielle R. Bajakian<sup>3</sup>, Andreas H. Hielscher<sup>1</sup>; <sup>1</sup>Biomedical Engineering, Columbia Univ., USA; <sup>2</sup>Radiology, Columbia Univ., USA; <sup>3</sup>Surgery, Columbia Univ. Medical Center, USA. We propose a perfusion model that can quantify blood flow in relation to arterial occlusion due to plaque accumulation in peripheral arterial disease patients. Model parameters can be of help to PAD diagnosis.

#### OF4D.7 • 17:45

**Dynamic Relationship Between Local Cerebral Blood Volume and Systemic Mean Arterial Pressure in the Frequency-Domain**, Kristen Tgavalekos<sup>1</sup>, Thao T. Pham<sup>1</sup>, Nishanth Krishnamurthy<sup>1</sup>, Angelo Sassaroli<sup>1</sup>, Sergio Fantini<sup>1</sup>; <sup>1</sup>Tufts Univ., USA. Coherent oscillations in cerebral blood volume and mean arterial pressure were concurrently measured. Transfer function analysis was performed to characterize their relationship in terms of relative amplitude and phase at frequencies 0.04-0.20 Hz.

# Key to Authors and Presiders

## A

A K, Nandakumaran - OTu2D.4  
Aasmul, Soren - CW4B.7  
Abbate, Francesca - OTH4D.1  
Abdalmalak, Androu - BF2C.2, JTu3A.63, OW4C.4  
Abdeladim, Lamiae - JW3A.62, MF2A.2  
Abdelfattah, Ahmed - BW2C.3  
Abi Haidar, Darine - JTh3A.20  
Abu Jawdeh, Elie G. - BF2C.3  
Adam, Yoav - BW2C.3  
Adams, Stephen R. - BF3C.2  
Adesnik, Hillel - BW2C.2  
Afara, Isaac O. - JTu3A.27, JW3A.38, OF4D.3, OTu4D.5  
Agar, Nathalie - MW2A.2  
Agochukwu, Nneamaka - CF3B.6, OW2D.4  
Ahmed, Irfan - JTh3A.50, JW3A.42  
Ahnen, Linda - JW3A.24, OF4D.5  
Aidukas, Tomas - MTu4A.2  
Akemann, Walther - BTh4C.2  
Akitegetse, Cleoplace - BF3C.4  
Akkin, Taner - JW3A.58  
Akula, James D. - JTu3A.11  
Ala-Myllymäki, Juho P. - JW3A.38  
Alessi-Fox, Christi - MTh2A.1  
Alfonso Garcia, Alba - CW4B.4  
Alford, Simon - JW3A.53  
Algarawia, Maha - JW3A.45  
Allegra Mascaro, Anna L. - BTh2C.2, BTu2C.5, JTu3A.47  
Allier, Cédric - JTh3A.28  
Almadi, Mohamed - JTu3A.49  
Almassalha, Luay M. - MW2A.4  
Alonzo, Carlo - JTh1A.1  
Altoe, Mirella - CTu4B.6  
Amaral, Marcello M. - JTh3A.46  
Ana, Patricia A. - JTh3A.46  
Anastasio, Mark A. - OF1D.5, OW4C.5  
Anazodo, Udunna C. - BF2C.2  
Anctil, Gabriel - JTu3A.16  
Anderson, Afrouz - BTh2C.5, JW3A.52  
Andersson Engels, Stefan - CF3B.4, CTu2B, OF1D, OF1D.2, OF1D.3  
Andresen, Bjørn - OW4C.2  
Andresen, Esben R. - BF3C.5  
Angelucci, Alessandra - JW3A.57  
Antaki, James F. - JTu3A.41  
Antolovic, Ivan - JW3A.24  
Aouad, Rony - CF3B.6  
Apiou-Sbirlea, Gabriela - MTh4A.1  
Applegate, Matthew B. - OF2D.3  
Aranda, Gloria - OTH4D.5  
Arbelaez, Ana Maria - JTh3A.52  
Arnal, Bastien - JTh3A.24, JTh3A.30  
Arridge, Simon - JTu3A.25  
Askinas, Carly - JTu3A.4  
Attia, Amalina E. - CF3B.7  
Augustin, Marco - BF4C.3, OTh2D.3  
Avila Rencoret, Fernando B. - CF1B.5  
Avtzi, Stella - CW2B.6  
Azimani, Hicham - JTu3A.33  
Aziz-Sultan, Mohammad A. - JW3A.54  
Azzahrani, Ahmad - JTh3A.35, JW3A.26

## B

Bachmann, Luciano - JTu3A.44  
Backman, Vadim - CTh2B.1, MW2A.4  
Bada, Henrietta S. - BF2C.3  
Badaoui, Hawraa - CTu2B.4  
Badon, Amaury - BF4C.5  
Badve, Sunil - MF3A.1  
Baesso, Mauro L. - JTh3A.43  
Baets, Roel - CW4B.7  
Bahrani, Ahmed - OW2D.4  
Bajakian, Danielle R. - CW4B.3, CW4B.6, OF4D.6  
Baker, Christopher - BTu2C.2  
Baker, Wesley - BF2C.2, CF3B.2, CW2B.2, JTh3A.61, JTu3A.54, OF4D.1, OTu2D, OW2D.5  
Bakker Schut, Tom - CF1B.2  
Balberg, Michal - JTh3A.32  
Bale, Gemma - JW3A.50  
Balu, Ramani - BF2C.2, JTu3A.54, OF4D.1  
Bancelin, Stéphane - JW3A.17  
Bandara, Aloka - CTh4B.6  
Barber, Nathaniel E. - OW2D.3  
Barbiero, Martina - JTh3A.21  
Bardet, Pierre-Luc - JTu3A.61  
Barkalifa, Ronit - CF4B.3  
Barnett, Susan - BTh4C.4  
Barrett, Douglas - JW3A.55  
Barroso, Margarida - CTh4B.4, JTh3A.19  
Barsi, James - JW3A.10  
Bartley, Aundrea - JTu3A.55  
Bauer, Adam Q. - BTh2C.1, BTh2C.4, JTh3A.58, OW4C.5  
Baumann, Bernhard - BF4C.3, OTh2D.3  
Baxter, Grant A. - BTh2C.1, BTh2C.4, JTh3A.58  
Bayarmagnai, Battuya - JTu3A.13  
Beaurepaire, Emmanuel - JW3A.62, MF2A.2  
Behera, Anurag - JW3A.30  
Beier, Frank - JW3A.8  
Bélanger, Erik - JTu3A.16  
Belfield, Kevin D. - JW3A.65  
Bell, David - MTh4A.3  
Benetti, Carolina - JTh3A.46  
Benirschke, David - JTh3A.27  
Benoit, Danielle S. - OW2D.3  
Benosman, Ryad - OF3D.5  
Bento, antonio C. - JTh3A.43  
Berdún, Sergio - CW2B.7  
Berg, Robert A. - CW2B.5  
Berger, Michel - JW3A.27  
Bergman, Aviv - MF3A.3  
Bergonzi, Karla M. - JW3A.51  
Bernatchez, Alyson - JTu3A.16  
Bernhardt, Erica B. - JTh3A.13  
Berthelton, Xavier - OF3D.5  
Berzin, Tyler M. - CF2B.4  
Bettega, Georges - JW3A.27  
Betz, Vaughn - JTu3A.9  
Bewley, Arnaud - CTu2B.3  
Bhargava, Rohit - MW2A.1  
Bice, Annie R. - BTh2C.1, BTu2C.6  
Bigio, Irving J. - OTu4D.3  
Billings, Jacob - JTh3A.59, JW3A.59  
Binini, Noemi - BTu2C.2  
Biswas, Arindam - JW3A.20  
Bjaalie, Jan - JTu3A.62  
Blackwell, Megan - JTu3A.53

Blair, Steve - JW3A.57  
Blandin, Pierre - JTh3A.28  
Bliznuks, Dmitrijs - JTh3A.7  
Boas, David A. - JTh3A.33, JTu3A.53, JW3A.56, OF4D.4  
Bobadilla Mendez, Carolina - MW4A.4  
Boetti, Nadia G. - OF2D.6  
Bohndiek, Sarah - OF2D.1  
Boitor, Radu - CF1B.2  
Bold, Richard - CTu4B.4  
Bolton, McLean - BTu2C.2  
Bolos, Daniel - JW3A.6  
Boorady, Timothy - CW2B.2, CW2B.5  
Boppard, Stephen A. - CF4B.3, JW1A.1, OTh2D.2  
Borda, Luis - JTh3A.6, JTu3A.7, JW3A.44  
Bordy, Thomas - JTh3A.28  
Borron, Halen - JTh3A.1  
Borycki, Dawid M. - OTu2D.2  
Bossy, Emmanuel - JTh3A.24, JTh3A.30  
Bouma, Brett - JW3A.67  
Bourdieu, Laurent - BTh4C.2, BTh4C.5  
bourel, Emilie - JTu3A.5  
Bouwman, Géraud - BF3C.5  
Bovetti, Serena - BTu2C.2  
Bozkurt, Alican - MTh2A.1  
Bozsanyi, Szabolcs - JW3A.12  
Bradley, Jonathan - BTh4C.2  
Braeuer, Bastian - JTh3A.42  
Brankov, Jovan G. - JTu3A.29, OTh4D.7  
Bratinov, George - CW2B.2, CW2B.5  
Bravo, Jaime J. - JTh3A.36  
Brickley, Stephen - JTu3A.48  
Brier, Lindsey M. - BTu2C.6, JTh3A.58  
Brix, Sarah - JTh3A.39  
Brizion, Sébastien - MF2A.2  
Brock, Jane - MTh4A.4  
Brommer, Harold - OTu4D.5  
Bronzi, Marco - BW2C.5  
Brooks, Dana H. - MTh2A.1  
Brown, J. Quincy - JTu3A.4, JW3A.6, MF1A.1, MF1A.4  
Brown, Tyra - MF2A.5  
Brown, William - OF3D.7  
Bruchas, Michael - BTh2C.1  
Bryan, Leah - OW2D.6  
Bubel, Tracy M. - OW2D.7  
Buchmann, Jens - OW4D.4  
Buckley, Erin - BF2C.5, JTu3A.58, JW3A.48, JW3A.66, OTu4D, OW2D.6  
Buffone, Dillon A. - JW3A.20  
Bumstead, Jonathan - JTh3A.60  
Burns-Yocum, Tracy M. - BTu4C.3, JTh3A.55, JW3A.51  
Busch, David R. - CW2B.2, JTu3A.54, JW3A.10, OF4D.1, OTh4D.3, OW2D.5  
Busch, Theresa M. - CF2B.6  
Buttafava, Mauro - JTu3A.20, OTh4D.5

## C

Cahill, Lucas C. - MF2A.1  
Calà Lesina, Antonino - JW3A.17  
Califa, Ran - JW3A.23  
Campaoli, Costanza - BTu2C.5  
Campbell, Robert E. - BW2C.3  
Camps-Renom, Pol - CW2B.6  
Cannon, Kelli - JTu3A.55

Cantaut-Belarif, Yasmine - JTu3A.61  
Cantow, Kathleen - JTh3A.39  
Cao, Xu - JTh3A.13, JTu3A.38  
Cao, Yingchun - CW4B.2  
Cardenaz de la Hoz, Edgar - JTu3A.13  
Cardoso, George - JTu3A.44  
Carlen, Peter L.- BTh2C.3  
Carp, Stefan A.- BTh2C.7, JTh3A.3, JTh3A.49,  
JTu3A.53, JTu3A.64, JW3A.41, OF4D.4  
Caspers, Peter - CF1B.2  
Cassano, Enrico - OTh4D.1  
Cassidy, Jeffrey - JTu3A.9  
Castelletto, Stefania - JTh3A.21  
Castro, Lidia - CW2B.4  
Castro, Pedro - JW3A.37  
Castro-Hoshino, Lidiane V.- JTh3A.43  
Chaigne, Thomas - JTh3A.24  
Chaiken, Joseph - JW3A.2  
Chandler, John E.- MW2A.4  
Chaney, Eric - CF4B.3  
Chang, Chia-Kai - MF3A.2  
Charbon, Edoardo - JW3A.24, OF4D.5  
Chard, Ryan - BF4C.2  
Charnley, Mirren - JTh3A.21  
Chastagnier, Yan - BTh4C.5  
Chavarha, Mariya - BTh4C.2  
Chen, Fuyao - MTh4A.2  
Chen, Li - CF3B.6  
Chen, Michael - MF3A.5  
Chen, Sez-Jade - JTh3A.19  
Chen, Siyu - JTu3A.59, OTh2D.7  
Chen, Xueli - JTu3A.38  
Chen, Xun - JTh3A.26, JTh3A.31  
Chen, Ye - JTh3A.21  
Chen, Yi - MF3A.1  
Chenegros, Guillaume - OF3D.5  
Cheng, Ji-Xin - CW4B.2, MW2A.5  
Cheng, Xiaojun - JTu3A.53  
Cheng, Yiming - JW3A.65  
Cheng, Yunzhou - JW3A.57  
Cherry, Katelin D.- CTu2B.4  
Ching-Roa, Vincent Ralph D.- JW3A.22  
Chinni, Bhargava - OW4D.2  
Choe, Regine - CF3B.1, JW3A.22, OTh4D,  
OW2D.3, OW2D.7  
Choi, Heejin - JW3A.67  
Choi, Honggu - CTu4B.7  
Chong, Sanghoon - JW3A.25, JW3A.63  
Chong, Shau Poh - BTu4C.2  
Chowdhry, Fatima - BTh2C.5  
Chowdhury, Shwetadwip - MF3A.5  
Chu, Kengyeh K.- CF4B.6, OF3D.3  
Chuah, Sai Yee - CF3B.7  
Chue-Sang, Joseph - JTu3A.6  
Chung, Kwanghun - JW3A.67  
Chung, So H.- OW2D.5  
Chuttani, Ram - CF2B.4  
Cioni, Olivier - JTh3A.28  
Cochran, Jeffrey M.- OTh4D.3, OW2D.5  
Cohen, Adam E.- BW2C.3  
Cohen, Andrew - JTu3A.13  
Cohen, Ari - JTu3A.4  
Coll, Jean-Luc - JW3A.27  
Colombo, Lorenzo - OTu2D.1, OW2D.2  
Condat, Laurent - JTh3A.45  
Connolly, James - MF2A.1  
Conti, Emilia - BTh2C.2, JTu3A.47  
Contini, Davide - OF2D.6, OTh4D.5, OTu2D.1,  
OTu2D.5, OW2D.2, OW4C.2  
Cormier, Jayne - OF4D.4

Corr, David T.- JTh3A.47  
Cortese, Lorenzo - CW2B.7, OF4D, OTh4D.5,  
OTu2D.5  
Cossart, Rosa - BF3C.5  
Costantini, Irene - JTh3A.64, JTu3A.62  
Côté, Daniel - JTh3A.4  
Cote, Daniel C.- BF1C, BF3C.4, JTh3A.60  
Cote, Francois - BF3C.4  
Cotta, Gianluca - CW2B.6  
Cowdrick, Kyle - JW3A.66  
Cox, Brian - JW3A.32, OF3D.7  
Cox, David D.- BW2C.3  
Crepeau, Joel - BF3C.4  
Crose, Michael - JW3A.32, OF3D.3, OF3D.7  
Crouch, Brian - CF2B.2  
Cubeddu, Rinaldo - JW3A.43, OF4D.2, OTh4D.1,  
OTu4D.1  
Culver, Joseph P.- BTh2C.1, BTh2C.4, BTu2C.6,  
BTu4C.3, JTh3A.52, JTh3A.58, JTh3A.60,  
JTu3A.20, JW3A.51, OF2D.2, OTu2D.6,  
OW4C.5, OW4C.7  
Cunningham, Brian T.- MW2A.3  
Cutrone, Alissa - JW3A.10  
Czarske, Juergen W.- OF2D.5  
Czarske, Jürgen - JW3A.19

## D

Da Silva, Anabela - JW3A.21  
Dabrowski, Wojciech - JTu3A.50  
Dai, Qionghai - BF4C.6  
Dai, Xianjin - BTu4C.4  
Dai, Yunpeng - JTu3A.38  
Dale, Anders M.- JW3A.56  
Dalla Mora, Alberto - CF2B.3, JW3A.30, JW3A.43,  
OF2D.6, OTh4D.5, OTu2D.1, OTu2D.5,  
OW2D.2  
Darrow, Morgan - CTu4B.4  
Dashtestani, Hadis - BTh2C.5, JW3A.52  
Davis, Arthur - JTu3A.33  
Davis, Tyler - JTu3A.3  
Dawant, Benoit - MTh4A.2  
De Carli, Agnese - OW4C.2  
de Fraguier, Sixte - OTh4D.5  
de Jesus, Rebeca - JW3A.47  
de la Zerma, Adam - OF3D.1  
de Melis, Mirko - CW4B.7  
de Ribaupierre, Sandrine - OW4C.4  
De, Suvranu - JTh3A.53  
Deán-Ben, Xosé Luís - JTh3A.44  
DeCampi, William M.- CW4B.5  
DeFusco, Patricia - OTh4D.2  
Dehghani, Hamid - CF2B.3, JTh3A.37, OF2D.2,  
OTu4D.5, OTh4D.6  
DeHoog, Edward - JTu3A.6  
Delahunt, Charles - MTh4A.3  
Delgado-Mederos, Raquel - CW2B.6  
Delogu, Alessio - JTu3A.48  
Dempsey, Eugene - CF3B.4  
Deng, Bin - JTh3A.49, JW3A.2, OF4D.4  
Dent, Paul - JW3A.2  
DePaoli, Damon - BF3C.4, JTh3A.4  
Derjabo, Aleksandrs - JTh3A.7  
Desa, Danielle E.- OW2D.3  
Desai, Manishi - CF4B.2  
Desjardins, Adrien E.- JW3A.4  
Desjardins, Lise - JW3A.8  
Desroches, Joannie - OW4C.6  
Desrosiers, Patrick - BF1C.1  
Detre, John A.- BF2C.2, OF4D.1

Devaux, Bertrand - JTh3A.20  
Devor, Anna - BF3C.2, BTh4C, JW3A.56  
Dewhirst, Mark - CF2B.2  
di Costanzo, Aldo - JW3A.24, OF4D.5  
Di Giovanna, Antonino Paolo - JTu3A.62  
Di Sieno, Laura - JW3A.30, OF2D.6  
Dickensheets, David L.- MW4A.1  
Dieudonné, Stephane - BTh4C.2, BTu2C  
DiMaria-Ghalili, Rose Ann - CF2B.7  
Dinten, Jean-Marc - JTh3A.45  
Dintzis, Suzanne M.- CTu4B.2  
Diop, Mamadou - BF2C.2, BF2C.4, BTu4C,  
JTu3A.54, JTu3A.63, JW3A.50, JW3A.8,  
OF4D.1, OW4C.4  
Dmochowski, Jacek - JTh3A.56  
Do, Daihung - MF2A.1  
Dogariu, Aristide - CW4B.5  
Dogra, Vikram - OW4D.2  
Dolui, Sudipto - BF2C.2  
Dominguez, Christian T.- JTu3A.44  
Dominik, Nikolas - CTh2B.5  
Dong, Biqin - BW2C.7, MW2A.4  
Dong, Kui - JTu3A.36  
Dorian, Paul - BTh2C.6  
Dot, Audrey - JW3A.27  
Dougherty, Joseph D.- BTu2C.6  
Doulgerakis-Kontoudis, Matthaios - OF2D.2  
Dragojević, Tanja - JTu3A.20, OTu2D.6  
Dray, Nicolas - JW3A.62  
Drozdzov, Gilad - OW4D.6  
Druon, Frédéric - JW3A.62  
Druzhkova, Irina - JTu3A.14  
Du, Ming - BF4C.2  
Dubois, Arnaud - JTu3A.33  
Dudenkova, Varvara - JTu3A.14, JW3A.7  
Duerr, Erik - JTu3A.53  
Dumas, John P.- OF2D.3  
Duperron, Matthieu - CW4B.7  
Durduran, Turgut - BF2C.1, CF2B.3, CW2B.4,  
CW2B.6, CW2B.7, JTu3A.20, JW3A.21,  
OTu4D.5, OTu2D.1, OTu2D.4, OTu2D.5,  
OTu2D.6, OW2D.2, OW4C.2  
Dussaux, Clara - BTh4C.5  
Dy, Jennifer G.- MTh2A.1  
Dyer, Eva - BF4C.2, JW3A.48

## E

Earles, Susan - JTh3A.35, JW3A.26  
Ebner, Michael - JTu3A.8  
Eckert, Regina - MF3A.5  
Edgar, Julia - BTh4C.4  
Eggebrecht, Adam T.- JTh3A.52, JW3A.51, OF2D,  
OF2D.2, OW4C.5, OW4C.7  
Einevoll, Gaute T.- JW3A.56  
Eisel, Max - JTu3A.12  
Eixarch, Elisenda - CW2B.7  
Elagin, Vadim - JW3A.7  
Eldridge, Will J.- OF3D.3  
Elfer, Katherine N.- JTu3A.4, JW3A.6, MF1A.4  
Eliceiri, Kevin - MTh2A.3  
Ellis, Ian - CTu4B.5  
Ellwood, Roger - JTh3A.5  
Elsheikh, Somaia - CF1B.2  
Elson, Daniel S.- CF1B.5  
Erdmann, Rainer - OTu4D.2, OW2D.2  
Erfanzadeh, Mohsen - JTh3A.40  
Ericson, Marica - MF2A, MF4A.3  
Erkol, Hakan - JTh3A.16, JW3A.45  
Escobar Acevedo, Marco Antonio - JTu3A.10

Eshein, Adam - MW2A.4  
 Esipova, Tatiana V.- JW3A.63  
 Eskaros, Adel - MTh2A.4  
 Esmaeili Pourfarhangi, Kamyar - JTu3A.13  
 Eugui, Pablo - BF4C.3, OTh2D.3  
 Evans, Casey - JTu3A.53

## F

Fabbri, Dan - MTh4A.2  
 Fainman, Yeshaiahu - BF3C.2, JW3A.56  
 Fang, Qianqian - JTh3A.17, JTh3A.3, JTh3A.38,  
 JTh3A.41, JTh3A.49, JTu3A.30, JTu3A.52,  
 JTu3A.64, OF4D.4  
 Fang, Yuhong - JTu3A.36  
 Fantini, Sergio - BTu4C.5, CW2B.3, JTh3A.32,  
 JTu3A.39, JW3A.40, JW3A.64, OF4D.7  
 Farhi, Samouil L.- BW2C.3  
 Farina, Andrea - CF2B.3, JTu3A.25, OF2D.6,  
 OF4D.2, OTu4D.1  
 Farwell, D. Gregory - CTu2B.3  
 Farzam, Parisa - BTh2C.7, JTh3A.33, JTu3A.23,  
 JW3A.41, JW3A.54  
 Farzam, Parya - BTh2C.7, JW3A.41, JW3A.54  
 Faulkner, Denzel E.- JTh3A.47  
 Faulkner-Jones, Beverly - MF2A.1  
 Fawzi, Amani - OTh2D.7  
 Feldchtein, Felix - CF4B.5  
 Fellin, Tommaso - BTu2C.2, BW2C.5  
 Feng, Jinchao - JTh3A.61, JTu3A.28  
 Feng, Xin - MW4A.3  
 Fereidouni, Farzad - MF1A.3  
 Ferguson, R. D.- JTu3A.11  
 Fernandez, Cristianne M.- JTh3A.6, JTu3A.7,  
 JW3A.44  
 Ferocino, Edoardo - JTu3A.25, JW3A.43  
 Ferrer, Marc - OTh2D.5  
 Ferrer-Ortas, Jülia - JW3A.62  
 Ferri, Christopher G.- BF3C.2, JW3A.56  
 Filer, Andrew - OTh4D.6  
 Fillioe, Seth - JW3A.2  
 Finnilä, Mikko - JTu3A.27  
 Fiolka, Reto P.- MTu2A.1  
 Fishell, Andrew - BTu4C.3, JTh3A.52  
 Fisher, Andrew M.- JTu3A.11  
 Flemming, Bert - JTh3A.39  
 Floyd, Thomas F.- JW3A.10  
 Fodor, Jozsua - BTh4C.5  
 Fong, Christopher J.- CW4B.3, CW4B.6, JW3A.1,  
 OF4D.6  
 Forli, Angelo - BTu2C.2  
 Forti, Amanda M.- OW2D.3  
 Fossum, Eric - JTu1A.1  
 Fox, Ben - CTh4B.6  
 Franceschini, Maria Angela - BF2C, BTh2C.7,  
 JTh3A.33, JTu3A.53, JW3A.41, JW3A.54,  
 CW2B.1, JTu3A.23  
 Franz, Erich S.- JTu3A.11  
 Frascioni, Paolo - JTh3A.64, JTu3A.62  
 French, David N.- JTu3A.55  
 Fried, Guy - CF2B.7  
 Fujimaki, Mitsue - JTh3A.43  
 Fujimoto, James - MF2A.1  
 Fumagalli, Monica - OW4C.2

## G

Galey, Jean-Baptiste - MF2A.2  
 Galliano, Gretchen - JTu3A.4  
 Galwaduge, P. T.- BF3C.3  
 Gan, Yu - OTh2D.6

Ganapathy, Vidya - MW4A.4  
 Gandjbakhche, Amir - BTh2C.5, JW3A.52  
 Gandour-Edwards, Regina - CTu2B.3  
 Gannon, Kimberly P.- OF4D.1  
 Garcia, Eduardo - OTh4D.5  
 Garcia, Javier - JW3A.23  
 Garcia, N Missael - JTu3A.3  
 Gelikonov, Grigory V.- CF4B.5  
 Gentile, Javier - CW2B.2  
 Georgakoudi, Irene - JTh1A.1  
 Georges, Patrick - JW3A.62  
 Gerald, Eric - JTu3A.17  
 Gerega, Anna - JTh3A.62, OTu2D.3  
 Giacalone, Giacomo - CW2B.6  
 Giacomelli, Michael G.- CTu4B, MF2A.1, MTh4A  
 Gigan, Sylvain - OF1D, OF1D.1  
 Giles, Robert - MF4A.4  
 Gill, Jonathan V.- BTu2C.3  
 Gill, Melissa - MTh2A.1  
 Gillenwater, Ann - CTu2B.4  
 Giordano, Anthony - JTu3A.49  
 Giovannella, Martina - OW4C.2  
 Giraldo, Juan - JTu3A.49  
 Girshovitz, Pinhas - JTh3A.32  
 Gladkova, Natalia D.- CF4B.5  
 Gladstein, Scott - MW2A.4  
 Gladytz, Thomas - JTh3A.39, JW3A.31  
 Glaser, Adam - MF3A, MTu2A.4  
 Gligorijevic, Bojana - JTu3A.13, MF3A.3  
 Go, Mary Ann - BTh4C.3  
 Godavarty, Anuradha - JTh3A.11, JTh3A.6,  
 JTu3A.7, JW3A.44  
 Goh, Chia C.- JW3A.10  
 Gokmen-Polar, Yesim - MF3A.1  
 Golberg, Mark - JW3A.23  
 Goldstein, Lee E.- JTu3A.11  
 Golubyatnikov, German - JTh3A.8  
 Gomes, Anderson S.- JTh3A.15, JTh3A.46  
 Gomis, Ramon - OTh4D.5  
 Gong, Wei - JTu3A.36  
 Gong, Yuzhu - JTu3A.38  
 Gonzalez, Mariacarla - JTu3A.6  
 Gonzalez-Lima, Francisco - JTh3A.56, JW3A.55  
 Goodisman, Jerry - JW3A.2  
 Goodman, Laurie - MF3A.1  
 Goodwin, Matthew S.- JTu3A.55  
 Göpfert, Luisa - JW3A.33  
 Goyette, Andréanne - OW4C.6  
 Graham, Jasmine Y.- CTh4B.2  
 Grama, Abhinav - BW2C.3  
 Gratacós, Eduard - CW2B.7  
 Gray, Gary - JTu3A.55  
 Greenberg, Joel H.- JW3A.63  
 Greenwald, Stephen - CW4B.7  
 Gregori Pla, Clara - CW2B.6  
 Greisen, Gorm - OW4C.2  
 Grieve, Kate - OF3D.5  
 Gritton, Howard - BW2C.6  
 Gropman, Andrea - BTh2C.5  
 Grosenick, Dirk - JTh3A.39, JW3A.31  
 Gruev, Viktor - JTu3A.3  
 Gu, Min - JTh3A.21  
 Guadagno, Claudia - OF4D.2  
 Gubarkova, Ekaterina - JW3A.7  
 Guck, Jochen - OF2D.5  
 Guesmi, Khmaies - JW3A.62  
 Gulsen, Gultekin - JTh3A.16, JW3A.45  
 Gunther, Jacqueline - CTu4B.6, OF1D.2, OF1D.3  
 Guo, Qiongyu - OTh2D.5  
 Gupta, Saurabh - JTu3A.46

Gurden, Hirac - JTu3A.57  
 Gursoy, Doga - BF4C.2  
 Guzmán-Cabrera, Rafael - JTu3A.10  
 Guzman-Sepulveda, Jose - CW4B.5, JTu3A.10

## H

Ha, Richard S.- CTu4B.6  
 Hadway, Jennifer - JW3A.8  
 Haghani, Sasan - JTh3A.54  
 Haig, Bernadette - JTh3A.25  
 Haj-Hosseini, Neda - BTh2C.8  
 Halem, Milton - JW3A.52  
 Hallbeck, Martin - BTh2C.8  
 Halperin, Irene - CF2B.3  
 Haluszka, Dora - JW3A.12  
 Han, Songfeng - CF3B.1, JW3A.22, OW2D.3,  
 OW2D.7  
 Han, Tao - CF3B.3  
 Han, Xue - BW2C.6  
 Han, Zichao - OW4D.2  
 Hanna, Marc - JW3A.62  
 Hanzu, Felicia - CF2B.3, OTh4D.5  
 Haorah, James - JW3A.65  
 Haroon, Attiya - MF4A.2  
 Harper, Danielle - BF4C.3, OTh2D.3  
 Harvey, Andrew R.- BTh4C.4, MTu4A.2  
 Haudenschild, Anne K.- CW4B.4  
 Hawxby, Alan - JTh3A.1  
 He, Lian - BF2C.2, CF3B.2, JTu3A.54, OF4D.1  
 Hebisch, Christoph - CTu4B.4  
 Heflin, James - CTh4B.6  
 Hemm, Simone - CTh2B.3  
 Hendon, Christine - OTh2D.4, OTh2D.6  
 Hendon, Christine P.- JW3A.35, OF3D.2  
 Hershman, Dawn - CTu4B.6  
 Herve, Lionel - JTh3A.28, JTh3A.45  
 Herzog, Walter - JTu3A.27  
 Hewko, Mark - JTh3A.48  
 Hibshoosh, Hanina - CTu4B.6  
 Hielscher, Andreas H.- CTu4B.6, CW4B.3, CW4B.6,  
 JTh3A.34, OF4D.6, JTh3A.12, JW3A.1  
 Hill, Malcolm C.- CF4B.3  
 Hillman, Elizabeth M.- BF3C.3, BW2C.1  
 Hitzenberger, Christoph K.- BF4C.3, OTh2D.3  
 Ho, Chris Jun Hui - CF3B.7  
 Ho, Derek S.- CF4B.6  
 Hoi, Jennifer W.- CW4B.3, CW4B.6, JW3A.1,  
 OF4D.6  
 Holler, Stephen - JTh3A.25  
 Hollman, Joseph - OTu2D.6  
 Hollmann, Joseph L.- JTu3A.20  
 Homma, Shu - JTu3A.43  
 Hoppe, Alexander - JTh3A.39  
 Horning, Matthew - MTh4A.3  
 Howard, Scott S.- JTh3A.27  
 Hu, Bihe - JW3A.6  
 Hu, Liming - MTh4A.3  
 Huang, Chong - BF2C.3, CF3B.6, OW2D.4  
 Huang, Pin-Chieh - CF4B.3, OTh2D.2  
 Huang, Sheng-Lung - MF3A.2  
 Huang, Yongyang - OTh2D.5  
 Huang, Zheng - JTu3A.36  
 Huber, Bertrand R.- JTu3A.11  
 Hui, Jie - CW4B.2  
 Huisken, Jan - BF1C.2, BF4C

## I

leva, Francesca - OTh4D.1  
 Intes, Xavier - CTh4B.4, JTh3A.19, JTh3A.47,  
 JTh3A.51, JTh3A.53, JTu3A.30, OF2D.4,  
 OTu4D.4  
 Inzana, Thomas - CTh4B.6  
 loussoufovitch, Seva - JW3A.8  
 Irwin, Daniel - OW2D.4  
 Iskander-Rizk, Sophinese - OW4D.1  
 Itzkan, Irving - CF2B.4  
 Iyer, Vivek - OTh2D.4

## J

Jacobsen, Chris - BF4C.2  
 Jagasia, Madan H.- MTh4A.2  
 Jager, Polona - JTu3A.48  
 Jaiswal, Mayoore - MTh4A.3  
 Jalal, Shadia - CTu4B.7  
 Javid, Sara - CTu4B.2  
 Jelly, Evan T.- JW3A.32, OF3D.3  
 Jeong, Sejin - CW2B.2, CW2B.5  
 Jermain, Peter R.- MW4A.3  
 Jerwick, Jason R.- CF4B.7  
 Jha, Abhinav Kumar - JTu3A.51  
 Jia, Kebin - JTh3A.61, JTu3A.28  
 Jiang, Huabei - BTu4C.4, JW3A.16, OTh4D.4  
 Jiang, Jingjing - JW3A.24, OF4D.5  
 Jiang, Shudong - JTh3A.13  
 Jiang, Yuxin - CF3B.3  
 Jin, Long - OW4D.7  
 Jones, Jake D.- CTh4B.3  
 Joseph, Cecil S.- MF4A.4  
 Joukainen, Antti - OF4D.3  
 Juchaux, Marjorie - JTh3A.20  
 Justicia, Carles - OTu2D.6

## K

K, Murali - OTu2D.4  
 Kacprzak, Michal - CW2B.4, JTu3A.50  
 Kadhim, Ahmed C.- JTh3A.35, JW3A.26  
 Kaeli, David - JTh3A.38  
 Kaile, Kacie - JTh3A.11  
 Kainerstorfer, Jana M.- JTu3A.40, JTu3A.41,  
 OW4C, OW4C.3  
 Kalganova, Tatyana - JTh3A.8  
 Kalia, Vrinda - JW3A.47  
 Kalinsky, Kevin - CTu4B.6  
 Kallis, Penelope - JTh3A.6, JTu3A.7, JW3A.44  
 Kallmayer, Christine - JW3A.57  
 Kalloor, Francis - OW4D.2  
 Kalume, Aiambale - JW3A.39  
 Kalyanov, Alexander - JW3A.24, OF4D.5  
 Kang, DongKyun - MTu4A, MW4A.2  
 Kang, Soyoun - CTu4B.2  
 Kantamneni, Harini - MW4A.4  
 Kaplan, Bernhard - OW4D.4  
 Karaliota, Sevasti - JTh1A.1  
 Karalis, Katia P.- JTh1A.1  
 Karrobi, Kavon - JTu3A.31  
 Kasthuri, Narayanan - BF4C.2  
 Katz, Ori - JTh3A.24  
 Kauffman, Kevin - JTu3A.3  
 Kaufman, Peter A.- JTh3A.13  
 Kavuri, Venkaiah C.- BF2C.2, CF3B.2, JTu3A.54,  
 OF4D.1  
 Keilholz, Shella - JTh3A.59, JW3A.59  
 Kermanian, Riley - JW3A.52  
 Kewin, Matthew D.- JW3A.50, OW4C.4

Khaksari, Kosar - JW3A.40  
 Khalid, Mahro - JTu3A.63  
 Khan, Umar - CF2B.4  
 Khandavilli, Dinesh - JTh3A.11  
 Khatib, Mirna E.- JW3A.63  
 Khilov, Aleksander - JW3A.9  
 Kholiqov, Oybek - BTu4C.2, OTu2D.2  
 Kilbaugh, Todd J.- CW2B.2, CW2B.5  
 Kilic, Kivilcim - JW3A.56  
 Kilpatrick, LaTonya - JTh3A.5  
 Kim, Hyun K. - CW4B.6, JTh3A.34  
 Kim, Hyun Keol - CTu4B.6, CW4B.3, JTh3A.12,  
 JW3A.1, OF4D.6  
 Kim, Jeong J.- BW2C.3  
 Kim, Sanghoon - JW3A.32, OF3D.7  
 Kim, Seung Hyun - JW3A.22  
 Kim, Youngwan - CW4B.3, CW4B.6, JTh3A.34,  
 JW3A.1  
 Kingsford, William - JTu3A.9  
 Kingsley, David - JTh3A.47  
 Kioulos, Charalambos - JW3A.17  
 Kirillin, Mikhail - JW3A.36, JW3A.9, OW4D.5  
 Kirsner, Robert - JTh3A.6, JTu3A.7, JW3A.44  
 Kiseleva, Elena B.- CF4B.5  
 Kiss, Norbert - JTh3A.29, JW3A.12  
 Klapshina, Larisa - JTh3A.10  
 Klose, Alexander D.- JTu3A.24  
 Knutson, Kristine - JW3A.52  
 Ko, Tiffany - CF3B.2, CW2B.2, CW2B.5  
 Kobayashi Frisk, Lisa - BTh2C.8  
 Kofke, Adrew - BF2C.2, JTu3A.54  
 Kofke, W. Andrew - OF4D.1  
 Kole, Ayeeshik - CW4B.2  
 Kolenderska, Sylwia - JTh3A.42  
 Koloydenko, Alexey - CF1B.2, CTu4B.5  
 Konda, Pavan Chandra - BTh4C.4, MTu4A.2  
 Kong, Kenny - CF1B.2  
 Kong, Lingjie - BF4C.6  
 Kong, Nan - MW2A.5  
 Konugolu Venkata Sekar, Sanathana - CF2B.3,  
 OF2D.6, OF4D.2, OTh4D.5, OTu2D.1,  
 OTu2D.5, OTu4D.1, OTu4D.2, OW2D.2  
 Kopans, Daniel B.- OF4D.4  
 Korhonen, Rami - JTu3A.27  
 Kose, Kivanc - MF1A, MTh2A.1  
 Koukourakis, Nektarios - JW3A.19  
 Kovarovic, Brandon J.- JW3A.10  
 Kraft, Andrew - BTh2C.1, JTh3A.60  
 Kreitinger, Seth - MW4A.1  
 Kress, Jeremy G.- JTh3A.63  
 Kreysing, Moritz - JW3A.19  
 Krischak, Katharina - OTh4D.5  
 Krishnamurthy, Nishanth - CW2B.3, JW3A.64,  
 OF4D.7  
 Krite Svanberg, Emilie - CF3B.4  
 Kröll, Stefan - OF1D.3  
 Krolopp, Adam - JTh3A.29  
 Kruizinga, Pieter - OW4D.1  
 Krupp, Karl - JTu3A.6  
 Krzyston, Jakob - JW3A.48  
 Ksenofontov, Sergey - CF4B.5  
 Kulkarni, Kusum - CF1B.2  
 Kumamoto, Takuma - JW3A.62  
 Kumavor, Patrick D.- JTh3A.40  
 Kurtzman, Scott - OTh4D.2  
 Kwasinski, Rebecca J.- JTh3A.6, JTu3A.7, JW3A.44  
 Kymissis, Ioannis - JTh3A.34

## L

Lachowska, Martyna - JTh3A.62  
 Lafci, Berkan - JTh3A.44  
 Lafontant, Alec - CF2B.7  
 Landsness, Eric C.- JTh3A.58  
 Lange, Marta - JTh3A.7  
 Lanka, Pranav - OF4D.2  
 Lapointe, Nicolas - BF3C.4, JTh3A.4  
 Lartizien, Rodolphe - JW3A.27  
 Lau, Condon - JTh3A.50, JW3A.42  
 Laufer, Jan - OW4D.4  
 Lautz, Andrew - CW2B.5  
 Leblond, Frederic - OW4C.6  
 Lecoq, Jerome - JW3A.60  
 Lediju Bell, Muynatu - OW4D  
 Lee, Christian R.- BTu2C.4  
 Lee, Jin-Moo - BTh2C.1, JTh3A.58  
 Lee, Jong hwan - JTh3A.12  
 Lee, Jonghwan - JTu3A.34  
 Lee, Julia S.- JTu3A.34  
 Lee, Kelvin C.- MF3A.4  
 Lee, Seung Yup - JTu3A.58, JW3A.48, OW2D.6  
 Lee, Ting-Yim - JW3A.8  
 Leergard, Trygve - JTu3A.62  
 Légaré, François - JW3A.17  
 Léger, Jean-François - BTh4C.5  
 Legouis, Renaud - MF2A.2  
 Leiva, Kevin - JTh3A.11, JTh3A.6, JTu3A.7,  
 JW3A.44  
 Leproux, Anais - OTh4D.3, OW2D.5  
 Lerman, Gilad M.- BTu2C.3  
 Lessard, Simon - OW4C.6  
 Levecq, Olivier - JTu3A.33  
 Levene, Michael J.- JW3A.18  
 Levenson, Richard M.- MF1A.3, MTu2A  
 Levesque, Martin - BF3C.4  
 Lévesque, Sébastien A. - JTu3A.16  
 Levi, Ofer - BTh2C.3  
 Lewin, Peter - CF2B.7  
 Li, Airong - JW3A.33  
 Li, Canyu - CF4B.7  
 Li, Changhui - CF3B.3  
 Li, Cynthia - OTh4D.7  
 Li, Hao - BW2C.7  
 Li, Jun - JTh3A.63  
 Li, Kenneth - JTu3A.24  
 Li, Martin - CF2B.2  
 Li, Weijun - JTu3A.36  
 Li, Wenze - BF3C.3  
 Li, Xingde - CF1B.4, OTh2D.1  
 Li, Xiuting - CF3B.7  
 Li, Yang - JTh3A.26, JTh3A.31  
 Li, Yanlu - CW4B.7  
 Li, Yinan - JTu3A.28  
 Li, Yue - MW2A.4  
 Li, Zhe - CTu4B.7, JTh3A.61, JTu3A.28  
 Liang, Jimin - JTu3A.38  
 Liang, Wenxuan - CF1B.4  
 Liang, Yizhi - OW4D.7  
 Liao, Chien-Sheng - MW2A.5  
 Libert, Nicolas - OF3D.5  
 Licht, Daniel - CW2B.2, CW2B.5, OF4D.1, OW4C.1  
 Lichtenegger, Antonia - BF4C.3, OTh2D.3  
 Liebert, Adam - JTh3A.62, JTu3A.50, OTu2D.3  
 Liew, Amanda - JW3A.66  
 Lighter, Daniel - OTh4D.6  
 Lihacova, Ilze - JTh3A.7  
 Lilge, Lothar - JTu3A.9  
 Lim, Emerson - CTu4B.6, JTh3A.12

Lima, Cassio - JTu3A.42  
 Lin, Haonan - MW2A.5  
 Lin, Michael - BTh4C.2  
 Lin, Pao T.- JTh3A.23, JTu3A.22, JW3A.11  
 Lin, Steve - BTh2C.6  
 Lin, Wei - JW3A.10  
 Lin, Wei-Chiang - JTu3A.49  
 Lin, Yuxi - CW2B.2, CW2B.5  
 Lindner, Claus - CF2B.3  
 Lindner, Scott - JW3A.24, OF4D.5  
 Ling, Yuye - JW3A.35  
 Liu, Chao - JW3A.58, OW4D.7  
 Liu, Hanli - BTu4C.1, JTh3A.56, JW3A.55  
 Liu, Jonathan T.- CTu4B.2, MTu2A.4  
 Liu, Pengyu - JTh3A.61  
 Liu, Qi - JTu3A.59  
 Liu, Rui - BW2C.4, JTu3A.60, JW3A.61  
 Liu, Tianbo - MW4A.1  
 Liu, Wenzhong - OTh2D.7  
 Liu, Xinglei - JW3A.65  
 Liu, Yajing - CF2B.5  
 Liu, Zhiyi - JTh1A.1, JTh3A.18  
 Liu, Ziping - OW2D.7  
 Livet, Jean - JW3A.62  
 Lo Presti, Giuseppe - CW2B.7, OTh4D.5, OTu2D.5  
 Lockwood, Joshua - BTh2C.3  
 Loginova, Daria - JW3A.36, JW3A.9  
 Lopes, Daniela - JTh3A.15  
 Lorincz, Kende - JW3A.12  
 Lou, Shan - BW2C.3  
 Loulier, Karine - JW3A.62  
 Loza-Álvarez, Pablo - JTh3A.14  
 Lu, Helen - OF3D.2  
 Lu, Wenqi - JTu3A.32  
 Luby-Phelps, Katherine - CF1B.4  
 Lucchesi, Jessica - BTu2C.5  
 Luethy, Sam J.- JTu3A.4, JW3A.3, MF1A.4  
 Luk, Alex - JTh3A.16, JW3A.45  
 Lukina, Maria - JTu3A.14, JW3A.7  
 Lundqvist, Mats - JTh3A.49  
 Lye, Theresa - OTh2D.6  
 Lynch, Jennifer - CW2B.2

## M

Ma, Yutao - CF4B.7  
 Macdonald, Callum - JW3A.21  
 Macdonald, Rainer - JW3A.31  
 Macmillan, Douglas - CTu4B.5  
 Madhivanan, Purnima - JTu3A.6  
 Mahadevan, Jagadeesh - JTh3A.11  
 Mahadevan-Jansen, Anita - CF1B.1, CW2B  
 Mahendroo, Mala - CF1B.4  
 Mahmoudzadeh, Mahdi - JTu3A.5  
 Mahn, Mathias - BTu2C.2  
 Mahou, Pierre - JW3A.62, MF2A.2  
 Majeed, Waqas - JTh3A.59, JW3A.59  
 Malda, Jos - OTu4D.5  
 Malkinson, Guy - MF2A.2  
 Maloney, Benjamin W.- CTu4B.3  
 Mancini, Irina - OTu4D.5  
 Maneas, Efthymios - JW3A.4  
 Maniewski, Roman - JTu3A.50  
 Manninen, Aki - JW3A.14  
 Manoochehri, Mana - JTu3A.5  
 Marboe, Charles - OTh2D.6  
 Marcu, Laura - CTu2B.3, CTu4B, CTu4B.4, CW4B.4  
 Mardinly, Alan - BW2C.2  
 Margolis, David J.- BTu2C.4  
 Marinov, Radoslav - JTu3A.3

Markel, Vadim A.- JW3A.21, JW3A.25  
 Markman, Zeev - JW3A.23  
 Markow, Zachary - BTu4C.3, OW4C.5  
 Markwardt, Niklas - CTh2B.5  
 Marone, Alessandro - CTu4B.6, CW4B.3, CW4B.6,  
 JTh3A.34, OF4D.6  
 Marquet, Pierre - JTu3A.16  
 Marro Sánchez, Mónica - JTh3A.14  
 Mars, Jérôme - JTh3A.45  
 Martelli, Fabrizio - JTu3A.25, JW3A.30, OTu4D.1  
 Martí-Fàbregas, Joan - CW2B.6  
 Martin, Hannah - CF2B.2  
 Martinelli, Matheus B.- JTu3A.44  
 Martinenghi, Edoardo - JW3A.43, OW2D.2  
 Martinez, Amy - CF2B.2  
 Maruccia, Federica - CW2B.4, CW2B.6  
 Maslennikova, Anna V.- CF4B.5, JTh3A.8  
 Mata Pavia, Juan - JW3A.24, OF4D.5  
 Mathieson, Keith - JW3A.57  
 Mathieu, Benjamin - BTh4C.2  
 Matveev, Lev A.- CF4B.5  
 Mavroudis, Constantine D.- CW2B.2, CW2B.5  
 Mayos, Mercedes - CW2B.6  
 Mazdeyasna, Siavash - BF2C.3, OW2D.4  
 Mazzamuto, Giacomo - JTh3A.64, JTu3A.62  
 McAlinden, Niall - JW3A.57  
 McCammon, Susan D.- MF2A.5  
 McClatchy, David M.- CTu4B.3  
 McCracken, Courtney - OW2D.6  
 McCutcheon, Kelly - CTh4B.6  
 McEvoy, Andrew - JTu3A.8  
 McGorty, Ryan - JTu3A.17  
 McGuire, Shawn - MTh4A.3  
 McLean, James P.- JW3A.35, OF3D.2  
 McMahan, Lori - JTu3A.55  
 Medina Neto, Antonio - JTh3A.43  
 Mehanian, Courosh - MTh4A.3  
 Mehidine, Hussein - JTh3A.20  
 Mehrabi, Mehraz - JTh3A.16, JW3A.45  
 Melchior, Richard W.- CW2B.2  
 Men, Jing - JW3A.33  
 Menneteau, Mathilde - JTh3A.28  
 Mensah-Brown, Kobina - CW2B.2, CW2B.5  
 Mensen, Armand - JTh3A.58  
 Mercep, Elena - JTh3A.44  
 Mertz, Jerome - BF4C.5, BW2C.6, CF3B.8  
 Messaddeq, Younes - JTh3A.4  
 Micera, Silvestro - BTh2C.2  
 Mikhaylova, Irina - OW4D.5  
 Milanese, Daniel - OF2D.6  
 Milej, Daniel F.- BF2C.2, JTu3A.54, JTu3A.63,  
 OF4D.1, OW4C.4  
 Miller, Joann - CF2B.6  
 Milos, Peter - BTh2C.8  
 Mimura, Tetsuya - JTu3A.43  
 Minaeva, Olga V.- JTu3A.11  
 Minnema, Jordi - OW2D.2  
 Miserocchi, Anna - JTu3A.8  
 Mittal, Shachi - MW2A.1  
 Moghe, Prabhas V.- MW4A.4  
 Moiseev, Alexander - CF4B.5  
 Molano-Mazón, Manuel - BW2C.5  
 Möllmert, Stephanie - OF2D.5  
 Molnar, Gabor - JTh3A.29  
 Moncaster, Juliet A.- JTu3A.11  
 Monnier, Philippe - BTh2C.3  
 Monroy, Guillermo L.- CF4B.3  
 Montagni, Elena - JTu3A.47  
 Montejo, Karla - JTu3A.6  
 Moore, Gerald A.- JTu3A.48

Moore, Michael G. - CTu2B.3  
 Moore, Richard - OF4D.4  
 Mora, Mireia - CF2B.3, OTh4D.5  
 Morales, Sophie - JTh3A.28, JTh3A.45  
 Morano, Vincent - CW2B.2  
 Morawiec, Magdalena - JTu3A.50  
 Moretti, Claudio - BTu2C.2  
 Morgan, Ryan - CW2B.5  
 Morrison, Laura - JTh3A.62, JW3A.8  
 Mosca, Sara - OTu4D.1, OTu4D.2  
 Moscatelli, Frank A.- JW3A.25  
 Mostafa, Atahar - OF1D.5  
 Mostrom, James - JW3A.2  
 Mota, Claudia - JTh3A.15  
 Muccigrosso, David - OW4C.7  
 Muck, Martina - BF4C.3, OTh2D.3  
 Mugnes, Jean-Michel - JTu3A.16  
 Mujat, Mircea - JTu3A.11  
 Mullen, Michael T.- OF4D.1  
 Munger, Karl - JTh1A.1  
 Muthukrishnan, Varalakshmi - JTh3A.11  
 Mylonas, George P.- CF1B.5

## N

Nadkarni, Vinay M.- CW2B.5  
 Najafzadeh, Laleh - BTu2C.4, JTh3A.54  
 Nalawade, Sahil - JW3A.55  
 Nandy, Sreyankar - JTh3A.40, JW3A.46  
 Narayanan, Sivakumar - JTh3A.11  
 Narsipur, Sriram - JW3A.2  
 Nasu, Hatsuko - JTu3A.43  
 Naughton, Thomas J.- JW3A.14  
 Navarro, Fabrice - JTh3A.28  
 Neel, Victor - MF4A.4  
 Neidrauer, Michael - CF2B.7  
 Nelson, Leonard Y.- CTh4B.2  
 Nemani, Arun - JTh3A.53  
 Ness, Steven - CF4B.2  
 Ness, Torbjørn V.- JW3A.56  
 Newbold, Dillan J.- BTu4C.3  
 Nezafati, Maysam - JTh3A.59  
 Nguyen, The-Quyen - MW2A.4  
 Ni, Ming - JW3A.13  
 Nie, Liming - CF2B.5  
 Nieman, Gary - JW3A.2  
 Niendorf, Thoralf - JTh3A.39  
 Nina-Paravecino, Fanny - JTh3A.38  
 Ning, Yuan - CF4B.7  
 Nirenberg, Shelia - JW1A.2  
 Nishimura, Goro - JTu3A.2  
 Nishioka, Norman S.- CTu2B.2  
 Nisoli, Enzo - OF4D.2  
 Nissinen, Jan - OF2D.6  
 Noimark, Sacha - JW3A.4  
 Nolte, David D.- CTu4B.7  
 Nosrati, Reyhaneh - BTh2C.6  
 Notingher, Ioan - CF1B.2, CTu4B.5  
 Nouizi, Farouk - JTh3A.16, JW3A.45  
 Novak, Michael A.- CF4B.3  
 Novitskaya, Tatiana - MTh2A.4

## O

Obaid, Sami - OW4C.6  
 O'Brien, Peter - CW4B.7  
 Occhi-Alexandre, Ingrid G.- JTh3A.43  
 Ochoa, Marlen I.- OF2D.4, OTu4D.4  
 Odintsov, Boris - OTh2D.2  
 Ogura, Hiroyuki - JTu3A.43  
 Ohmae, Etsuko - JTu3A.43

Ojanen, Simo - JTu3A.27  
Oldenburg, Ian A.- BW2C.2  
Olivo, Malini C.- CF3B.7  
Olson, Eben - JW3A.18  
Olson, Jonathan - JTh3A.36  
Ong, Yihong - CF2B.6, JW3A.25, JW3A.63  
Orive Miguel, David - JTh3A.45  
Orlova, Anna - JTh3A.8, OW4D.5  
Orlova, Natalia - JW3A.60  
Orr, Harry - JW3A.58  
Orsini, Francesco - JTh3A.64, JTu3A.62  
Orukari, Inema - BTh2C.4  
Osina, Ilze - JTh3A.7  
Ourselin, Sebastien - JTu3A.8, JW3A.4  
Ozana, Nisan - JW3A.23  
Ozcan, Aydogan - MTh2A.2

## P

Pacheco Tobo, Andrea L.- CF3B.4  
Paganoni, Anna Maria - OTh4D.1  
Pagliuzzi, Marco - CF2B.3, OTu2D.1, OTu2D.5,  
OW2D.2, OW4C.2  
Pain, Frederic - JTu3A.57  
Pal, Rahul - MF2A.5  
Pallud, Johan - JTh3A.20  
Palmer, Gregory - CF2B.2  
Pan, Wen-Ju - JTh3A.59, JW3A.59  
Pan, Yongle - JW3A.39  
Panzeri, Stefano - BW2C.5  
Paragas, Neal - JTu3A.24  
Parent, Martin - JTh3A.4  
Park, Jasmine - JTh3A.60  
Park, Jong K.- MF2A.3  
Parot, Vicente J.- BW2C.3  
Parthasarathy, Ashwin B.- CF3B.2, JW3A.20,  
JW3A.25, JW3A.63, OF4D.1, OW2D  
Pasquini, Maria - BTh2C.2  
Patel, Kripa B.- BF3C.3  
Patel, Nirav J. - JW3A.54  
Patel, Rakesh - MF4A.4  
Patel, Sanjay - JW3A.28  
Patterson, Melanie D.- MTh4A.2  
Paulsen, Keith D.- CTu4B.3, JTh3A.13, JTh3A.36  
Pavlosky, William - BF2C.2  
Pavlov, Mikhail V.- JTh3A.8  
Pavone, Francesco S.- BF4C.1, BTh2C.2, JTh3A.64,  
JTu3A.47, JTu3A.62  
Pavone, Francesco Saverio - BTu2C.5  
Pegard, Nicolas C.- BW2C.2  
Pena, Ana-Maria - MF2A.2  
Pera, Vivian - JTu3A.31  
Pereira, Daisa - JTh3A.15  
Perekatova, Valeriya - JW3A.36, OW4D.5  
Perelman, Lev T.- CF2B.4  
Perez-Clavijo, Francisco - JTh3A.6, JTu3A.7,  
JW3A.44  
Perriollat, Mathieu - JW3A.27  
Perroy, Julie - BTh4C.5  
Peru, Deborah - JTh3A.5  
Peterson, Charles - JW3A.2  
Peterson, Gary - MW4A.1  
Pham, Thao T.- CW2B.3, JW3A.64, OF4D.7  
Phipps, Jennifer - CTu2B.3, CTu4B.4  
Pian, Qi - JTh3A.51, OTu4D.4  
Piao, Daqing (Daching) - JTh3A.1, JW3A.28  
Pichette, Julien - OW4C.6  
Picot, Fabien - OW4C.6  
Pierce, Mark C.- JTh3A.5, MW4A.4, OF2D.3

Pifferi, Antonio - CF2B.3, JTu3A.25, JW3A.30,  
JW3A.43, OF2D.6, OF4D.2, OTh4D.1,  
OTh4D.5, OTu2D.1, OTu2D.5, OTu4D.1,  
OTu4D.2, OW2D.2, OW4C.2  
Pitkääho, Tomi - JW3A.14  
Planat-Chretien, Anne - JW3A.27  
Plekhanov, Vladimir - JTh3A.8  
Pleskow, Douglas K.- CF2B.4  
Plorina, Emilija Vija - JTh3A.7  
Poca, María Antonia - CW2B.4  
Pogue, Brian W.- CTu2B.1, CTu4B.3, JTh3A.13  
Pohlmann, Andreas - JTh3A.39  
Polucha, Collin - JTu3A.34  
Pongratz, Thomas - JTu3A.12  
Poon, Chien - JTh3A.63  
Popescu, Gabriel - MF1A.2  
Popp, Juergen - CTh4B, CTh4B.1  
Portaluppi, Davide - JTu3A.20  
Porter, Ryan G.- CF4B.3  
Potcoava, Mariana - JW3A.53  
Pouli, Dimitra - JTh1A.1  
Poulon, Fanny - JTh3A.20  
Powell, Samuel - OW4D.4  
Prakash, Ammu - JTh3A.48  
Prakash, Mithilesh - OF4D.3  
Proctor, Ashley R.- CF3B.1, OW2D.3, OW2D.7  
Prohaska, Steffen - OW4D.4  
Pulawski, Przemyslaw - JTu3A.50  
Puppels, Gerwin - CF1B.2  
Pybus, Alyssa - JW3A.66

## Q

Qiu, Le - CF2B.4  
Qiu, Suimin - MF2A.5  
Qu, Dovina - OF3D.2  
Qu, Jason Z. - BTh2C.7, JW3A.41  
Quarta, Eros - BTu2C.5  
Quinn, Kyle P.- CTh4B.3, JTh1A.1

## R

Racheli, Noam - JTh3A.32  
Radabaugh, Jeffrey - CF3B.6  
Raghavan, Guruprasad - JTu3A.41  
Rahmim, Arman - JTu3A.51  
Rahn, Rachel M.- BTu2C.6  
Rainwater, Orion - JW3A.58  
Rajadhyaksha, Milind M.- MTh2A.1, MW4A,  
MW4A.1  
Rajaram, Ajay - JTu3A.63, JW3A.50, OW4C.4  
Raju, Michael - OF1D.2  
Rakha, Emad - CTu4B.5  
Ramachandran, Siddharth - CTh4B.6  
Ramanujam, Nimmi - CF2B.2  
Ramanujam, Nirmala - CTu4B.1  
Ramella-Roman, Jessica - JTu3A.6  
Ramirez, Gabriel A.- CF3B.1, JW3A.22, OW2D.3,  
OW2D.7  
Ramser, Hallie E.- CTh4B.3  
Ramunno, Lora - JW3A.17  
Rao, Babar - MF4A.2  
Rao, Navalgund - OW4D.2  
Raveendran, Tara - JTu3A.46  
Razansky, Daniel - CF3B.7, JTh3A.44  
Reddy, Divya D.- JW3A.55  
Reder, Nicholas - CTu4B.2  
Reiche, Christopher - JW3A.57  
Reiner, Thomas - MTu4A.4  
Reisman, Matthew D.- JTh3A.60, OW4C.5  
Ren, Jian - BF4C.4, JW3A.67

Ren, Jingxuan - JW3A.22, OW2D.3  
Renna, Marco - OTh4D.5  
Resta, Francesco - BTh2C.2, JTu3A.47  
Rey-Perez, Anna - CW2B.4  
Riaz, Muhammad - JTh3A.35  
Ricci, Andrew - OTh4D.2  
Richards-Kortum, Rebecca - CTu2B.4  
Richter, Ed - JTh3A.52  
Richter, Johan - BTh2C.8, CTh2B.3  
Rieppo, Lassi - OF4D.3  
Rieth, Loren - JW3A.57  
Rigneault, Hervé - BF3C.5  
Rinberg, Dmitry - BTu2C.3  
Ringuette, Dene - BTh2C.3  
Rioux-Pellerin, Émile - JTu3A.16  
Rippe, Lars - OF1D.3  
Ristaniemi, Aapo - JW3A.29  
Ritter, Alfred - CTh4B.6  
Riveiro Vilaboa, Marilyn - CW2B.4  
Rivera, Marcela - JTh3A.52  
Riviere, Ryan - JTh3A.25  
Rizzo, Elizabeth J.- CTu4B.3  
Robbins, Constance M.- JTu3A.41  
Roberge, Cassandra E.- JTh3A.47  
Roberts, David - JTh3A.36  
Robledo, Edwin A.- JTh3A.11, JTh3A.6, JTu3A.7,  
JW3A.44  
Roblyer, Darren M.- JTu3A.31, OF2D.3  
Rodriguez, Shelagh - JW3A.53  
Rodriguez, Erik A.- BF3C.2  
Roetzer, Thomas - OTh2D.3  
Roffilli, Matteo - JTh3A.64  
Rohrbach, Daniel J.- JTh3A.63  
Rosalen, Pedro L.- JTh3A.43  
Rosen, Ike - JTh3A.60  
Rosenthal, Amir - JTu3A.37, OW4D.6  
Rosenthal, Tami M.- CW2B.2  
Rosinski, Bogdan - OTh4D.5  
Roy, Debasish - JTu3A.46  
Roy, Sayon - CF4B.2  
Roy, Vincent - JTu3A.16  
Rozsa, Balazs - BTu2C.1  
Ruan, Haowen - BF3C.6  
Rubin, Erin - JTh3A.1  
Rubin, Joshua B.- BTh2C.4  
Rudkouskaya, Alena - CTh4B.4, JTh3A.19  
Rueden, Curtis T.- MTh2A.3  
Ruers, Theo J.- CF1B, CTh2B.6  
Ruesch, Alexander - JTu3A.40, OW4C.3  
Rühm, Adrian - CTh2B.5  
Ruogu, Fang - JW3A.44  
Russell, Sarah - JTh3A.21  
Rykhlik, Pavel - JTh3A.8

## S

Saarakkala, Simo - JTu3A.27  
Sacconi, Leonardo - BTh2C.2, BTu2C.5, JTh3A.64,  
JTu3A.47  
Sadegh, Sanaz - BF3C.2  
Saggau, Peter - JW3A.60  
Sahel, Jose-Alain - OF3D.5  
Sahin, Sule - JTh3A.3  
Sahuquillo, Juan - CW2B.4  
Sahyoun, Christine C.- JTh3A.5  
Saini, Neal - JTh3A.26  
Saisan, Payam A.- BF3C.2  
Sakadzic, Sava - JW3A.56  
Sakahara, Harumi - JTu3A.43  
Saknite, Inga - MTh4A.2

- Saksena, Mansi - OF4D.4  
 Sakulsaengprapha, Vorada - CF1B.4  
 Salsabilian, Shiva - BTu2C.4  
 Samaei, Saeed - OTu2D.3  
 Sanchez Majos, Salvador - JW3A.24, OF4D.5  
 Sanders, Bharat B.- JW3A.66, OW2D.6  
 Sarin, Jaakko K.- JTu3A.27, OF4D.3, OTu4D.5  
 Sassaroli, Angelo - CW2B.3, JTu3A.39, JW3A.40, JW3A.64, OF4D.7  
 Satalin, Joshua - JW3A.2  
 Sathialingam, Eashani - OW2D.6  
 Sato, Francielle - JTh3A.43  
 Sawhney, Mandeep - CF2B.4  
 Sawosz, Piotr - JTu3A.50, OTu2D.3  
 Scharf, Robert - JW3A.57  
 Scheel, Julia - CW2B.4  
 Scheslavskiy, Vladislav - JW3A.7  
 Schiavo, Kellie L.- CW2B.2  
 Schlaggar, Bradley L.- BTu4C.3  
 Schlüßler, Raimund - OF2D.5  
 Schmidt, Alexander - CW2B.2  
 Schmitt, Samantha - JTu3A.40, OW4C.3  
 Schüler, Ralf - CW4B.7  
 Schultz, Simon - BTh4C.3, JTu3A.48  
 Schutzman, Richard - JTh3A.11, JTh3A.6, JTu3A.7, JW3A.44  
 Schwartz, Nadav - CF3B.2  
 Schwarz, Ariel - JW3A.23  
 Schwarz, Richard - CTu2B.4  
 Sedova, Elena S.- CF4B.5  
 See, Alfred P. - JW3A.54  
 Seeliger, Erdmann - JTh3A.39  
 Segers, Patrick - CW4B.7  
 Seibel, Eric J.- CTh4B.2  
 Selb, Juliette - BTh2C.7, JW3A.41  
 Sevilla, Nicole - JTu3A.6  
 Shade, Brandon C.- CW2B.2  
 Shaik, Mohammed A.- BF3C.3  
 Shakhova, Natalia - JTh3A.8  
 Shan, Tianqi - OW4D.3  
 Shao, Di - CF4B.2  
 Sharma, Rohit - JW3A.57  
 Shatrovov, Oleg - JTu3A.53  
 Shechter, Revital - JTh3A.32  
 Shemer, Amir - JW3A.23  
 Shen, Qi - MF3A.1  
 Sherafati, Arefeh - JW3A.51  
 Sherif, Sherif S.- JTh3A.48  
 Shi, Dongqing - BTh4C.2  
 Shi, Taixiang - OTh4D.4  
 Shimony, Joshua S.- BTh2C.4  
 Shipp, Dustin - CF1B.2, CTu4B.5  
 Shirmanova, Marina - JTu3A.14, JW3A.7  
 Shkalova, Lubov - JTh3A.8  
 Shlivko, Irena - JW3A.7  
 Shoham, Shy - BTu2C.3  
 Sholl, Andrew - MF1A.1, MF1A.4  
 Shribak, Michael I.- MTu4A.5  
 Shu, Xiao - BW2C.7, JTu3A.59, OTh2D.7  
 Shulevitz, Henry J. - JTh3A.34  
 Siegel, Adrew - JTu3A.53  
 Siegel, Joshua S.- BTh2C.4  
 Silberstein, Jonathan - MF1A.4  
 Silva, Elizabete D.- JTh3A.46  
 Silvestri, Ludovico - JTh3A.64, JTu3A.62  
 Singh, Bhawana - OF4D.4  
 Singh, Mithun K.- JW3A.4  
 Singh-Moon, Rajinder P.- OTh2D.4  
 Sinha, Lagnojita - JTu3A.29, OTh4D.7  
 Sinsuebphon, Nattawut - CTh4B.4, JTh3A.19  
 Siret, David - JTu3A.33  
 Sirotkina, Marina - CF4B.5  
 Siu, Dickson M.- MTu4A.3  
 Sivankutty, Siddharth - BF3C.5  
 Sloat, Charles J.- JTh3A.47  
 Smith, Matthew A.- JTu3A.40, OW4C.3  
 Smith, Spencer - BF3C  
 Smolina, Ekaterina - OW4D.5  
 Smyser, Christopher - JTh3A.52  
 Snatarpia, Joshua - JW3A.39  
 Snyder, Abraham Z.- JTh3A.58  
 So, Hayden - MF3A.4  
 So, Peter T.- MF2A.3  
 Sobh, Nahil A.- OTh2D.2  
 Soleimanzad, Haleh - JTu3A.57  
 Song, Chaolong - JW3A.16  
 Song, Ge - JW3A.32, OF3D.7  
 Song, Weiye - CF4B.2  
 Soulez, Gilles - OW4C.6  
 Sowa, Michael - JTh3A.48  
 Sowah, Johanan N. - JTh3A.34  
 Spicer, Graham - MW2A.4  
 Spigulis, Janis - JTh3A.7  
 Spillman, Darold R.- OTh2D.2  
 Spinelli, Lorenzo - OF4D.2, OTu2D.5, OW4C.2  
 Squarcia, Mattia - CF2B.3, OTh4D.5  
 Srinivas, Vijaya - JTu3A.6  
 Srinivasan, Vivek J.- BTu4C.2, OTu2D.2  
 Sroka, Ronald - CTh2B.5, JTu3A.12  
 St. Lawrence, Keith - BF2C.2, JTh3A.62, JTu3A.54, JTu3A.63, JW3A.50, JW3A.8, OF4D.1, OW4C.4  
 Starkweather, Zack - JTu3A.23  
 Steelman, Zachary - CF4B.6  
 Steinmann, Richard - JW3A.2  
 Stenroth, Lauri - JW3A.29  
 Stepp, Herbert - CTh2B.5  
 Sternberg, Jenna - JTu3A.61  
 Stringari, Chiara - MF2A.2  
 Strittmatter, Frank - JTu3A.12  
 Ströbl, Stephan - JTu3A.12  
 Sturek, Michael - CW4B.2  
 Styles, Iain - JTu3A.32, OTh4D.6  
 Subhash, Hreshm M.- JTh3A.5  
 Subochev, Pavel - JW3A.36, OW4D.5  
 Sun, Cheng - BW2C.7, MW2A.4  
 Sun, Chi-Kuang - MF4A.1  
 sun, hanlin - OTh4D.4  
 Sun, Zhonghua - JTh3A.61, JTu3A.28  
 Sunar, Ulas - CF3B.5, CF4B.4, CTh2B.2, JTh3A.63  
 Supatto, Willy - JW3A.62, MF2A.2  
 Suter, Melissa - CF2B, CF4B.1  
 Sutton, Robert M.- CW2B.5  
 Suzuki, Hiroaki - JTu3A.43  
 Suzuki, Norihiro - JTu3A.43  
 Swan, Carly - JW3A.6  
 Szabo, Vivien - BTh4C.5  
 Szipocs, Robert - JTh3A.29, JW3A.12
- T**
- Tabassum, Syeda - JTu3A.31  
 Tachtsidis, Ilias - JW3A.50  
 Tagliabue, Susanna - CW2B.4  
 Takasaki, Kevin - JTu3A.60  
 Tamas, Gabor - JTh3A.29  
 Tamborini, Davide - JTh3A.33, JTu3A.20, JTu3A.53  
 Tan, Mei Chee - MW4A.4  
 Tang, Anson H.- MTu4A.3  
 Tannenbaum, Susan - OTh4D.2  
 Tanzi, Rudolph - JW3A.33
- Taroni, Paola - CF2B.3, JTu3A.25, JW3A.43, OF4D.2, OTh4D.1, OTh4D.5, OTu2D.5, OTu4D.1  
 Tathireddy, Prashant - JW3A.57  
 Tatka, Jakub - JW3A.10  
 te Moller, Nikae - OTu4D.5  
 Tellis, Jay - JW3A.6  
 Teng, Fei - JTu3A.31  
 Terada, Raquel S.- JTh3A.43  
 Tgavalekos, Kristen - CW2B.3, JTu3A.39, JW3A.40, JW3A.64, OF4D.7  
 Thambayah, Ashvin - JTu3A.35  
 Thng, Steven Tian Guan - CF3B.7  
 Thompson, Sarah M. - JTh3A.34  
 Thouvenin, Olivier - BTh4C.1, JTu3A.61  
 Thunemann, Martin - BF3C.2, JW3A.56  
 Tichauer, Kenneth M.- JTu3A.29, OTh4D.7  
 Titus, Steven - OTh2D.5  
 Tiwari, Saumya - MW2A.1  
 Tkaczyk, Eric - MF4A, MTh4A.2  
 Tommasin, Daniela - CW4B.7  
 Tong, Shanbao - JTu3A.59  
 Torniaainen, Jari E.- JW3A.29  
 Toronov, Vladislav - BTh2C.6  
 Torres, Richard - JW3A.18  
 Torres, Veronica C.- OTh4D.7  
 Torricelli, Alessandro - OTu2D.1, OW2D.2, OW4C.2  
 Tosi, Alberto - OTh4D.5  
 Töyräs, Juha - JTu3A.27, JW3A.29, JW3A.38, OF4D.3, OTu4D.5  
 Tozer, Samuel - JW3A.62  
 Tran, Anh Phong - JTh3A.17, JTu3A.52  
 Tremblay, Marie-André - OW4C.6  
 Tricoli, Ugo - JW3A.21  
 Tripathy, Kalyan - BTu4C.3  
 Tripathy, Pooja - BTu4C.3  
 Tromberg, Bruce J.- CF2B.1, CF3B, OTh4D.3, OW2D.5  
 Tseng, Hua-an - BW2C.6  
 Tsia, Kevin - MF3A.4, MTu4A.3  
 Tsvirkun, Viktor - BF3C.5  
 Tsyboulski, Dmitri - JW3A.60  
 Tulman, David - JTu3A.4, MF1A.4  
 Turchin, Ilya - JTh3A.8, JW3A.36, JW3A.9, OW4D.5  
 Turek, John - CTu4B.7  
 Turschak, Emily - JTu3A.60  
 Turzhitsky, Vladimir - CF2B.4
- U**
- Uddin, K M Shihab - OF1D.5  
 Ueda, Yukio - JTu3A.43  
 Unger, Jakob - CTu2B.3, CTu4B.4  
 Unlu, Burcin - JTh3A.16
- V**
- Vaghefi, Ehsan - JTh3A.42  
 Vaitkevicius, Henrikas - JW3A.54  
 Valdes, Claudia - JTh3A.52  
 Valentini, Gianluca - OTu4D.1, OTu4D.2  
 Valley, Matthew - JTu3A.60  
 van der Kolk, Jarno N.- JW3A.17  
 van der Steen, Antonius - OW4D.1  
 van Soest, Gijs - OW4D.1  
 van Weeren, René - OTu4D.5  
 Vanegas, Morris D.- JTh3A.3, JTu3A.64  
 Vanholsbeeck, Frederique - JTh3A.42  
 Vanholsbeeck, Frédérique - JTu3A.35  
 Vanvincq, Olivier - BF3C.5  
 Vargas, Gracie - MF2A.5

Varlet, Pascale - JTh3A.20  
 Varma, Hari - OTu2D.4  
 Varma, Sandeep - CF1B.2  
 Varone, Antonio - JTh1A.1  
 Vasu, Ram - JTu3A.46  
 Vavadi, Hamed - OF1D.4, OTh4D.2  
 Vecchia, Dania - BTu2C.2  
 Veesa, Joshua Deepak - JTh3A.37  
 Ventalon, Cathie - BTh4C.5  
 Vercauteren, Tom - JTu3A.8  
 Vescovi, Rafael - BF4C.2  
 Vidal, Ernesto - OTu2D.6  
 Vigneswaran, Nadarajah - CTu2B.4  
 Villa, Federica - JTu3A.20  
 Villarreal, Paula - MF2A.5  
 Villette, Vincent - BTh4C.2  
 Vilov, Sergey - JTh3A.24, JTh3A.30  
 Vinogradov, Sergei A.- BF3C.2, JW3A.63  
 Vishwanath, Karthik - JW3A.47  
 Viswanathan, Mohan - JTh3A.11  
 Vitkin, Alex - CF4B.5  
 Vitkin, Edward - CF2B.4  
 Voleti, Venkatakaushik - BF3C.3

## W

Wabnitz, Heidrun - JW3A.31  
 Wada, Hiroko - JTu3A.43  
 Wadduwage, Dushan - MF2A.3  
 Waller, Laura - BW2C.2, MF3A.5  
 Wallois, Fabrice - JTu3A.5  
 Walsh, Alex - MF2A.4, MW2A  
 Walther, Andreas - OF1D.3  
 Wang, Chuji - JW3A.39  
 Wang, Jianing - MTh4A.2  
 Wang, Jing - JTu3A.17  
 Wang, Lidai - OW4D.7  
 Wang, Lin - CF3B.2  
 Wang, Maolin - MF3A.4  
 Wang, Mingyi - JTu3A.21  
 Wang, Pu - MW2A.5  
 Wang, Xiaofang - CF4B.7, OTh2D.5  
 Wang, Xinlong - JTh3A.56, JW3A.55  
 Wang, Yihong - CF4B.7  
 Wang, Yu - CTu4B.2  
 Wårdell, Karin - BTh2C.8, CTh2B.3  
 wartak, andreas - OTh2D.3  
 Waspe, Adam C.- BTh2C.3  
 Waters, Jack - JTu3A.60  
 Watters, Valérie - JTu3A.16  
 Wax, Adam - CF4B.6, JW3A.32, OF3D.3, OF3D.7  
 Weber, Timothy D.- CF3B.8  
 wei, Xianlin - OTh4D.4  
 Weigel, Udo M.- OTh4D.5, OTu2D.5, OW4C.2  
 Weingarten, Michael - CF2B.7  
 Wells, Wendy A.- CTu4B.3  
 Wenceslao Evans, Stephen - BTh4C.2  
 West, Simeon J.- JW3A.4  
 Wikonkál, Norbert - JW3A.12  
 Williams, Amber - JW3A.47  
 Williams, Michelle - CTu2B.4  
 Wilson, Benjamin - MTh4A.3  
 Woehrer, Adelheid - BF4C.3, OTh2D.3  
 Woessner, Alan - CTh4B.3  
 Wojnarowicz, Mark W.- JTu3A.11  
 Wojtkiewicz, Stanislaw - OTh4D.5  
 Wolf, Martin - JW3A.24, OF4D.5  
 Won, Jungeun - CF4B.3  
 Wong, Dean - JTu3A.51  
 Wong, Kenneth - MTu4A.3

Wong, Lesley - CF3B.6, OW2D.4  
 Wood, Levi - JW3A.66  
 Wright, Harlan - JTh3A.1  
 Wright, Patrick - JTh3A.58, JTh3A.60  
 Wu, Kuan C. - JTh3A.33  
 Wu, Melissa - BTh2C.7  
 Wu, Min - OW4D.1  
 wu, nanshou - JTu3A.21  
 Wyart, Claire - BTh4C.1, JTu3A.61  
 Wykes, Victoria - JTu3A.8  
 Wyzlic, Angelika - JW3A.33

## X

Xia, Wenfeng - JW3A.4  
 Xiao, Rui - CW2B.2  
 Xiao, Sheng - BW2C.6  
 Xie, Enyuan - JW3A.57  
 Xie, Hao - BF4C.6  
 Xie, Shusen - JTu3A.36  
 Xie, Yijing - JTu3A.8  
 Xu, Chen - OTh4D.2  
 Xu, Chris - BF3C.1, BW2C  
 Xu, Tao - CF4B.7  
 Xu, Weihao - OF4D.6

## Y

Yaguang, Zeng - JTu3A.21  
 Yamagata, Masahito - BW2C.3  
 Yamashita, Yutaka - JTu3A.43  
 Yan, Pingkun - OF2D.4  
 Yan, Shijie - JTh3A.17  
 Yang, Changhui - BF3C.6  
 Yang, Eric - CTu2B.4  
 Yang, Fang - CF3B.3  
 Yang, Fugang - JTu3A.26  
 Yang, Guojian - JTu3A.21  
 yang, hao - BTu4C.4, JW3A.16, OTh4D.4  
 Yang, Jason - JTu3A.40, JTu3A.41, OW4C.3  
 Yang, Lin - JW3A.31  
 Yang, Meng - CF3B.3  
 Yang, Mu-Han - BF3C.2  
 Yang, Shan - CTh4B.5  
 Yang, Yanlong - JTh3A.31  
 Yao, Baoli - JTh3A.31  
 Yao, Gang - MTu4A.1  
 Yao, Ruoyang - JTh3A.51, JTu3A.30, OF2D.4  
 Yao, Xinwen - OTh2D.4, OTh2D.6  
 Yaroslavsky, Anna N.- MF4A.4, MTh2A, MW4A.3  
 Yassine, Abdul-Amir - JTu3A.9  
 Ye, Tong - JTh3A.26, JTh3A.31  
 Yeh, Kevin - MW2A.1  
 Yi, Ji - CF4B.2  
 Yizhar, Ofer - BTu2C.2  
 Yodh, Arjun G.- BF2C.2, CF2B.6, CF3B.2, CW2B.2, CW2B.5, JTh3A.61, JTu1A.2, JTu3A.54, JW3A.10, JW3A.25, JW3A.63, OF4D.1, OTh4D.3, OW2D.5  
 Yoo, Hongki - CW4B, CW4B.1  
 Yoon, Jonghee - OF2D.1  
 Yoshimoto, Kenji - JTu3A.43  
 Yoshitake, Tadayuki - MF2A.1  
 Yoshizawa, Nobuko - JTu3A.43  
 Yu, Guoqiang - BF2C.3, CF3B.6, OW2D.4  
 Yu, Hang - BF3C.3  
 Yu, Leiming - JTh3A.38, JTh3A.41  
 Yuan, Yaoshen - JTh3A.41

## Z

Zagaynova, Elena - CF4B.5, JTu3A.14, JW3A.7  
 Zaidel, Lynette - JTh3A.5  
 Zaitsev, Vladimir Y.- CF4B.5  
 Zakharov, Yuri - CF2B.4  
 Zalesky, Zeev - JW3A.23  
 Zanoletti, Marta - OTu2D.5  
 Zaragoza, Rachel - JW3A.52  
 Zaryab, Mohammad - OTh2D.4  
 Zeng, Haishan - MW4A.5  
 Zeng, Xianxu - CF4B.7  
 Zezell, Denise M.- JTh3A.15, JTh3A.46, JTu3A.42, JW3A.37  
 Zhan, Yonghua - JTu3A.38  
 Zhang, Chao - JW3A.24, OF4D.5  
 Zhang, Hao F.- BW2C.7, JTu3A.59, MW2A.4, OTh2D.7  
 Zhang, Lei - CF2B.4, CF4B.2  
 Zhang, Linlin - CF4B.7  
 Zhang, Qiming - JTh3A.21  
 Zhang, Sui - CF4B.2  
 Zhang, Xian - BW2C.7  
 Zhang, Xiaoran - CF4B.7  
 Zhang, Yide - JTh3A.27  
 Zhang, Yuanlong - BF4C.6  
 Zhang, Zhan - CF4B.7  
 Zhao, Lingyi - CF3B.3  
 Zhao, Mingjun - BF2C.3, CF3B.6, OW2D.4  
 Zhao, Yan - JTh3A.13  
 Zhao, Yang - JW3A.32, OF3D.3  
 Zhao, Yanyu - OF2D.3  
 Zheng, Corey - JTu3A.58  
 Zhou, Chao - CF4B.7, JW3A.33, OF3D, OTh2D.5  
 Zhou, Feifei - OTh4D.2  
 Zhou, Wenjun - BTu4C.2  
 Zhou, Xiang - MW2A.4  
 Zhou, Yaxuan - CTh4B.2  
 Zhu, Caigang - CF2B.2  
 Zhu, Jinghao - CW4B.7  
 Zhu, Lei - CF3B.3  
 Zhu, Li - JTh3A.54  
 Zhu, Qing - JTh3A.40, OF1D.4, OF1D.5, OTh4D.2  
 Zhu, Timothy C. - CF2B.6  
 Zhu, Yansong - JTu3A.51  
 Zhuo, Shuangmu - JW3A.13  
 Zijlstra, Andries - MTh2A.4  
 Zimmermann, Bernhard B.- JTh3A.3, JTh3A.33, JTu3A.53, OF4D.4  
 Zolda, Pamela - OTh4D.5  
 Zou, Jinyun - OTh2D.5  
 Zsigmond, Peter - CTh2B.3  
 Zubkov, Leonid - CF2B.7  
 Zuo, Ziwei - CTh4B.6  
 Zuschtrater, Werner - OTu4D.2

Sponsored and Managed by



Gold Corporate Sponsor

**HAMAMATSU**

Silver Corporate Sponsor



Corporate Sponsors



**AXIOM OPTICS**

Exhibitors

**Energetiq Technology, Inc.**

**ISS, Inc.**

**PicoQuant Photonics North America, Inc.**